“The most incomprehensible thing about the world is that it is comprehensible”

- Albert Einstein

University of Alberta

ICHNOLOGY, SEDIMENTOLOGY, STRATIGRAPHY, AND TRACE FOSSIL-PERMEABILITY RELATIONSHIPS IN THE UPPER CRETACEOUS MEDICINE HAT MEMBER, MEDICINE HAT GAS FIELD, SOUTHEAST ALBERTA, CANADA

by

ANDREW DAVID LA CROIX

A thesis submitted to the Faculty of Graduate Studies and Research in partial fulfillment of the requirements for the degree of

MASTER OF SCIENCE

DEPARTMENT OF EARTH AND ATMOSPHERIC SCIENCES

Fall 2010
Edmonton, Alberta

Examining Committee

Dr. S. George Pemberton, Department of Earth and Atmospheric Sciences, University of Alberta

Dr. Murray Gingras, Department of Earth and Atmospheric Sciences, University of Alberta

Dr. Michael Ranger, Department of Earth and Atmospheric Sciences, University of Alberta

Dr. Heather Proctor, Department of Biological Sciences, University of Alberta

DEDICATION

This thesis is dedicated to my parents, David and Carol. My accomplishments would not have been possible without your endless love and support. Your encouragement, patience, and quiet concern helped me through the toughest times, while your gracious and humble demeanor kept me grounded when I was successful. I am forever indebted to you for fostering in me a curiosity about the world, and most importantly, teaching me that through perseverance and hard work anything is possible. You are dear to my heart and I love you both.

ABSTRACT

The Upper Cretaceous Medicine Hat Member (Niobrara Formation) in western Canada contains abundant reserves of biogenic natural gas. In the Medicine Hat gas field area of southeast Alberta, nineteen cored intervals were examined and classified based on primary physical and biogenic sedimentary structures. Core analysis and stratigraphic mapping determined that the Medicine Hat Member strata consist of stacked, regionally extensive, lobate geobodies that prograde to the north. Employing spot-minipermeametry, the effect of biogenic rock fabrics on the reservoir characteristics was assessed. X-ray micro-computed tomography was conducted on four samples from a reservoir interval to visualize the geometry and distribution of burrow-associated heterogeneity. The results demonstrate that planiform bioturbate textures locally enhance the storage and transmission of natural gas in Medicine Hat reservoirs.

ACKNOWLEDGEMENTS

Many have helped me on my journey to attain an M.Sc. and they should not go without recognition. My thesis began as a seed of insight planted in my mind by George and Murray, and they gave me the freedom and support to sprout the ideas into a form that could be understood and digested by the scientific community. I am forever indebted to you both for allowing me the opportunity to become a member of such a productive and knowledgeable research group. Moreover, without your seemingly endless geological wisdom, prowess in the field, and unparalleled mentorship I certainly would not have become the geologist I am today. In my time as your pupil I have come to regard you both as friends.

I also would like to acknowledge those in the Ichnology Research Group (IRG), past and present. Had many of you not shared your valuable insight and experiences gained during your graduate studies and passed them on to newer members of the group I would be lost. Particularly, I'd like to thank Curtis Lettely for taking me under his wing in the early part of my study and ensuring that I did not stray far from the important aspects. B.C. Yang, thank you for your helpful insight, and for guiding me through the laborious process of core logging. Ryan King, you were always helpful for bouncing ideas off of, and suffered long and tedious edits of manuscripts for which I am thankful. Thank you to Lynn Dafoe for numerous insights into the world of sedimentology, ichnology, stratigraphy, and thesis preparation. To Ryan Lemiski, a sincere nod of appreciation for your support, advise, and mentorship as together we struggled through the study of rocks that leave much to be desired. Last but not least, I'd like to thank Jesse Schoengut and Greg Baniak for helping break up the days with intricate discussions of both geology and sports related topics, I'd certainly have gone crazy without your friendship. The list of IRG members could go on for pages, and those not mentioned by name all helped in some way and you are not forgotten.

Finally, I would like to acknowledge the financial and logistical support of the companies who sponsored my thesis through the Milk River Consortium: Nexen, Conocco Phillips, and Total. Specifically, I'd like to thank Dr. Dale Leckie and Cindy Robinson at Nexen for allowing me to closely examine some of their cores, and for their encouragement and feedback during our meetings in Calgary.

TABLE OF CONTENTS

LIST OF TABLES

LIST OF FIGURES

LIST OF SYMBOLS AND ABBREVIATIONS

FACIES/SEDIMENTOLOGY

*F*A1	Facies Association 1
FA2	Facies Association 2
FA3	Facies Association 3
FA4	Facies Association 4
HCS	Hummocky Cross-Stratification
M_{lb}	Laminated Claystone (Burrowed)
M_{ln}	Laminated Claystone (Unburrowed)
M_{mb}	Structureless Claystone (Burrowed)
M_{mn}	Structureless Claystone (Unburrowed)
S_h	Hummocky Cross-stratified Sandstone
S_p	Planar Stratified Sandstone
S_w	Wave-ripple Cross-laminated Sandstone
S_c	Combined-flow-ripple Cross-laminated Sandstone
S_{mb}	Homogeneous Sandstone (Burrowed)
S_{mn}	Homogeneous Sandstone (Unburrowed)
Z_{lb}	Laminated Siltstone (Burrowed)
Z_{ln}	Laminated Siltstone (Unburrowed)
Z_{mb}	Massive Siltstone (Burrowed)
Z_{mn}	Massive Siltstone (Unburrowed)

STRATIGRAPHY

FS	Flooding Surface
HST	Highstand Systems Tract
SB	Sequence Boundary

LIST OF SYMBOLS AND ABBREVIATIONS CONT.

ICHNOFOSSILS

As	*Asterosoma*
Cy	*Cylindrichnus*
fu	fugichnia
MS	"mantle and swirl"
Pa	*Palaeophycus*
Ph	*Phycosiphon*
Pl	*Planolites*
Ps	*Psilonichnus*
Rh	*Rhyzocorallium*
Sch	*Schaubcylindrichnus freyi*
Sc	*Scolicia*
Sk	*Skolithos*
Si	*Siphonichnus*
Te	*Teichichnus*
Th	*Thalassinoides*
Zo	*Zoophycos*

ICHNOFOSSIL OCCURENCE

vr	Very Rare
r	Rare
m	Moderately Common
c	Common

MISCELLANEOUS

BI	Bioturbation Index
CT	Computed Tomography
K_a	Air Permeability
MRI	Magnetic Resonance Imaging
PDP	Pulse Decay Permeameter
PDPK	Pressure Decay Profile Permeameter
SEM	Scanning Electron Microprobe
TCF	Trillion Cubic Feet
WCSB	Western Canada Sedimentary Basin

CHAPTER I — INTRODUCTION

Currently, the energy industry faces a major shift in paradigm. Conventional petroleum reserves are on the decline, and demand for energy is ever increasing. Global production of natural gas must significantly increase over the next two decades in order to meet the world's energy needs, as estimates suggest that roughly half of conventional natural gas resources have already been exploited. As a result, unconventional resources will bear the burden as a long-term solution to supplement the high demand for energy in industrialized and developing markets alike (Odedra et al., 2005). Total global consumption of natural gas increases by 1.6% per year, on average, and is estimated to reach 153 trillion cubic feet (TCF) by 2030 (EIA, 2009). Furthermore, oil prices are projected to increase once again after 2012, and remain high through the forecast period. Therefore, consumers will look to natural gas for their energy needs when possible because of its less expensive cost and lower greenhouse gas emissions compared to coal or oil, among other factors (EIA, 2009). Though at current production rates conventional reserves will suffice for approximately the next 60 years (Odedra et al., 2005), unconventional resources are replacing declining conventional petroleum systems.

The definition of an unconventional petroleum system is dependent upon perception. Economic factors distinguished the difference between conventional and unconventional resources in North America during the 1970's. Coalbed methane, tight sands, and shale gas were at best marginally economic, and thus, were considered unconventional. However, these resources have since become economically viable, and many now regard such play types to be conventional (Law and Curtis, 2002). With the exception of economics, there are fundamental geologic characteristics that can be used to define unconventional systems. Whereas conventional resources are generally buoyancy-driven, discrete accumulations, occurring in structural or stratigraphic traps, unconventional systems are characterized by regionally pervasive accumulations, independent of structure and stratigraphy, that are not driven by buoyancy forces (Law and Curtis, 2002). As unconventional gas emerges as a viable alternative, exploration geoscientists are revisiting traditional ideas about the generation, expulsion, migration, entrapment, and reservoir characteristics of natural gas systems (Law and Curtis, 2002).

Immense volumes of methane are contained in regionally extensive, relatively fine-grained, and low-permeability intervals worldwide, but in large part, they are poorly understood. In the northern Great Plains of the United States and Canada, methanogenic bacteria charged a blanket of shallow Cretaceous sediments during early burial (Shurr and Ridgley, 2002; Odedra et al., 2005). These intervals provide a composite source, seal, and trap for the accumulation of natural gas. The Medicine Hat Member of the Niobrara Formation in southeast Alberta and southwest Saskatchewan is particularly important, as it contains between 4 and 6 TCF (O'Connell, 2003). Combined with the Milk River/Lea Park, and the Second White Specks formations, the units constitute the largest gas fields discovered in Canada (Figure I-1) (O'Connell, 2003). However, little has been published on their geological characteristics, for a myriad of reasons. Firstly, natural gas in the shallow reservoirs occurs in broad, lobate sandstone bodies. Stratigraphic analysis as a result, is generally not regarded as an important exploration tool. Secondly, the strata are exceptionally rich in smectite clays, and as a result, primary physical and biogenic sedimentary structures are often obscured. Moreover, until recently the fields were only marginally economic because of their low recovery rates, thus they were not deemed important to geologists exploring in the Western Canada Sedimentary Basin (O'Connell, 2003).

This present thesis integrates ichnology, sedimentology, and stratigraphy to understand the depositional environments and stratigraphic architecture of the Upper Cretaceous Medicine Hat Member in southeast Alberta. Porosity and permeability data are integrated with the sedimentological and ichnological observations, to investigate the role of bioturbate textures on unconventional resource quality. Ichnology has proven to be a viable tool for palaeoenvironmental and stratigraphic interpretation. However, by and large, in the sedimentological literature bioturbation is equated with sediment homogenization, and thus holds negative connotations with regard to the storativity, and deliverability of hydrocarbons. This thesis reveals that bioturbate textures can, in fact, provide appreciable, quantifiable enhancement of permeability, whereby the admixing of sand into otherwise silt- and clay-rich sediment increases porosity.

This thesis concentrates on the Medicine Hat gas field as the study area. It is located in Townships 8-22, Ranges 1-9W4, and contains more than 17 000 wells, of which at least 16 000 penetrate the Medicine Hat Member. Nineteen

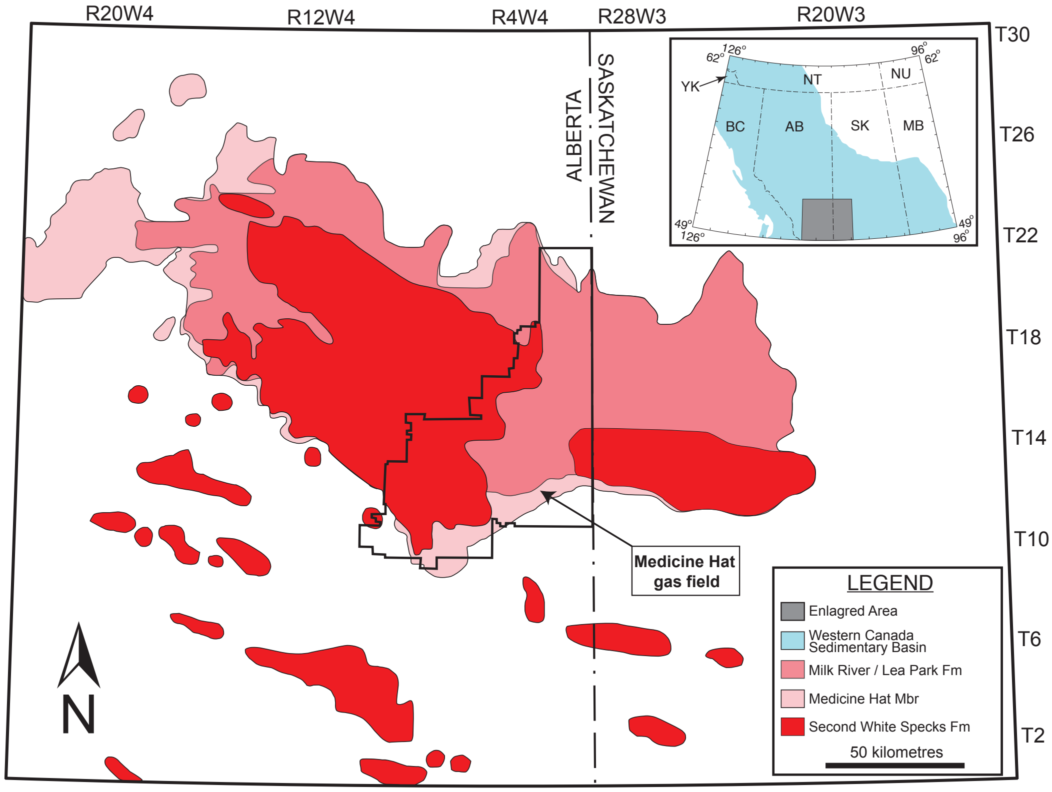

FIGURE I-1: Distribution of Upper Cretaceous gas fields in southeast Alberta and southwest Saskatchewan. The combined reserves of the Milk River/Lea Park Formation, Medicine Hat Member (Niobrara Formation), and Second White Specks Formation comprise the largest gas accumulation discovered in Canada to date. The Medicine Hat gas field (study area) is shown for reference. Modified from O'Connell (2003), and Lemiski (2010).

cored intervals were chosen for analysis and inclusion in the dataset. Well data is relatively more abundant in the north and east of the study area, as a result of comingled production from three Upper Cretaceous intervals (e.g., Milk River Formation, Medicine Hat Member, and Second White Specks Formation). The Medicine Hat Member is Santonian in age, overlies the Verger Member, and below the First White Specks Member of the Niobrara Formation. A more detailed discussion of the stratigraphy is provided in Chapter III.

Chapter II describes the recurring facies in the Medicine Hat Member in terms of physical sedimentary structures and ichnofossil content. The facies are grouped into repeating packages (facies associations), where each is attributed to a specific depositional environment in a subaqueous clinoform-shaped succession. The merits of the interpretations are discussed, and compared with the other sedimentological studies in the region by Schröder-Adams et al. (1997), Nielsen (2002), and Nielsen et al. (2008).

Chapter III introduces the reader to the stratigraphic relationships of the Medicine Hat Member to the laterally adjacent and bounding strata. A brief history of previous work proceeds a lithostratigraphic analysis based upon a network of cross-sections comprising 41 wells, tied to 19 measured sections. The lithostratigraphic interpretations are then used in a sequence stratigraphic framework, with particular emphasis on the development of autogenic and allogenic surfaces in the study area. Chapter III concludes with a comparison and discussion of the results with the most recent regional studies of Upper Cretaceous stratigraphy by Nielsen (2002) and Nielsen et al. (2003).

Chapter IV puts the ichnological observations from Chapter II into a reservoir characterization context. Spot-minipermeametry and micro-CT techniques were applied to investigate the role of trace fossils in altering the porosity distribution and permeability fields of pervasively bioturbated intervals. Spot-minipermeametry data is compared against permeability data from Nexen Inc., and the test results are discussed in terms of the statistical relationship between layered heterogeneity and anisotropy. Furthermore, micro-CT data provides easily interpreted three-dimensional volumes and serial slice x-ray images of density heterogeneity that support earlier observations about the nature of burrowing and its possible effects on the conduits for fluid flow.

REFERENCES

(EIA) Energy Information Administration, 2009, International Energy Outlook 2009: Natural Gas, Report DOE/EIA – 0484. World Wide Web Address: http://www.eia.doe.gove/oiaf/ieo/nat_gas.html

Law, B.E., and Curtis, J.B., 2002, Introduction to unconventional petroleum systems, American Association of Petroleum Geologists Bulletin, v. 86, p. 1851-1852.

Nielsen, K.S., 2002, Lithostratigraphy, sequence stratigraphy and palaeoenvironments of the Upper Colorado Group in southern Alberta and southwestern Saskatchewan: definition of the Carlile and Niobrara formations (Upper Turonian to Upper Santonian), unpublished Ph.D. thesis, Carleton University, Ottawa, Canada.

Nielsen, K.S., Schröder-Adams, C.J., and Leckie, D.A., 2003, A new stratigraphic framework for the Upper Colorado Group (Cretaceous) in southern Alberta and southwestern Saskatchewan, Canada, Bulletin of Canadian Petroleum Geology, v. 51, p. 304-346.

Nielsen, K.S., Schröder-Adams, C.J., Leckie, D.A., Haggart, J.W., Elberdak, K., 2008, Turonian to Santonian palaeoevironmental changes in the Cretaceous Western Interior Sea: The Carlile and Niobrara formations in southern Alberta and southwestern Saskatchewan, Canada, Palaeogeography, Palaeoclimatology, Palaeogeography, v. 270, p. 64-91.

O'Connell, S.C., 2003, The Second White Specks, Medicine Hat and Milk River formations – A shallow gas workshop, consult. rep.

Odedra, A., Burley, S.D., Lewis, A., Hardman, M., and Haynes, P., 2005, The world according to gas, *in* Dore, A.G., and Vining, B.A., eds., Petroleum Geology: North-West Europe and Global Perspectives, Proceedings of the 6th Petroleum Geology Conference, p. 571.-586.

Schröder-Adams, C.J., Adams, P.J., Leckie, D.A., Bloch, J., Craig, J., and El-Dien, S.A.S, 1997, Upper Cretaceous Medicine Hat Formation and First White Speckled Shale in southeastern Alberta: Evidence for localized shallow water deposition, Bulletin of Canadian Petroleum Geology, v. 45, p. 356-376

Shurr, G.W., and Ridgley, J.L, 2002, Unconventional shallow biogenic gas systems, American Association of Petroleum Geologists, Bulletin, v. 86, p. 1939-1969.

CHAPTER II — FACIES ANALYSIS AND PALAEOENVIRONMENTAL INTERPRETATION OF THE MEDICINE HAT MEMBER, MEDICINE HAT GAS FIELD, SOUTHEAST ALBERTA, CANADA

INTRODUCTION

The term facies was originally introduced by Gressly (1838) to describe rock units with specific biological characteristics that could be traced laterally across the Jura Mountains of Europe. Since its original inception, several different ideologies of what constitutes a facies have been proposed and the use of the term has long been a subject of debate (Reading, 1996 and references within; Miall, 1999 and references within). Different definitions of facies are used depending upon the scale of a particular study and the nature of data under consideration. A particular facies scheme may be based upon consideration of the biologicalal aspects of a rock unit (biofacies) or the physical and chemical characteristics that distinguish it from other rock units (lithofacies). In general, however, a facies should be useful in the interpretation of the rock record and have some degree of lateral correlation according to Walther's Law.

The integration of sedimentology and ichnology in this study of the Medicine Hat Member reveals nine facies in terms of sedimentary structures, lithology, and trace fossils (Table II-1). The prime focus was to characterize the interval at a local scale (i.e., within the Medicine Hat gas field) for interpreting a depositional setting by understanding the physical and biological processes that affected the distribution and nature of small-scale units. Consequently, the facies classification scheme hinges upon a lithofacies-style breakdown where sub-facies may be defined upon the nature of bioturbation. The scheme emphasizes small-scale features for the interpretation of individual depositional events by integrating observations of primary physical and biogenic sedimentary structures. The decision to subdivide the strata of the Medicine Hat Member in this manner is a direct result of the nature of the dataset, which consists of nineteen cored intervals from the Medicine Hat as field and their respective wire-line log suites (Figure II-1; Appendix A).

Description	Occurrence/Contacts	Sedimentological Characteristics	Ichnological Characteristics	Interpretation
Facies Class S: Sandstone (>70% sand) Sp Planar parallel stratified sandstone	• sharp lower contact, gradational upper contact • most commonly at the base of sand units, grades upwards into FSh, FSw, FSc or more rarely FZl • 1-10 mm thick	• planar parallel laminations, varying between 1-1.5 mm thick	• bioturbation is almost entirely absent • rarely burrowed into from overlying units or bioturbated base by Sk, Cy, Pl, Pa, Ps or Te • diminutive burrow sizes	• deposition above storm wave base • event bed such as a tempestite or hyperpycnal flow depending upon location • physicochemical environmental stress
Sh Hummocky cross-stratified sandstone	• sharp or gradational lower contact, gradational upper contact • overlies FSp and underlies FSw or FSc most commonly • increasing presence upwards • 0.5 - 3 cm thick	• low angle parallel laminations • wavelengths 30 - 60 cm		• deposition above storm wave base • oscillatory dominated, combined flow conditions
Sw Wave-ripple cross-laminated sandstone	• gradational lower contact, sharp upper contact • overlies FSp or FSh • underlies FZl, FZm, FMl and FMm • <0.5 – 10 mm thick	• wave ripple cross-laminations • ripple height <1 cm • wavelengths 5 – 10 cm	• low to locally moderately bioturbated • locally low diversity, including: Pl, Th, Pa, Sc • diminutive burrow sizes	• deposition above storm wave base • waning flow from tempestites, or oscillatory wave agitation • physicochemical environmental stress
Sc Combined-flow-ripple cross-laminated sandstone	• gradational lower contact, sharp upper contact • overlies FSp or FSh • underlies FZl, FZm, FMl and FMm • <0.5 – 10 mm thick	• combined flow ripple cross-laminations • rounded ripple crest/form • ripple height <1 cm • wavelengths 5 – 10 cm	• same as FSw	• deposition above storm wave base • waning flow from hyperpycnal flows • physicochemical environmental stress
Smb Structureless sandstone, burrowed	• generally bioturbated lower contact, sharp upper contact • often near top of coarsening upward cycles • 0.5 – 6 cm thick	• sedimentary structures apparently absent, maybe obscured by bioturbation? • bioturbate texture	• low to moderately bioturbated • locally low diversity, including; Pl, Th, Cy, Pa, Sc, As, Sk, Sch. freyi, Ps, Te • diminutive burrow sizes	• rapid sedimentation and/or cannibalization of other sandy facies • physicochemical environmental stress
Smn Structureless sandstone, unburrowed	• sharp lower and upper contacts • 0.5 – 6 cm thick	• sedimentary structures are apparently absent		• rapid sedimentation and/or ?cannibalization of other sandy facies • crevasse splay deposition

TABLE II-1

Facies Class Z: Siltstone (30-70% sand)				
Zlb Laminated siltstone, burrowed	• bioturbated, gradational or sharp lower contact; bioturbated or sharp upper contact • interstratified with any FS, FZ or FM • more common in distal settings, decreasing abundance upwards • 0.2 – 10 cm thick	• planar parallel laminations • thin, discontinuous sand stringers (starved ripples?) scattered shell fragments (concave up and concave down) • soft sedimentary deformation; micro flame structures, load casts, micro-faults, recumbent ichnofossils • bioturbate texture • white calcareous specks (coccoliths)	• moderately bioturbated • locally low diversity, including: Pl, Si, Pa, Th, Cy, Sc, As, Ph, Sk, Sch. freyi, Ps, Te, horizontal spreitenated traces (rare) • traces with vertical elements are often recumbent • diminutive burrow sizes	• fair weather deposition above • suspension settling • physicochemical environmental stress
Zln Laminated siltstone, unburrowed	• gradational or sharp lower contact, bioturbated or sharp upper contact • interstratified with any FS, FZ or FM • more common than FZlb in proximal settings, decreasing abundance upwards	• planar parallel laminations • thin, discontinuous sand vf sand stringers (starved ripples?) • scattered shell fragments (concave up and concave down) • soft sedimentary deformation; micro flame structures, load casts, micro-faults • white calcareous specks (coccoliths)		• fair weather deposition above • suspension settling • physicochemical environmental stress
Zmb Structureless siltstone, burrowed	• bioturbated or sharp lower contact; bioturbated, sharp or gradational upper contacts • interstratified with any FS, FZ or FM • decreases in abundance upwards • 0.2 – 5 cm thick	• apparently structureless • thin, discontinuous sand stringers and lenses • recumbent ichnofossils • bioturbate texture • scattered shell fragments (concave up and concave down) • white calcareous specks (coccoliths)	• moderately bioturbated • locally low diversity, including: Pl, Si, Pa, Th, Cy, Sc, As, Ph, Sk, Sch. freyi, Ps, Te, horizontal spreitenated traces (rare) • traces with vertical elements are often recumbent • diminutive burrow sizes	• fair weather deposition above • cannibalization of laminated facies by infaunal organisms? • physicochemical environmental stress
Zmn Structureless siltstone, unburrowed	• sharp lower contact; sharp, gradational or bioturbated upper contact • interstratified with any FS, FZ or FM • decreases in abundance upwards • 0.2 – 5 cm thick	• apparently structureless • thin, discontinuous sand stringers and lenses • scattered shell fragments (concave up and concave down) • white calcareous specks (coccoliths)		• fair weather deposition above • rapid sedimentation rate? • physicochemical environmental stress

TABLE II-1 (continued)

Facies Class M: Claystone (<30% sand)				
Mlb Laminated claystone, burrowed	• sharp to gradational lower and upper contacts • interstratified with any FS, FZ or FM • sharp lower contact; sharp, gradational or bioturbated upper contact • ranges from 0.5 – 5 cm thick • decreases in thickness and abundance upwards • significantly more common in the NE portion of the study area	• millimeter-scale planar-parallel lamination • rare bivalve shell fragments (concave-up and concave-down) • white calcareous specks (coccoliths)	• low levels of bioturbation • locally low diversity, including: Pl, Sk, Cy, Ph, Si • diminutive burrow sizes	• slow suspension settling of clay sized particles
Mln Laminated claystone, unburrowed	• sharp to gradational lower and upper contacts • interstratified with any FS, FZ or FM • sharp lower contact; sharp, gradational or bioturbated upper contact • ranges from 0.5 – 5 cm thick • decreases in thickness and abundance upwards • significantly more common in the NE portion of the study area	• millimeter-scale planar-parallel laminations • rare bivalve shell fragments (concave-up and concave-down) • white calcareous specks (coccoliths)		• slow suspension settling of clay sized particles
Mmb Structureless claystone, burrowed	• gradational or sharp lower contact; sharp upper contact • most commonly found sharply above sandy facies • may be interstratified with any FS or FZ • generally only occurs in distal settings, decreases in abundance upwards • 0.5 – 5 cm thick	• apparently structureless • bioturbate texture	• low intensity of bioturbation • low diversity, including: Pl, Si, Cy, Sk, Ph • diminutive burrow sizes	• rapid deposition from fresh water input (freshets) • enough transit time for organisms to burrow • physicochemical environmental stress
Mmn Structureless claystone, unburrowed	• gradational or sharp lower contact; sharp upper contact • most commonly found sharply above sandy facies • may be interstratified with any FS or FZ • generally only occurs in distal settings, decreases in abundance upwards • 0.5 – 5 cm thick	• apparently structureless		• rapid deposition from fresh water input (freshets) • physicochemical environmental stress

TABLE II-1 (continued): Summary of facies descriptions and classification scheme constructed in this study based on sedimentological and ichnological observations during core logging of Medicine Hat Member strata (Medicine Hat gas field, southeast Alberta). For further detail refer to main body of text. Abreviations and terminology are defined in list of abbreviations at beginning of thesis.

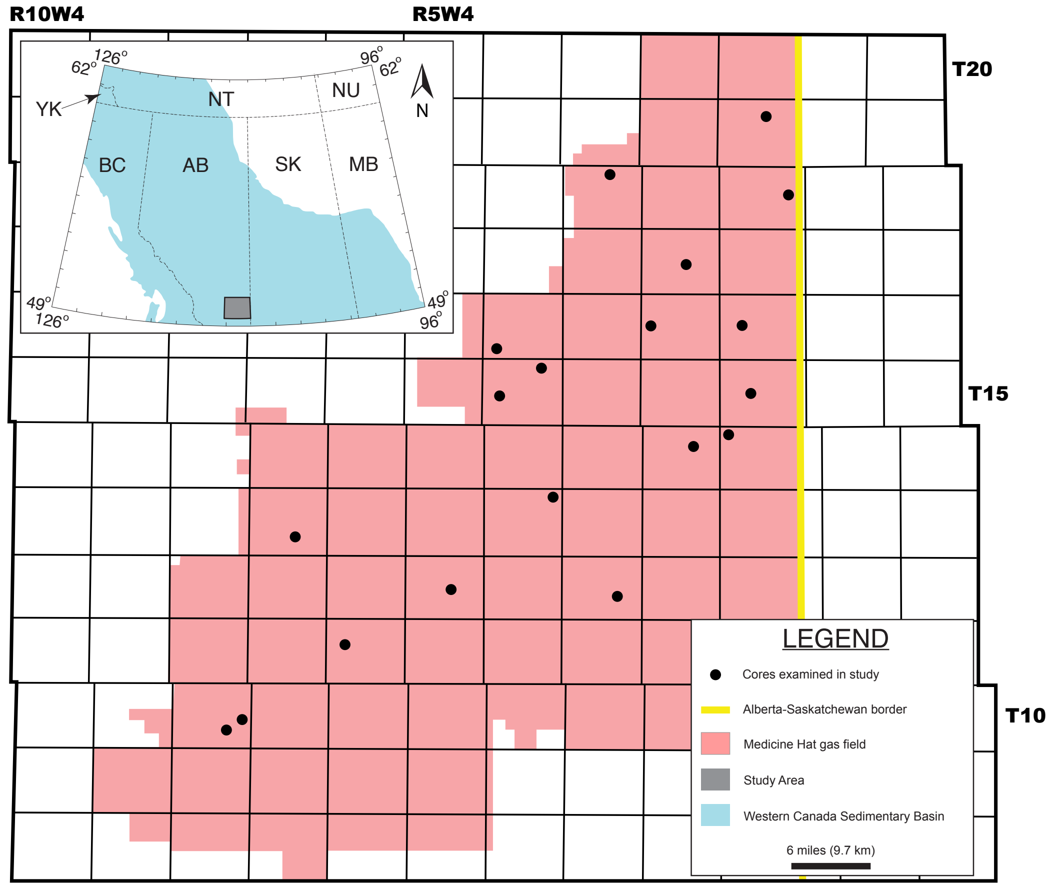

FIGURE II-1: The 19 cores examined in this study of the Medicine Hat gas field. The top left inset shows the study area in relation to the Western Canada Sedimentary Basin. The boundaries of the Medicine Hat field are from Accumap©, 2008. The field spans north-south from approximately Township 8 to 20, and east-west from Range 1 to 9, west of the 4th meridian. For core UWI's and detailed strip logs see Appendix A.

FACIES DESCRIPTIONS AND INTERPRETATIONS

Facies S_p: Planar Stratified Sandstone

Facies S_p consists of very-fine lower to fine-grained, moderately sorted sandstone. The sandstone has sharp contacts at its base and gradational contacts at the top, commonly grading upward into the facies S_h, S_w, S_c, or more rarely, Z_l. The thickness of the facies S_p ranges from 0.1 to 1 cm. Planar-stratification is the sole primary physical sedimentary structure that defines the facies. Individual planar laminae vary between 1 and 1.5 mm; there are subtle grain size variations within single laminae and no bedding plane features. Trace fossils are rare in facies S_p, present only as top-down burrows from overlying units, or less commonly as bioturbated bases. Bioturbation is primarily evident as indistinct mottling, however, some traces have morphologies similar to the ichnogenera *Skolithos, Cylindrichnus, Planolites, Palaeophycus, Psilonichnus* and *Teichichnus.*

Interpretation of Facies S_p

Plane bedding is primarily the result of deposition through vertical accretion of moving bed-loads, as the result of sudden changes in flow competence. Particularly, in the very fine to fine-grained S_p, planar lamination is interpreted to represent upper flow-regime conditions with fluid velocities between approximately 60-110 cm/s (Southard and Boguchwal, 1990). Based upon the stratigraphic position of facies S_p, upper flow-regime conditions can be inferred to be the result of two processes: wave energy, and unidirectional currents such as hyperpycnal flows.

The ichnology observed in the facies S_p suggest that trace-making organisms are strongly influenced by physico-chemical stresses (MacEachern et al., 2008). The trace fossils observed are predominantly diminutive and limited in ethological diversity, representing an impoverished signature of the *Cruziana* Ichnofacies. Faunal opportunism is inferred from the absence of burrows in the bulk of the facies, except for rare top-down burrows created after energy conditions decreased to a level that was conducive to colonization. Sedimentation rate and high-energy conditions were the most important physico-chemical stresses.

Facies S_h: Hummocky Cross-stratified Sandstone

Facies S_h comprises very fine to fine-grained, moderately sorted sandstone. The lower contact of the facies ranges from sharp to gradational, though the upper contact is consistently gradational. The facies commonly overlies the facies S_p and is found below facies S_w or S_c. There is an increase in the abundance of facies S_h towards the top of Facies Association 1. Generally, the sandstone is 0.5 to 3 cm thick. Primary sedimentary structures are limited to low-angle, parallel lamination with erosive bases. Laminae thicken laterally from 1 to 1.5 mm but remain parallel to the basal erosive surface so as to appear fan-like. These characteristics resemble hummocky cross-stratification. The amplitude of hummocks ranges between 2 and 3 cm, and wavelengths range from ca. 30 to 60 cm. Bioturbation is completely absent from the facies S_h.

Interpretation of Facies S_h

Hummocky cross-stratification (HCS) has long been recognized as a highly variable sedimentary structure found in shallow, storm-dominated marine settings in both the modern and rock record (Harms et al., 1976). Combined-flow conditions, dominated by oscillation, are proposed to be the primary depositional conditions that generate HCS (Duke et al., 1991; Ito et al., 2001). Recently, Yang et al. (2006) suggested that the wavelength of HCS is primarily proportional to bottom orbital diameter, and increases with decreasing water depth from the shelf to the surf zone, and then decreases landward (*see also* Ito et al., 2001).

Based upon the observations of other authors (e.g., Harms et al., 1975; Duke et al., 1991; Ito et al., 2001; Yang et al., 2006), the presence of HCS within the Medicine Hat Member infers combined-flow conditions, dominated by oscillation. By applying the simple formula presented in Yang et al. (2006), the bottom orbital diameters in the study area are calculated to range between 40 and 80 cm. Since bottom orbital diameters are non-unique, two contrasting interpretations of palaeo-water depths are possible: shallow-water above fair weather wave base, or relatively deeper water below fair weather wave base. However, the ichnology of silty and muddy deposits that are interstratified with the HCS indicate significant physico-chemical environmental stresses during the time of deposition (MacEachern et al., 2008). The possible stresses include episodic salinity fluctuation and high sedimentation rates. From these observations, the HCS in the study area are attributed to deposition in a proximal location with respect to the shoreline, above fair weather wave base.

Facies S_w: Wave-ripple Cross-laminated Sandstone

Facies S_w consists of very fine to fine-grained, moderately sorted sandstone demarcated with a gradational lower contact and sharp upper contact. Typically facies S_w overlies the facies S_p or S_h and is observed below facies Z_l, Z_m, M_l or M_m. The thickness of the facies is variable and ranges between 0.05 and 1 cm. Wave-ripples are the sole physical sedimentary structure observed in facies S_w, combining to form cross-stratification. The ripples have symmetric profiles with slightly pointed crests and range from 0.5 to 1 cm in amplitude. Bioturbation is localized in facies S_w, however the degree of burrow reworking is very low. Trace fossils are best ascribed to the ichnogenera *Planolites, Thalassinoides, Palaeophycus* and *Scolicia.*

Interpretation of Facies S_w

Ripples with symmetric profiles and pointed crests are widely recognized as bedforms produced by oscillatory currents. When the bedforms migrate in upper flow-regimes, cross-stratification is the resulting structure. In the Medicine Hat Member, wave-ripple cross-laminated sandstone (facies S_w) is closely associated with HCS, planar laminated sandstone and various siltstone facies. This leads to the interpretation that the facies represents deposition from fair weather waves or the waning-flow stages of storm events in a setting above fair weather wave base. More, the trace fossils observed within facies S_w indicate that physico-chemical environmental stresses were present during deposition (MacEachern et al., 2008). Simple deposit-feeding forms and a distinct lack of filter-feeding behaviors, consistent with a stressed expression of the *Cruziana* Ichnofacies, dominate the suite of ichnofossils. Therefore, the major stresses are interpreted to be high-energy conditions and shifting sandy substrates. Facies S_w was deposited above storm wave base.

Facies S_c: Combined-flow-ripple Cross-laminated Sandstone

Facies S_c is physically very similar to facies S_w: very fine to fine-grained, moderately sorted sandstone with a gradational lower contact and sharp upper contact. Facies S_c is observed to overlie the facies S_p or S_h and underlies facies Z_l, Z_m, M_l or M_m. The variation in thickness of facies S_c is the same as facies S_w, ranging from 0.5 to 10 mm. Combined-flow ripples are the only primary physical sedimentary structure observed and cross-stratification is the resulting stratification type. The combined-flow ripples have rounded form sets, amplitudes of up to 1 cm, and wavelengths of 3 to 5 cm. Bioturbation is present locally where ichnofossils are morphologically similar to *Planolites, Thalassinoides, Palaeophycus* and *Scolicia.*

Interpretation of Facies S_c

Combined-flow is defined as the combination of two or more flow types in both space and time (Dumas et al., 2005). Bedforms and stratification produced by combined-flow regimes include combined-flow ripples and their resulting cross-stratification. Combined-flow ripples are recognized within the Medicine Hat Member by asymmetric profiles and smooth, rounded crests. The occurrence of facies S_c (i.e., associated with HCS, wave-ripple cross-stratification and planar lamination) aids in the interpretation that the ripples are the result of the combined affects of oscillatory, wave-generated currents at an oblique angle of incidence to the shoreline. Deposition of the facies is inferred to have occurred above storm wave base.

Facies S_{mb}/S_{mn}: Homogeneous Sandstone (Burrowed and Unburrowed)

Facies S_m is composed of fine to medium-grained, poorly to moderately sorted sandstone. Two sub-facies constitute the facies S_m: bioturbated (facies S_{mb}) and non-bioturbated (facies S_{mn}). The lower contact ranges from sharp to bioturbated and the upper contact is sharp. The sandstone varies between 0.5 and 6 cm thick. Facies S_m is commonly observed at the top of coarsening-upwards cycles in Facies Association 1 or Facies Association 4. Physical sedimentary structures are not observed, likely obscured by bioturbation. However, biogenic structures are locally observed (in facies S_{mb}) and consist of a low diversity suite that may include trace fossils that closely resemble *Planolites, Thalassinoides, Cylindrichnus, Palaeophycus, Scolicia, Asterosoma, Skolithos, Schaubcylindrichnus freyi, Psilonichnus* and *Teichichnus.*

Interpretation of Facies S_{mb}/S_{mn}

Homogenous beds lack internal structure. The bedding style can be formed in several ways including rapid deposition of sediment by turbulent flow, and alternatively, by the obliteration of primary physical structures from faunal reworking. Within the Medicine Hat Member, facies S_m is interpreted to be the result of two distinctly different modes of deposition: rapid deposition from episodic high-energy events (facies S_{mn}) and biogenic reworking of previously deposited sandstone facies (facies S_{mb}). The interpretations are based on the relationship between each sub-facies and the surrounding facies. The presence of scattered traces within facies S_{mb} distinguishes it from the facies S_{mn}.

Facies Z_{lb}/Z_{ln}: Laminated Siltstone (Burrowed and Unburrowed)

Facies Z_l is a very common facies in the Medicine Hat Member and consists of dark grey siltstone with a lower contact that ranges from bioturbated, to gradational, to sharp, and an upper contact that is bioturbated or sharp. The facies can be divided into two sub-facies based upon bioturbation: facies Z_{lb} (burrowed) and facies Z_{ln} (unburrowed). Both sub-facies are observed interstratified with the facies S_p, S_h, S_w, S_c, S_m, Z_m, M_m and M_l. Typical thicknesses range between 0.2 and 10 cm. Overall, facies Z_l is characterized by planar lamination with thin, discontinuous, very-fine sandstone stringers (starved ripples?). Soft sedimentary structures such as micro-flames, load casts, micro-faults, and recumbent ichnofabrics are common. Scattered shell fragments (concave-up and concave-down) and white calcareous specks (coccoliths) are accessories that are locally observed.

Facies Z_{lb} has a bioturbate texture with low to moderate burrowing intensities. Trace fossil suites are locally low diversity, diminutive, and include forms closely related to the ichnogenera *Planolites, Siphonichnus, Palaeophycus, Thalassinoides, Cylindrichnus, Scolicia, Asterosoma, Phycosiphon, Skolithos, Schaubcylindrichnus freyi, Psilonichnus, Teichichnus* and rare horizontal spreitenated traces. Traces in the vertical plane are commonly recumbent.

Interpretation of Facies Z_{lb}/Z_{ln}

Fine-scale plane bedding (lamination) in fine-grained sediments is the result of slow, steady deposition of suspended sediment. The laminated nature of facies Z_l, lacking any significant faunal reworking, indicates that sedimentation rates were high, the transport time of the bed or bedsets into the historical layer was faster than biogenic colonization (Wheatcroft, 1990), or other physico-chemical stresses were present during the time of deposition. Based upon the stressed ichnologic signature observed within the facies, sedimentation rate and salinity were likely among the most important physico-chemical environmental stresses affecting the depositional system (MacEachern et al., 2008). Consequently, facies Z_l is interpreted to represent fair weather sedimentation in a setting with high concentrations of suspended sediment and reduced salinity. Deposition under these conditions ranged from above fair weather wave base to below storm wave base.

Facies Z_{mb}/Z_{mn}: Structureless Siltstone (Burrowed and Unburrowed)

Facies Z_m is strikingly similar to Z_l, differing only in the nature of physical sedimentary structures and thickness. Two sub-facies are recognized: burrowed (facies Z_{mb}) and unburrowed (facies Z_{mn}). A bioturbated or sharp lower contact is observed, while the upper contact may be sharp, gradational or bioturbated. Facies Z_m varies between 0.2 and 5 cm thick. In general, the unit decreases in abundance upwards and is interstratified with the facies S_p, S_h, S_w, S_c, S_m, Z_l, M_m and M_l. Physical sedimentary structures are not observed in facies Z_m (i.e., it is apparently structureless), however, thin, discontinuous very-fine sandstone stringers and lenses occur locally. Scattered shell fragments (concave-up and concave-down) and white calcareous specks (coccoliths) are common accessories.

A bioturbate texture of low to moderate burrowing intensity characterizes facies Z_{mb}. The ichnology of facies Z_m constitutes a low diversity suite of diminutive traces that closely resemble the ichnogenera *Planolites, Siphonichnus, Palaeophycus, Thalassinoides, Cylindrichnus, Scolicia, Asterosoma, Phycosiphon, Skolithos, Schaubcylindrichnus freyi, Psilonichnus, Teichichnus* and rare horizontal spreitenated traces. Traces that are normally vertically oriented, such as *Skolithos,* are generally recumbent.

Interpretation of Facies Z_m/Z_{mn}

Based on visual observation of hand specimens, the siltstone facies Z_m is homogeneous, apparently lacking internal structure. Commonly, structureless deposits are the result of rapid deposition from turbulent flow; facies Z_{mn} is interpreted to be the result of episodic event style deposition. Episodic event beds differ in nature depending upon their location with respect to the dip-profile. Therefore, they may be derived from gravity-driven currents in the northeastern (distal) part of the study area, or alternatively, from fresh water influx to the southwestern (proximal) portion of the Medicine Hat field. The sub-facies Z_{mb} resulted from biogenic reworking of these beds soon after deposition. In conclusion, facies Z_m is inferred to be the result of deposition above storm wave base.

Facies M_{lb}/M_{ln}: Laminated Claystone (Burrowed and Unburrowed)

Facies M_l is characteristically 0.5 to 5 cm thick with upper and lower contacts that range from sharp to gradational. The laminated claystone facies is found throughout the Medicine Hat Member, but is significantly more common in the northeastern parts of the study area. Generally, M_l decreases in thickness and abundance upwards and is found interstratified with all sandstone and siltstone facies. Primary physical sedimentary structures are limited to millimeter-scale planar lamination. Rare shell fragments (concave-up and concave-down) and white calcareous specks (coccoliths) are accessory. The facies can be subdivided into burrowed (facies M_{lb}) and unburrowed (facies M_{ln}) sub-facies. Trace fossils are observed in facies M_{lb}, but are limited in size and abundance. A very low diversity suite of trace fossils such as *Planolites*, *Skolithos*, *Cylindrichnus*, *Phycosiphon* and *Siphonichnus* characterizes the ichnology.

Interpretation of Facies M_{lb}/ M_{ln}

The interpretation of facies M_l varies throughout the study area. In southwestern locations, the facies is interpreted to be the deposits resulting from suspension settling of fine-grained fractions under the influence of physico-chemical stresses. These stresses include salinity, high suspended-sediment concentration, and periodic emplacement of storm-induced event-deposits. A gradation exists between the depositional conditions described above and those interpreted in the northeastern (distal) locations. In distal settings laminated claystone is inferred to be from suspension settling where high suspended-sediment loads, salinity and periodic emplacement of gravity-driven event-deposition are the main physico-chemical environmental stresses.

Facies M_{mb}/M_{mn}: Structureless Claystone (Burrowed and Unburrowed)

Facies M_m is subtly different than facies M_l, though many commonalities exist. Facies M_m varies between 0.5 and 5 cm thick with a sharp to gradational lower contact, and sharp upper contact. The facies is commonly observed to sit abruptly above sandy facies (e.g., facies S_p, S_h, S_w, S_c, S_m), however it is also interstratified with facies Z_l, Z_m and M_l. Facies M_m lacks primary physical sedimentary structures and appears homogeneous. Two sub-facies are defined: burrowed (facies M_{mb}) and unburrowed (facies M_{mn}). The burrowed sub-facies has a bioturbate texture that consists of a low diversity suite of diminutive trace fossils that include forms such as *Planolites, Skolithos, Cylindrichnus, Phycosiphon* and *Siphonichnus.* Overall, bioturbation is poorly developed with low burrowing intensities.

Interpretation of Facies M_{mb}/M_{mn}

Massive claystone in the Medicine Hat Member (M_m) is inferred to be the result of a single process: periodic rapid deposition from density-currents with high suspended-sediment concentrations. The observations are based on the presence of an abrupt, sharp basal contact that appears discordant with the surrounding strata. Moreover, facies M_m is often thicker than the surrounding deposits, supporting the interpretation that the currents depositing the sediment contained abundant suspended-loads. Trace fossils are rare, locally observed in the massive claystone and indicate opportunistic colonization, presumably after initial deposition (Pemberton et al., 1992).

FACIES ASSOCIATIONS

Individual facies have limited interpretive value when taken in isolation, due to the non-unique processes that form physical and biogenic sedimentary structures. Observation of the context in which facies occur, with reference to neighboring units, allows more meaningful environmental inferences to be made by eliminating alternative interpretations. Thus, by grouping facies into genetically related packages, those that recur together without being separated by a hiatus in deposition, an assessment of the parameters that controlled sedimentation can lead to inferences about likely environments of deposition. Therefore, facies associations are essential in developing a palaeoenvironmental reconstruction.

The facies associations in the Medicine Hat Member were derived from observations of the recurrence of specific facies (e.g., Table II-1), noting changes in thickness, abundance, ichnology, and relationships to surrounding strata. Differences in these parameters are often subtle and the boundaries between facies associations are chosen somewhat arbitrarily. However, the division of facies associations is based upon specific physical and biological criteria that indicate important changes in the environment in which the sediments were deposited. From this outlook, four distinct associations are described, corresponding to a proximal subaqeous foreset, distal subaqeous foreset, proximal bottomset, and subaqeuous bay settings. The descriptions follow a proximal to distal trend that conveniently corresponds to the relative abundance of each setting in the study area.

A shorthand system was used to hasten the description of the ichnologic elements that were observed in the facies associations. Specifically, the abundance of particular ichnogenera in the suite of trace fossils were described as being very rare (vr), rare (r), moderately common (m), and common (c).

Facies Association 1 (FA1): Proximal Foreset Association

Sedimentology of FA1

Facies Association 1 (Figure II-2) overlies FA2, FA3, or more rarely FA4, and comprises sets of recurring sandy facies (e.g. facies S_p, S_h, S_w, S_c and S_m) interstratified with siltstone and claystone facies (e.g. facies Z_l, Z_m and M_m). Sandstone beds and bedsets vary between 2 and 10 cm thick, are most commonly 3 to 8 cm thick, and are typically very fine to fine-grained. The succession is sharp-based but may be subtly erosional. The lowermost sandy facies is planar laminated, with individual laminae that are less than a millimeter thick. Low angle (<15°) planar to wavy lamination, interpreted to represent hummocky-cross stratification (HCS) pass into wave, and more rarely, combined-flow rippled sandstones that commonly caps the succession.

The siltstone facies occur as normally graded tops of sandstone successions and also as discrete sharp-based strata. Siltstone ranges from 1 to 3 cm thick. The facies may be parallel laminated or structureless, with or without burrowing. Comminuted plant debris and interstitial clay are common.

The claystone within FA1 occurs as 1 to 3 cm thick strata. The facies is often fissile and sharply overlies both siltstone and sandstone facies. The claystone is structureless and bioturbation is common, but is sporadically distributed.

Facies Association 1 shows a progressive upwards increase in the frequency and thickness of sandstone facies (Figure II-3). This corresponds to a concomitant decrease in siltstone and claystone. Characteristically, the association is 8 to 10 m thick and contains any number of partial to complete successions stacked upon one another. Amalgamated sands are rare and found only in the top 2 to 3 m.

Ichnology of FA1

Burrowing is sporadic in FA1. Traces have a particularly patchy distribution and are largely confined to the siltstone and claystone facies. Characteristically, the trace fossil assemblage is of low to moderate diversity with low burrowing intensities (BI 0 to BI 2; Taylor and Goldring, 1993).

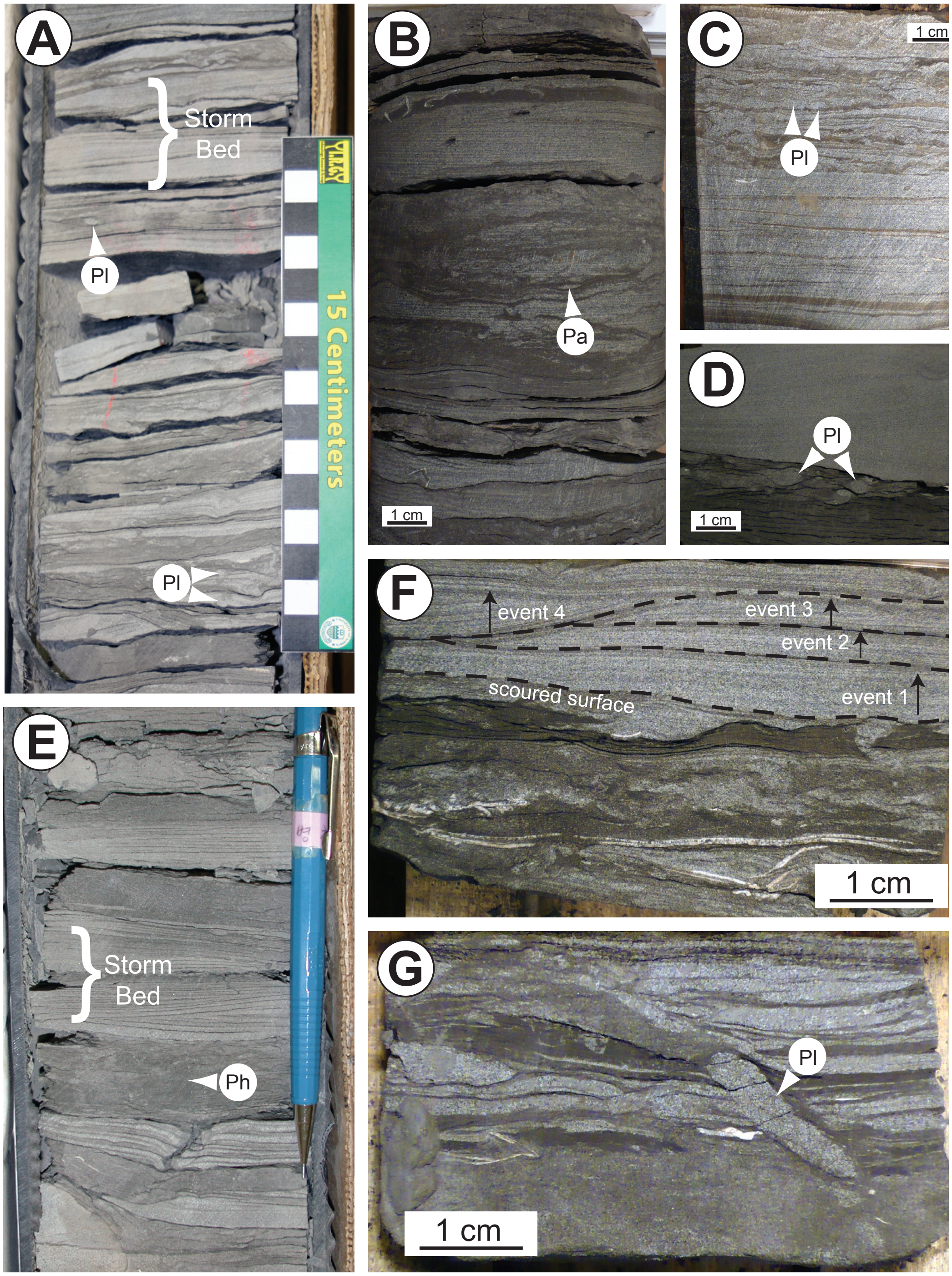

FIGURE II-2: FA1-Proximal Foreset Deposits of the Medicine Hat Member.
(A) Planar to wavy laminated fine sandstone with intervening dark sandy siltstone in the top few meters of FA1. The sandstones are interpreted as tempestites, while the sandy siltstones represent fair-weather deposition. Trace fossils are sporadically distributed and consist mainly of *Planolites* (Pl). Well 6-10-10-8W4, depth 321.5 m. (B) Planar laminated fine sandstone with intervening dark sandy siltstone showing sporadic bioturbate texture. A single *Palaeophycus* (Pa) trace can be recognized within the burrow mottling. Well 11-15-12-5W4, depth 337.7 m. (C) Planar-laminated fine sandstone with very thin intervening sandy siltstone at the top of FA1. These tempestites are nearly amalgamated but lack the full succession of storm-generated physical sedimentary structures. More, biogenic reworking by *Planolites* (Pl) burrows is contrasted

FIGURE II-2 continued: against non-bioturbated strata. Well 11-15-12-5W4, depth 332.5 m. (D) Low-angle parallel to subparallel laminated fine sandstone sharply overlying siltstone with bioturbated top. Note that overlying laminae in the sandstone are at an angle to the truncation surface. Also, the laminae decrease in inclination upwards, consistent with HCS. Burrows in the siltstone consist only of *Planolites* (Pl). Well 2/7-13-10-8W4, depth 318.5 m. (E) Low-angle planar-parallel to subparallel laminated fine sandstone and intervening siltstone. The structure in the sandstone is interpreted to represent HCS, and thought to be the result of storm deposition. Siltstone contains sporadically distributed *Phycosiphon* (Ph). Well 6-10-10-8W4, depth 323.75 m. (F) Low-angle planar-parallel to subparallel laminated fine sandstone atop mottled silty claystone. A few indistinct traces burrow the top of the silty claystone, which represents intervening fair-weather deposits between storm events. Four distinct events can be discerned above a scoured contact, as storm beds amalgamated. Well 2/7-13-10-8W4, depth 319.1 m. (G) An inclined *Planolites* (Pl) burrowing down through a mottled remnant of storm deposition into the intervening fair-weather siltstone and mudstone. Well 11-11-12-3W4, depth 444.5 m.

Traces are often deformed and rarely attributable to specific ichnogenera, so the majority of the ichnology is indistinct burrow mottling. Ichnogenera that are recognized include *Planolites* (c), *Thalassinoides* (vr-r), *Palaeophycus* (m-c), *Schaubcylindrichnus freyi* (r-m), cryptic *Phycosiphon* (r), *Skolithos* (r-m), *Cylindrichnus* (r), *Psilonichnus* (r), and fugichnia (r). The majority of trace Traces are often deformed and rarely attributable to specific ichnogenera, so the majority of the ichnology is indistinct burrow mottling. Ichnogenera that are recognized include Planolites (c), Thalassinoides (vr-r), Palaeophycus (m-c), Schaubcylindrichnus freyi (r-m), cryptic Phycosiphon (r), Skolithos (r-m), Cylindrichnus (r), Psilonichnus (r), and fugichnia (r). The majority of trace fossils are diminutive in size. are diminutive in size.

Ichnofossils are largely confined to the siltstones and claystones at the top of sandy units. Horizontally oriented passive-carnivore and deposit-feeding structures dominate the trace fossil assemblage of FA1. Traces with vertical orientations such as *Skolithos, Cylindrichnus,* and *Psilonichnus* are notably less common. Identification of specific ichnofossils is hindered by the fine grain-size and cryptic appearance of the sediments.

Interpretation of FA1

Overall, Facies Association 1 has an upwards-coarsening profile (Figure II-3). The increase in the thickness and frequency of sandstone strata is coupled with a synchronous decrease in siltstone and claystone. At the base of FA1,

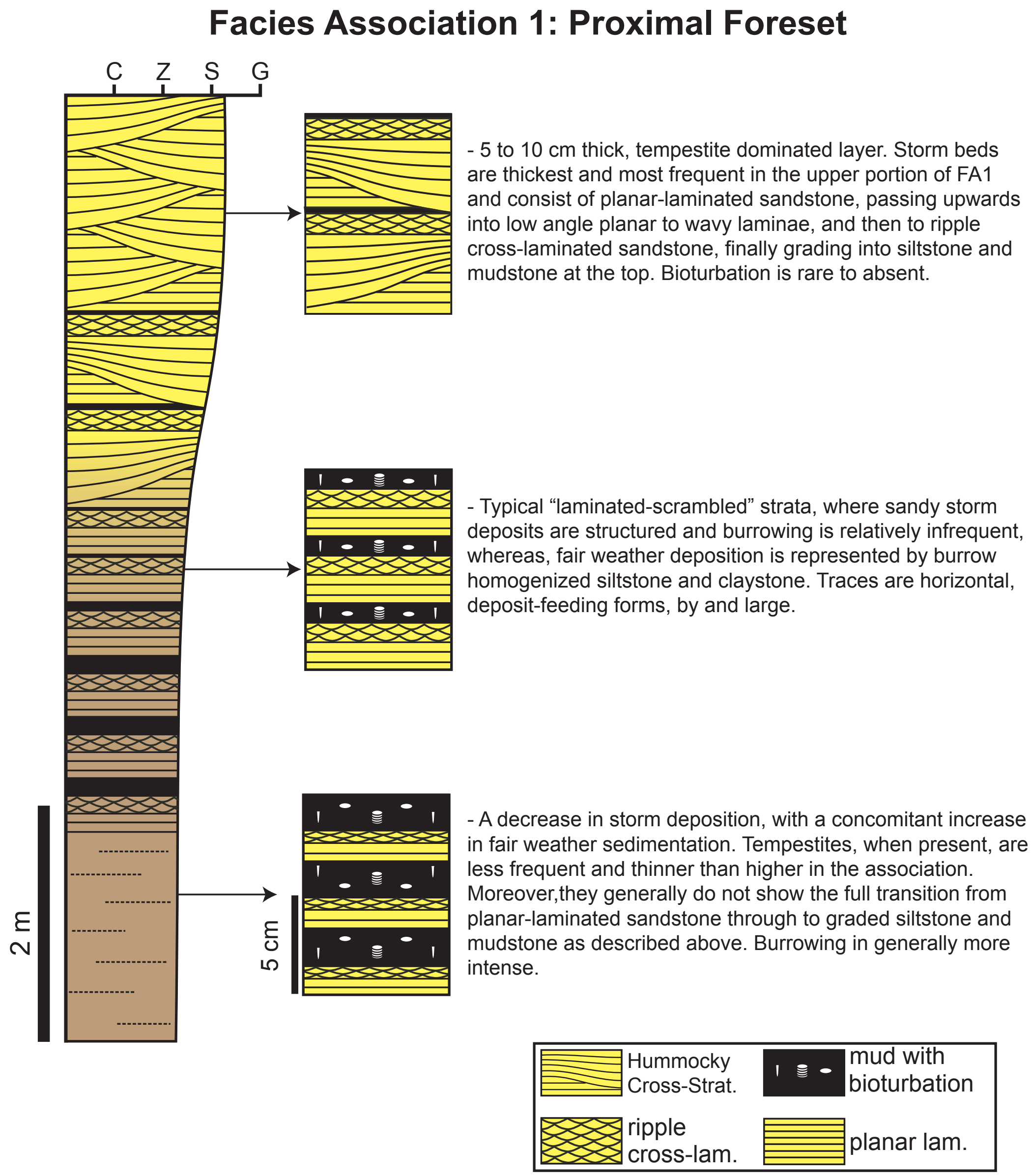

Figure II-3: A schematic illustration of an idealized section of FA1. The association shows a progressive increase in the thickness and frequency of sandstone facies towards the top, with a concomitant decrease in siltstone and claystone. When fully preserved, sandstone successions contain planar laminae passing upwards into hummocky cross-stratification, followed by current (or combined flow) ripples, grading into siltstone and claystone. Any number of partial to complete successions may be preserved, however, sandstones are best preserved and often amalgamated at the top of the association. Burrowing is a very sporadic element of FA1.

sandstone comprises less than ca. 50% of the sediment by volume, increasing to greater than approximately 80% near the top. In rare instances, sandstones may be amalgamated at the top of the association.

Thin, millimeter to centimeter-scale packages of interstratified siltstone and claystone prevail throughout FA1, decreasing in abundance upwards. These packages contain soft sedimentary features such as micro-flame structures and convolute bedding. Soft sedimentary deformation can be attributed to relatively high sedimentation rates loading poorly consolidated fine-grained sediments. It is important to note that the siltstones and claystones do not show any indications of oscillatory currents, and therefore, were likely deposited during times of fair weather, not influenced by waves. It is suspected that wave energy was baffled by water turbidity down dip of FA1 and that these sediments were deposited from suspension. Alternatively, hyperpycnal flows may have played a role in the development of the rhythmically stratified facies, a process that is increasingly recognized in the modern and rock record (Felix et al., 2006; Bhattacharya and MacEachern, 2009).

The siltstone and claystone facies in FA1 contain the bulk of biogenic sedimentary structures. The ichnology of these beds and bedsets is typical of ecologically stressed environments, periodically affected by episodic depositional events (Pemberton et al., 1992; MacEachern, 1994). Low diversity, diminutive trace suites are evidence for physico-chemical environmental stresses in the system (MacEachern et al., 2008). The presence of *Planolites, Phycosiphon, Palaeophycus,* and *Schaubcylindrichnus freyi* represent the establishment of passive carnivore and deposit-feeding behaviors following event deposition. More rarely, *Skolithos* can be observed within these units, and may be interpreted as a head-down deposit-feeding ethology (Gingras et al., 1999).

The stressed ichnologic suite, with rare suspension-feeding traces, suggests suspension fallout of fine-grained sediment between events or, overall high sedimentation rates. Suspended sediment may preclude colonization by filter feeding fauna in two ways: by clogging filter-feeding apparatuses, and by decreasing the concentration of organic detritus so that organisms must filter significantly more volume of sediment (Moslow and Pemberton, 1988; Buatois and Angriman, 1992; MacEachern et al., 2008). The patchy distribution of burrowing suggests that higher energy events were relatively frequent, thus minimal time was available for faunal colonization and biogenic reworking of the sediment.

Several physical sedimentary structures within the sandstone facies indicate reworking by wave energy. These include low angle planar to wavy laminae (interpreted as HCS), wave-ripples, and combined-flow ripples. The sedimentary structures are arranged in a recurring order: i.e., planar parallel lamination grading into HCS, followed by wave or combined-flow ripples grading into siltstones and claystones. These recurring bedsets record high-energy oscillatory conditions grading into waning flow conditions and a return back to fair weather suspension settling of fine-grained sediments. The succession is interpreted to represent tempestites in a setting above fair weather wave base (Pemberton and Frey, 1984; Aigner, 1985; Pemberton et al., 1992). The nature of the sandstones indicates that the storms/waves were the primary agent of reworking during the deposition of FA1 (Davis and Hayes, 1984; Reading, 1996). Ichnological evidence is indicative of sediment reworking by tempestites. Sandstones have very low degrees of bioturbation, or bioturbation is absent. Moreover, the presence of fugichnia, although uncommon, signifies that sedimentation rates were high, forcing fauna to continually re-equilibrate to the sediment-water interface. Burrowing into the sandstone units from the overlying, fine-grained fair weather deposits signals a return to ambient conditions (Pemberton et al., 1992).

Physical and biogenic sedimentary structures are consistent with a setting characterized by episodic, rapid deposition and wave reworking, coupled with quiescent conditions dominated by suspension settling or rapid deposition of fines. Biogenic structures and the overall nature of burrowing are indicative of a setting with significant physico-chemical environmental stresses (MacEachern et al., 2008). The stresses are interpreted to be rapid deposition rates, salinity reductions, episodic emplacement of event beds and high degrees of suspended sediments. The overall coarsening upwards nature of the association is indication of progradation. Facies Association 1 is stratigraphically the highest association and has been interpreted to be the most proximal association. Therefore, FA1 is interpreted to represent deposition in a proximal part of a subaqeous clinoform, in a predominantly fine-grained setting.

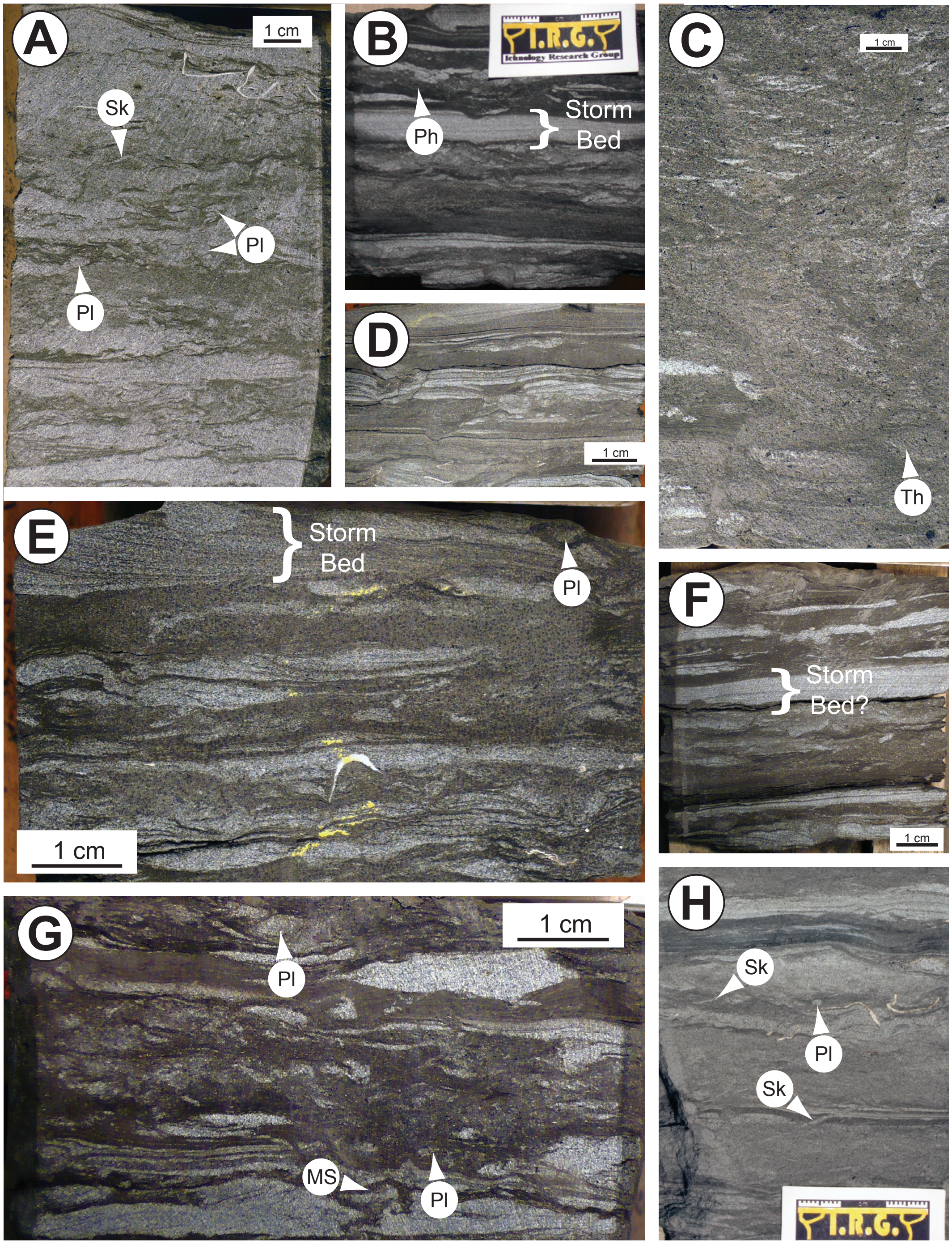

Figure II-4: FA2-Distal Foreset Deposits of the Medicine Hat Member.
(A) Burrowed interstratified fine sandstone and siltstone near the top of FA2. The planar-parallel laminated sandstones are only poorly preserved, representing burrow-reworked portions of tempestites. An example of a depauperate, inclined *Skolithos* (Sk) demonstrating downslope sediment creep is shown in the top portion of the photo. A cross-sectional view through a small *Planolites* (Pl) burrow into siltstone is shown in the bottom half. Well 14-36-13-4W4, depth 401.3 m. (B) Thinly interstratified claystone and low-angle planar-laminated fine sandstone observed in the middle of FA2. The planar-parallel laminated sandstone represents the preserved portion of tempestites. Indistict burrow mottling and cryptic *Phycosiphon* (Ph) indicate faunal colonization during intervening fair-weather conditions between storm events. Well 7-19-16-2W4, depth 547m.

FIGURE II-4 continued: (C) Highly homogenized silty sandstone with only rarely preserved evidence of tempestites near the base of the photo. Well 14-36-13-4W4, depth 400.6 m. (D) Siltstone with thin interstratified fine sandstone laminae. Sandstone laminae near the top of the photo show slight waviness. Indistinct burrow mottling characterizes the center of the photo. Well 2/6-26-14-2W4, depth 516.8 m. (E) Indistinctly burrow mottled fine sandstone and siltstone. Low-angle planar-parallel to subparallel laminated sandstone at the top is interpreted as the stoss side of a current ripple. Burrowing has homogenized the rest of the photo with only rare preserved sand laminae. Well 2/6-26-14-2W4, depth 512.9 m. (F) Thinly interstratified fine sandstone and silty claystone. A few planar-parallel sand laminae represent the preservation of tempestites in a distal position of the subaqeous foreset. Indistict burrow mottling demonstrates faunal colonization during intervening fair-weather deposition between storm events. Well 7-19-16-2W4, depth 547.25 m. (G) An interval of relatively intense bioturbation within previously interstratified fine sandstone and siltstone. The majority of burrowing is indistinct, however an excellent cross-sectional view of a depauperate *Planolites* (Pl) burrow is observed at the top of the photo. Moreover, a good example of a "mantle and swirl" burrow indicating soupy substrates is present (MS). A thin massive appearing claystone lamina, interpreted as a freshet, occurs in the top of the photo, below the *Planolites* (Pl) burrow. Well 7-35-15-4W4, depth 485.4 m. (H) Interstratified burrowed fine sandstone and silty claystone. The fine sandstone has been homogenized by traces such as *Planolites* (Pl) and *Skolithos* (Sk). In addition, the recumbent *Skolithos* indicate downslope sediment shearing or creep. Near the top of the photo is a partially reworked claystone lamina, interpreted as a freshet. Well 7-19-16-2W4, depth 544.75 m.

Facies Association 2 (FA2): Mid to Distal Foreset Association

Sedimentology of FA2

The upward transition from FA3 to FA2 is often gradational but, in rare instances, can be sharp. The facies association is split into 3 facies based upon grain-size, with a variety of sub-facies depending upon the nature of sedimentary structures and bioturbation (Figure II-4). The facies range from very-fine sandstone (e.g., facies S_p, S_w, S_c and S_m) through siltstone (e.g., facies Z_l and Z_m) and claystone (facies M_m). Overall, FA2 is less sandy than FA1, but shares many similarities. These include an overall coarsening-upwards profile, a suite of traces representing stressed environmental conditions, and similar facies, although there are important differences in the thickness and distribution of the facies. Facies Association 2 ranges between 8 and 10 m thick, but may be as thick as 15 m.

The sandstone facies commonly consist of horizontal planar laminated very-fine sand grading upwards into wave-ripple cross-laminated coarse silt or very-fine sand. In FA2, there is a distinct absence of low angle (<15°) planar to wavy lamination, that were interpreted in FA1 to be hummocky cross-stratification. Typically, the horizontal planar laminated sandstone is 1 to 1.5 cm

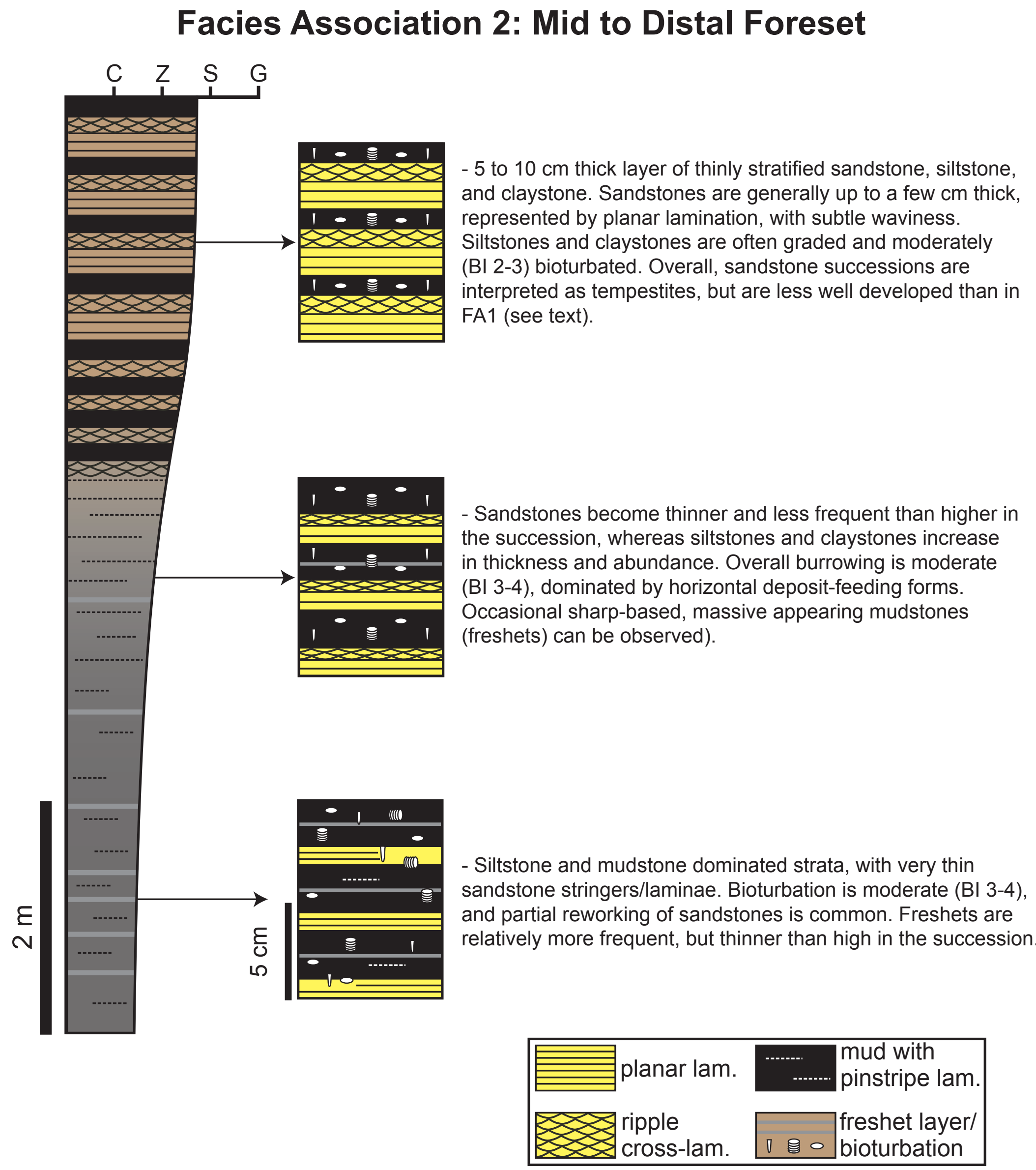

Figure II-5: A schematic illustration of an idealized section of FA2. Similar to FA1, FA2 is typified by a coarsening-upwards profile where sandstone facies progressively increase in thickness and frequency. Siltstone and claystone concurrently decrease with increasing sandstone content. Tempestites occur in FA2, but are not as well developed, as HCS is generally not observed to be part of a typical storm deposited succession. Generally, ichnofossils are sporadically distributed, but to a lesser degree than in FA1. Overall however, traces are the most common in FA2, compared to FA1 or FA3.

thick, whereas the wave-ripple cross-laminated siltstone/sandstone is 0.75 to 1 cm thick. In all cases, an individual sandstone succession is less than 3 cm thick.

Siltstone facies in FA2 are found as normally graded tops to the ripple cross-laminated sandstone, or more rarely, as sharp-based strata. These can range from 1 to 4 cm in thickness, but are commonly between 2 and 3 cm thick. In FA2, siltstone may be planar laminated or massive and is commonly bioturbated. Soft sedimentary deformation features such as micro-flame structures, micro-faults and convolute stratification are common.

Claystone comprises the tops to the fining-upwards successions that recur throughout FA2, or more rarely, isolated sharp-based strata. The claystone is massive and may overlie siltstone or sandstone. Bioturbation is most common in the claystone portion of FA2. Soft sedimentary deformation and recumbent ichnofabrics are also common in the claystone.

Overall, FA2 is typified by a coarsening-upwards profile, in which sandstone facies increase in thickness and frequency with a concurrent decrease in siltstone and claystone (Figure II-5). However, the facies association is ultimately composed of numerous stacked fining-upwards successions that become sandier upwards. These fining-upwards units are between 3 and 7 cm, but most commonly are between 4 and 5 cm thick. Planar laminated sandstone is absent at the base of the succession, but becomes common 2 to 3 m above the lower contact, and the dominant facies near the top of FA2.

Ichnology of FA2

Biogenic structures are moderately common in the siltstone and claystone facies and less common in the sandstones of FA2. The ichnology can be described as low to moderately diverse, with low burrowing intensity (BI 0 to BI 2; Taylor and Goldring, 1993). The traces observed include: *Planolites* (c), *Phycosiphon* (vr), *Thalassinoides* (vr), *Teichichnus* (r), *Schaubcylindrichnus freyi* (vr-r), *Palaeophycus* (r-m), *Skolithos* (r-m), *Cylindrichnus* (vr), *Siphonichnus* (vr), rare horizontal spreitenated traces (*Rhizocorallium* or *Scolicia),* and fugichnia (vr). However, generally the ichnology is manifested as indistinct burrow mottling, presumably dominated by deposit-feeding forms.

There is a sporadic nature to the burrowing observed in FA2, though the burrows are more evenly distributed than in FA1 or FA3. Traces are most common in the fine-grained fractions, but there is considerable biogenic reworking of the sandstone facies, likely because the transit time of these strata into the "historical layer” was conducive to faunal colonization (Wheatcroft, 1990). The suite of ichnofossils is dominated by diminutive sub-horizontal to horizontal forms. Nevertheless, bent or recumbent *Skolithos* are relatively common and are thought to be the result of simple shear or inclined depositional surfaces (Gingras and Bann, 2006).

Interpretation of FA2

Facies Association 2 can generally be described as rhythmically stratified siltstone and claystone facies, passing upwards into sharp-based, wave reworked, sand-dominated facies. An overall increase in wave- and current-generated structures towards the top of FA2 is observed, but their thickness and nature differ from FA1. Wave-generated bedsets in FA2 are manifested as thinner, planar lamination passing upwards into wave (or combined-flow) ripple cross-lamination. The perceived lack of HCS, typical in wave- and storm-generated deposits, is explained by deeper water depths (relative to FA1), where particle oscillations have a larger orbital diameter. The result is long-wavelength HCS that are not readily recognized in core. Thus, if present, they may have been interpreted as horizontal planar lamination.

Deformation features such as micro-faults and small loading structures are frequent in the fine-grained fractions of FA2. The development of such features can be attributed to four main causes: 1) high sedimentation rates, 2) under-consolidation of fine-grained sediments resulting in excess pore-fluid pressure, 3) rapid decomposition of organic detritus forming methane, adding to the pore fluid pressure, and 4) wave-agitation/shocking of sediments by large waves/storms (Coleman, 1988; Reading, 1996; Hildebrandt and Egenhoff, 2007; Matsumoto et al., 2008).

Many trace fossils of FA2 show substantial penecontemporaneous deformation consistent with incremental down-slope sediment creep (Gingras and Bann, 2006). Although the depositional environment was dominated by very shallow depositional gradients (ca. 0.15°), it appears that the gradients were steep enough to promote down slope creep/deformation. The deformation is primarily observed in ichnogenera such as *Skolithos*.

On the whole, the ichnology of FA2 is indicative of prevailing physico-chemical environmental stresses within the system (MacEachern et al., 2008). Filter-feeding trace fossils are subtly more common than in FA1, found burrowed into the sandy facies from above. The dominance of small, horizontal deposit-feeding traces and traces of passive carnivores indicate that there was significant suspended sediment in the water column. Certainly, salinity, thixotropic substrates (fluid muds), and deposition rates were among the stresses affecting faunal habitats (Bhattacharya and MacEachern, 2009). Moreover, burrowing is more pervasive throughout FA2, a result of lower energy conditions and adequate time for faunal colonization of substrates.

Facies Association 2 can be interpreted to be the deposits of the distal foreset region on a subaqeous clinoform. An overall coarsening-upwards profile in combination with wave-generated physical sedimentary structures, and stressed ichnologic indicators aid in the interpretation. The lack of HCS in tempestite deposits, common soft sedimentary deformation features, and a decrease in the sporadic nature of bioturbation all indicate that FA2 is more distal than FA1.

Facies Association 3 (FA3): Proximal Bottomset Association

Sedimentology of FA3

Facies Association 3 is made of a complex arrangement of sandstone (e.g., facies S_p), siltstone (e.g., facies Z_l and Z_m) and claystone (e.g., facies M_m) facies, with numerous sub-facies based upon sedimentary structures and ichnology (Figure II-6). Facies Association 3 sharply to gradationally passes into FA2. In the study area, the general thickness of FA3 is poorly constrained because cores do not completely penetrate the association. Estimated thicknesses from the wire-line cross-sections in Chapter III range from 10 m to upwards of 50 m, where several strata are interpreted to be stacked.

Facies Association 3 comprises thinly stratified sandstones, siltstones, and claystones with an overall coarsening-upwards profile (Figure II-7). Sandstones are seldom thicker than 1 cm, and most often are less than 5 mm. Sandy facies are very-fine at the coarsest. Sharp-based planar lamination, rarely with subtle waviness, is the most common physical sedimentary structure observed. Soft

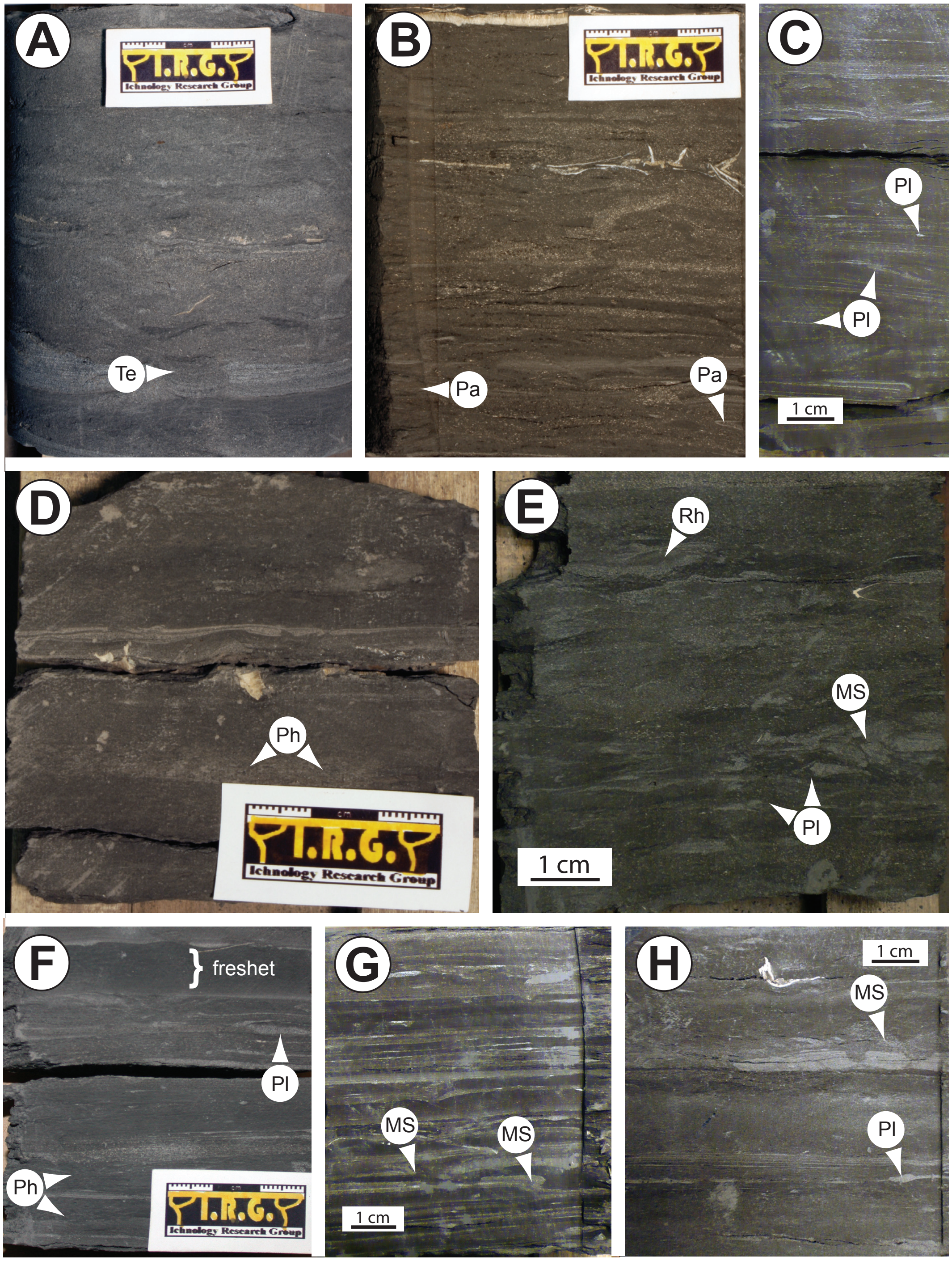

Figure II-6: FA3-Proximal Bottomset Deposits of the Medicine Hat Member.
(A) Sandy siltstone with a few fine-grained pin-stripe sand laminae. The siltstone has been sporadically bioturbated by indistinct forms, disrupting the laminae. Near the bottom is a fine-grained low-angle planar-parallel laminated stratum up to 1 centimeter thick that is burrowed by *Teichichnus* (Te). Well 10-26-19-1W4, depth 511.3 m. (B) Silty claystone with rare pin-strip fine sand laminae. The example shows the very sporadic nature of burrowing, dominated by single ichnogenera (in this case *Palaeophycus* (Pa)). Well 10-26-19-1W4, depth 513.6 m. (C) Claystone with thinly interlaminated ("pin-stripe" laminated) fine-sandstone. Well 16-16-15-1W4, depth 521.6 m. (D) Claystone containing a few fine-grained sandstone pin-stripe laminae. The example is barren of burrowing, except for a thin horizon cryptically bioturbated by *Phycosiphon* (Ph).

Figure II-6 continued: Well 10-26-19-1W4, depth 512.9 m. (E) Burrow mottled silty claystone showing the sporadic nature of bioturbation within FA3. Traces are limited to two ichnogenera: *Rhyzocorallium* (Rh) and *Planolites* (Pl), as well as “mantle and swirl” burrowing (MS) in soupy substrate. Well 10-26-19-1W4, depth 512.5 m. (F) Silty claystone with rare fine sandstone pin-stripe laminae. Burrowing is sporadically distributed with only rare horizons of cryptic *Phycosiphon* (Ph), or scattered *Planolites* (Pl). The massive appearing mudstone laminae near the top of the photo is interpreted as a freshet carried basinward by fresh water influx following the culmination of a storm. Well 7-19-16-2W4, depth 549.2 m. (G) Finely interlaminated fine sandstone and silty claystone. A few subtle examples of soft sedimentary deformation can be observed, particularly in the middle and right side of the photo in the bottom half. Moreover, “mantle and swirl” burrows (MS) can be observed. This is most representative of the uppermost portion of FA3. Well 16-15-17-2W4, depth 542.2 m. (H) Clayey siltstone with interstratified fine sandstone. The sandstone is manifested as pin-strip laminae with subtle waviness near the base of the photo, and as relatively thicker wavy laminae near the top. Trace fossils are almost completely absent, with exception of a few indistinct forms burrowing down into the upper sand laminae and “mantle and swirl” traces (MS). Well 7-24-18-1W4, depth 500.1 m.

sediment deformation is also common, evident as convolute stratification, micro-flame structures and micro-faults.

The bulk of FA3 is composed of siltstone and claystone. Silt- and clay-sized fractions appear similar in hand sample. Silt grades into clay and the same physical characteristics are observed. Sand content was used as the primary discriminator, based on visual estimations (silt is 30-70% sand content, clay is <30% sand content). The fine-grained sediments (siltstone and claystone) are present as finely interlaminated strata, found gradationally atop sandstone facies. Thicknesses of the siltstone/claystones can vary between 0.5 and 5 cm. Sharp-based, massive claystones, 1 to 4 cm thick, are intermittently distributed. Physical sedimentary structures include planar laminae and soft sedimentary deformation structures including flame structures, micro-faults, recumbent ichnofabrics and convolute stratification.

As in FA1 and FA2, an overall coarsening-upwards profile characterizes FA3 (Figure II-7). A general increase in sand thickness and frequency occurs concomitantly with a decrease in thickness and abundance of siltstone and claystone facies. Concave-up and concave-down shell fragments and calcareous white specks (coccoliths) are common in FA3. The shell fragments are disarticulated.

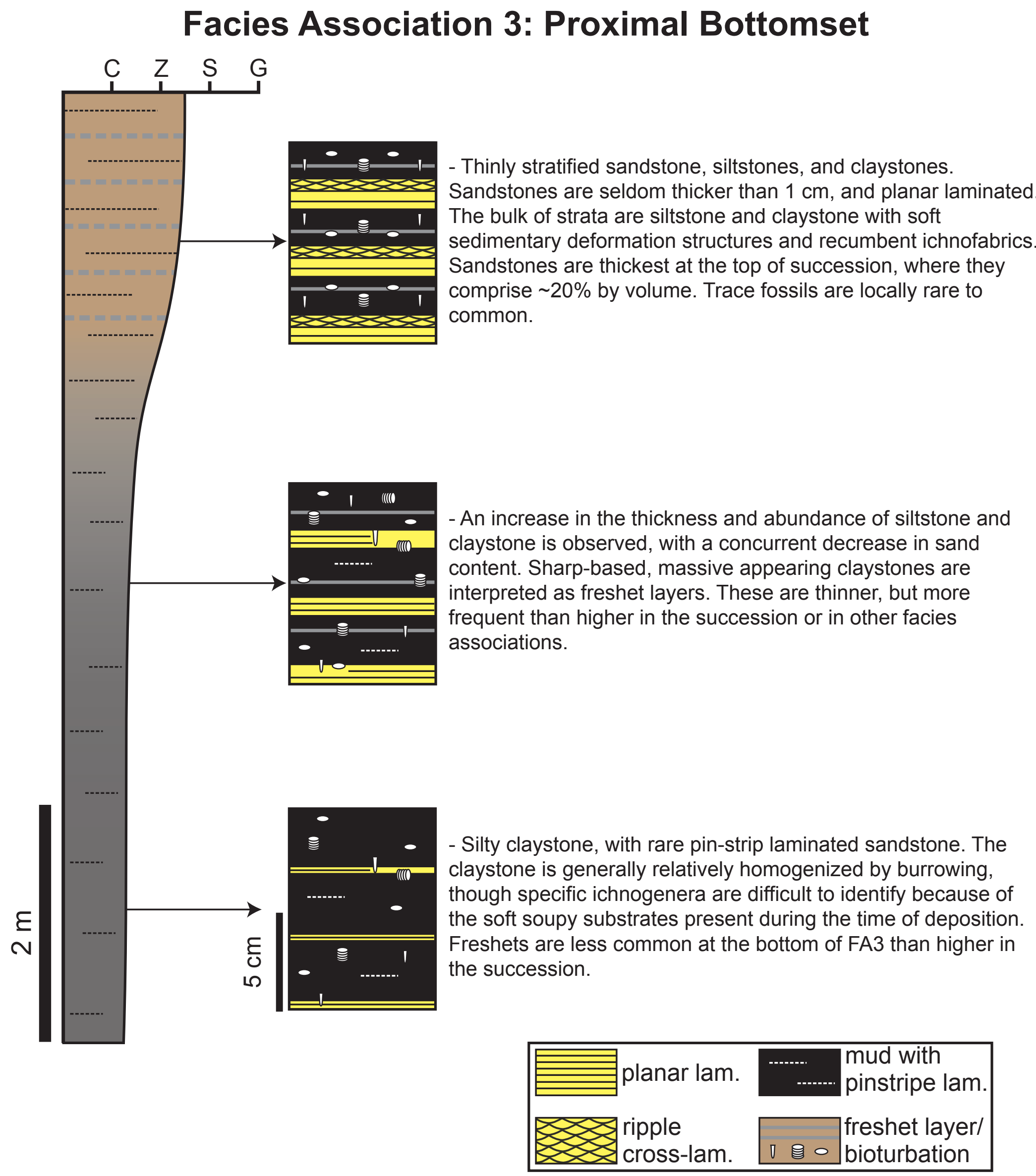

Figure II-7: A schematic illustration of an idealized section of FA3. The facies association is composed of thinly stratified sandstones, siltstones, and claystones organized into an overall coarsening-upwards package. Sedimentary structures in the sandstone are limited to wavy laminae, soft sedimentary deformation, or rarely ripple cross lamination near the top of the section. Siltstone and claystones are generally well laminated or structureless. The massive/structureless claystones are interpreted to represent freshets carried down the clinoform following the culmination of storm events in the foreset region. Overall, burrowing is sparse, likely due to compaction of the silts and clays, or trace makers moving through thixotropic substrates.

Ichnology of FA3

The trace fossil assemblage of FA3 is generally characterized by a low to moderate diversity of ichnogenera, with very low burrowing intensities (BI 0 to

BI 1; Taylor and Goldring, 1993) that are more sporadically distributed than in FA1 or FA2. The trace fossils observed include *Palaeophycus* (r-m), *Planolites* (r-m), *Teichichnus* (m), *Asterosoma* (r-m), *Skolithos* (m), cryptic *Phycosiphon* (r), and rare horizontal spreitenated traces interpreted as *Rhizocorallium.* Unlike FA1 and FA2, architecturally complex ichnofossils (i.e. *Asterosoma, Rhyzocorallium,* and *Teichichnus*) are locally observed in FA3. Burrow mottling dominates the ichnology of the facies association - traces are deformed and there is a degree of uncertainty in assigning specific ichnogenera. Many have similarities to the “mantle and swirl” traces of Lobza and Schieber (1999).

Interpretation of FA3

The physical sedimentology of FA3 is indicative of high sedimentation rates in a low-energy setting, episodically affected by event deposition. Siltstone and claystone dominate the association with minor thin, isolated sandstone stringers and lenses. Sand lenses are more frequent and increase in thickness upwards, resulting in an overall coarsening-upwards profile. Fine-grained sediments (silts and clays) are predominantly laminated and often are convoluted by soft sedimentary deformation. Siltstones and claystones are interpreted to be deposits from suspension settling, below fair weather wave base, or alternatively, the result of event deposition of thixotropic fluid-muds (Gingras et al., 1998; Bhattacharya and MacEachern, 2009). Sandstone lenses and stringers are the down-dip expression of storms on the proximal foreset region. They are gradationally succeeded by normally graded siltstone and claystone. Deposition of these deposits was driven by wind-forced and storm surge currents (Nelson, 1982) and they can be considered distal tempestites (Reineck and Singh, 1972; Aigner and Reineck, 1982). A distinctly different mode of event sedimentation can be observed from abundant sharp-based, massive claystones intermittently distributed, but generally occurring within 10 cm of sandstone lamination. The claystones range from 2 to 4 cm thick. They are thought to represent freshets deposited during times of high water discharge following storm events that created hyperpycnal conditions, allowing for rapid basinal deposition of massive claystones. These deposits are considered to be hyperpycnites/turbidites.

The ichnology of Facies Association 3 is the most important aspect for high-resolution interpretation of the depositional environment. The presence of a stressed, distal *Cruziana* Ichnofacies contrasts with the ichnology of more proximal locations in the study area, which are dominated by a stressed proximal *Cruziana* Ichnofacies. Important differences in the character of bioturbation are seen in the overall degree of bioturbation, the types of burrows, and burrow sizes. In FA1 and FA2, trace fossil suites are overwhelmingly composed of deposit-feeding behaviors (primarily *Palaeophycus* and *Planolites*) with a paucity of traces by presumed suspension-feeding fauna. In addition, fugichnia occur locally as a faunal response to high sedimentation rates. Burrowing is sporadically distributed with low bioturbation intensities and diminutive traces. In contrast, FA3 contains relatively larger trace fossils, though not fully developed, which are more sporadically distributed throughout the sediment and occur in smaller quantities. The trace fossil suite observed shows decreased proportions, or an absence, of passive carnivore dwelling structures (specifically *Palaeophycus* and *Schaubcylindrichnus freyi)* matched by the presence, or increase in the proportion, of complex forms representing grazing or deposit-feeding structures (e.g., *Teichichnus, Asterosoma* and *Phycosiphon*). Moreover, fugichnia are not observed in the siltstone dominated FA3, which is evidence for relatively slower deposition rates. This signature indicates that although physico-chemically stressed (as in FA1 and FA2), FA3 occupied a setting that suffered lower rates of sediment influx and were less frequently affected by salinity fluctuations (MacEachern et al., 2008). An important caveat to the overall lower sedimentation rate is the presence of "mantle and swirl" traces (cf. Lobza and Schieber, 1999), demonstrating that certain muddy intervals were deposited rapidly as soupy substrates. The mud likely was carried down the foreset region and deposited on the bottomset as the result of shocking by storm waves or hyperpycnal flows (Bhattacharya and MacEachern, 2009).

Based upon sedimentological and ichnological criteria, FA3 is interpreted to represent deposition in a proximal part of the bottomset of a subaqeous clinoform. The stratigraphic affinity (i.e., occurring below FA1 and FA2, and interdigitating with FA2) and accessories (i.e., fragmental shells) support this interpretation.

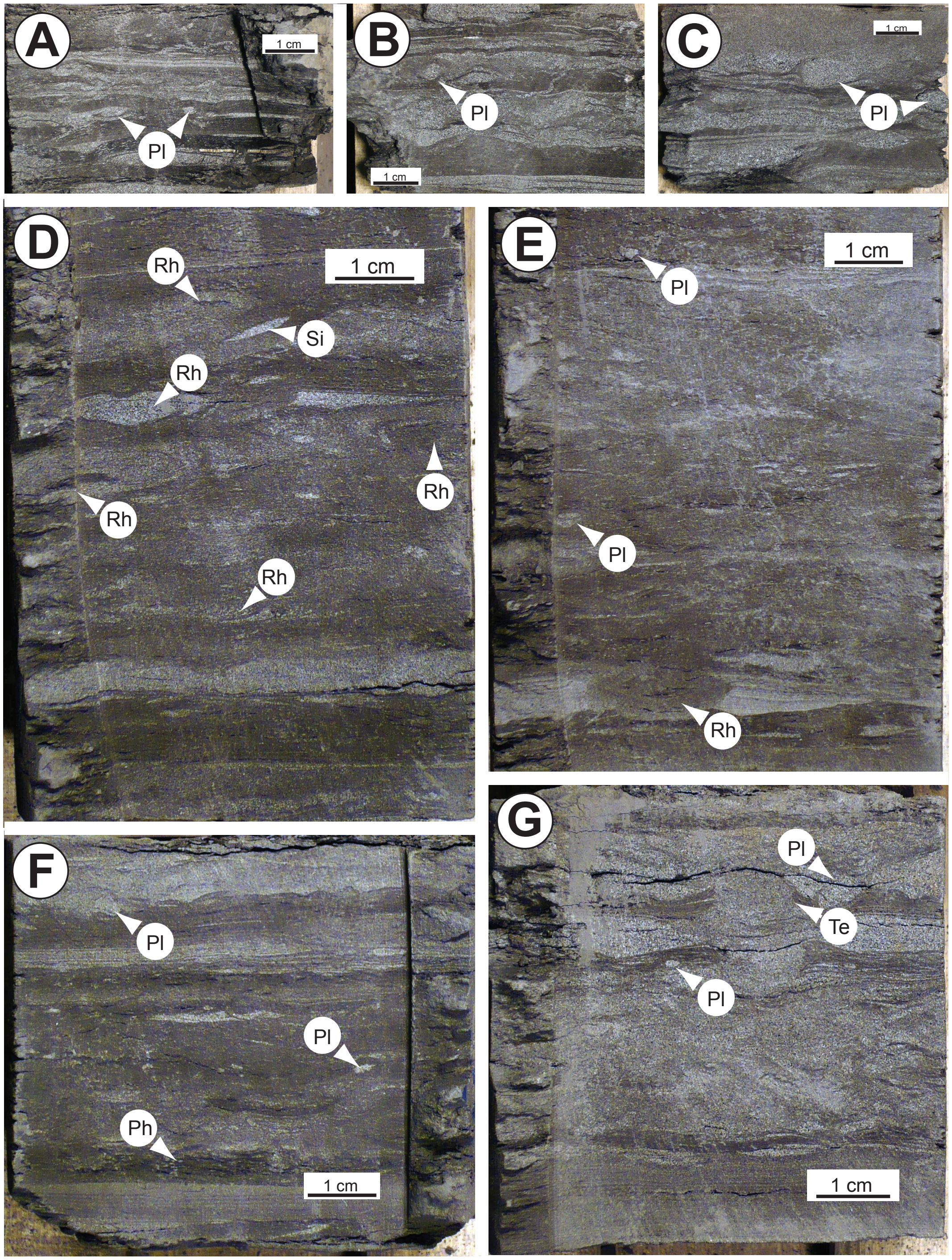

Figure II-8: FA4-Subaqeous Bay Deposits of the Medicine Hat Member.
(A) Moderately burrowed (BI 3-4), interlaminated fine-sandstone and siltstone. Trace fossils are dominated by indistinct horizontal forms and *Planolites* (Pl). Near the top of the photo rhythmic sand-silt couplets indicate a subtle tidal influence. Syneresis cracks are common in the top portion of the photo. Well 11-21-16-1W4, depth 577.4 m. (B) Interstratified fine-sandstone, siltstone, and claystone with low to moderate burrowing intensity (BI 2-3). Bioturbation is evident as indistinct mottling, with only rare identifiable traces such as *Planolites* (Pl). Rhythmically interlaminated sand-silt couplets are shown near the top and base of the photo. Syneresis cracks are common in the top portion of the photo. Well 11-21-16-1W4, depth 575.45 m. (C) Interstratified fine sandstone, siltstone, and claystone with low burrowing intensity (BI 2). Sand-silt couplets

FIGURE II-8 continued: occur scattered throughout the photo. The base of a rapidly deposited, massive sandstone can be observed near the top with an undulatory, bioturbated base. The only ichnogenera present is *Planolites* (Pl). Well 11-21-16-1W4, depth 576.6 m. (D) Moderately bioturbated (BI 3-4) clayey siltstone with a thin, massive sandstone laminae near the bottom of the photo. Most traces are indistinct, however, two ichnogenera can be recognized; *Rhyzocorallium* (Rh) and *Siphonichnus* (Si). Well 6-10-13-7W4, depth 381.3 m. (E) Heavily bioturbated (BI 4-5) sandy siltstone, with rarely preserved fine-sand laminae. Trace fossils are indistinct, with exception of a diminutive *Rhyzocorallium* (Rh) cross-cutting a sand laminae near the base of the photo, and rare *Planolites* (Pl). Well 6-10-13-7W4, depth 384.8 m. (F) Interstratified clayey siltstone, massive sandstone and thinly laminated sandstone with low burrowing intensity (BI 2). Burrowing is limited to two ichnogenera, diminutive *Planolites* (Pl) and cryptic *Phycosiphon* (Ph). Fine sand-silt couplets are noted near the base and top of the photo, indicating a subtle tidal influence on sedimentation. The massive sandstone with an undulatory/bioturbated base at the top of the photo was a rapidly deposited event bed that was churned by bioturbating organisms because the transit time of the bed into the historical layer was relatively slow. Well 6-10-13-7W4, depth 373.8 m. (G) Heavily bioturbated (BI 4-5) silty sandstone. The majority of traces are indistinct forms, however a well-formed, diminutive *Teichichnus* (Te) is shown in the top half of the photo, as well as a few *Planolites* (Pl) burrows. Well 6-10-13-7W4, depth 371.8 m.

Facies Association 4 (FA4): Subaqeous Bay Association

Sedimentology of FA4

Facies Association 4 abruptly overlies FA2 or FA3, and passes sharply upwards into FA1, FA2 or FA3. The facies association is primarily composed of fine-grained sediments (siltstone and claystone), with minor thinly interstratified sandstones, arranged in an overall coarsening-upwards package (Figure II-8; Figure II-9). FA4 contains unique physical sedimentary structures and ichnology that require the designation of a separate facies association. However, FA4 is relatively uncommon, and is only observed in a few locations within the study area.

Sandstone facies within FA4 are manifested in two distinct ways: 1) as thin laminae (facies S_p), finely interlaminated between siltstone and claystone and, 2) as thinly bedded, massive sandstones (facies S_m) with sharp, and commonly bioturbated bases. Individual sandstone laminae are always less than 0.5 mm thick and are found closely spaced together in packages up to 1 cm thick. There is a subtle rhythmicity to the sandstone-siltstone packages, but it is commonly obscured by bioturbation. The homogenous sandstones have undulatory/bioturbated bases and range between 0.5 and 2 cm thick. Both sandstone facies are very fine-grained.

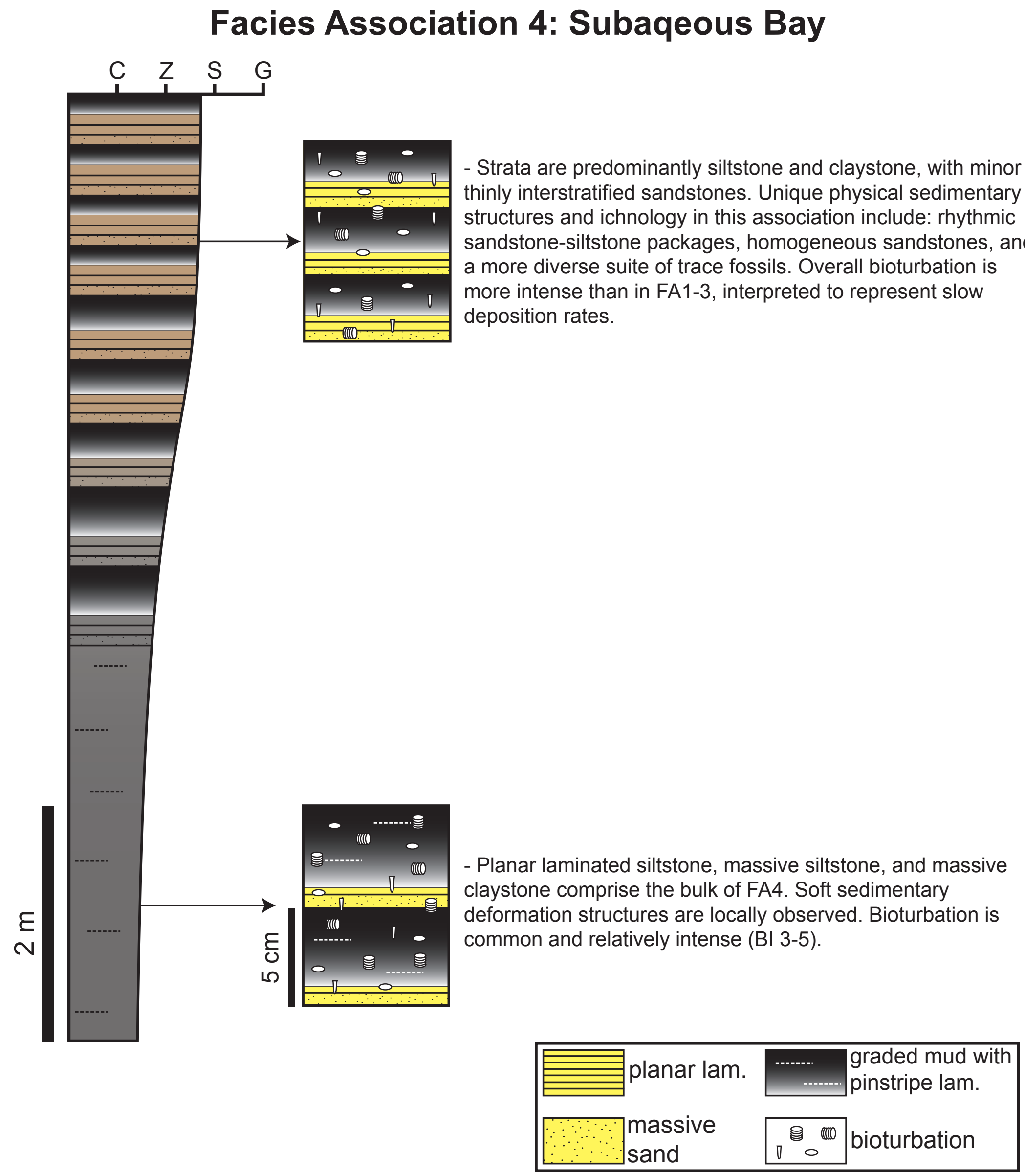

Figure II-9: A schematic illustration of an idealized section of FA4. The association comprises a coarsening-upwards succession of heavily bioturbated siltstones and claystones, with a minor sandstone component. Siltstones and claystones are either well laminated, or homogenized by burrowing, whereas the sandstones occur as thin, isolated planar laminated strata, or structureless laminae. The ichnology is the most important aspect of FA4, where the trace fossils and trace fossil suites are more robust, diverse, and evenly distributed than in the other facies associations. Facies Association 4 is interpreted to represent relatively slow deposition rates in a quiescent subaqeous bay setting, between actively prograding clinoforms.

Planar laminated siltstone (facies Z_p), massive siltstone (facies Z_m) and massive claystone (facies M_m) make up the bulk of FA4. Planar laminated siltstone is found in thin siltstone-sandstone packages, or as individual units from 0.5 to 3 cm thick. The siltstones in the sandstone-siltstone packages are always less than 0.5 mm thick. Massive siltstones (30-70% sand content) and massive claystones (<30% sand content) are observed to range in thickness from 0.5 to 3 cm. These facies have sharp bases and are distinctly structureless, though soft sedimentary features are locally common.

Ichnology of FA4

The ichnofossils in FA4 can generally be described as a low diversity suite with moderate to high bioturbation intensities (BI 3 to BI 5; Taylor and Goldring, 1993) and diminutive sizes. Ichnogenera observed within the association include *Planolites* (r-m), *Teichichnus* (r-m), *Siphonichnus* (r-m), *Rhizocorallium* (m), and *Zoophycos* (r). Trace fossils are generally poorly developed and commonly obscured by crosscutting relationships and an overall fine grain-size.

Interpretation of FA4

Aspects of the sedimentology indicate sedimentation from suspension settling was common in FA4. Sedimentary structures in the fine-grained media are limited to finely laminated and massive facies. The facies association displays no evidence of reworking by oscillatory currents (waves), however, biogenic reworking is common. Certainly, the depositional environment was significantly protected from wave-action. Subtle rhythmically interlaminated sandstone and siltstone is interpreted to represent tidal influence. Silts in these bedsets were deposited during slack-water conditions, while the sand component was deposited from traction. Sand-grade sediments were originally supplied to the bays from high-energy events, carrying the sediment in a landward direction. An abundance of tidal structures is not observed in FA1-3 because wave energy was stronger and the tidal range was comparatively small (Davis and Hayes, 1984).

In FA4, relatively thicker, structureless sandstones with sharp bases and tops are interpreted to be the result of rapid sedimentation events. The most likely mechanism was sediment-gravity flows, initiated during storms, increasing water velocity in an otherwise quiescent setting. The mass-movement events built momentum under the force of gravity and carried sand away from the topographically higher clinoforms - thin, massive sheet-sands were the result.

The ichnology of FA4 is unique for the Medicine Hat Member and distinct from FA1-3. Overall, the diversity of trace fossils is relatively limited when compared to fully marine suites (Gingras et al., 2008; MacEachern et al., 2008). Moreover, ichnofossils are diminutive and difficult to observe, and are manifested as subtle contrast between silt- and sand-sized fractions. However, the bioturbation intensity is higher than observed in other facies associations, resulting in varying degrees of sediment homogenization, and in certain cases, near complete destruction of original physical sedimentary structures. It is certain that physico-chemical environmental stresses were imparted on the sedimentary environment, such as episodes of salinity reduction and episodic high-energy conditions. Slow deposition rates are interpreted from the nature of burrowing intensity, which allowed an adequate colonization time for fauna occupying this ecological niche.

Finally, the stratigraphic affinity of FA4 is an important consideration for its interpretation. Facies Association 4 is limited in thickness and lateral continuity; it occurs as isolated packages with sporadic distributions. It is likely that the facies association had low preservation potential and other occurrences of the environment were not preserved.

Based upon consideration of the physical sedimentology, ichnology and stratigraphy of FA4, it is interpreted to represent quiescent subaqeous bays, protected from significant wave and current energy. As the clinoforms of the Medicine Hat were autocyclically switching, bays between them allowed for slow deposition in brackish water. However, since bays tend to be shallow (Reading, 1996), they are easily scoured away and do not survive into the rock record.

OVERVIEW AND DISCUSSION

Facies Associations 1-3

The Medicine Hat Member of the Niobrara Formation reflects a complex subaqeous clinoform shaped succession, dominated by fine-caliber sediments. Bay deposits are intermittently distributed, representing locations where no significant sand was deposited between the clinoforms, or where preservation of the foreset region was poor. Integrating ichnology and sedimentology provides insight into the physical and chemical stresses present during the time of deposition, leading to a refined palaeoenvironmental interpretation. In the Medicine Hat gas field, the succession is interpreted as a mixed wave- and river-influenced system, frequently affected by storms.

The most proximal facies association, FA1, reflects deposition in a proximal location on the foreset of a subaqeous clinoform under moderate storm-influence. Stacked, sharp-based, fining-upwards sandstone intervals interstratified with thin sporadically bioturbated siltstones and claystones supports proximal tempestites from high frequency storms. The cyclicity of low angle planar laminated sandstones passing gradationally into HCS and wave-ripples with a distinct lack of biogenic structures is typical of storm-generated deposits (Aigner, 1985). Such sandy facies represent winnowed, wave- and storm-reworked sediment. The intervening siltstones and claystones account for suspension fallout of fine material genetically related to the storm sandstones. In addition, a large proportion of silt and clay were deposited as floccules and subjected to post-depositional compaction, destroying the evidence of such depositional conditions (Macquaker and Bohacs, 2007; Schieber et al., 2007). Only subtle fluctuations in energy conditions, or differences in the sediment supplied by the source, were required to accumulate the fine-grained fractions. Studies of the modern Suriname coast and Amazon delta provide excellent examples of high-energy settings where fine-silts and clays are deposited in great quantities (Wells and Coleman, 1981; Rine and Ginsburg, 1985; Nittrouer et al., 1986). The sporadic nature of low diversity burrowing with low bioturbation intensities within the siltstones and claystones supports episodic event-deposition. Depauperate traces indicate that fluctuations in salinity were among the physico-chemical stresses imparted upon infaunal and epifaunal organisms. The absence of suspension-feeding structures suggests that sandstone facies were rapidly buried, and/or, water turbidity was generally high (MacEachern et al., 2005). The delta-front of storm-dominated systems is one such setting characterized by these conditions.

Facies Association 2, constituting a distal position on the foreset of a subaqeous clinoform, shows a decrease in storm-generated deposition when compared to FA1. Sandstone intervals are sharp-based and coarsen-upwards with physical sedimentary structures indicative of oscillatory wave-generated currents. However, hummocky cross-stratifcation is not present in the sandstone intervals of FA2, and therefore, tempestites are characterized by planar lamination succeeded by wave-ripple cross-lamination and capped gradationally with siltstone and claystone. The lack of HCS structures is consistent with the interpretation that deposition occurred at depths where wave-orbital diameters were large, resulting in long-wavelength HCS that are not readily recognized in core datasets. The most compelling evidence for the interpretation of FA2 is the ichnology and sedimentary structures in the siltstone and claystone facies. Silt and clay sized particles become widespread distally on the subaqeous clinoform, where storm-generated deposits are not well developed. These fine-grained deposits occur as graded tops to the ripple-cross laminated sandstones, and as isolated, sharp-based units. Aspects of the physical sedimentology, such as micro-flame structures, convolute bedding, and micro-faults are an indication that sedimentation rates were high. The development of these structures may also be related to rapid decomposition of organic detritus, under-consolidation, and or shocking by high-energy storm events. Overall, the trace fossil suite is dominated by deposit-feeding and passive carnivore behaviors, providing evidence for a high suspended-sediment concentration during deposition (MacEachern et al., 2005). Furthermore, strained ichnofabrics are commonplace in the finer grain-size fractions, demonstrating frequent down-slope sediment creep (Gingras and Bann, 2006). The observations from FA2 are consistent with physical and biologicalal processes in a distal position on a delta-front.

Facies Associations 1 and 2 make up the foreset portion of a clinoform succession that progrades basinward over a siltstone and claystone dominated bottomset (FA3). These two facies associations show that the Medicine Hat system was wave-influenced, as wave- and storm-generated features are abundant in the upward coarsening profiles. Sedimentological features including erosive bases, abundant HCS and wave-ripple cross-stratification, combined with the lack of tidally produced structures, indicates that very little, if any tidal influence affected deposition in the proximal portion of the delta (cf. Davis and Hayes, 1984). Though tempestites are common in the foreset, intervening siltstone and claystone strata are also common. In the Medicine Hat Member, the majority of sediment was finer than 0.25 mm (fine-grained sand). Consequently, a significant proportion of the proximal foreset consists of silt and clay. Energy conditions were certainly high enough to allow for winnowing of the fine silt- and clay-sized particles, but flocculation and generally high suspended-sediment concentrations resulted in deposition interstitially between the sand. The remaining fine-grained sediment favored buoyancy dominated mixing (Orton and Reading, 1993), and ultimately resulted in an extremely gradual, progressive deposition pattern observed throughout the region.

Facies Associations 3, comprising the bottomset portion of the subaqeous clinoforms in the Medicine Hat Member, reflects lower energy conditions than FA1 and FA2. The association contains abundant siltstone and claystone with only a minor sandstone component. Storm deposition is present on the bottomset, but differs in its representation from the foreset region. Whereas in the foreset, wave-generated currents rework sediments and deposit them as fining-upwards cycles containing HCS and wave-ripples, in the bottomsets, storm deposits are derived from reworking of sediments from the foreset. The succession is manifest as thin planar laminated sandstone passing gradationally into graded siltstone with claystone caps. Presumably, these are a distal expression of tempestites formed during large storms, when wave energy was able to scour and deposit sediment well below fair weather wave base. A second type of event stratification can be observed in FA3, represented by sharp-based claystone units with graded tops. Thin sandstone stringers are occasionally found at their base. Following the culmination of coastal storm events, fresh water discharge reached a maximum and debouched abundant fine-grained material that bypassed the foreset region and was deposited on the bottomset via density currents (Mulder and Syvitski, 1995; MacEachern et al., 2005; Bhattacharya and MacEachern, 2009). The deposits have many analogous characteristics to turbidites, specifically the B-D-E divisions (Bouma, 1962). The ichnological signature associated with the sharp-based claystones is significant for the interpretation of storm-induced freshets/turbidites on the bottomset (Gingras et al., 1998; Bhattacharya and MacEachern, 2009). Trace fossils representing the stressed distal *Cruziana* Ichnofacies dominate the background, ambient sedimentation. Similar trace fossils burrow the storm-induced freshets/turbidites as the fair weather deposits – there is no indication of “doomed pioneers” which were entrained in distal turbidites (Follmi and Grimm, 1990). Faunal opportunism in a physico-chemical stressful environment is typical of deltaic settings, making discrimination of ambient conditions and event deposition a challenge (MacEachern et al., 2005). Nevertheless, the ichnology indicates a marine setting periodically affected by salinity fluctuations and increased sedimentation rates (MacEachern et al., 2005; MacEachern et al., 2008). Moreover, recumbent ichnofabrics demonstrating down-slope creep of fine-grained media (Gingras and Bann, 2006) are common in FA3. The inclined *Skolithos* traces are easily mistaken for very small *Planolites,* but recognition of their true affinity is important for understanding the mechanisms of deposition for the siltstone and claystone. Other soft sedimentary deformation structures are readily observed and include micro-flame structures and convolute bedding. The prodelta or proximal bottomset of a subaqeous clinoform is one common setting characterized by a number of sedimentological and ichnological criteria described above.

Proximality Trends in Tempestites

A conspicuous proximality trend is observed within the storm deposits of the Medicine Hat Member (Figure II-10). The trend is a major piece of evidence for determining the depth that particular successions were deposited in (cf. Aigner and Reineck, 1982). Tempestites in proximal locations consist of planar lamination passing upwards into HCS, succeeded by ripple cross-lamination, and followed gradationally by siltstone grading into claystone. In contrast, distal tempestites are characterized by very thin planar laminated (rarely wavy-laminated) fine-grained sandstone, followed by normally graded siltstone passing into claystone. The proximity of a given succession to a hypothesized shoreline can be deduced by considering the systematic changes in the nature of stratification. Considerable variation in storm deposition exists in any given succession, the result of numerous storms of varying strength. Nevertheless, meaningful generalizations can be made regarding the relative abundance of sandstone, the nature of sedimentary structures, the frequency and thickness of storm deposits and the nature of bioturbation (Aigner and Reineck, 1982). On the whole, the proportion of sand decreases seaward with a concomitant increase in claystone. The same pattern is commonly observed in dip-profiles in marine settings and is controlled by the capacity of storm-induced currents to transport sand offshore. In the Medicine Hat Member, the frequency and thickness of storm deposits decreases down-profile, and correspondingly, the preservation of fair weather sedimentation increases. It is likely that tempestites would decrease in frequency landward of FA1, however no record of deposition in a more proximal

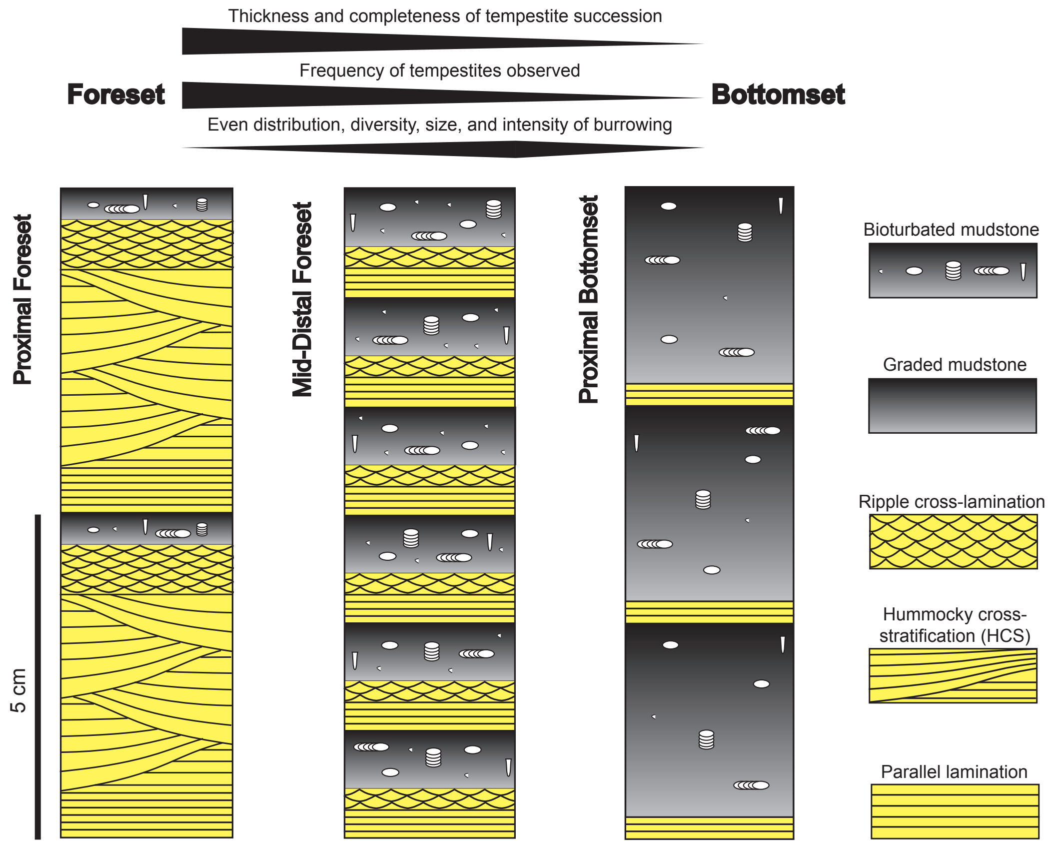

Figure II-10: Proximality trends in the storm deposits within the Medicine Hat Member. The trends are important for determining the depth at which a particular tempestite succession was deposited. Proximal tempestites show the full gradation from planar laminated sandstone passing upwards into HCS, followed by ripple (or combined-flow) cross-lamination, grading into siltststone and claystone. Trace fossils are diminutive and sporadically distributed between the storm deposits; they are primarily limited to the silt and clay dominated facies. In contrast, distal tempesites are characterized by planar laminated sandstone abruptly passing upwards into siltstone and claystone, without HCS or ripple cross-lamination. Ichnofossils are relatively more widespread, larger, and more diverse overall. However, considerable variation in the tempestites is observed, regardless of proximity as a result of numerous storms of varying strength.

setting was observed in the study area. The nature of sedimentary structures changes considerably proximally to distally. In general, fewer structures are observed in the tempestites basinward; HCS is the first structure absent from the succession, followed by ripple cross-lamination and then a significant decrease in the thickness and abundance of planar laminated sandstone. Planar laminated siltstone and graded siltstone and claystone are generally ubiquitous. Bioturbation is an important factor in considering the frequency with which storm waves made contact with the sediment-water interface. In the proximal tempestites, bioturbation is completely absent from the sandstone and very sporadically distributed in the intervening siltstone and claystone facies. Colonization by epifaunal and infaunal organisms was minimal due to a high periodicity of storm occurrence. Bioturbation increases in an offshore direction to the distal foreset region, and then decreases into the bottomset region. Near the toe of the foresets, intervening fair weather deposits are burrowed and the tops of tempestites are occasionally colonized, demonstrating a systematic decrease in the strength and periodicity of storms. More, the nature of bioturbation represents physico-chemically stressed conditions throughout the study area (MacEachern et al., 2005; MacEachern et al., 2008).

Facies Association 4

Facies Association 4, representing deposition in subaqeous bays between active clinoform progradation, is a complex arrangement of interlaminated sandstone, siltstone and claystone laid down in a quiescent setting protected from significant energy. Physical sedimentary structures highlight that deposition was predominantly from suspension settling under some amount, albeit small, of tidal influence. Thin, rhythmically interlaminated siltstone and sandstone show the alternation between deposition during slack water and fluctuating tides. No evidence of wave reworking is observed in FA4. Sand grains in the subaqeous bays were derived from splays, or delivered during storms by flood tidal currents. Event deposition is present in FA4, but is less conspicuous than the successions located on the active delta. Sediment-gravity flows deposited thin, massive sheet-sandstones absent of burrowing. These high-energy flows, initiated as levees were breached, and momentum from gravity carried the sediment to the middle of the bays. The ichnology of FA4 is significantly different from the active portions of the clinoform sedimentation in FA1-FA3. Trace fossils are low in diversity and depauperate, but burrowing intensities are obviously greater than observed on the foresets or bottomsets. Very low sedimentation rates account for the high degree of faunal induced sediment homogenization, resulting in near obliteration of primary physical sedimentary structures. The characteristics illustrated above are common for quiescent subaqeous bays.

Evidence for a Deltaic Interpretation

Contrary to Gilbert's (1885) classical definition of a delta, where steeply dipping foresets are deposited over finer-grained, flat lying bottom sets, not all deltas have well developed subaerial expressions (Nittroeur et al., 1986). Paralic topset facies are commonly reworked or entirely removed during transgression, leaving little if any evidence of distributary and coastal plain deposition (Bhattacharya and Giosan, 2003). In this study, cored intervals in the Medicine Hat gas field contain subaqueous deposits that have been interpreted as possible sediments from a deltaic environment under mixed fluvial- and wave-influence (Figure II-11). Subaerial environments associated with distributary channels were not noted. A similar problem identifying major fluvial systems and coastal plain complexes is found in the Jurassic Brent Group of the North Sea (Reading, 1996). Nevertheless, the terms foreset and bottomset are applicable to the stratigraphic architecture of the various elements seen in the Medicine Hat (i.e., FA1, FA2 and FA3). The Medicine Hat comprises distinct accretionary deposits that stand well above the regional topography. However, the lack of paralic deposits means that to a large extent the palaeoenvironmental interpretation of the Medicine Hat Member hinges upon the effective integration of ichnology and sedimentology at local and regional scales. Understanding the faunal responses to variations in the hydraulic regime and sediment supply characteristics gives valuable insight into the dynamic processes that ultimately resulted in its deposition.

In this study, a process-based approach to the Medicine Hat system was favored. The method concentrated on differences in the processes of updrift and downdrift portions of the clinoforms, and the effect they had on the nature of facies and facies architecture (cf. Bhattacharya and Giosan, 2003). This ideology differs significantly from the classical tripartite model, which primarily considers the relative effects of rivers, tides and waves on delta morphology (Wright and Coleman, 1973; Galloway, 1975). Erroneous interpretations of the hydrodynamic processes and resulting facies architecture can occur when one tries to force fit a particular system into one of the end-member categories (Orton and Reading, 1993; Bhattacharya and Giosan, 2003).

Overall, the distribution of the Medicine Hat Member is characterized by broad facies belts (see Chapter III) with subtle variations in basinward and alongshore directions (NE and NW-SE, respectively). The system appears

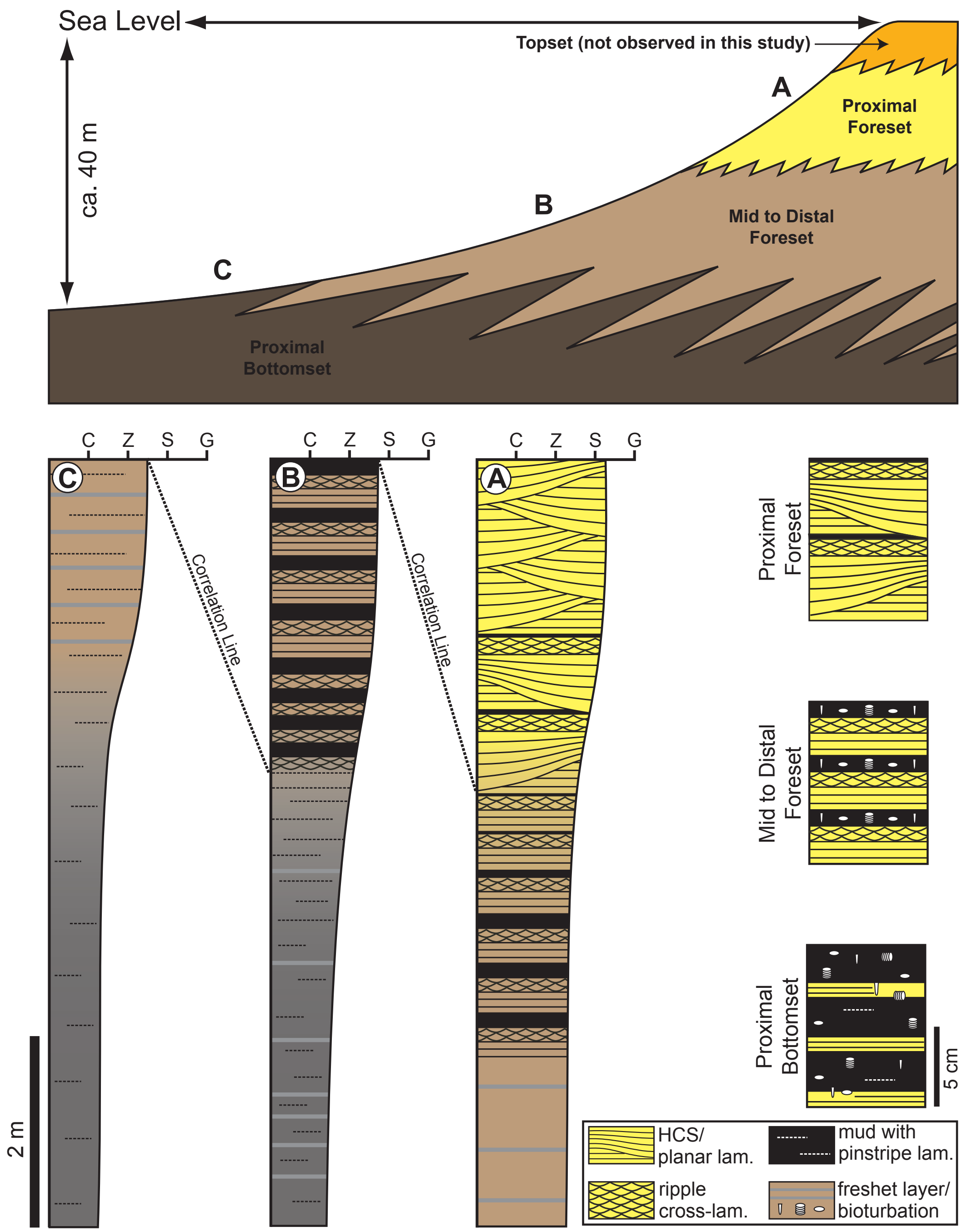

Figure II-11: A summary of the proximal to distal relationship between the three major facies associations: FA1, FA2, and FA3. Facies Association 1 is interpreted to be the deposits occurring in a proximal part of the foreset region. Facies Association 2 is thought to represent sediments accumulated in a distal position on the foreset. Facies Association 3 is inferred to be the result of sedimentation in the proximal part of the bottomset region. All three facies associations have coarsening-upwards profiles, but differ in the nature of sedimentary structures and ichnology.

to have a degree of symmetry, with an asymmetry index well below 200 (cf. Bhattacharya and Giosan, 2003). The ratio of net alongshore-transport of sediment to fresh water discharge is low. Despite indications of wave influence in the sedimentological characteristics observed (i.e., abundant wave-ripples, etc.), there were also temporally and spatially significant fluvial effects on the distribution and character of sedimentation (i.e., hyperpycnal flows/turbidites in the bottomset region). Bay fills within individual clinoforms were deposited at a higher frequency than the clinoforms themselves (cf. Coleman, 1988). The subtle lobate geometry of the foresets with subaqeous bay deposits further attests to the importance of fresh water discharge. The deposition of the Medicine Hat, by and large, was controlled by the interplay between wave processes and the influx of fresh water. Overall, the system was dominated by waves, but during episodic flooding it switched to a river-dominated state. The nature of the fluvial influence was dependent upon the duration and magnitude of floods and post-flood storms (cf. Rodriguez et al., 2000). These fluctuations were undoubtedly related to temporal variations in weather and climate (monsoonal rains, seasonal changes in river discharge) (MacEachern et al., 2005).

The alongshore profile of facies observed in the Medicine Hat gas field does not show marked changes in the nature of sedimentary structures and ichnology. Two possible mechanisms may account for this phenomenon: 1) the cores in the study area are all located on the same side of a large clinoform lobe or, 2) the clinoforms are relatively symmetric where fresh water discharge processes are important compared to alongshore sediment transport. The latter is felt to be the probable cause of the observed facies distribution. It is possible that a regionally sheltered palaeogeography (i.e., regional embayment) played a role in precluding alongshore currents. The system is characterized by a shallow dip-gradient where fine-grained sediment was supplied in abundance. Today, the large majority of the world's deltas supply large volumes of mud to the coastline (Nittrouer et al., 1986; Orton and Reading, 1993). The high suspended-load subdued wave action by increasing the overall viscosity of water (Rodriguez et al., 2000; MacEachern et al., 2005), and as a result, in the long term the coast was in a dissipative state (Wright, 1982; Wright et al., 1982; Wright and Short, 1984).

Evidence Against the Deltaic Interpretation and an Alternative Hypothesis

The interpretation presented in this study that the Medicine Hat Member in southeastern Alberta represents a subaqeous clinoform deposit, similar in aspects to river- and wave-influenced deltas, certainly is not accepted by all geologists familiar with the regional sedimentology and stratigraphy. There are important elements of deltaic systems that are notably absent from the Medicine Hat interval, and therefore, hinder consensus on its depositional affinity. Specifically, there are four strong arguments against the delta interpretation that could not be adequately resolved in this study. The first point of contention is the discrete lack of subaerial deposits that are stratigraphically equivalent to the Medicine Hat. Nowhere in the southeastern portion of Alberta can Santonian-aged paralic sediments be observed (i.e., distributary channels feeding the delta, coastal plain deposits, etc.). In fact, sedimentary geologists working in the Upper Cretaceous provide the argument that paralic environments cannot even be found far to the south in Montana (Nielsen, 2002; Nielsen et al., 2008; D. Leckie, pers. comm., 2009; Pedersen et al., 2010). The second problem with the delta interpretation is the location of the Medicine Hat Member with respect to the Western Interior Seaway. Particularly, palaeogeographic reconstructions have shown that the Medicine Hat gas field occurs far from the palaeoshoreline of the Western Interior Seaway. Therefore, despite the relative influence of the Sweetgrass Arch on the geometry and depositional character (i.e., relatively shallower water depths), many authors have an issue with invoking a “true” marginal marine setting for the Medicine Hat strata (Hankel et al., 1989; Schröder-Adams et al., 1997; Schröder-Adams et al., 1998; Nielsen, 2002; Nielsen et al., 2003; Nielsen et al., 2008; Leckie, pers. comm., 2009; Pedersen et al., 2010). That being said, Nielsen et al. (2008), infer that the Sweetgrass Arch (Bow Island Arch) was a subtle subaqeous high of less than 10 m water depth; the shallow water depth is consistent with the physical sedimentary structures observed in this study. Third, the micropaleontology of the Medicine Hat Member is a piece of evidence that contrasts with the physico-chemically stressed suite of trace fossils. The work by Nielsen (2002), and Nielsen et al. (2008), interpreted that the microfossils and nannofossils within the interval are indicative of fully marine oceanic conditions, particularly in the finer-grained fractions in southeastern Alberta. These observations contrast significantly from the interpreted physico-chemically stressed conditions indicated by the depauperate, sporadically distributed, and limited ichnogenera observed here. Finally, Pedersen et al. (2010) analyzed thin sections of the fine-grained fractions, noting that the muds are dominantly reworked sediments, indicating that they were deposited and later transported farther offshore via sediment bypass.

The four pieces of evidence discussed above provide the backbone of the leading alternative hypothesis for the unique setting in which the Medicine Hat Member was deposited. Only a few examples of modern or ancient analogues to laterally extensive sandstone bodies occurring in shale-dominated intervals exist, and the terms shoals, bars, or ridges do not suffice (Nielsen et al., 2008). Therefore, to these authors, the general statement that deposition occurred in a sandy offshore to shelf environment, under the influence of waves and geostrophic currents, is the best explanation (Hankel et al., 1989; Schröder-Adams et al., 1997; Schröder-Adams et al., 1998; Nielsen, 2002; Nielsen et al., 2003; Nielsen et al., 2008; Pedersen et al., 2010). Pedersen et al. (2010), prefer the terminology "detached fine-grained shelf edge wedges" to describe the unit. However, based on the sedimentological and ichnological observations, it is unclear how significant volumes of sandy sediment with evidence of frequent high-energy events, and physico-chemically stressed epifaunal and infaunal responses could occur in such a distal setting.

CONCLUSIONS

The Upper Cretaceous Medicine Hat Member (Niobrara Formation) of southeastern Alberta, Canada, is a thin, gas-charged deposit that is interpreted as a fine-grained progradational clinoform succession. The integration of ichnological and sedimentological data suggest that deposition occurred in a shallow marine setting, where wave/storm and river processes were the dominant modes of sediment transport. Moreover, a high proportion of siltstone and claystone resulted in proximal flocculation, distal fluid-muds and hyperpycnal flows/turbidites. Evidence reflecting the depositional affinities comprise coarsening upwards units containing planar lamination, HCS and wave-ripples, an impoverished marine suite of trace fossils with elements of the *Cruziana* Ichnofacies and a marked absence of the *Skolithos* Ichnofacies (MacEachern et al., 2005; Gingras et al., 2008), soft sedimentary deformation features (convolute bedding, micro-faults, flame structures, etc.), and strained ichnofabrics indicating downslope movement of unconsolidated substrates (Gingras and Bann, 2006). Further support for the interpretation was based on the dominance of deposit-feeding trace fossils, the short wavelengths of HCS, sharp-based homogeneous claystone intervals, and the overall distribution of burrowing. The clinoforms are hypothesized to be relatively symmetric, owing to dissipation of energy, interpreted from the lateral similarity of facies.

In general, the Medicine Hat strata are arranged in coarsening-upwards units, 5-15 m thick, consisting of laminated to burrowed siltstone and claystone, interlaminated siltstone and sandstone with sporadic bioturbation, and tempestite successions with rare burrowing in the intervening fair weather deposits. The abundance of wave-generated physical sedimentary structures, in conjunction with the presence of hyperpycnal flows/turbidites from river floods, in concert with only small variations in ichnology and sedimentary facies along-strike, result in the interpretation that the Medicine Hat Member represents a fine-grained, wave- and fluvial-influenced expression of a subaqueous delta system. Few rock record or modern examples of a system strikingly similar to the Medicine Hat exist in the literature; a good analogue is the modern Brazos delta system in Texas discussed in detail in Chapter III (Rodriguez et al., 2000). Similar deposits may be under-represented because of the difficulties in integrating ichnological and sedimentological data in silt and clay rich intervals, particularly in the rock record.

Several physico-chemical environmental stresses helped shape the Medicine Hat Member and were recorded by the trace fossil assemblage observed in the strata. These stressed assemblages are more characteristic of deltaic deposits than those of fully marine shoreface and offshore settings (Gingras et al., 1999; MacEachern et al., 2005; MacEachern et al., 2008; Bhattacharya and MacEachern, 2009), as had previously been interpreted (Nielsen, 2002; Nielsen et al., 2003; Nielsen et al., 2008). The stresses are manifest in a number of ways which include: 1) decreased trace fossil diversities, 2) diminutive ichnofossil sizes, 3) reduced and fluctuating bioturbation intensities, 4) sporadic trace fossil distribution, 5) deformed burrows of sediment swimming organisms (cf. Lobza and Schieber, 1999), 6) assemblages dominated by a single ichnogenus (generally *Planolites* or *Palaeophycus*).

This study highlights a gap in the literature on fine-grained clinoform shaped systems. Differentiating between strandplain successions and deltaic protuberances can be difficult without the aid of ichnological assessment. Integrating concepts from ichnology and sedimentology has proven to be an effective tool for detailed palaeoenvironmental interpretations of this economically important interval. The work has shown that the Medicine Hat Member may have a deltaic affinity, and thus, the mapping of reservoir units based upon older models can be improved upon. This new insight may lead to updated reserve calculations, and ultimately, improved exploration and production of natural gas from the Medicine Hat gas field.

REFERENCES

Aigner, T., 1985, Storm depositional systems – dynamic stratigraphy in modern and ancient shallow-marine sequences. *In:* G.M. Friedman, H.J. Neugebauer and A. Seilacher (eds.), Lecture Notes in Earth Sciences 3, Springer-Verlag, New York, 174p.

Aigner, T., and Reineck, H., 1982, Proximality trends in the modern storm sands from the Helgoland Bight (North Sea) and their implications for basin analysis, Senckenbergiana Maritima, v. 14, p. 183-215.

Bhattacharya, J.P., and MacEachern, J.A., 2009, Hyperpycnal rivers and prodeltaic shelves in the Cretaceous Seaway of North America, Journal of Sedimentary Research, v. 79, p. 184-209.

Bhattacharya, J.P., and Giosan, L., 2003, Wave-influenced deltas: geomorphological implications for facies reconstruction, Sedimentology, v. 50, p. 187-210.

Bouma, A.H., 1962, Sedimentology of some flysch deposits, Amsterdam, Elsevier, 168p.

Buatois, L.A., and Angriman, O.L., 1992, The ichnology of a submarine braided channel complex: the Whiskey Bay Formation, Cretaceous of James Ross Island, Antarctica, Paleogeography, Paleoclimatology, Paleoecology, v. 94, p. 119-140.

Coleman, J.M., 1988, Dynamic changes and processes in the Mississippi River delta, Bulletin of the Geological Society of America, v. 100, p. 999-1015.

Davis, R.A, and Hayes, M.O., 1984, What is a wave-dominated coast?, Marine Geology, v. 60, p. 313-329.

Duke, W.L., Arnott, R.W.C., and Cheel, R.J., 1991, Shelf sandstones and hummocky cross-stratification: new insights on a stormy debate, Geology, v. 19, p. 625-628.

Dumas, S., Arnott, R.W.C., Southard, J.B., 2005, Experiments on oscillatory-flow and combined-flow bed forms: implications for interpreting parts of the shallow-marine sedimentary record, Journal of Sedimentary Research, v. 75, p. 501-513.

Felix, M., Peakall, J., and McCaffrey, W.D., 2006, Relative importance of processes that govern the generation of particulate hyperpycnal flows, Journal of Sedimentary Research, v. 76, p. 382-387.

Follmi, K.B., and Grimm, K.A., 1990, Doomed pioneers: gravity-flow deposition and bioturbation in marine oxygen-deficient environments, Geology, v. 18. p. 1069-1072.

Galloway, W.E., 1975, Process framework for describing the morphologic and stratigraphic evolution of deltaic depositional systems, In: *Deltas, Models for Exploration* (Ed. M.L. Broussard), p. 87-98, Houston Geological Society, Houston, Texas.

Gilbert, G.K., 1885, The topographic features of lake shores, Annual Report of the U.S. Geological Survey #5, p. 75-123.

Gingras, M.K., MacEachern, J.A., and Pemberton, S.G., 1998, A comparative analysis of the ichnology of wave- and river-dominated allomembers of the Upper Cretaceous Dunvegan Formation, Bulletin of Canadian Petroleum Geology, v. 46, p. 51-73.

Gingras, M.K., and Bann, K.L., 2006, The bend justifies the leans: interpreting recumbent ichnofabrics, Journal of Sedimentary Research, v. 76, p. 483-492.

Gingras, M.K., Bann, K.L., MacEachern, J.A., and Pemberton, S.G., 2008, A conceptual framework for the application of trace fossils, *in* Applied Ichnology, SEPM Short Course Notes #52, p. 5-30.

Gressly, A., 1838, Observations géologiques sur le Jura Soleurois, Neue Denkschr. Allg. Schweiz, Ges. Ges. Naturw., v. 2, p. 1-112.

Hankel, R.C., Davies, G.R., and Krouse, H.R., 1989, Eastern Medicine Hat gas field: a shallow, Upper Cretaceous, bacteriogenic gas reservoir of southeastern Alberta, Bulletin of Canadian Petroleum Geology, v. 37, p. 98-112.

Harms, J.C., Southard, J.B., Spearing, D.R., and Walker, R.G., 1975, Depositional environments as interpreted from primary sedimentary structures and stratification sequences. SEPM Short Course Notes #2, 161 p.

Hildebrandt, C., and Egenhoff, S., 2007, Shallow-marine massive sandstone sheets as indicators of palaeoseismic liquefaction – An example from the Ordovician shelf of central Bolivia, Sedimentary Geology, v. 202, p. 581-595.

Ito, M., Ishigaki, A., Nishikawa, T., and Saito, T., 2001, Temporal variation in the wave-length of hummocky cross-stratification: implications for storm intensity through Mesozoic and Cenozoic, Geology, v. 29, p. 87-89.

Lobza, V., and Schieber, J., 1999, Biogenic sedimentary structures produced by worms in soupy, soft muds: observations from the Chattanooga Shale (Upper Devonian) and experiments, Journal of Sedimentary Research, v. 69, p. 1041-1049.

MacEachern, J.A., 1994, Integrating ichnology with sedimentology: sequence stratigraphy and palaeoenvironmental interpretation of the Viking and Peach River Formations, west-central Alberta, unpublished Ph.D. thesis, University of Alberta, 566p.

MacEachern, J.A., Bann, K.L., Bhattacharya, J.P., and Howell, C.D., 2005, Ichnology of deltas: organism responses to the dynamic interplay of rivers, waves, storms, and tides, *in* River Deltas – Concepts, Models, and Examples, SEPM Special Publication #83, p. 49-85.

MacEachern, J.A., Pemberton, S.G., Bann, K.L., and Gingras, M.K., 2008, Departures from the archetypal ichnofacies: effective recognition of environmental stress in the rock record, *in* Applied Ichnology, SEPM Short Course Notes #52, p. 69-93.

Macquaker, J.H.S., and Bohacs, K.M., 2007, On the accumulation of mud, Science, v. 318, p. 1734-1735.

Matsumoto, D., Naruse, H., Fujino, S., Surphawajruksakul, A., Jarupongsakul, N.S., and Murayama, M., 2008, Truncated flame structures within a deposit of the Indian Ocean Tsunami: evidence of syn-sedimentary deformation, Sedimentology, v. 55, p. 1559-1570.

Miall, A.D, 1999, Principles of Sedimentary Basin Analysis (third edition), Springer-Verlag, Berlin Heidelberg, Germany.

Moslow, T.F., and Pemberton, S.G., 1988, An integrated approach to the sedimentological analysis of some Lower Cretaceous shoreface and delta front sandstone sequences, Canadian Society of Petroleum Geologists Memoir, v. 15, p. 373-386.

Mulder, T., and Syvitski, J.P.M., 1995, Turbidity currents generated at river mouths during exceptional discharges to the world's oceans, Journal of Geology, v. 103, p. 285-299.

Nelson, C.H., 1982, Modern shallow-water graded sand layers from storm surges, Bering Shelf: a mimic of Bouma sequences and turbidite systems, Journal of Sedimentary Petrology, v. 52, p. 534-545.

Nielsen, K.S., 2002, Lithostratigraphy, sequence stratigraphy and palaeoenvironments of the Upper Colorado Group in southern Alberta and southwestern Saskatchewan: definition of the Carlile and Niobrara formations (Upper Turonian to Upper Santonian), unpublished Ph.D. thesis, Carleton University, Ottawa, Canada.

Nielsen, K.S., Schröder-Adams, C.J., and Leckie, D.A., 2003, A new stratigraphic framework for the Upper Colorado Group (Cretaceous) in southern Alberta and southwestern Saskatchewan, Canada, Bulletin of Canadian Petroleum Geology, v. 51, p. 304-346.

Nielsen, K.S., Schröder-Adams, C.J., Leckie, D.A., Haggart, J.W., and Elberdak, K., 2008, Turonian to Santonian paleoevironmental changes in the Cretaceous Western Interior Sea: The Carlile and Niobrara formations in southern Alberta and southwestern Saskatchewan, Canada, Palaeogeography, Palaeoclimatology, Palaeogeography, v. 270, p. 64-91.

Nittrouer, C.A., Kuehl, S.A., DeMaster, D.J., and Kowsmann, R.O., 1986, The deltaic nature of Amazon shelf sedimentation, Geological Society of America Bulletin, v. 97, p. 444-458.

Orton, G.J., and Reading, H.G., 1993, Variability of deltaic processes in terms of sediment supply, with particular emphasis on grain-size, Sedimentology, v. 40, p. 475-512.

Pedersen, P.K., Macquaker, J.H., and Hart, B., 2010, Detached fine-grained shelf edge wedges within shale dominated successions, depositional model and reservoir significance, American Association of Petroleum Geologists, Conference Abstracts.

Pemberton, S.G., and Frey, R.W., 1984, Ichnology of a storm-influenced shallow marine sequence: Cardium Formation (Upper Cretaceous) at Seebe, Alberta. *In:* D.F. Stott and D.J. Glass (eds.), The Mesozoic of middle North America, Canadian Society of Petroleum Geologists Memoir 9, p. 281-304.

Pemberton, S.G., MacEachern, J.A., and Ranger, M.J., 1992, Ichnology and event stratigraphy: the use of trace fossils in recognizing tempestites. *in* Pemberton, S.G., ed., Applications of Ichnology to Petroleum Exploration: Society of Economic Paleontologists and Mineralogists Core Workshop 17, Society of Economic Paleontologists and Mineralogists, Tulsa, p. 85-117.

Reading, H.G.,1996, Sedimentary Environments and Facies (third edition), Blackwell Scientific Publications, Boston, 615p.

Reineck, H.E., and Singh, I.B., 1972, Genesis of laminated sand and graded rhythmites in storm-sand layers of shelf mud, Sedimentology, v. 18, p. 123-128.

Rine, J.M., and Ginsburg, R.N., 1985, Depositional facies of a mud shoreface in Suriname, South America – a mud analogue to sandy, shallow-marine deposits, Journal of Sedimentary Petrology, v. 55, p. 633-652.

RODRIQUEZ, A.B., HAMILTON, M.D., AND ANDERSON, J.B., 2000, Facies and evolution of the modern Brazos Delta, Texas: wave versus flood influence, Journal of Sedimentary Research, v. 70, p. 283-295.

SCHIEBER, J., SOUTHARD, J, AND THAISEN, K., 2007, Accretion of claystone beds from migrating floccule ripples, Science, v. 318, p. 1760-1762.

SCHRÖDER-ADAMS, C.J., ADAMS, P.J., LECKIE, D.A., BLOCH, J., CRAIG, J., SEIF EL-DEIN, S.A., 1997, Upper Cretaceous Medicine Hat Formation and First White Speckled Shale in southeastern Alberta: evidence for localized shallow water deposition, Bulletin of Canadian Petroleum Geology, v. 45, p. 356-376.

SCHRÖDER-ADAMS, C.J., ADAMS, P.J., HAGGART, J., LECKIE, D.A., BLOCH, J., CRAIG, J., AND MCINTYRE, D.J., 1998, An integrated paleontological approach to reservoir problems: Upper Cretaceous Medicine Hat Formation and First White Speckled Shale in southern Alberta, Canada, Palaios, v. 13, p. 361-375.

SOUTHARD, J.B., AND BOGUCHWAL, L.A., 1990, Bed configurations in steady unidirectional water flows. Part 2. Synthesis of flume data, Journal of Sedimentary Research, v. 60, p. 658-679.

TAYLOR, A.M., AND GOLDRING, R., 1993, Description and analysis of bioturbation and ichnofabric, Journal of the Geological Society of London, v. 150, p. 141-148.

WELLS, J.T., AND COLEMAN, J.M., 1981, Physical processes and fine-grained sediment dynamics, coast of Surinam, South America, Journal of Sedimentary Petrology, v. 51, p. 1053-1068.

WHEATCROFT, R.A., 1990, Preservation of sedimentary event layers, Geology, v. 18, p. 843-845.

WRIGHT, L.D., 1982, Field observations of long-period, surf-zone standing waves in relation to contrasting beach morphologies, Australian Journal of Marine and Freshwater Research, v. 33, p. 181-201.

WRIGHT, L.D., AND COLEMAN, J.M., 1973, Variations in morphology of major river deltas as a function of ocean wave and river discharge regimes, American Association of Petroleum Geologists Bulletin, v. 57, p. 370-398.

Wright, L.D., Guza, R.T., and Short, A.D., 1982, Dynamics of a high-energy dissipative surf zone, Marine Geology, v. 45, p. 41-62.

Wright, L.D., and Nittrouer, C.A., 1995, Dispersal of river sediments in coastal seas: six contrasting cases, Estuaries, v. 18, p. 494-508.

Wright, L.D., and Short, A.D., 1984, Morphodynamic variability of surf zones and beaches: a synthesis, Marine Geology, v. 56, p. 93-118.

Yang, B., Dalrymple, R.W., and Chun, S., 2006, The significance of hummocky cross-stratification (HCS) wavelengths: evidence from an open-coast tidal flat, South Korea, Journal of Sedimentary Research, v. 76, p. 2-8.

CHAPTER III — LITHO- AND SEQUENCE-STRATIGRAPHIC ANALYSIS OF THE MEDICINE HAT MEMBER, MEDICINE HAT GAS FIELD, SOUTHEAST ALBERTA, CANADA

INTRODUCTION

The upper Colorado Group in southern Alberta is a poorly understood interval in the Western Canada Sedimentary Basin. While a formal stratigraphic nomenclature for the lower Colorado Group has been in place for some time (i.e. Bloch et al, 1993), a detailed stratigraphic nomenclature for the upper Colorado Group has not been compiled until recently (Schröder-Adams et al., 1998; Nielsen, 2002; Nielsen et al., 2003). This chapter is intended to build upon this newly established stratigraphy for the upper Colorado Group, specifically the Medicine Hat Member, which resides within the Niobrara Formation (Figure III-1). Herein, a combination of litho- and sequence-stratigraphic methodologies is implemented to highlight the spatial and temporal significance of the sedimentological and ichnological observations discussed in Chapter II. In concert, the two chapters support a subaqeous, clinoform-shaped depositional body for the Medicine Hat Member in the area of the Medicine Hat gas field of southeastern Alberta.

PREVIOUS WORK AND HISTORICAL OVERVIEW OF STRATIGRAPHY

Initial descriptions of the subsurface geology in southern Alberta placed the Niobrara Formation and the Medicine Hat gas horizon within the Colorado Group interval (Downling, 1917). Dowling et al. (1919) then produced the first formal map and described a "broad, low anticline plunging north into the central plains" (pg.13), a feature that is now known as the Bow Island Arch (the northern extension of the Sweetgrass Arch, a more generalized term that is preferred in this thesis). Later, Spratt (1931) correlated the Colorado Group from northern Montana to the subsurface of the Alberta plains. He subdivided the group into a lower sand-prone unit, and an upper, more shaly interval, which are now recognized as the lower and upper Colorado Group, respectively. The Alberta

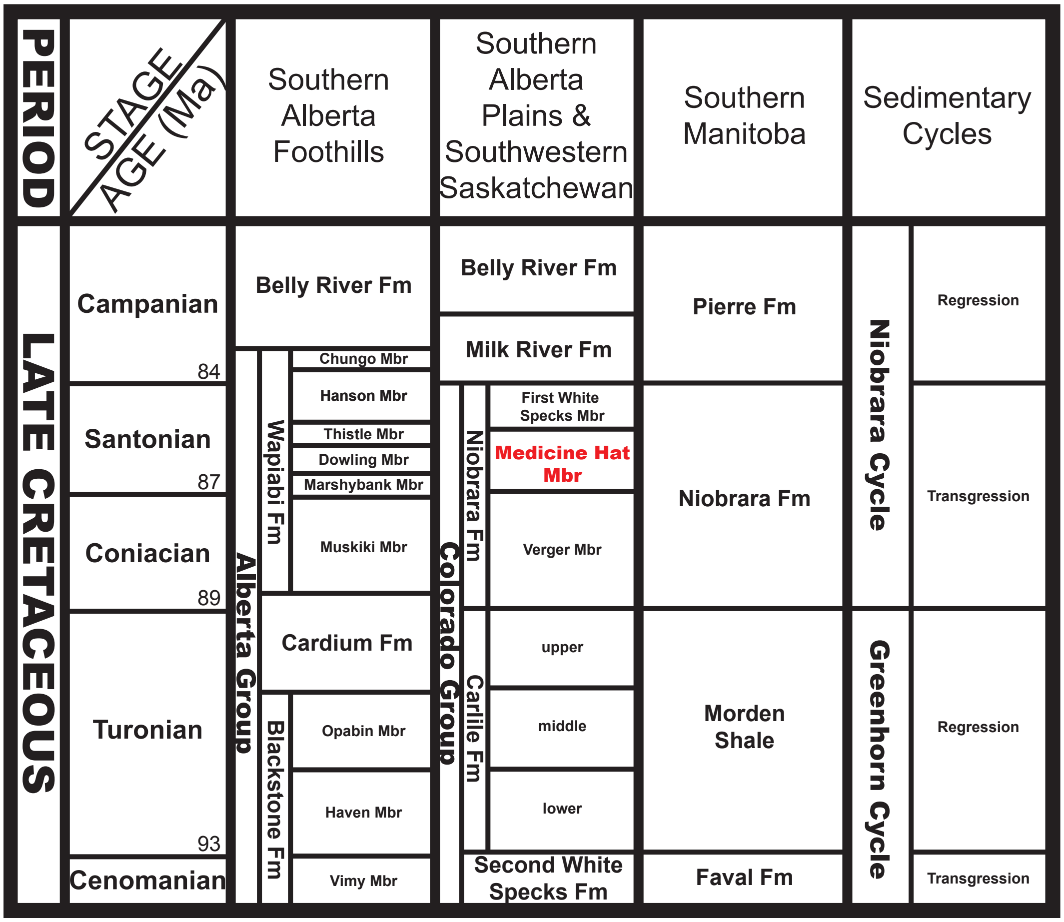

Figure III-1: Late Cretaceous stratigraphic relationships in the southern interior of North America. The Medicine Hat Member (shown in red) is roughly correlated with the Marshybank, Dowling, and Thistle members in the southern Alberta Foothills, and with the Niobrara Formation in southern Saskatchewan and Manitoba. The Medicine Hat Member was deposited during the transgressive portion of the Niobrara sea level cycle, and is Santonian in age. Modified from Nielsen (2002), and Nielsen et al. (2003).

Group was then defined and demonstrated to be equivalent to the Colorado Shale and lower Milk River Formation in the Foothills of southern Alberta by Russell and Landes (1940). The exact placement of the contact between the units, however, was indistinguishable at the time by a limited macrofossil biostratigraphic framework (Russell and Landes, 1940; Nielsen et al., 2003).

Cobban (1951), and Cobban et al. (1959), correlated the Alberta shale in the southern plains of Alberta to the Colorado Group of northwestern Montana. From then forth, the strata overlying the Mannville Group, and below the Milk River/Lea Park formations in the southern plains, were referred to as the Colorado Group in Canadian literature (e.g. Stott, 1963; Stott, 1984; Caldwell et al., 1978;

Simpson, 1982; Simpson 1984; Schröder-Adams et al., 1997; Schröder-Adams et al., 1998; Nielsen et al., 2003). More specifically, the upper Colorado Group refers to the interval overlying the Second White Specks Formation and underlying the Milk River/Lea Park formations (Caldwell et al., 1978; Nielsen, 2002).

The original correlation of the Medicine Hat and First White Speckled Shale members to the Wapiabi Formation of the Alberta Foothills was established using Foraminifera (Wall, 1967). These correlations were later refined, showing that the Medicine Hat Member specifically correlates with the Marshybank and Dowling members in the southern Foothills (Wall and Rosen, 1977), and the Dowling Member, Wapiabi Formation and Puskwaskau Formation, in the west-central Foothills and plains (Plint, 1991). Correlations of the Medicine Hat Member were also made with the lower Vermillion River Formation in Saskatchewan (North and Caldwell, 1975), and the Niobrara Formation of Manitoba and Montana (McNeil and Caldwell, 1981).

Most recently, studies of the upper Colorado Group stratigraphy have focused on subdividing the interval into formal units (Nielsen, 2002; Nielsen et al., 2003), and using microfossils to biostratigraphically differentiate between the intervals (Schröder-Adams et al., 1998). Nielsen (2002), and Nielsen et al. (2003), introduced the Carlile (lower) and Niobrara (upper) formations for the upper Colorado Group. The Carlile Formation was subdivided into an informal lower, middle, and upper unit. It is interpreted to represent the upper regressive phase of the Greenhorn sea-level cycle (Nielsen, 2002; Nielsen et al., 2003). The Niobrara was split into the lower Verger Member, the middle Medicine Hat Member, and the upper First White Speckled Shale Member (Figure III-1). Deposition of the Niobrara Formation occurred during the transgressive portion of the Niobrara sea-level cycle (Nielsen, 2002; Nielsen et al., 2003). These second-order sea level cycles are thoroughly described from the Late Cretaceous Interior Seaway of Canada and the United States (Kaufmann, 1967; McNeil and Caldwell, 1981). The studies of Nielsen (2002), and Nielsen et al. (2003), selected the well 16-4-22-15W4 as the type section for the Niobrara Formation.

Schröder-Adams et al. (1998), incorrectly referred to the Medicine Hat Member as the “Medicine Hat Formation,” due to the lack of formal stratigraphic terminology for the upper Colorado Group existing at the time. However, their work, using macrofossils, microfossils, nannofossils and palynology in a biostratigraphic framework, proved that the "Medicine Hat Formation" falls within the Santonian stage, allowing for differentiation from the informally named "Sweetgrass Member," a sand-rich interval found within the First White Speckled Shale Member. The studies of Nielsen (2002), Nielsen et al. (2003), and Schröder-Adams et al. (1998), provide relatively extensive examples of wire-line log signatures for the upper Colorado Group. Furthermore, a regional interpretation of the complex sequence stratigraphy was attempted through a series of wire-line cross-sections spanning southern Alberta (Nielsen, 2002; Nielsen et al., 2003).

While it is clear that aspects of the upper Colorado Group stratigraphy have been established on a regional scale (Nielsen 2002; Nielsen et al., 2003; Nielsen et al., 2008), to date, authors have not concerned themselves with the local stratigraphy, related to small-scale depositional trends, in the Medicine Hat gas field. Therefore, the primary focus of this chapter is to introduce sequence stratigraphic concepts that are tied to lithostratigraphic units in order to understand the spatial and temporal significance of the major lithofacies observed within the Medicine Hat Member, in the region of the Medicine Hat gas field. This analysis will demonstrate the stratigraphic rationale for imparting a subaqueous clinoform depositional model, and provide evidence that important petroleum reservoir units can be mapped and targeted with a higher degree of predictability than previously recognized.

PALEOGEOGRAPHY AND TECTONIC SETTING

The Late Cretaceous in the western interior of North America was punctuated by repeated inundations of the Western Interior Seaway into the Western Canadian Foreland Basin (Schröder-Adams et al., 1997). During the deposition of the Niobrara Formation (late Turonian to early Campanian), the interaction of sea-level change and tectonics played a major role on the distribution of sedimentary environments. The Niobrara transgressive cycle, combined with downflexing of the western margin of the North American Craton, resulted in a regional sea-level highstand (Leckie and Smith, 1992).

The Niobrara highstand was characterized by the incursion of a broad, shallow marine seaway (Western Interior Seaway), which trended north and connected the Tethys Ocean (Gulf of Mexico) to the Boreal Sea (Gill and Cobban,

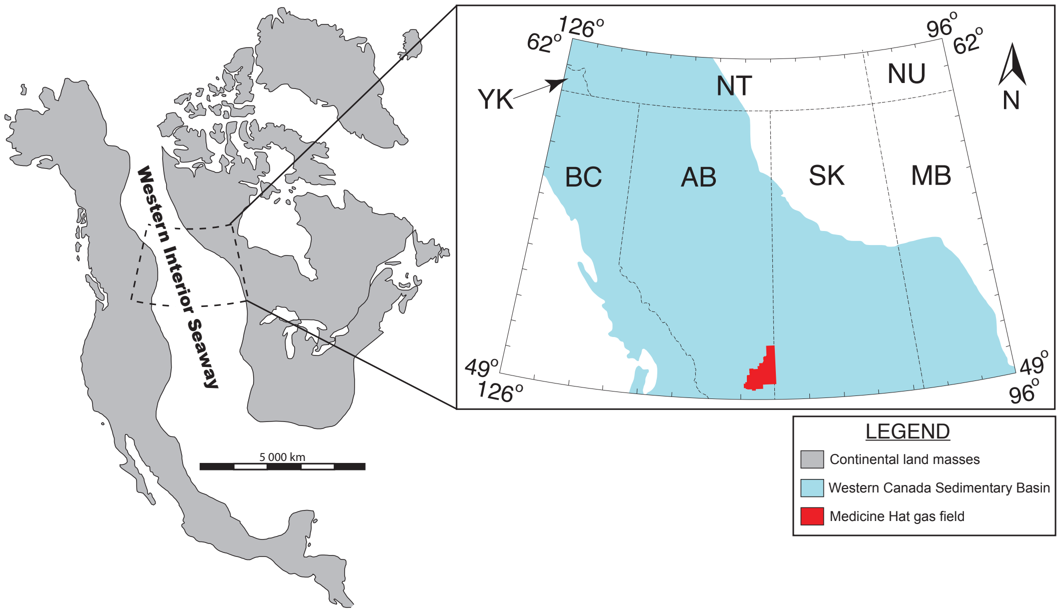

Figure III-2: The palaeogeography of North America during the Late Cretaceous. North America was inundated by a broad, shallow marine seaway (Western Interior Seaway) that trended north and connected the Tethys Ocean with the Boreal Sea. The seaway was bounded to the west by the rising cordillera, and to the east by the North American craton. Modified from Gill and Cobban (1973).

1973). The seaway was bound to the west by the rising cordillera, which ran along the Pacific Ocean, all the way from what is now Alaska to Central America (Figure III-2). At its widest, the seaway stretched up to 1600 kilometres. The sediments that were shed from the cordillera were ultimately the source for clastic fill within the western side of the basin, while the eastern side received sediment from the North American Craton. The cordilleran highland was relatively narrow, occupying approximately 500 000 square kilometres (Gill and Cobban, 1973).

The Sweetgrass Arch was a prominent palaeogeographic feature in the evolving interior of North America throughout the Cretaceous Period (Figure III-3). The history of the anticline dates back to the Silurian, with reactivation during the Mesozoic (Stelk, 1975). The broad anticline controlled the distribution of sediment deposited into the southern plains, resulting in sand being deposited in a setting otherwise dominated by shale (Schröder-Adams et al., 1997). Sediment from the mountains was "screened" across the high, starving the coarse-fraction from being supplied to the Williston Basin in the east (Stelck, 1975). Following studies on the basement control of deposition in the Western Canadian Sedimentary Basin (Stelck, 1975; Lorenz, 1982), the Sweetgrass Arch, a positive-relief tectonic feature, has been used to explain the presence of shallow marine

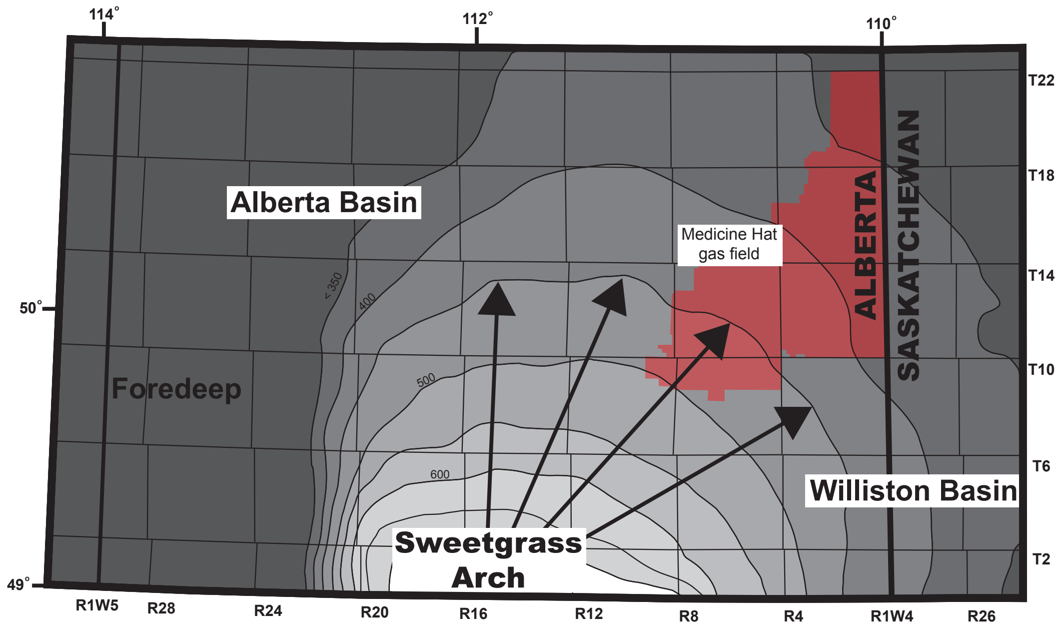

Figure III-3: The Sweetgrass Arch, a prominent palaeogeographic feature in the Western Canada Sedimentary Basin throughout the Cretaceous Period. The broad anticline affected the distribution of sediment deposited in the southern plains, screening the coarse-fraction from reaching the eastern part of southern Alberta. The feature has been used to explain the presence of relatively shallow marine deposits in an otherwise deeper marine setting (e.g., Schröder-Adams et al., 1997; Schröder-Adams et al., 1998). Modified from Nielsen, 2002.

fauna and sediments within a dominantly deeper marine setting (Schröder-Adams et al., 1997; Schröder-Adams et al., 1998).

METHODS AND STRATIGRAPHIC APPROACH

Petrophysical wire-line logs from 41 wells and 19 measured core intervals were used to construct a network of seven stratigraphic cross-sections (Figure III-4). The ideal wells were those that had an appropriate wire-line log suite necessary to produce accurate correlations, namely modern gamma-ray and resistivity logs. Well spacing was chosen to achieve maximum coverage across the Medicine Hat gas field, which spans approximately fourteen townships south to north, from Townships 8 to 22, and nine townships east to west, from Ranges 1 to 9, west of the fourth meridian. The field covers an area of approximately 12 000 square kilometres.

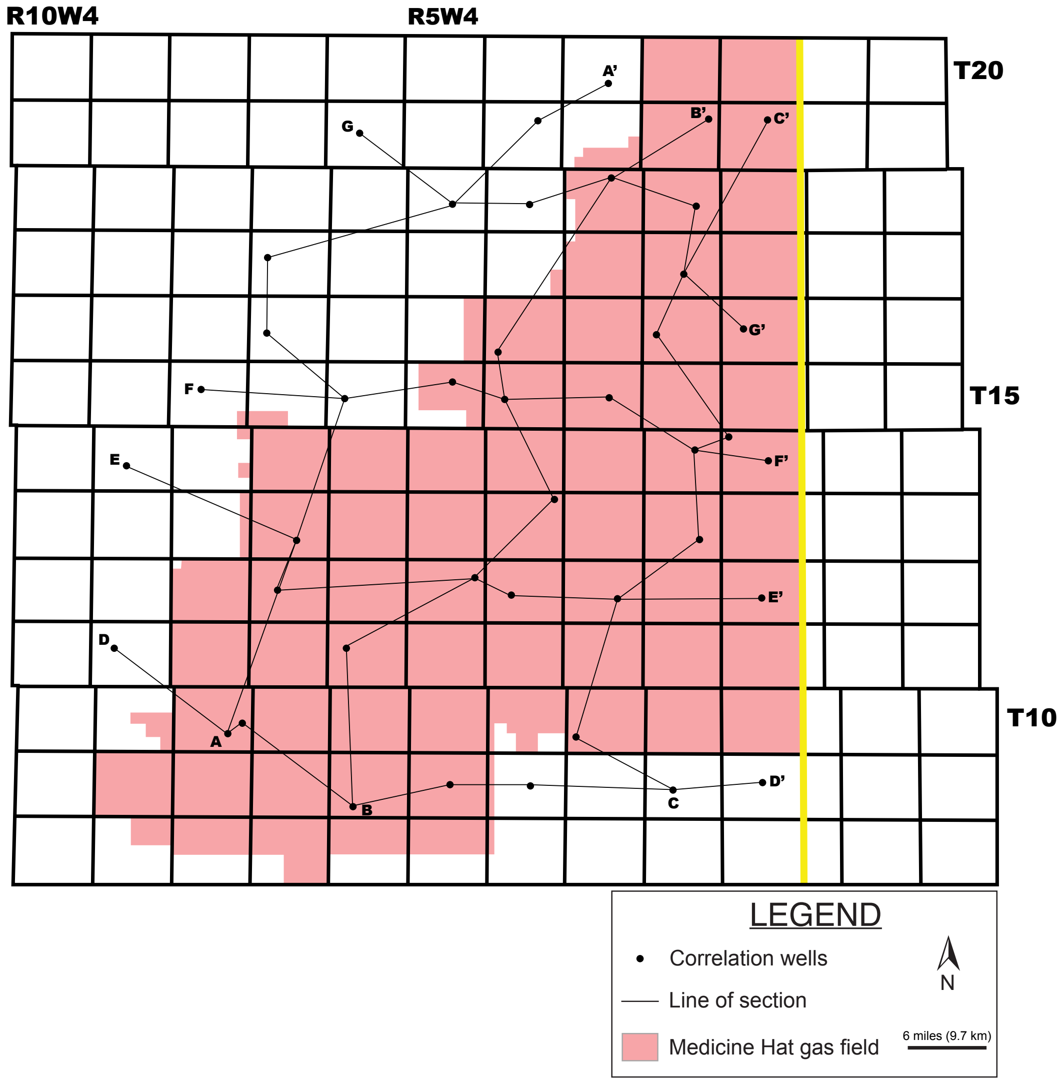

Figure III-4: The network of seven stratigraphic cross-sections used for stratigraphic analysis of the Medicine Hat Member. The cross-sections used petrophysical wire-line logs from 41 wells and 19 measured core intervals. Well spacing was chosen to achieve maximum coverage across the Medicine Hat gas field. Sections A-A', B-B', and C-C' are approximately dip-oriented, whereas sections D-D', E-E', F-F', and G-G' are arranged approximately strike-oriented.

Cored intervals were logged in terms of grain-size, primary physical sedimentary structures, ichnology, and the nature of facies contacts. Based upon the core data, a facies classification scheme was erected and a depositional system was interpreted (see Chapter II). Individual facies associations from logged sections were compared against their corresponding wire-line log signatures in order to recognize the facies associations in wells where no core data was available. This method was then applied to produce cross-sections of the Medicine Hat Member, which were correlated to visualize the lithostratigraphic architecture.

Three dip-oriented cross-sections (A-A', B-B', and C-C'; Figure III-5 to Figure III-7), and four strike-oriented cross-sections (D-D', E-E', F-F', and G-G'; Figure III-8 to Figure III-11) comprise the network. All the wells are tied to core, and a number of wells are used in both strike- and dip-sections. The Sweetgrass Arch to the west of the study area was subtly resolved in these cross-sections (see Figure III-8).

The approach herein is primarily lithostratigraphic, where bedset/facies association contacts are not implied as time-lines. The sequence stratigraphic interpretation and discussion to follow give insight into the basinal processes controlling facies architecture and a very general chronology of deposition. For a broader regional chronostratigaphy, one should consider the work by Schröder-Adams et al. (1998), Nielsen (2002), and Nielsen et al. (2003).

DESCRIPTION AND INTERPRETATION OF STRATIGRAPHIC CROSS-SECTIONS

All sections in this study hang on a datum at the top of the Second White Specks Formation, which closely approximates the configuration of the region at the time of deposition. This zone displays several distinctively high gamma-ray spikes, making log picks easy. Formation tops for units other than the Medicine Hat are based on the upper Colorado Group stratigraphy presented in Schröder-Adams et al. (1997), Nielsen (2002), and Nielsen et al. (2003).

Descriptions and Lithostratigraphic Correlation

Location of Sections

Section A, the first of three dip-oriented sections, is on the western margin of the Medicine Hat gas field, and comprises eight wells from 6-10-10-8W4 north to 6-10-20-3W4, a distance of approximately 130 kilometres (Figure III-5). Section B is oriented through the middle of the field and encompasses eight wells, from 10-4-9-6W4 in the south to 13-24-19-2W4 in the north, a distance of 126 kilometres (Figure III-6). The third dip-section, Section C, is composed of nine

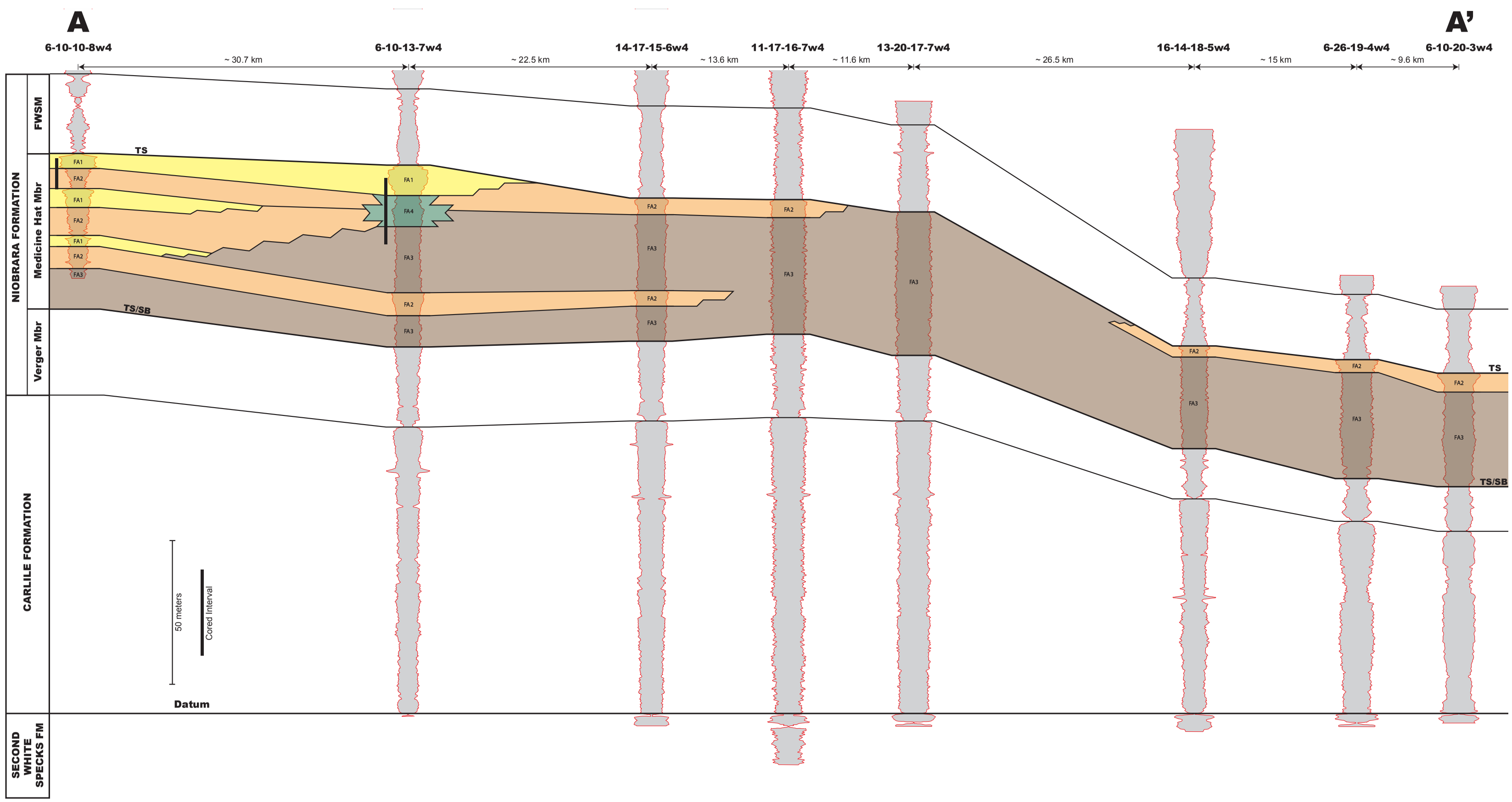

Figure III-5: Stratigraphic cross-section A-A'. The section is the first of three dip-oriented sections in the network of cross-sections, roughly tracing the western limit of the Medicine Hat gas field. The section contains eight wells, from 6-10-10-8W4 in the south, to 6-10-20-3W4 in the north, a distance of 130 km. Three stacked parasequences are interpreted in the southern part of the section, as well as one bay deposit. FA1 is shown in yellow, FA2 in orange, FA3 brown, and FA4 in green. Cored intervals are marked by solid black lines next to the respective curves. Gamma-gamma curves (butterfly curves) were used for accurate correlations. The datum for all sections is the top of the Second White Specks Formation. Transgressive surfaces are denoted by TS, and sequence boundaries are marked by the abbreviation SB. See body of text for discussion of interpretations.

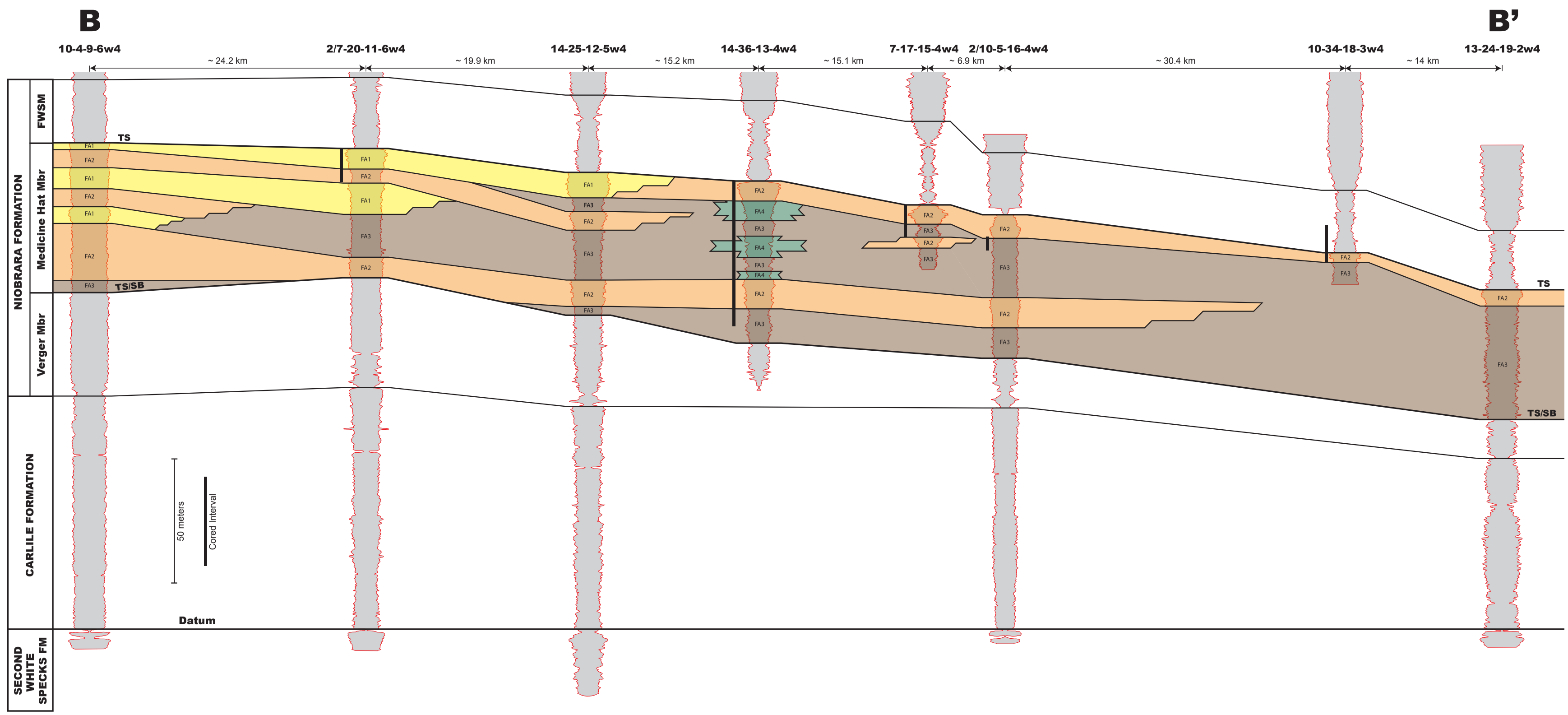

Figure III-6: Stratigraphic cross-section B-B’. The section is the second of three dip-oriented sections in the network of cross-sections, roughly tracing the middle of the Medicine Hat gas field. The section contains eight wells, from 10-4-9-6W4 in the south, to 13-24-19-2W4 in the north, a distance of 126 km. Three stacked paraseqences are interpreted in the southern part of the section, as well as one subaqueous bay. FA1 is shown in yellow, FA2 in orange, FA3 in brown, and FA4 in green. Cored intervals are marked by solid black lines next to the respective curves. Gamma-gamma curves (butterfly curves) were used for accurate correlations. The datum for all sections is the top of the Second White Specks Formation. Transgressive surfaces are denoted by TS, and sequence boundaries are marked by the abbreviation SB. See body of text for discussion of interpretations.

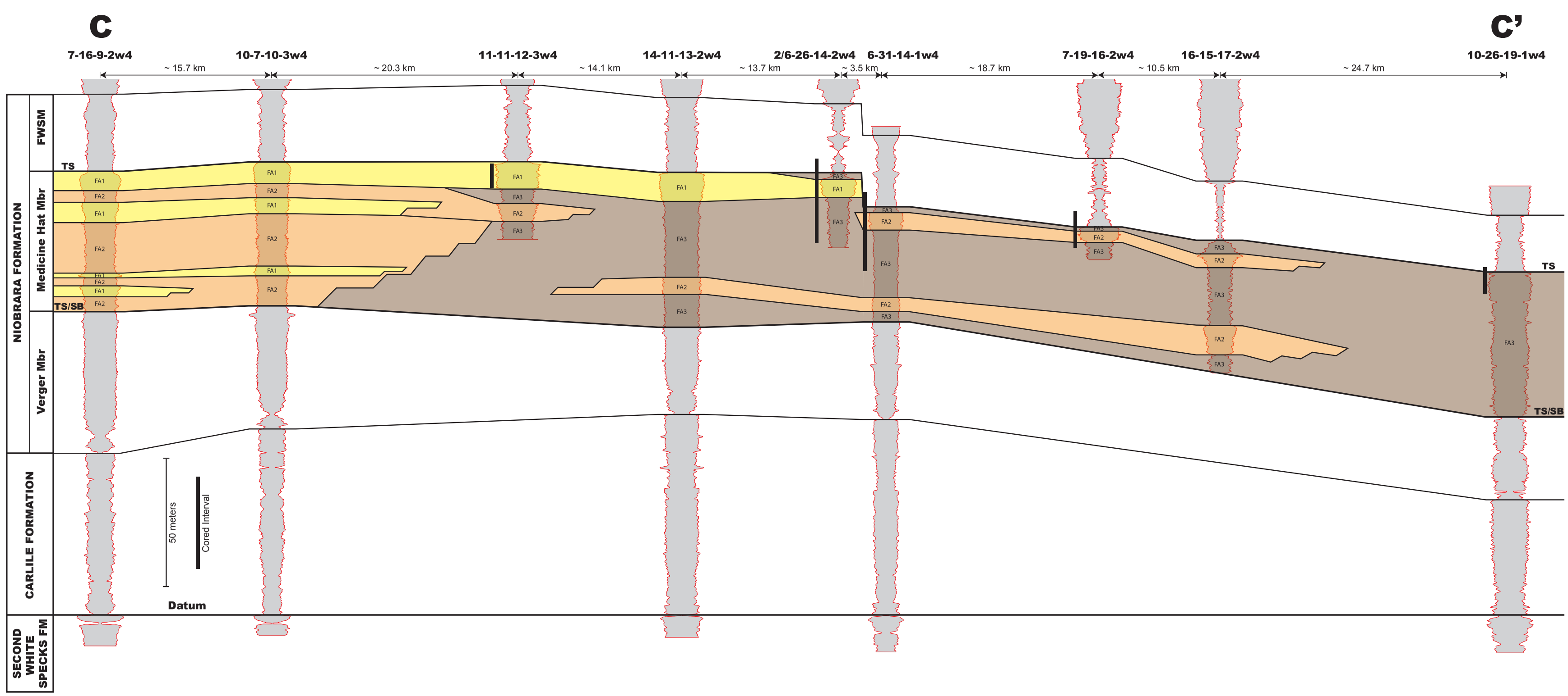

Figure III-7: Stratigraphic cross-section C-C'. The section is the third of three dip-oriented sections in the network of cross-sections, roughly tracing the eastern limit of the Medicine Hat gas field. The section contains nine wells, from 7-16-9-2W4 in the south, to 10-26-19-1W4 in the north, a distance of 121 km. Four stacked paraseqences are observed in the southern part of the section. FA1 is shown in yellow, FA2 in orange, FA3 in brown, and FA4 in green. Cored intervals are marked by solid black lines next to the respective curves. Gamma-gamma curves (butterfly curves) were used for accurate correlations. The datum for all sections is the top of the Second White Specks Formation. Transgressive surfaces are denoted by TS, and sequence boundaries are marked by the abbreviation SB. See body of text for discussion of interpretations.

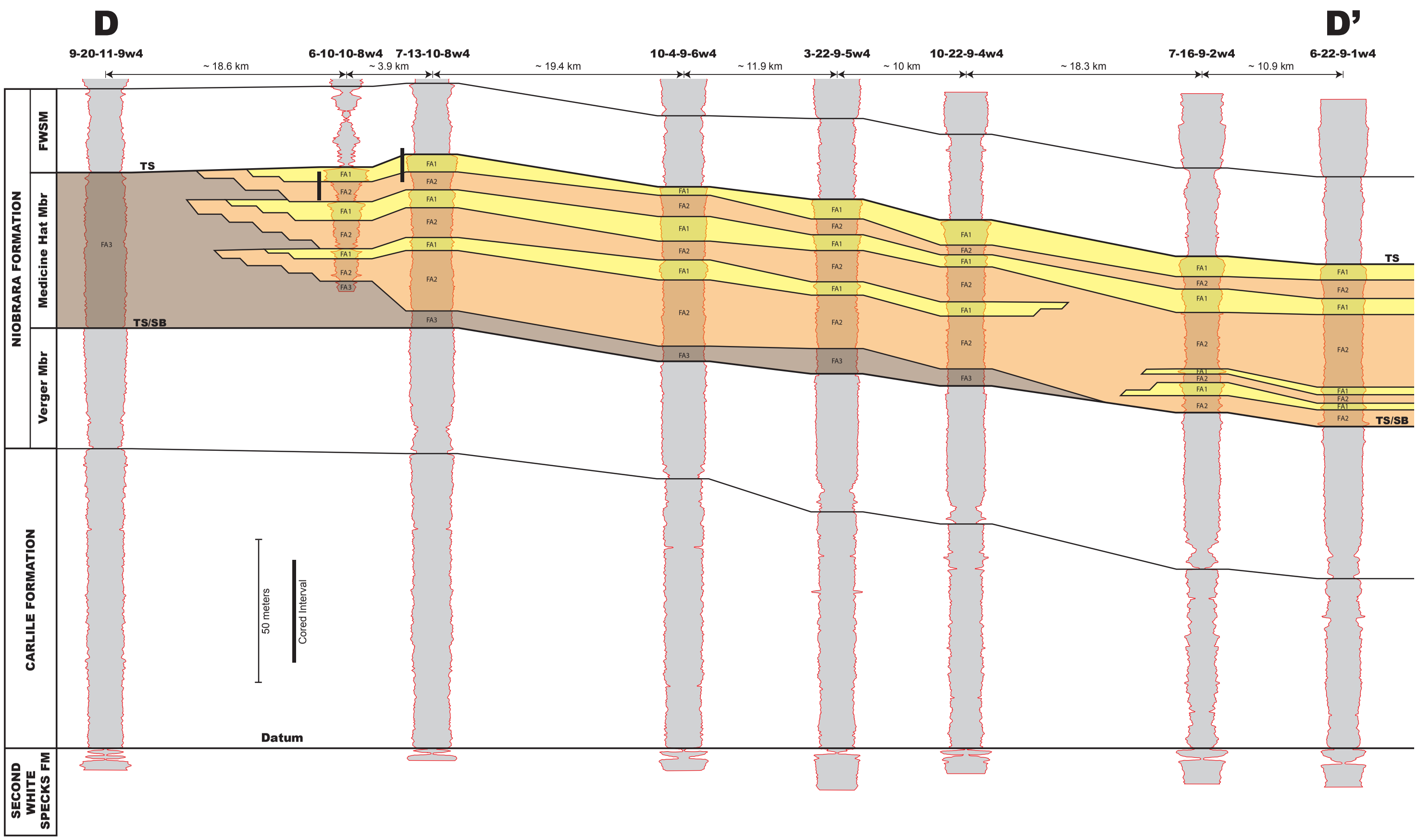

Figure III-8: Stratigraphic cross-section D-D’. The section is the first of four strike-oriented sections in the network of cross-sections, located near the southern limit of the Medicine Hat gas field. The section contains eight wells, from 9-20-11-9W4 in the west, to 6-22-9-1W4 in the east, a distance of over 93 km. All five parasequences occuring in the Medicine Hat Member can be seen in the section. FA1 is shown in yellow, FA2 in orange, FA3 in brown, and FA4 in green. Cored intervals are marked by solid black lines next to the respective curves. Gamma-gamma curves (butterfly curves) were used for accurate correlations. The datum for all sections is the top of the Second White Specks Formation. Transgressive surfaces are denoted by TS, and sequence boundaries are marked by the abbreviation SB. See body of text for discussion of interpretations.

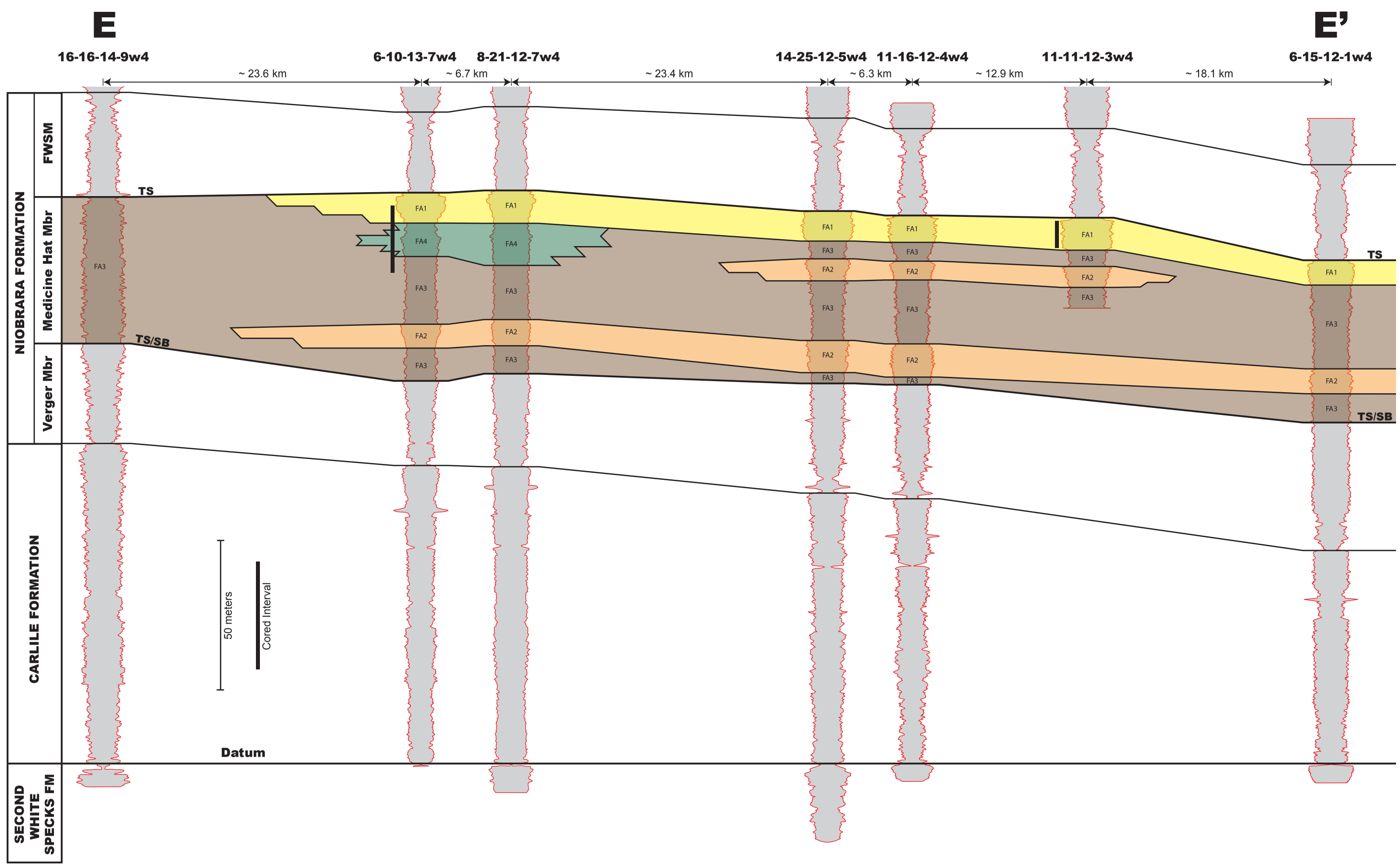

Figure III-9: Stratigraphic cross-section E-E’. The section is the second of four strike-oriented sections in the network of cross-sections, located in the mid-southern portion of the Medicine Hat gas field. The section contains seven wells, from 16-16-14-9W4 in the west, to 6-15-12-1W4 in the east, a distance of 91 km. Portions of two parasequences and one bay deposit can be observed in the section. FA1 is shown in yellow, FA2 in orange, FA3 in brown, and FA4 in green. Cored intervals are marked by solid black lines next to the respective curves. Gamma-gamma curves (butterfly curves) were used for accurate correlations. The datum for all sections is the top of the Second White Specks Formation. Transgressive surfaces are denoted by TS, and sequence boundaries are marked by the abbreviation SB. See body of text for discussion of interpretations.

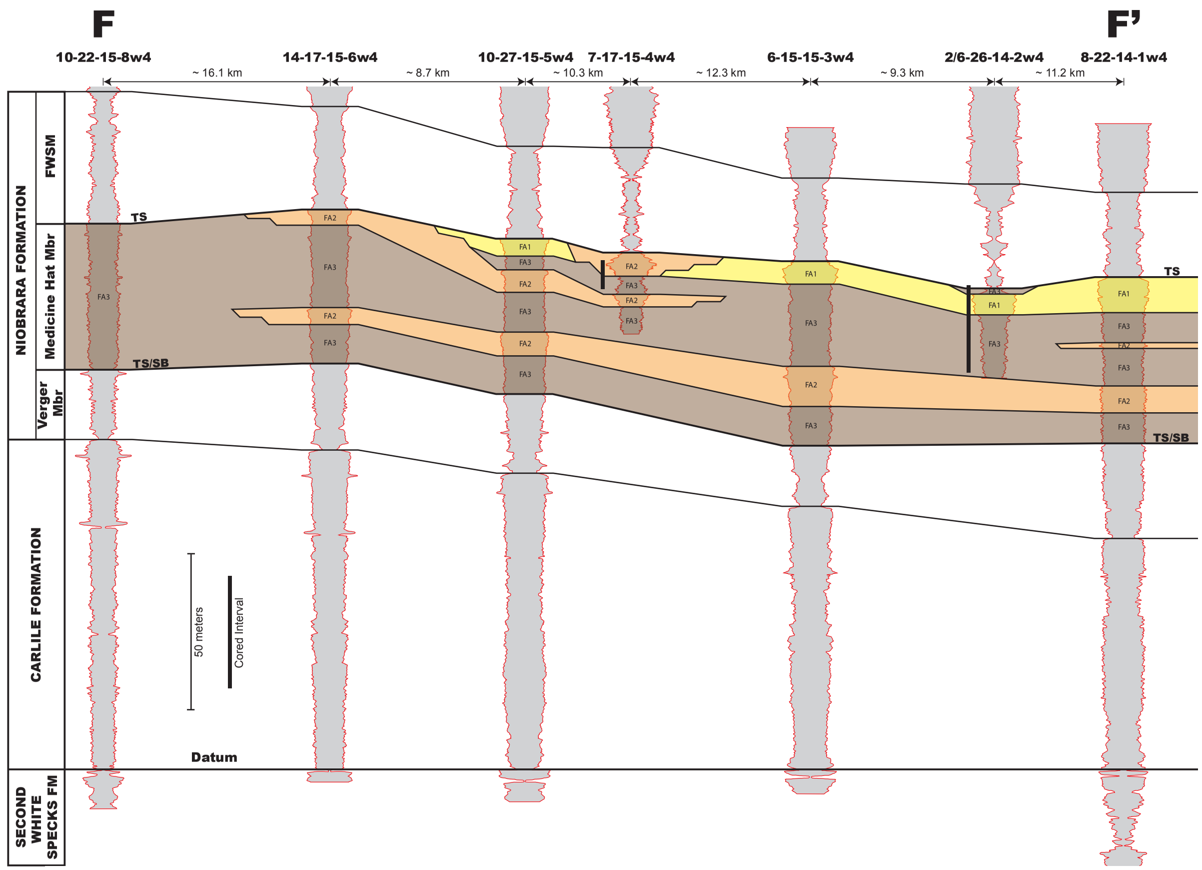

Figure III-10: Stratigraphic cross-section F-F'. The section is the third of four strike-oriented sections in the network of cross-sections, located in the mid-northern portion of the Medicine Hat gas field. The section contains seven wells, from 10-22-15-8W4 in the west, to 8-22-14-1W4 in the east, a distance of 73 km. Portions of at least two parasequences can be observed in the section. FA1 is shown in yellow, FA2 in orange, FA3 in brown, and FA4 in green. Cored intervals are marked by solid black lines next to the respective curves. Gamma-gamma curves (butterfly curves) were used for accurate correlations. The datum for all sections is the top of the Second White Specks Formation. Transgressive surfaces are denoted by TS, and sequence boundaries are marked by the abbreviation SB. See body of text for discussion of interpretations.

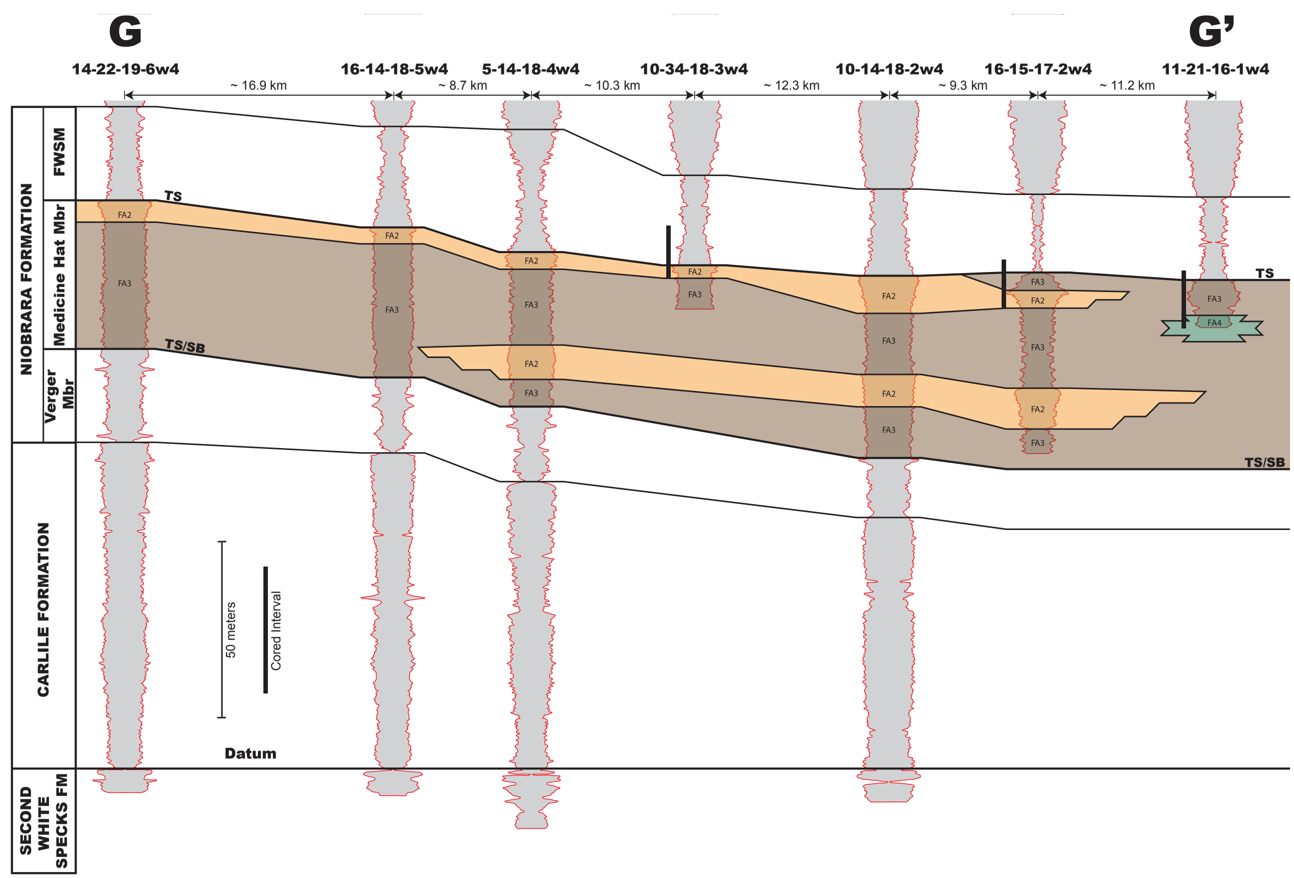

Figure III-11: Stratigraphic cross-section G-G'. The section is the last of four strike-oriented sections in the network of cross-sections, located roughly at the northern limit of the Medicine Hat gas field. The section contains seven wells, from 14-22-19-6W4 in the west, to 11-21-16-1W4 in the east, a distance of 69 km. The toe of two parasequences and one bay deposit can be observed in the section. FA1 is shown in yellow, FA2 in orange, FA3 in brown, and FA4 in green. Cored intervals are marked by solid black lines next to the respective curves. Gamma-gamma curves (butterfly curves) were used for accurate correlations. The datum for all sections is the top of the Second White Specks Formation. Transgressive surfaces are denoted by TS, and sequence boundaries are marked by the abbreviation SB. See body of text for discussion of interpretations.

wells spanning 121 kilometres, from 7-16-9-2W4 to 10-26-19-1W4 (Figure III-7).

Four cross-sections were arranged orthogonal to the dip-sections, demonstrating the along-strike variation in the Medicine Hat stratigraphy. Section D strikes east to west and contains eight wells that stretch over 93 kilometres, from 9-20-11-9W4 to 6-22-9-1W4 (Figure III-8). Further north, Section E, comprises seven wells, from 16-16-14-9W4 to 6-15-12-1W4, a span of 91 kilometres (Figure III-9). Section F encompasses seven wells that extend approximately 73 kilometres, from 10-22-15-8W4 in the west to 8-22-14-1W4 to the east (Figure III-10). Finally, Section G consists of seven wells from 14-22-19-6W4 to 11-21-16-1W4, covering roughly 69 kilometres of section (Figure III-11).

Contacts and Lithostratigraphic Units

Five stacked cycles of deposition are observed in the study area. The base of the first cycle occurs on an unconformable contact with the underlying, shaly Verger Member. The contact is a pebbly lag that contains a thin layer of calcareous ooids, glauconite, fish and bone debris, and is cemented with siderite (Nielsen, 2002; Nielsen et al., 2003; Nielsen et al., 2008). Subtle evidence of reworked palaeosols was observed in the lag (Nielsen, 2002). Across the majority of the study area, bottomset deposits (FA3) occur above the contact, with exception of the extreme southeast portion (Sections C and D; Figures III-7 and III-8), where a relatively thin draping (less than 10 metres) of distal foreset strata (FA2) is present. The distal foreset extends northward into Township 10 and interdigitates with the bottomset. Above, a thin interval (up to 5 metres) of proximal foreset (FA1) sediments conformably overlay the distal foreset facies. The most sand-prone FA1 strata are confined to the southeastern corner of the field and stretch northwest to 10-3W4 (Figure III-12). Adjacent strata (distal foreset and bottomset) interdigitate with, and apron the locus of FA1 deposition to the north, and west. Stratal terminations are not observed up-dip (south), but basinward, they appear to downlap onto the Verger Member. A flooding surface at the top of the succession marks the end of the initial progradational cycle.

The second depositional cycle lies directly above a flooding surface and constitutes proximal foreset sediments, up to 4 metres thick, stacked over the more distal counterparts of FA2, which vary in thickness up to a few tens of

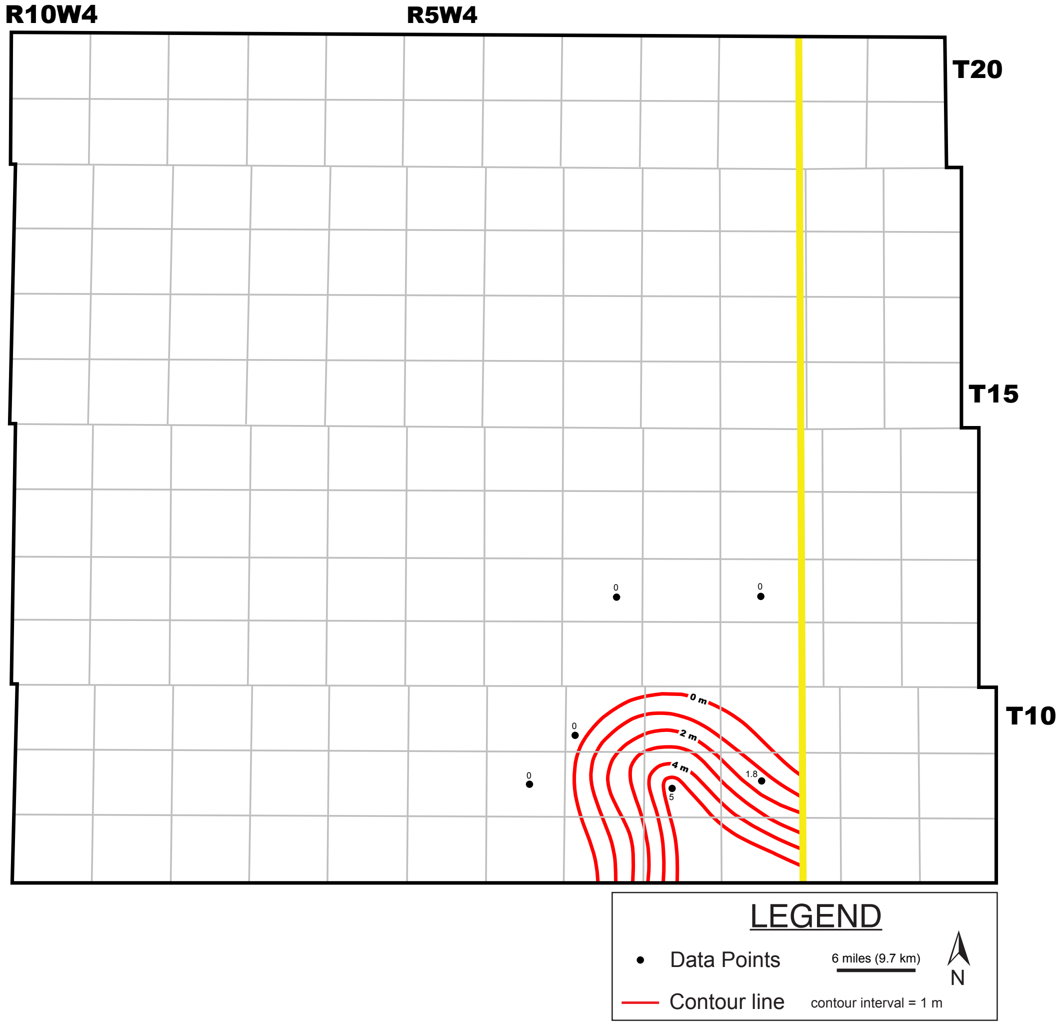

Figure III-12: An isopach map showing the distribution of the proximal foreset region (FA1), interpreted to represent part of the lowermost parasequence in the Medicine Hat gas field.

metres (Figure III-13). The proximal portion of the foreset is limited in extent; it is observed only in the southeast corner of the Medicine Hat field (Sections C and D; Figures III-7 and III-8). The locus of deposition for the proximal foreset occurs farther to the northeast, compared to the initial depositional succession, occurring around 10-2W4. Laterally adjacent to the foreset, strata interdigitate with the bottomset. The succession is observed downlapping older strata basinward. A flooding surface marks the top of this second progradational cycle.

The third succession is relatively thicker than those stratigraphically lower, with the proximal foreset ranging up to 7 metres thick in the study area (Figure III-14). The strata in this cycle occur above a flooding surface, separating it from older cycles. The proximal foreset is more widespread than lower foreset deposits,

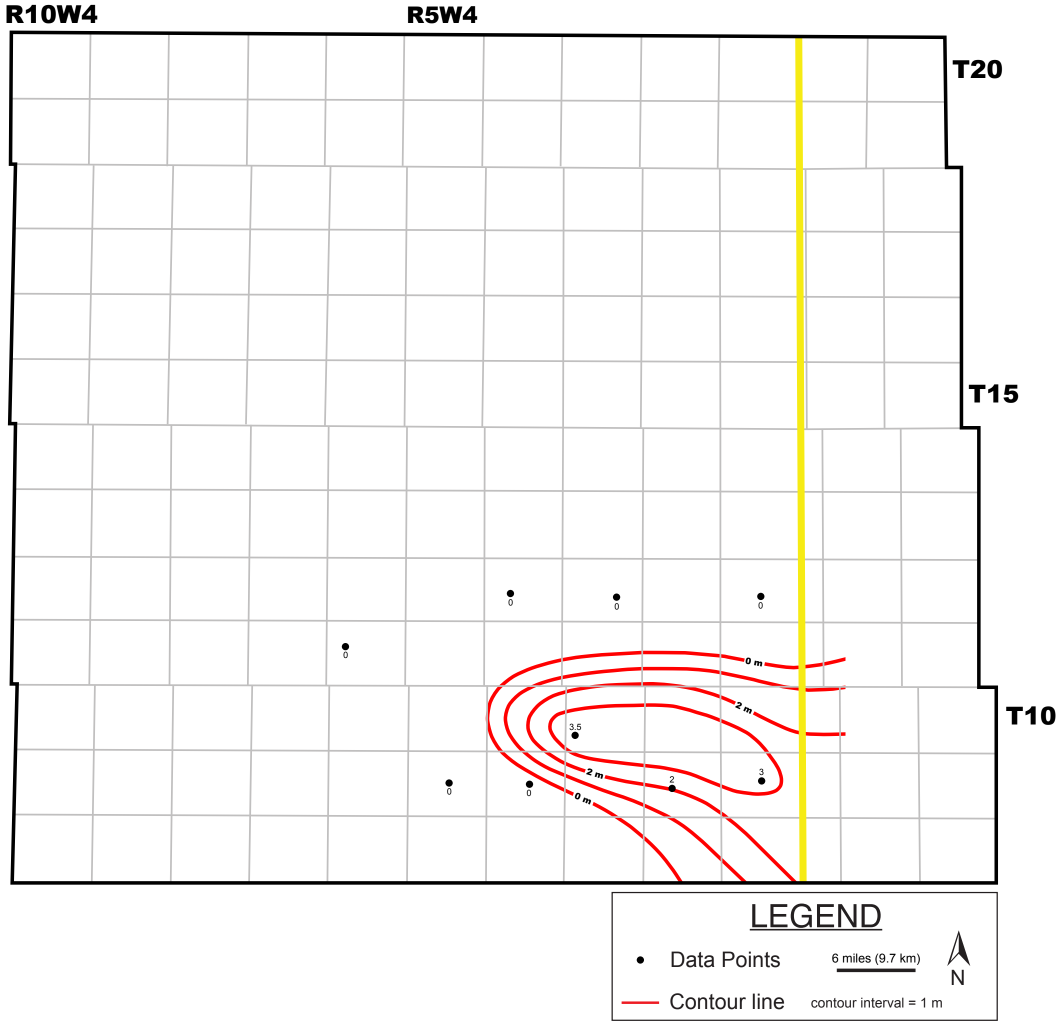

Figure III-13: An isopach map showing the distribution of the proximal foreset region (FA1), interpreted to represent part of the second parasequence in the Medicine Hat gas field.

being greater than 70 kilometres at the widest point. During deposition, the locus shifted southwest between 8-6W4 and 8-7W4. Undifferentiated bottomset sediments (FA3) are observed distal to the main foreset deposits (FA1 and FA2), and interdigitate with them. Overall, the deposits downlap older strata.

A fourth cycle comprises stacked relatively thick (tens of metres) distal foreset deposits, underlying thinner (up to 13 metres thick) proximal foreset strata. The succession is very similar sedimentologically to the underlying cycles. It is separated from Cycle C by a discontinuity (flooding) surface. The foreset (FA1 and FA2), occurs throughout the southern half of the Medicine Hat gas field, stretching west of 6-10-10-8W4, eastwards into Saskatchewan, and as far north as Township 14 (Figure III-15). The depocenter of this succession occurs

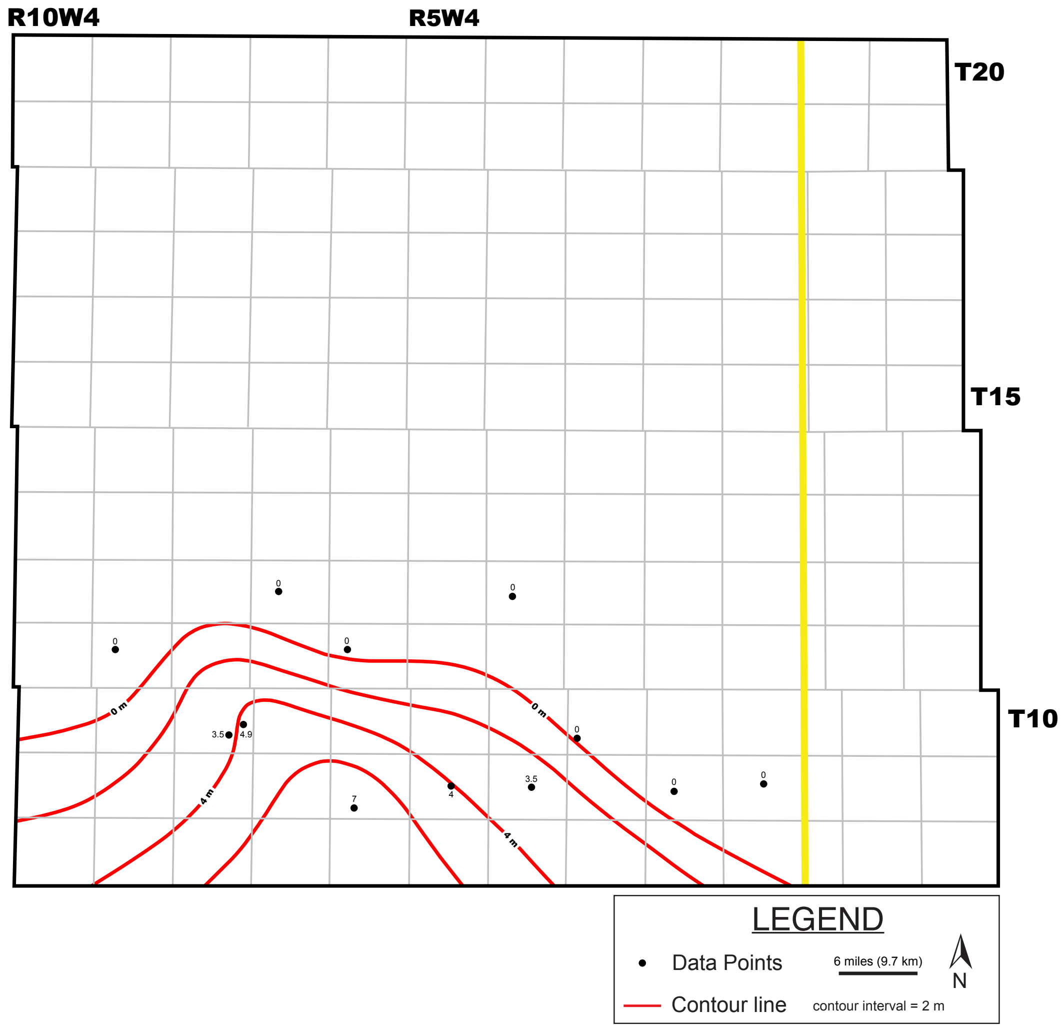

Figure III-14: An isopach map showing the distribution of the proximal foreset region (FA1), interpreted to represent part of the third parasequence in the Medicine Hat gas field.

approximately in 11-6W4, where up to 13 metres of proximal foreset sediments are preserved. Interdigitating distal foreset (FA2) and bottomset (FA3) strata mark the transition across which there is little significant deposition of sand, primarily to the north of the depocenter. The strata are observed to downlap onto the bottomset.

The fifth and youngest depositional cycle recognized in the Medicine Hat Member shows the greatest northward extension of proximal and distal foreset deposits. The cycle is composed of proximal foreset deposits (FA1), up to 11 metres thick, overlying thinner distal foreset (FA2) sediments. The deposits began west of 6-10-10-8W4, stretching east of the study area into Saskatchewan, and as far north as Township 16. The final phase of foreset building occured directly

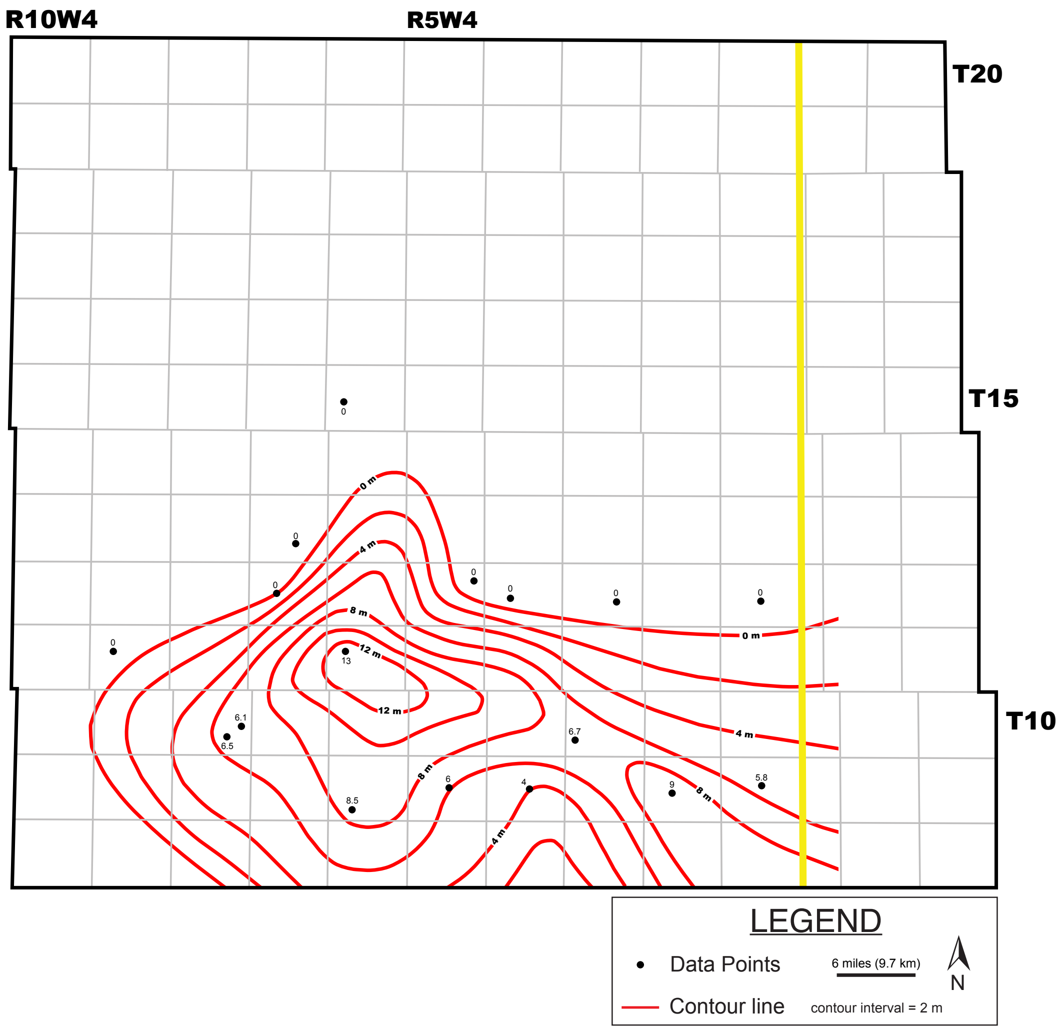

Figure III-15: An isopach map showing the distribution of the proximal foreset region (FA1), interpreted to represent part of the fourth parasequence in the Medicine Hat gas field.

above a flooding surface, separating it from the sediments of the next oldest cycle. The locus of sandstone deposition can be characterized as an arcuate band, approximately 2 townships wide (~20 kilometres), trending east to west, in the vicinity of Townships 12 and 13 (Figure III-16). Basinward of the foreset deposits, an interdigitating accumulation of thick (tens of metres) bottomset strata typifies the study area. The strata downlap onto the older Medicine Hat deposits. The five depositional cycles are summarized in Figure III-17, where each consecutive foreset is shown overlain upon its younger counterpart.

In addition to the five major cycles of foreset deposition, there are smaller, less significant sandy bodies that occur within subaqeous bays (FA4), between the actively prograding clinoforms (Figure III-18). Five bay deposits are mapped;

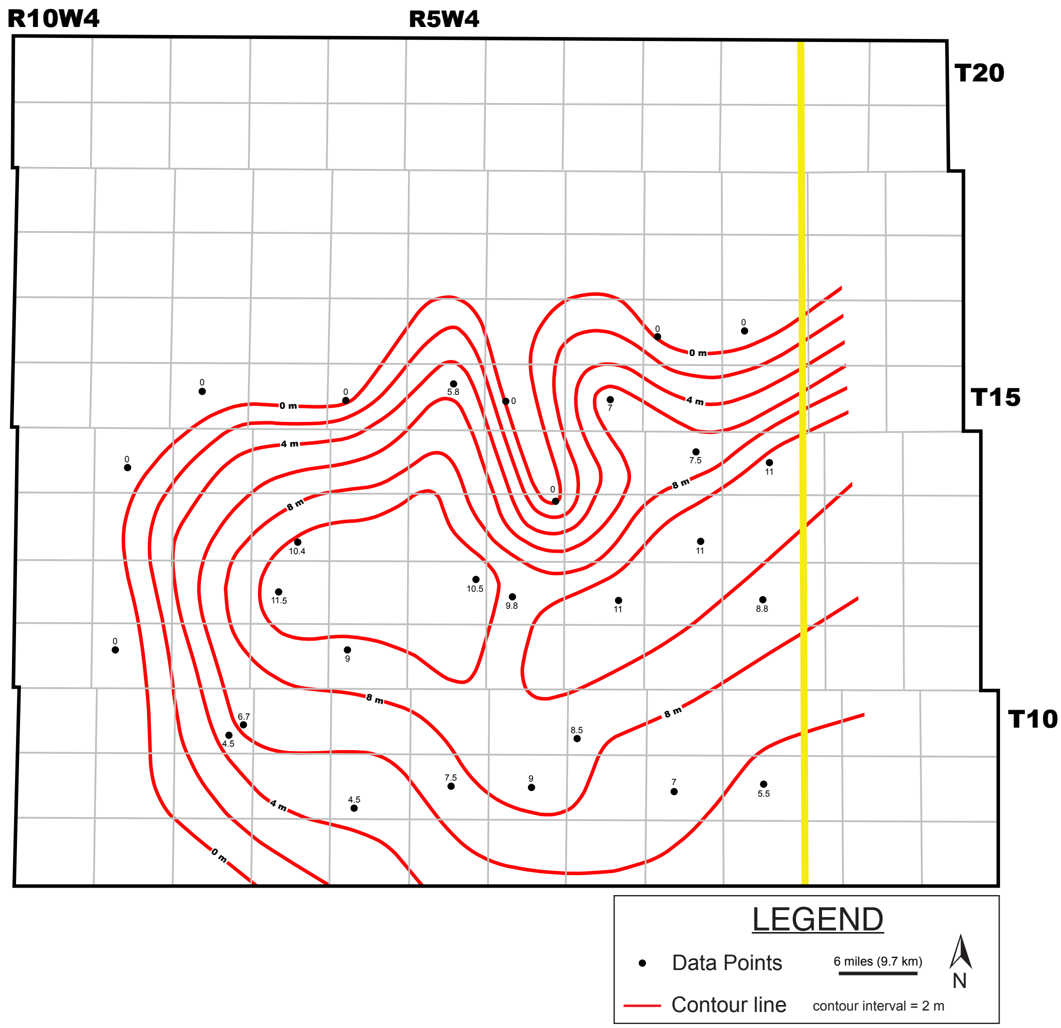

Figure III-16: An isopach map showing the distribution of the proximal foreset region (FA1), interpreted to represent part of the fifth parasequence in the Medicine Hat gas field.

they are inferred to be associated with the upper three stratigraphic cycles (Cycles 3, 4, and 5).

SEQUENCE STRATIGRAPHY

Sequence Stratigraphic Model

The network of cross-sections allowed for detailed observations of the depositional stratal stacking patterns. Using the principles and terminology of sequence stratigraphy (Catuneanu, 2006; Catuneanu et al., 2009; Van Wagoner et al., 1988; Van Wagoner et al., 1990), the Medicine Hat Member is put into a

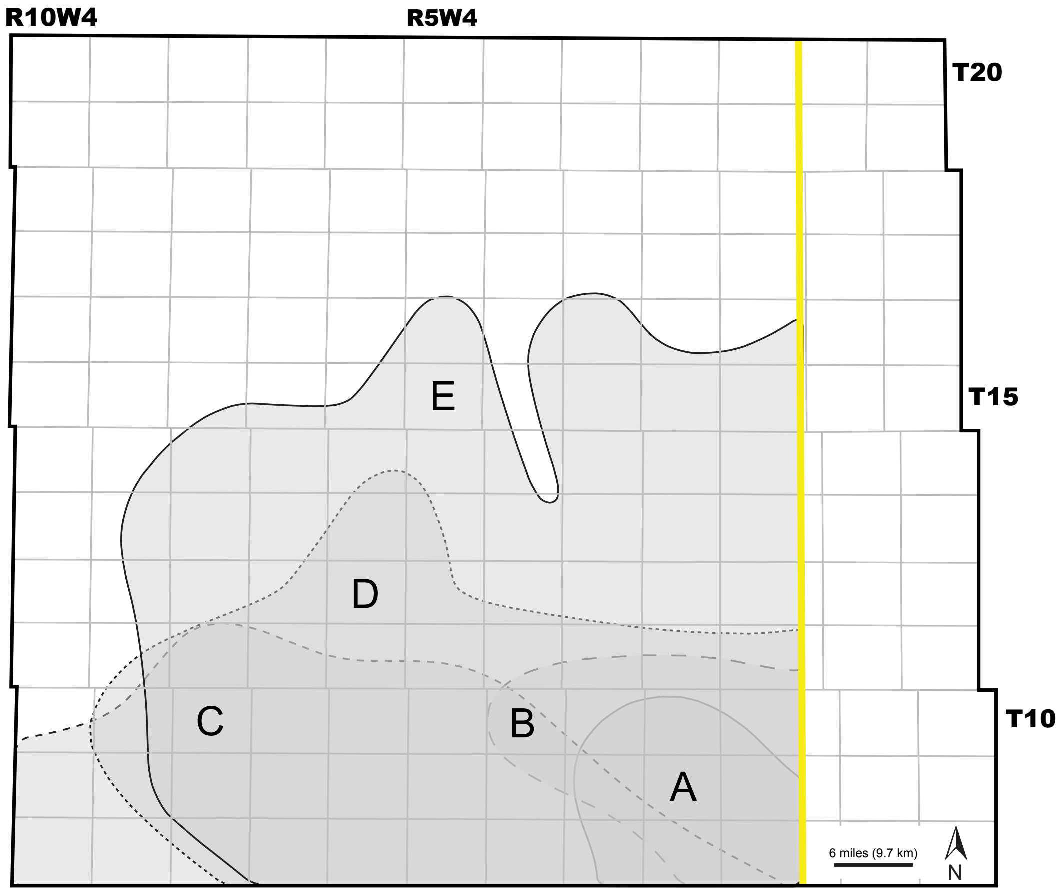

Figure III-17: Summary diagram showing the progradational nature of the parasequences in the Medicine Hat gas field region. The traced geobodies represent the various FA1 distributions through time with A being the oldest and E being the youngest.

quasi-chronostratigraphic framework, where the relationships to the underlying Verger Member and overlying First White Specks Member are explained by changes in relative sea-level.

A number of sequence stratigraphic models exist in the literature, the primary difference between them being the surfaces elevated to sequence boundary (Catuneanu, 2006; Catuneanu et al., 2009). Of the four most commonly applied models (i.e., Type-1 Depositional Sequences; Posamentier et al., 1988; Type-2 Depositional Sequences; Posamentier et al., 1988; Genetic Stratigraphic Sequences; Galloway, 1989; and Transgressive-Regressive Sequences; Embry and Johannessen, 1992), the Type-2 Depositional Sequence Model of Posamentier et al. (1988) is chosen herein to describe the sequence stratigraphy, because it uses the subaerial unconformity and its marine correlative conformity as the sequence boundary.

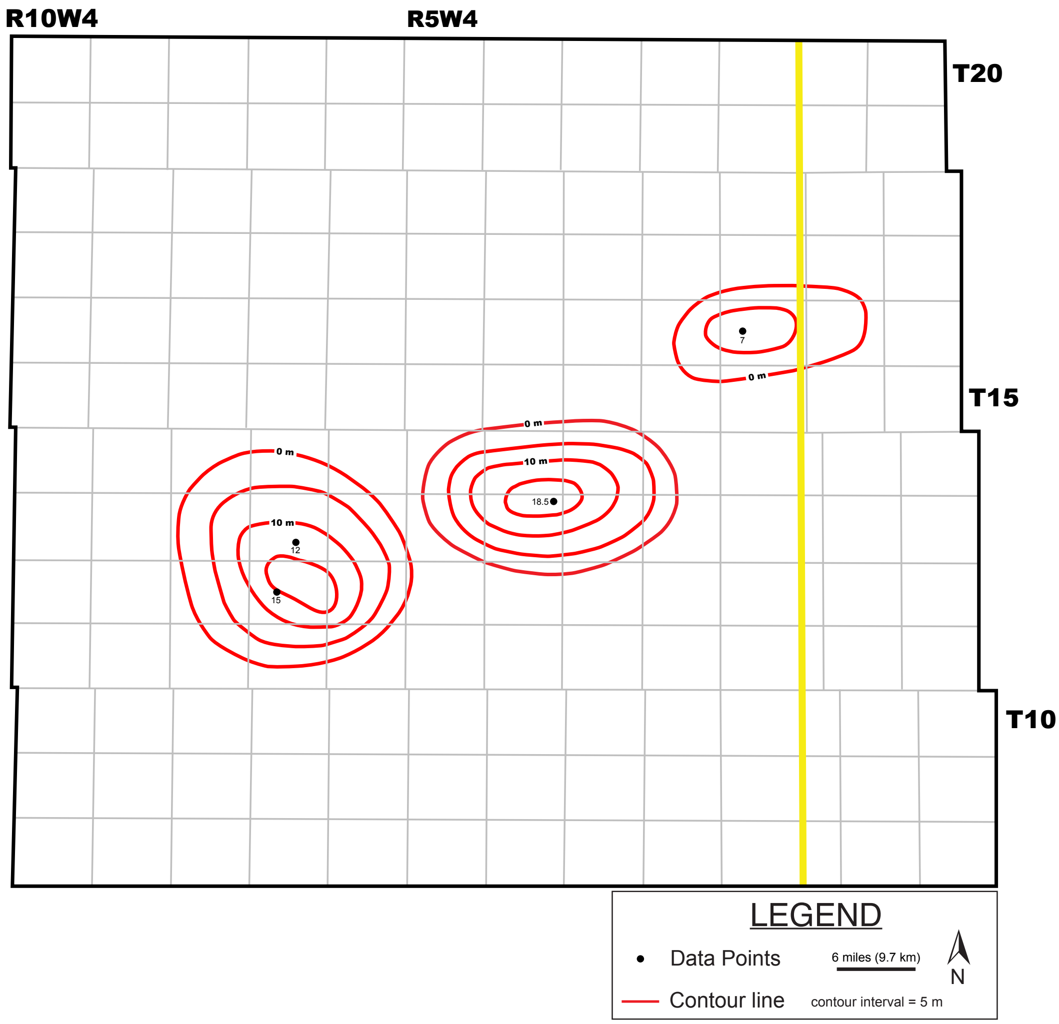

Figure III-18: An isopach map showing the distribution of FA4 (subaqueous bay deposits).

Surfaces and Parasequences

The disconformable lower contact of the Medicine Hat Member is a pebbly transgressive lag throughout much of southern Alberta. It was deposited as a result of an increase in relative sea-level that transgressed the Verger Member (Nielsen, 2002; Nielsen et al., 2003). The pebbly lag provides petrographic evidence for reworked palaeosols. Nielsen (2002), interpreted it to be the cannibalized lowstand deposits of the Verger Member, subsequently eroded during transgression. In a sequence stratigraphic framework, the surface reflects a co-planar sequence boundary/flooding surface.

Overall, the stratal stacking observed in the Medicine Hat gas field is interpreted as a progradational parasequence set (*sensu* Van Wagoner et al., 1990) comprising five parasequences. The parasequences show no significant change in the depositional regime. Each parasequence, excepting the lowermost and uppermost, is bound above and below by local flooding surfaces. The flooding surfaces are most likely autogenic - the result of cyclic clinoform progradation or short-term reductions in the relative ratios of sedimentation to available accommodation space. Moreover, the ratio of sedimentation to accommodation space appears to have increased through time as the Medicine Hat system evolved. This is evidenced by the presence of subaqeous bays in the upper three parasequences, combined with thicker and more widespread foreset deposits. The influence of the Sweetgrass Arch on sediment distribution appears to decrease throughout the deposition of the Medicine Hat Member. However, the broad anticline strongly affected deposition in the study area, as proximal (foreset) facies downlap and interdigitate with distal (bottomset and offshore) facies, within a short distance east and north of the gas field. This is contrary to the depositional systems that might be expected in a distal portion of the basin (Schröder-Adams et al., 1997). It is uncertain how far east the parasequences stretch, as the dataset was limited to southeastern Alberta, and cores and wire-line logs from southwestern Saskatchewan were not considered in the study. The interval has not been extensively studied to the east.

The upper bounding surface of the Medicine Hat parasequences is a sequence boundary that separates underlying prograding sandy strata from calcareous mud-prone strata (Nielsen, 2002; Nielsen et al., 2003). The surface is manifest as a decimetre thick concentration of shells, or calcareous debris, with variable amounts of reworking and dissolution. In some instances, the surface shows current and wave lineated belemnites. Presumably, the surface indicates subaerial exposure during a minor fall in sea-level, where calcareous debris was partially dissolved and reworked.

The major flooding event following deposition and exposure of Medicine Hat strata was the most extensive in the Niobrara sea-level cycle. This resulted in a dramatic increase in accommodation space that was matched by very low sedimentation rates (Nielsen, 2002). The water depths and depositional regime changed significantly, from a relatively shallow water system (this study) to a distal offshore environment (Nielsen, 2002). Throughout Medicine Hat time, accommodation space was created to the northwest, and filled from the southeast, as indicated by the northwest migration of the locus of deposition for each parasequence. It is interpreted that accommodation space was approximately matched by deposition, since progradation of the clinoforms dominated over aggradation. The shoreline trajectory is indicative of normal progradation as parasequences maintained a small degree of aggradation, opposed to forced regression, where younger parasequences have moved a significant distance offshore from older parasequences, without aggradation (Helland-Hansen and Martinsen, 1996; Catuneanu, 2006; Catuneanu et al., 2009). The upper bounding surface is interpreted to be a sequence boundary.

Systems Tracts

Sea-level periodically fluctuated throughout the Santonian in southern Alberta (Nielsen, 2002; Nielsen et al., 2003; Nielsen et al., 2008), resulting in a number of sequences and parasequences. Locally within the study area, relative sea-level (from combined eustacy and subsidence) was outpaced by sedimentation. The resulting progradational parasequences are illustrative of the complex relationship between tectonism (uplift and subsidence), eustacy, and sediment input differences on a regional scale. While parts of the basin experienced increases in relative sea-level, others experienced stillstand or a fall in relative sea-level during the deposition of the Niobrara Formation (Nielsen, 2002).

Based on the nature of the bounding sequence stratigraphic surfaces, where the base on the Medicine Hat Member is marked by a co-planar sequence boundary/flooding surface and the top is a sequence boundary, the progradational parasequence-set observed in the Medicine Hat gas field is interpreted as part of the Highstand Systems Tract (Posamentier et al., 1988; Catuneanu, 2006; Catuneanu et al., 2009). The flooding surface capping the unit resulted from an overall 2nd-order transgression (Niobrara Sea-level Cycle), where progradation of the Medicine Hat Member was a smaller-scale (3rd-order) relative sea-level fluctuation, that has been superimposed upon it. It is inferred that the First White Specks Member is a seperate sequence, backstepping to the south.

DISCUSSION

The stratal relationships in the Medicine Hat gas field are shown as a prograding parasequence set that is part of a HST. Based on the dataset and interpretations made in this study, it is not deemed necessary to locally invoke as complex a sequence stratigraphic interpretation as those of Nielsen (2002), Nielsen et al. (2003), and Nielsen et al. (2008). In the aforementioned studies, the Medicine Hat Member in southern Alberta is interpreted to comprise two sequences ("sequences F10 and F11"; Nielsen, 2002) that overlie a sequence boundary at the top of the Verger Member. Their sequence stratigraphic interpretation stems from using the Transgressive-regressive sequence model of Embry (1995), that uses major first flooding surfaces as sequence boundaries (Nielsen, 2002). The model was chosen because the author's deemed the surface the most easily recognizable surface in a lower shoreface to shelf environment. Within the two sequences of Nielsen (2002), a number of sand bodies are mapped throughout southern Alberta, and were inferred to belong to various Lowstand Systems Tracts, Transgressive Systems Tracts, and Highstand Systems Tracts. Particularly, four of the sand bodies mapped (i.e, Medicine Hat 4, 6, 6a, and 9 sandstones) appear to roughly correspond to the five highlighted in this study, though a direct correlation is difficult to understand and I have interpreted them all to belong to a single parasequence-set. It is difficult to place the results from this study into a wide-scale sequence stratigraphic framework, especially with the very local study area.

Choice of Datum

The datum used in the cross-sections corresponds to a series of regional bentonites that occur at the top of the Carlile Formation (Nielsen, 2002). The bentonite markers are an ideal choice for the datum because they are easily recognizable on wire-line logs, and were deposited with negligible stratigraphic dips. Coincidently, the bentonites were deposited just before a major change in the depositional regime occurred (Nielsen, 2002). The bentonite swarm indicates an increase in volcanic activity that coincided with a major tectonic episode in the Cordillera to the west, likely due to renewed thrusting in the south and southwest. Moreover, the renewed thrusting changed the overall basin geometry and source of sediment, resulting in marked differences in the lithology, sedimentology, geochemistry, and micropaleontology across the boundary. In the southern plains, the bentonites have been used as stratigraphic markers (Nielsen, 2002).

To illustrate the importance of choosing a suitable datum for the stratigraphic correlations, Section B-B’ was flattened on the top of the Colorado Group (Figure III-19). The surface caps the uppermost shaly interval, corresponding to the top of the First White Specks Member. There are two major downfalls in choosing such a datum, despite its easily recognizable wire-line log signature and objective possibility of being a flat palaeo-surface that would normally make it a good candidate for a datum. The first major problem in applying the datum reveals itself in observation of the lower bounding surface of the Medicine Hat Member (top of the Verger Member). Sections flattened on this datum show an overall surface dip to the south and southwest, which contrasts with the interpreted basinal dip. The basinal dip was affected by the uplift of the Sweetgrass Arch, making surface dips to the south and southwest unlikely. The second issue with the alternate datum is derived from the interpretation that the surface shows some degree of erosion, separating highstand deposits below from regressive deposits above (Nielsen, 2002; Payenberg, 2002). Therefore, flattening on such a datum is inherently wrong, as it imparts larger stratal dips than were likely to be present at the time of deposition.

Mapping the Bottomset Versus the Offshore

There is some uncertainty in mapping bottomset deposits in the distal portions of the Medicine Hat gas field. The main issue is in differentiating bottomset strata using wire-line log signatures from the laterally adjacent offshore strata, which both tend to have a very similar log response. Where gamma-ray wire-line log responses are tied to core, in the upper portion of the interval, and within regions demonstrated to have overlying foreset deposits, there is a higher degree of certainty in the interpretation of the bottomset as compared to the edge of the prograding clinoforms. However, the degree of uncertainty increases significantly as correlation is attempted distally to the locus of foreset deposition. This is especially the case in the cross-sections that flank the system to the north and west.

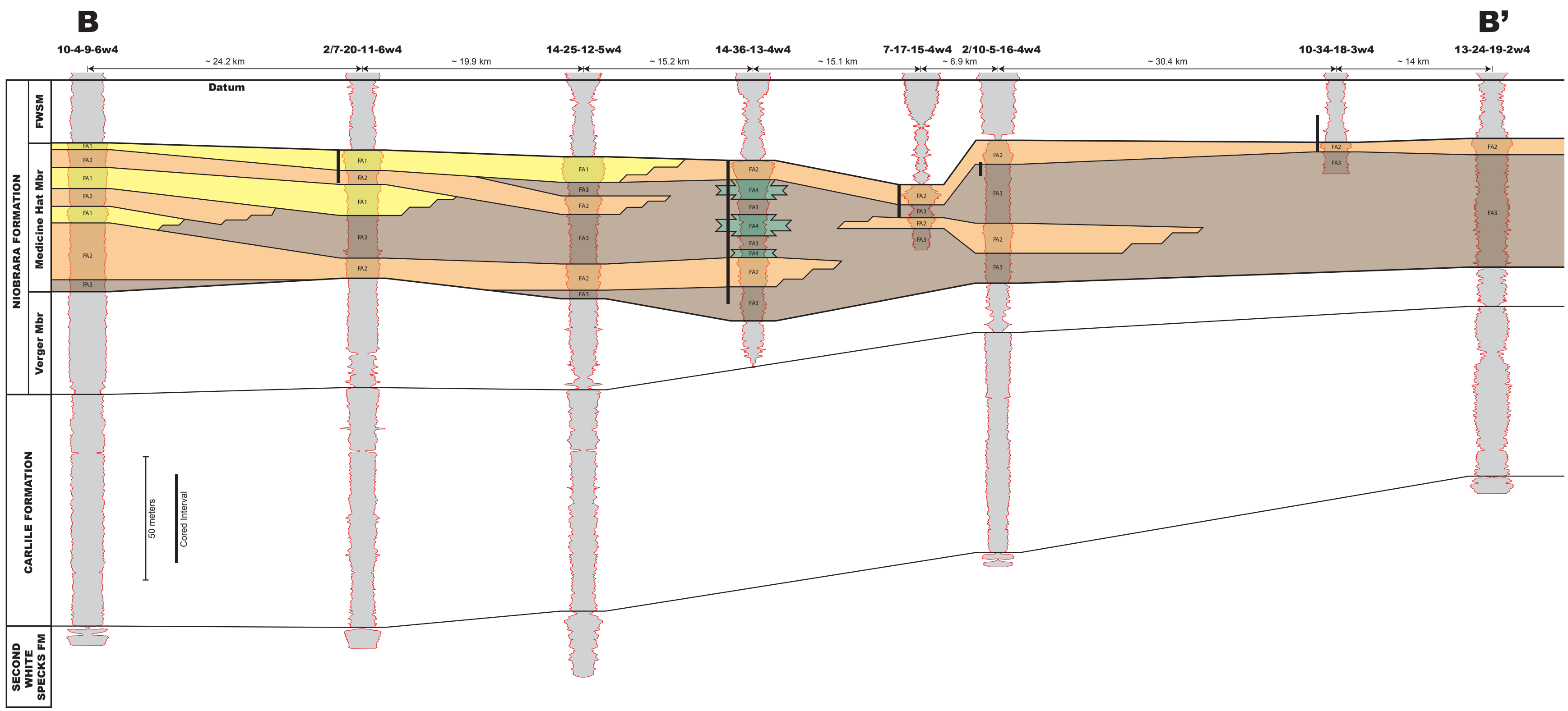

Figure III-19: Stratigraphic cross-section B-B' using a datum at the top of the Colorado Group. There are two main downfalls for utilizing such a datum, despite its easily recognizable wire-line log signature and objective possibility of being a flat palaeo-surface: 1) the sections show a regional dip to the west, contrary to the know dip to the east caused by the Sweetgrass Arch; and 2) the surface does not show any degree of erosion, as suggested by Nielsen (2002) and Payenberg (2002).

Lithostratigrapic Versus Chronostratigraphic Correlations

Admittedly, the stratigraphy presented here is likely over simplified with respect to the chronological aspect of clinoform deposition (see Gani and Bhattacharya, 2005). In the network of cross-sections, the correlations are denoted with solid lines that separate lithologically distinct units (facies associations) from one another. In reality, these are diachronous facies contacts that cut across time lines, following the depiction of delta geometries in Scrutton (1960). Unlike in outcrop examples, where sedimentary units and their entire bounding surfaces may be observable, the core data and wire-line logs do not continuously document the nature of stratal surfaces. Moreover, local seismic and chronometric data were not available for higher resolution correlations. Therefore, as simplistic as the lithostratigraphic correlations may be, they are preferred, and deemed to be objective observations that do not impart significant interpretations that cannot be substantiated by the dataset. It is accepted and understood that many of the solid facies correlation lines are highly diachronous and perhaps, with more data available, they could be re-drawn as “shazam lines” in the manner suggested by Gani and Bhattacharya (2005). However, the sections do provide strong evidence for low-angle clinoform geometries that are not simply layer-cakes.

COMPARISON WITH STRATIGRAPHY OF OTHER WAVE- AND RIVER-INFLUENCED SYSTEMS

The well known delta classification system of Galloway (1975) proposes that delta morphology and facies architecture are primarily controlled by the relative influence of rivers, waves, and tides. Wave-dominated deltas tend to have cuspate strand-plain morphologies, whereas in river-dominated settings deltas are lobate in plan-view according to the tripartite classification (Galloway, 1975; Rodriguez et al., 2000). More recently, deltas have been associated with other controlling parametres, namely grain-size, water depth, and the type of channels that feed the coastline (Orton and Reading, 1993). Certainly, the later approach affords more flexibility in the classification of complex systems. On the basis of the aforementioned criteria, and combined with the distinct sedimentological and ichnological observations, the Medicine Hat Member has been interpreted as a combined wave- and river-influenced subaqeous clinoform (Chapter II).

In studies of the modern Brazos delta, Texas (Rodriguez et al., 2000; Dellapenna et al., 2008) two distict phases of delta evolution were observed. The first wave-dominated phase formed a series of amalgamated beach ridges as sufficient sediment was supplied along the coast. The second constructive delta phase occurred as the longshore sand supply diminished and episodic flooding events created a series of outbuilding lobes that were subsequently reworked during the intervening time between high-discharge flooding events - a river-dominated process (Rodriquez et al., 2000). The Brazos delta shows the complex geometries that can arise from the interaction of wave- and river-influence.

In the Brazos coastal system, prodelta sediments dominate, constituting approximately 60% of the delta's volume (Rodriguez et al., 2000). Presumably, the dominance of fine-grained media is the result of the extremely low depositional gradients that prevented sand from being widely dispersed (Rodriguez et al., 2000; Dellapenna et al, 2008). The preservation potential of the prodelta becomes high compared to the delta-front sands, where wave-erosion depths are not deep enough to overcome subsidence (Rodriguez et al., 2000). Furthermore, the Brazos River is interesting in that it has been observed to flow both hyperpycnally and hypopycnally within a five kilometre radius of the river mouth (Dellapenna et al., 2008). In fact, it may be one of the only modern examples of a shallow gradient river that flows hyperpycnally, a mechanism that is used to explain the distribution of sedimentary structures and ichnology in the Medicine Hat (Chapter II).

The stratigraphic sections and plan-view morphology of the Brazos delta show similarity to the parasequences of the Medicine Hat system. The most obvious commonality is the downlapping clinoform morphology that defines all delta protrusions (Scrutton, 1960). Secondly, the Brazos delta is lobate proximal to the feeder system, but grades into a typical strandplain within a short distance of the river mouth. Parasequences of the Medicine Hat Member are also relatively lobate due to river-influence in the foreset, where the distribution of sediment into the basin is apron shaped (Olariu and Bhattacharya, 2006). Parasequences C and D however, map strandplain-like, especially to the west of the locus of deposition. It is possible that this indicates the direction of a subtle longshore current. Another similarity between the two lies in the relative proportion of prodelta/bottomset sediments. On the whole, the Medicine Hat Member has high volumes of bottomset deposits when compared to the amount of sandy foreset. Though the bottomset may not comprise 60% of the stratigraphy as in the Brazos (Rodriguez et al., 2000), the abundance of bottomset silts and clays is similar overall.

There is a major difference in scale between the Brazos delta and the Medicine Hat system. The Brazos delta grades from delta-plain and shoreface environments into the delta-front and prodelta over a distance of approximately 10 kilometres (Rodriguez et al., 2000). The Medicine Hat clinoforms, on the other hand, transition from foreset through to bottomset strata over more than 100 kilometres, with a distinct lack of paralic deposits preserved in the study area. This departs from the Brazos delta system and indeed many modern and rock record examples of deltaic environments. The Niobrara transgressive cycle is inferred to have removed any evidence of coastal plain deposition. Alternatively, an extensive coastal plain may not have existed at all (see Chapter II).

In the Yellow River delta, sourced from one of the largest river systems in the world, fine-grained sediment is transported both across, and along the shelf (Yang and Liu, 2007). The Yellow River discharges significant volumes of sediment to the Bohai Sea, where most of the fluvially derived sediment temporally remains trapped in the modern delta (Yang and Liu, 2007, and references within). In the Yellow River delta, significant silt and clay are deposited in a large subaqueous system. Sonar profiles reveal that the fine-fraction has built an omega-shaped clinoform that dips both landward and seaward, occurring along the shelf from the river-mouth. Basinal factors such as tides, waves, and geostrophic currents, cause a high proportion of the silt and clay to become re-suspended and transported hundreds of kilometres out of the Bohai Sea and into the Yellow Sea (Yang and Liu, 2007).

Yang and Liu (2007), showed that within the Yellow River system shear stresses are too great to allow significant deposition in the topset, due to the relatively strong oceanographic regime. This observation explains the predominance of progradational foreset and bottomset strata as basinal depths increase offshore. The most important aspect of the study, however, was the documentation of wide sediment dispersal (both along and across the shelf) in the Holocene highstand, where only a very small fraction escaped to the outer shelf or shelf break (Yang and Liu, 2007).

Comparison of the Medicine Hat strata in the study area with the Yellow River system yields a few notable similarities. The Medicine Hat Member, as mapped in this study, occurs as a series of widely distributed, clinoform shaped parasequences, where the largest parasequence (Parasequence E), covers an area of over 6000 km^2, in an overall sea-level highstand. Moreover, the depositional environments and associated strata represent a subaqeous clinoform, where progradational foresets dominate and no topsets are observed. Some important differences between the two fine-grained systems include the nature of clinoforms (i.e., sigmoidal shaped for the Medicine Hat versus omega-shaped in the Yellow River delta), and the basinal energy regimes affecting deposition, where locally the Cretaceous Interior Seaway shows low to moderate wave-action and geostrophic currents, as compared to a relatively high-energy basin in the Bohai and Yellow seas (Yang and Liu, 2007).

Certainly, the Medicine Hat system is not unique in a number of characteristics documented from modern coastal settings, with respect to stratigraphy and aerial extent. However, it appears that fine-grained, low-gradient subaqeous clinoforms are poorly represented in the literature on the rock record. This may be the result of certain depositional models becoming popular and scientists force-fitting their observations to them. In consequence, these models propagate and departures from the “norm” go unrecognized.

SUMMARY AND CONCLUSIONS

The Medicine Hat Member of the Niobrara Formation in southeastern Alberta is reinterpreted as a progradational parasequence set representing a 3rd-order Highstand Systems Tract (HST) superimposed upon the 2nd-order Niobrara sea-level transgression. The lower bounding surface of the parasequence set (Verger-Medicine Hat member contact) is a transgressive surface of erosion demarcated by a pebbly lag containing ooids, glauconite, and evidence of eroded palaeosols (Nielsen, 2002; Nielsen et al., 2003). The surface is relatively subtle on wire-line logs, and is recognized mainly by a sudden increase in the resistivity log response. However, previous studies (Nielsen, 2002; Nielsen et al., 2003) have demonstrated that a significant change occurs in the geochemistry, sedimentology, and micropaleontology across the boundary. The surface at the top of the Medicine Hat Member is sequence boundary where local calcareous debris indicates a period of exposure, prior to a transgression. The Medicine Hat-First

White Specks member contact is very obvious, shown by a sudden increase in the gamma-ray log response.

The parasequence-set observed in the Medicine Hat Member comprises five parasequences of a subaqeous clinoform shaped geobody. Each successive parasequence shows basinward shifts in facies that deposited sediment farther to the north and west than their underlying counterparts. The parasequences are composed of bottomset clays and silts, passing upwards into more sandy distal foreset deposits, and capped with proximal foreset sediments. The locus of deposition increased in area and moved northwest overall as the system evolved. The uplifting of the Sweetgrass Arch throughout the Upper Cretaceous affected the distribution of sediment in southeastern Alberta, and was an important controlling factor on the distribution of facies in the Medicine Hat gas field.

The stratigraphy, areal extent, and plan-view geometry of the foreset has analogies to modern examples of river- and wave-influenced deltas. The Brazos River delta in the Gulf of Mexico (Rodriguez et al., 2000; Dellapenna et al., 2008) and the Yellow River delta in the Bohai Sea (Yang and Liu, 2007) are used for comparison with the results of this study. An overall lobate geometry in the Medicine Hat parasequences, with subtle strandplain morphologies in parts of individual parasequences, characterizes the system. The low-gradient receiving basin and fine-grained sediment supplied were two of the most important factors for controlling the stratigraphic architecture. This study is a rock record example of silt and fine-grained sand being transported hundreds of kilometres from a relatively low-energy coast. With the documentation of such a system, similar deposits may be readily recognized in the study of other sedimentary units or their reinterpretation.

The local stratigraphy described herein is important for the exploration and development of natural gas in southeastern Alberta. Understanding the stratal architecture of the Medicine Hat Member in a sequence stratigraphic framework will yield better exploration models, is vital to calculating petroleum reserves, and has engineering applications for production from unconventional reservoirs.

REFERENCES

Bloch, J., Schröder-Adams, C.J., Leckie, D.A., McIntyre, D.J, Craig, J., and Staniland, M., 1993, Revised stratigraphy of the lower Colorado Group (Albian to Turonian), Western Canada, Bulletin of Canadian Petroleum Geology, v. 41, p. 325-348.

Caldwell, W.G.E., North, B.R., Stelck, C.R., and Wall, J.H., 1978, A foraminiferal zonal scheme for the Cretaceous System in the Interior Plains of Canada, *in* Western and Arctic Canadian Biostratigraphy, C.R. Stelck and B.D.E. Chatterton (eds.), Geological Association of Canada Special Paper 18, p. 495-575.

Catuneanu, O, 2006, Principles of Sequence Stratigraphy, Elsevier, Amsterdam, 374p.

Catuneanu, O., Abreu, V., Bhattacharya, J.P., Blum, M.D., Dalrymple, R.W., Eriksson, P.G., Fielding, C.R., Fisher, W.L., Galloway, W.E., Gibling, M.R., Giles, K.A., Holbrook, J.M., Jordan, R., Kendall, C.G.St.C., Macurda, B., Martinsen, O.J., Miall, A.D., Neal, J.E., Nummedal, D., Pomar, L., Posamentier, H.W., Pratt, B.R., Sarg, J.F., Shanley, K.W., Steel, R.J., Strasser, A., Tucker, M.E., and Winker, C., 2009, Towards the standarization of sequence stratigraphy, Earth-Science Reviews, v. 92, p. 1-33.

Cobban, W.A., 1951, Colorado Shale of central and northwestern Montana and equivalent rocks of the Black Hills, American Association of Petroleum Geologists Bulletin, v. 35, p. 2170-2198.

Cobban, W.A., Erdmann, C.E., Lemke, R.W., and Maughan, E.K., 1959, Revision of the Colorado Group on the Sweetgrass Arch, Montana, American Association of Petroleum Geologists Bulletin, v. 43, p. 2786-2796.

Dellapenna, T.M., Noll, C.J., Fielder, B.R., and Webster, R., 2008, Hypercynal flow within low gradient river deltas and implications for both sand and mud transport onto the shelf: Brazos River, Northern Gulf of Mexico, Search and Discovery Article #50091, American Association of Petroleum Geologists.

Dowling, D.B., 1917, The Southern Plains of Alberta, Geological Survey of Canada, Memoir 93, 200p.

Dowling, D.B., Slipper, S.E., and Mclearn, F.H., 1919, Investigations in the gas and oil fields of Alberta, Saskatchewan, and Manitoba, Geological Survey of Canada, Memoir 116, 89p.

Embry, A., and Johannessen, E., 1992, T-R sequence stratigraphy, facies analysis and reservoir distribution in the upper-most Triassic-Lower Jurassic succession, western Sverdrup Basin, Arctic Canada, *in* Artic Geology and Petroleum Potential, Vorren, T.O., Bergsager, E., Dahl-Stamnes, O.A., Holter, E., Johansen, B., Lie, E., and Lund, T.B. (eds.), Norwegian Petroleum Society, Special Publication 2, p. 121-146.

Embry, A.F., 1995, Sequence boundaries and sequence hierarchies: problems and proposals, *in* Sequence Stratigraphy: Advances and Applications for Exploration and Producing in Northwest Europe, Steel, R.J., Felt, V.L., Johannessen, E.P., and Mathieu, C. (eds.), Norweigian Petroleum Society (NPF), Special Publication 5, p. 1-11.

Galloway, W.E., 1975, Process framework for describing the morphologic and stratigraphic evolution of deltaic depositional systems, *in* Deltas, Models for Exploration, Broussard, M.L. (eds.), Houston Geological Society, Houston, Texas, p. 87-98.

Gani, MR., and Bhattacharya, J.P., 2005, Lithostratigraphy versus chronostratigraphy in facies correlations of Quaternary deltas: application of bedding correlations, *in* River Deltas – Concepts, Models, and Examples,

Gill, J., and Cobban, W., 1973, Stratigraphy and geologic history of the Montana Group and equivalent rocks, Montana, Wyoming, and North and South Dakota, United States Geological Survey, Professional Paper 776, 37p.

Helland-Hansen, W., and Martinsen, O.J., 1996, Shoreline trajectories and sequences: description of variable depositional-dip scenarios, Journal of Sedimentary Research, v. 66, p. 670-688.

Kaufmann, E.G., 1967, Coloradan macroinvertebrate assemblages, central Western Interior, *in* Palaeoenvironments of the Cretaceous seaway in the Western Interior, Colorado School of Mines, Golden Colorado, p. 67-143.

Leckie, D.A., and Smith, D.G., 1992, Regional setting, evolution, and depositional cycles of the Western Canada Foreland Basin, *in* Foreland Basins and Fold Belts, R.W. Macqueen and D.A. Leckie (eds.), American Association of Petroleum Geologists, Memoir 55, p. 9-46.

Lorenz, J.C., 1982, Lithospheric flexure and the history of the Sweetgrass Arch in northwestern Montana, *in* Geological Studies of the Cordilleran Thrust Belt, R.B. Powers (eds.), Rocky Mountain Association of Geologists, Denver, Colorado, p. 77-89.

McNeil, D.G., and Caldwell, W.G.E., 1981, Cretaceous rocks and their foraminifera in the Manitoba Escarpment, Geological Association of Canada, Special Paper 21, 439p.

Nielsen, K.S., 2002, Lithostratigraphy, sequence stratigrapy and palaeoenvironments of the Upper Colorado Group in southern Alberta and southwestern Saskatchewan: definition of the Carlile and Niobrara formations (Upper Turonian to Upper Santonian), unpublished Ph.D. thesis, Carleton University, Ottawa, Canada.

Nielsen, K.S., Schröder-Adams, C.J., and Leckie, D.A., 2003, A new stratigraphic framework for the Upper Colorado Group (Cretaceous) in southern Alberta and southwestern Saskatchewan, Canada, Bulletin of Canadian Petroleum Geology, v. 51, p. 304-346.

Nielsen, K.S., Schröder-Adams, C.J., Leckie, D.A., Haggart, J.W., Elberdak, K., 2008, Turonian to Santonian paleoevironmental changes in the Cretaceous Western Interior Sea: The Carlile and Niobrara formations in southern Alberta and southwestern Saskatchewan, Canada, Palaeogeography, Palaeoclimatology, Palaeogeography, v. 270, p. 64-91.

North, B.R., and Caldwell, W.G.E., 1975, Foraminiferal faunas in the Cretaceous system of Saskatchewan, *in* The Cretaceous System in the Western Interior of North America, W.G.E. Caldwell (eds.), Geological Association of Canada, Special Paper 13, p. 303-331.

Olariu, C., and Bhattacharya, J.P., 2006, Terminal distributary channels and delta front architecture of river-dominated delta systems, Journal of Sedimentary Research, v. 76, p. 212-233.

Orton, G.J., and Reading, H.G., 1993, Variability of deltaic processes in terms of sediment supply, with particular emphasis on grain-size, Sedimentology, v. 40, p. 475-512.

Rodriquez, A.B., Hamilton, M.D., and Anderson, J.B., 2000, Facies and evolution of the modern Brazos Delta, Texas: wave versus flood influence, Journal of Sedimentary Research, v. 70, p. 283-295.

Payenberg, T.H.D., 2002, Litho-, chrono- and allostratigraphy of the Santonian to Campanian Milk River and Eagle formations in southern Alberta and north-central Montana: Implications for differential subsidence in the Western Interior Foreland Basin, Unpublished Ph.D. Thesis, University of Toronto, Canada, 221p.

Plint, A.G., 1991, High-frequency relative sea-level oscillations in the Upper Cretaceous shelf clastics of the Alberta foreland basin: possible evidence for a glacio-eustatic control?, International Association of Sedimentologists, Special Publication 12, p. 409-428.

Posamentier, H.M., and Vail, P., 1988, Eustatic controls on clastic deposition II – sequence and systems tract models: *in* Sea-Level Changes: An Integrated Approach, C.K., Wilgus, B.S., Hastings, C.G.St.C., Posamentier, H.W., Roos, C.A., and Van Wagoner, J.C., Society of Economic Paleontologists and Minerologists, Special Publication 42, p. 125-154.

Russell, L.S., and Landes, R.W., 1940, Geology of the Southern Alberta Plains, Geological Survey of Canada, Memoir 221, 223p.

Rodriquez, A.B., Hamilton, M.D., and Anderson, J.B., 2000, Facies and evolution of the modern Brazos Delta, Texas: wave versus flood influence, Journal of Sedimentary Research, v. 70, p. 283-295.

Schröder-Adams, C.J., Adams, P.J., Leckie, D.A., Bloch, J., Craig, J., and El-Dien, S.A.S, 1997, Upper Cretaceous Medicine Hat Formation and First White Speckled Shale in southeastern Alberta: Evidence for localized shallow water deposition, Bulletin of Canadian Petroleum Geology, v. 45, p. 356-376.

Schröder-Adams, C.J., Adams, P.J., Haggart, J., Leckie, D.A., Bloch, J., Craig, J., and McIntyre, D.J., 1998, An integrated paleontological approach to reservoir problems: Upper Cretaceous Medicine Hat Formation and First White Speckled Shale in southern Alberta, Canada, Palaios, v. 13, p. 361-375.

Scrutton, P.C., 1960, Delta building and deltaic sequence, *in* Shepard, F.P., Phleger, F.B., and Van Andel, T.H., (eds), Recent Sediments, Northwest Gulf of Mexico, American Association of Petroleum Geologists, p. 82-102.

Simpson, F., 1982, Low-permeability gas reservoirs in marine Cretaceous sandstones of Saskatchewan, *in* Summary of Investigations 1982, Saskatchewan Geological Survey, Miscellaneous Report 82-4, p. 120-125.

Simpson, F., 1984, Hydrocarbon potential of low permeability marine Cretaceous sandstones of Saskatchewan, *in* The Mesozoic of Middle North America. A Selection of Papers from the Symposium on the Mesozoic of Middle North America, Calgary, Alberta, Canada, Canadian Society of Petroleum Geologists, p. 513-533.

Spratt, J.G., 1931, Stratigraphy of Colorado Shale in southern plains of Alberta, American Association of Petroleum Geologists Journal, v. 10, p. 228-240.

Stelk, C.R., 1975, Basement control of Cretaceous sand sequences in western Canada, Geological Association of Canada Special Paper, no.13, *in* Cretaceous System in the Western Interior of North America, p.427-440.

Stott, D.F., 1963, The Cretaceous Alberta Group and equivalent rocks, Rocky Mountain Foothills, Alberta, Geological Survey of Canada, Memoir 317, 306p.

Stott, D.F., 1984, Cretaceous sequences of the foothills of the Canadian Rocky Mountains, *in* The Mesozoic of North America, D.F. Stott and D.J. Glass (eds.), Canadian Society of Petroleum Geologists, Memoir 9, p. 85-108.

Van Wagoner, J.C., Posamentier, H.W., Mitchum, R.M., Vail, P.R., Sarg, J.F., Loutit, T.S., and Hardenbol, J., 1988, An overview of the fundamentals of sequence stratigraphy and key definitions, *in* Wilgus, C.K., Hastings, B.S., Kendall, C.G.St.C., Posamentier, H.W., Ross, C.A., and Van Wagoner, J.C., (eds.), Sea-level Changes – An Integrated Approach, SEPM, Special Publication 42, p. 39-45.

Van Wagoner, J.C., Mitchum, R.M., Campion, K.M., and Rahmanian, V.D., 1990, Siliciclastic Sequence Stratigraphy in Well Logs, Cores, and Outcrops: Concepts for High-Resolution Correlation of Time and Facies, American Association of Petroleum Geologists, Methods in Exploration 7, 55p.

Wall, J.H., 1967, Cretaceous foraminifera of the Rocky Mountain Foothills, Alberta, Research Council of Alberta, Bulletin 20, 185p.

Wall, J.H., and Rosene, R.K., 1977, Upper Cretaceous stratigraphy and micropaleontology of the Crowsnest Pass – Waterton Area, southern Alberta Foothills, Bulletin of Canadian Petroleum Geology, v. 25, p. 842-867.

Yang, Z.S., and Liu, J.P., 2007, A unique Yellow River-derived distal subaqueous delta in the Yellow Sea, Marine Geology, v. 240, p. 169-176.

CHAPTER IV — THE EFFECTS OF BIOTURBATION ON POROSITY AND PERMEABILITY IN RESERVOIR FACIES OF THE MEDICINE HAT MEMBER, MEDICINE HAT GAS FIELD, SOUTHEAST ALBERTA, CANADA

INTRODUCTION

Contemporary ichnological investigation has shown that the utility of trace fossils goes beyond palaeoenvironmental or stratigraphic application. Bioturbating organisms alter the sorting characteristics of sediments, leading to differential porosities and permeabilities between the burrow fills and surrounding matrix (Meadows and Tait, 1989; Lee and Foster, 1991; Pierret et al., 1999, 2002; Gingras et al., 2002a,b; Bastardie et al., 2003). Since trace fossils alter the textural attributes of porous media, in certain instances they may become the primary fluid conduits for the migration and production of oil, natural gas, and water (Gingras et al., 2004a; Pemberton and Gingras, 2005; Lemiski et al., in review).

Bioturbation of sediment is conventionally regarded to be detrimental to porosity and permeability (e.g. Weber, 1982; Castle et al., 2004; Worden and Morad, 2003; Zorn et al., 2010). Infaunal and epifaunal organisms churn laminated sediment, decreasing the overall sorting, producing a homogenous texture, and thereby reducing permeability. However, complete sediment homogenization is rare and primary sedimentary structures are most often disrupted, rather than obliterated (Bromely, 1996; Zorn et al., 2010). Moreover, bioturbation is often preserved as discrete, tubular, coarser grained entities encapsulated by finer matrix. As such, the contention that reservoir fluid flow is reduced or inhibited by biogenic processes is probably an oversimplification, especially in light of several examples of bioturbation-enhanced bulk permeability now presented in the geological literature (e.g., Dawson, 1978; Gunatilaka et al., 1987; Gingras et al., 1999; 2004a, b; McKinley et al., 2004; Sutton et al., 2004; Pemberton and Gingras, 2005; Gingras et al., 2007; Cunningham et al., 2009). Generally, two main mechanisms account for biogenically-enhanced permeability: 1) burrow-mediated modification of the primary depositional fabric, or alternatively, 2) diagenetic alteration of the sedimentary matrix via recrystallization (Pemberton and Gingras, 2005).

This chapter investigates the relationship between bioturbate textures in the Medicine Hat Member strata, and their corresponding effects on reservoir properties in the Medicine Hat gas field. Particularly, the study demonstrates that in the shallow, low-permeability, unconventional reservoirs of southeast Alberta, the porosity and permeability distribution is significantly affected by the nature and intensity of burrowing.

BACKGROUND

Bioturbating organisms such as earthworms, decapod crustaceans, amphipods, polychaetes, and meiofauna, create macropores in modern sediments that enhance porosity and permeability (e.g., Meadows and Tait, 1989; Lee and Foster, 1991; Pierret et al., 1999, 2002; Bastardie et al., 2003). In a seminal paper on ichnofossil-related permeability, Gingras et al. (1999) explored the effects of *Glossifungites* surfaces on permeability in Pleistocene deposits at Willipa Bay, Washington, by using numerical simulations, as well as laboratory and field measurements. The results of the study showed that the effective permeability of a substrate is preserved by the presence of sand filled burrows. More importantly, however, the study showed that permeability across the *Glossifungites* surfaces could be predicted to some degree.

In a later study the textural attributes of *Macaronichnus*-burrowed sandstone was visualized in three dimensions by utilizing magnetic resonance imaging (MRI) paired with petrographic techniques by Gingras et al. (2002a). Based upon the distribution of mineral grains and porosity, they surmised that the burrowed zones represented a dual-porosity flow network system (discussed below). A similar flow network was noted in Gingras et al. (2002b) in the rocks from the Palliser Formation from the Alberta Foothills. By imaging the textural attributes using MRI, and calibrating to petrographic observations, the resource quality of the burrowed carbonates was inferred to be reduced by bioturbation. Both studies presented the potential for using a new class of MRI technique as a powerful imaging tool for low-porosity reservoir rocks.

It was increasingly recognized that two different types of flow networks can be manifested in biogenic flow media: *dual-porosity*, and *dual-permeability* networks (Gingras et al., 2004b; Pemberton and Gingras, 2005). Dual-porosity systems are those characterized by burrow-associated permeability that is within two orders of magnitude relative to the permeability of the surrounding matrix. Dual-porosity occurs where burrow- and matrix-permeability are similar. Conversely, highly contrasting, well-defined permeability fields that differ by more than two orders of magnitude define dual-permeability systems. The type of flow system, combined with the stratigraphic stacking of the strata, were two important factors for classifying the various types of flow media in Pemberton and Gingras (2005).

Building upon the previous observations of biogenically enhanced permeability, Pemberton and Gingras (2005) classified and characterized the various types, emphasizing their role as a potentially important reservoir-development tool. These flow-media types form the basis upon which we can begin to describe and understand the potential effects of burrowing in reservoir units. Pemberton and Gingras' (2005) classification system is five-fold: 1) surface-constrained discrete textural heterogeneity; 2) non-surface-constrained discrete textural heterogeneity; 3) weakly defined textural heterogeneity; 4) diagenetic textural heterogeneity; and 5) cryptic biogenic heterogeneity.

PREVIOUS WORK

Little is formally documented on the reservoir properties and storage potential of the Medicine Hat Member in southeast Alberta. Only a single investigation into general porosity and permeability characteristics in the Medicine Hat gas field is publicly available (Hankel et al., 1989). In that study, Hankel et al. (1989) analysed thin sections from the eastern part of the Medicine Hat gas field to demonstrate that porosity in reservoir units mainly comprises primary intergranular and interparticle micropore types. The intergranular porosity was found to occur between framework grains in the siltstones and sandstones, whereas the interparticle micropores were observed between lightly compacted detrital clays (kaolinite) in the matrix and mudstones. Core analysis porosity ranged from 20 to 37% in the main reservoir unit ("Medicine Hat A" sandstone; Hankel et al., 1989), and air permeability measurements ranged from 10 to greater than 500 millidarcy (Hankel et al., 1989). However, point-count analyses from thin sections determined significantly lower porosity and permeability values compared to the results from core analyses. The observed discordance was attributed to the microporosity, which was not visible or quantifiable in thin sections. SEM examination of the poorly compacted clay-rich matrix supported this hypothesis (Hankel et al., 1989).

Although Hankel et al. (1989) outlined the basic types and ranges in values of porosity and permeability, the effects of biogenic structures on reservoirs properties have yet to be assessed. In the last decade, new concepts about the relationship between bioturbation and reservoir flow properties have emerged (e.g., Gingras et al., 1999; Gingras et al., 2002a,b; Gingras et al., 2004a; Pemberton and Gingras, 2005; Lemiski, 2010), and the burrowed intervals of the Medicine Hat Member provide an excellent opportunity to test and apply these concepts.

METHODS

Nexen Inc. provided a one third slabbed core from the 6-31-14-1W4 well for core analysis. Oil-based drilling fluids were used during the coring process, preserving the swelling-clay dominated core in pristine condition. Samples from one of the reservoir facies (FA2; see Chapter II) was selected for spot-minipermeametry and micro-CT analysis to assess intra-facies heterogeneity. Furthermore, the relationship between layered heterogeneity and anisotropy was examined between burrowed and unburrowed strata to assess the degree to which burrows are connected to form networks. The burrow networks, if present and extensive enough, have the potential to provide preferential fluid migration pathways for the production of hydrocarbons. This investigation was based upon the principles of hydrogeology presented in Freeze and Cherry (1979, Chapter 2), and references therein.

Due to the need for accurate and repeatable measurements, each sample was checked for micro-fractures, pitting, or other factors that might affect the quality of measurements. From the entire core, only five samples passed the quality-control requirements. A comparison between the results from spot-minipermeametry and micro-CT illustrates the power of integrating multiple non-destructive reservoir characterization techniques.

Facies Selection

In the Medicine Hat Member, four important facies associations recur through the study area (see Chapters II and III). Two of the four associations comprise the major reservoir units for the production of natural gas (FA1 and FA2, respectively). As minipermeametry is especially sensitive to the quality of core surfaces tested, where micro-fractures and clay swelling, among other issues, significantly affect the results, it was necessary to use core that was obtained via oil-based drilling fluids. Nexen Inc. allowed access to a high quality slabbed core in the central part of the study area (6-31-14-1W4; Appendix A), and thus, it was selected as an ideal candidate for comparing spot-minipermeametry and micro-CT techniques.

Spot-Minipermeametry

Spot-minipermeametry was conducted on selected facies from the 6-31-14-1W4 well using a Core Laboratories PDPK – 400 Pressure-Decay Profile Permeameter (PDPK – 400) (Figure IV-1A). The PDPK – 400 spot-minipermeameter is a device that measures gas (in this case nitrogen) permeability in the range from 0.001 millidarcy to greater than 30 Darcy (Core Laboratories Instruments, 1996). The major components of the instrument are the probe assembly/travelling case, a tank supplying nitrogen to the probe assembly, a core rack upon which the sample under investigation is placed, and a computer to store and display the measurement results. The probe assembly is composed of four calibrated, nitrogen-filled volumes (referred to as the "tank supply"). The front panel of the PDPK – 400 is where the measurement control devices are located. These controls comprise the tank supply and probe regulators, gauge displays, and a button to initiate permeability measurement.

The study utilized a one-centimeter grid pattern on fresh, slabbed core faces. To maintain consistent measurements and ensure adequate probe-tip seals, the core face was cleaned with compressed air prior to the experiments. To conduct the spot-minipermeametry testing, the first step was to place the sample on the core rack, securing it with rubber putty so that it would not be jarred during the measurement process. Next, the probe assembly and core rack were aligned

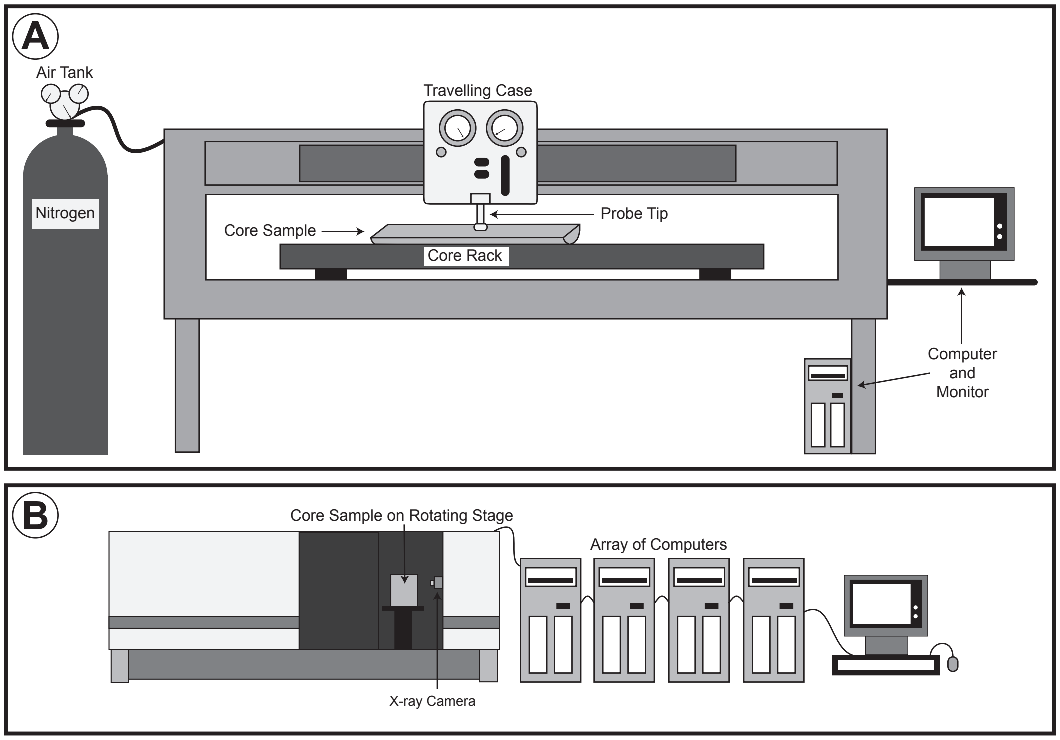

Figure IV-1: (A) Core Laboratories PDPK — 400 Pressure Decay Profile Permeameter. The main components have been labelled and described in text. Modified from Core Laboratories Instruments, 1996, and Lemiski, 2010. (B) SkyScan 1172 Desktop X-ray Microtomograph. The major components are labelled and described in text. Modified from SkyScan N.V., 2005.

to the starting position (the top left of the grid), and the probe's rubber O-ring tip (0.46 cm diameter) was sealed against the sample using the pneumatic cylinder. At this point, the computer-controlled probe valve was opened and allowed to flow, while the tank and probe pressure were recorded as a function of time. The maximum pressure-decay time allowed was 30 seconds. Five measurements from each point in the grid were taken before moving on to the next measurement location.

Upon completion of the spot-minipermeametry testing, the maximum and minimum values for each point were discarded, and the remaining three values were averaged. In certain instances, anomalous measurement values were recorded indicating a poor tip seal (from an uneven testing surface, edge effects, or microfractures). These values were removed from the dataset. Finally, the permeability fields were contoured using Surfer 9 gridding and contouring software (Rockware ®, Inc., 2009). Once contour maps of the permeability fields were generated in Surfer 9, they were edited to highlight the lithologically constrained nature of the permeability domains.

Limitations of the PDPK – 400 Spot-Minipermeameter

The main limitation of the PDPK – 400 spot-minipermeameter is the large size of the probe-tip compared to the ichnological heterogeneity. Although the smallest diameter was chosen for these experiments (~0.46 cm diameter), in many instances the tip was too large to accurately determine the permeability of the diminutive trace fossils found in the Medicine Hat Member. A second problem encountered during spot-minipermeametry testing was achieving a tight probe-tip seal. The surface of the core must be reasonably flat, and measurements at least one centimeter from the edge of the core in order to avoid a leaky seal from edge effects. Furthermore, in more than one instance microfractures were encountered in the fissile silt and mud laminae. This was solved by discarding the measurements and contouring the permeability fields in the absence of extraneous data points.

Graphs and Statistical Relationships Between Layered Heterogeneity and Anisotropy

On a relatively large scale, layered (approximately planiform) heterogeneity and anisotropy are related. Heterogeneity refers to the property of a porous medium where a measured parameter (in this case permeability) is different depending upon the location of measurement. The antonym of heterogeneous is homogeneous, that is, having the same parametric value everywhere. A related concept is isotropy. An isotropic system has permeability that is independent on the direction of measurement at a point in a geological formation. In contrast, in anisotropic systems permeability varies with the direction of measurement (e.g., vertical versus horizontal) (Freeze and Cherry, 1979).

In layered media, fluid flow occurs parallel to the layers. Where each layer is assumed to be homogeneous, Freeze and Cherry (1979) show that the system as a whole can be characterised as a single homogeneous, anisotropic layer. By applying a simple volume weighted arithmetic mean of the permeability of each layer, an estimation of the overall bulk permeability occurring parallel to stratification can be obtained. This relationship can be expressed as:

$$k_{arithmetic} = \sum_{i=1}^{n} \frac{k_i d_i}{d}$$

(Equation 3.1)

where k_i is the permeability of each layer, and d_i/d is the weighted volume.

For fluid flow occurring perpendicular to layered media, applying a volume-weighted harmonic mean provides an estimation of the bulk vertical permeability. The equation that describes the relationship is:

$$k_{harmonic} = \frac{1}{\sum_{i=1}^{n} \frac{d_i}{k_i d}}$$

(Equation 3.2)

Finally, the volume-weighted geometric mean of the permeability of multiple layers, is representative of homogeneous, isotropic systems where fluid flow occurs in all dimensions (Warren and Price, 1961). This type of bulk permeability is expressed as:

$$\ln(k_{geometric}) = \sum_{i=1}^{n} \frac{\ln(k_i) d_i}{d}$$

(Equation 3.3)

The weighted volume in equations 3.1-3.3 represents the volume occupied by burrows (burrowing intensity). That is, the unit volume was considered to comprise two portions, the burrows with their respective fills, and the surrounding matrix. Therefore, volume weighting was achieved by characterizing the burrowing intensity as a fraction of the total rock volume under consideration.

Based upon the relationships describing anisotropic and homogeneous permeability through multiple layers parallel and perpendicular to bedded units (i.e., equations 3.1 and 3.2), and isotropic, homogeneous permeability in unstructured units (i.e., equation 3.3), graphs of burrowing intensity versus permeability in an idealized unit volume were constructed. The graphs were bound by end-member permeability measurements determined from the minipermeametry dataset (Table IV-1). These curves show the relationship between measured spot permeability and core-plug "bulk" permeability, and permit identification of the permeability behaviour as arithmetic, harmonic, or geometric.

To produce the graphs, the lowest three permeability measurements from the spot-minipermeametry tests for each sample were averaged. These low values were observed to approximately correspond to the unburrowed (0% bioturbation), clay- or silt-rich matrix. On the other hand, in general, the highest permeability values occurred in, or were in very close proximity to the most heavily bioturbated fabrics. Therefore, the three highest values of measured permeability were averaged to approximate the 100% bioturbation end member. The three values chosen to average for each maximum and minimum were similar, generally within 15% of one another. Thus the end member values were a good approximation of the permeability associated with the burrows, and matrix, respectively.

Using the values obtained for 0% and 100% biogenically-altered permeability, the three types of average permeability were traced, corresponding to the full range of bioturbation intensity. These three averages correspond to different trends in flow behaviour, where the arithmetic mean represents flow dominated through the highest permeability conduits (i.e., the burrow fills), the harmonic mean represents flow dominated through the lower permeability conduits (i.e., the matrix), and the geometric mean represents flow in a relatively unstructured medium (i.e., no preference for burrows or matrix). Therefore, in general, the trend traced by the arithmetic mean can be thought of as flow through well connected burrow networks, whereas the trend traced by the harmonic mean indicates poorly connected, isolated burrowing, with many dead-end flow pathways. The trend of the geometric mean falls somewhere in between the other two cases, where fluid flow is not confined only to the burrow networks.

Sample	Matrix Permeabilities (mD)	Mean Matrix Permeability (mD)	Burrow Permeabilities (mD)	Mean Burrow Permeability (mD)
	0.003		61.6	
1	0.012	0.015	43.4	44.6
	0.030		28.8	
	0.261		159	
2	0.392	0.384	150	134.9
	0.498		95.7	
	0.134		99.3	
3	0.640	0.547	99.7	99.4
	0.868		99.1	
	0.083		68.6	
4	0.064	0.104	49.7	51.2
	0.166		35.2	
	0.009		10.8	
5	0.015	0.015	8.36	8.44
	0.020		6.16	

Table IV-1: Data used to construct burrowing intensity versus permeability graphs. The permeability measurements were taken from the spot-minipermeametry dataset and used to infer the permeability of 0% bioturbated media (the lowest values), and 100% bioturbated media (the highest values), respectively.

Nexen Inc. Profile Permeametry

All the graphs of average permeability are annotated with data from profile permeametry undertaken by Nexen Inc. on the same core (6-31-14-1W4) (Table IV-2). The permeability data was derived using a Pulse Decay Permeameter (PDP-200) that measures gas permeability in the range from 1.0 x 10^4 to 1 x 10^8 Darcy. The very low permeability range makes it ideal for the analysis of muddy intervals and other low permeability porous media. The permeability measurements were conducted at intervals ranging between centimeters and decimenters. Furthermore, the PDP-200 analysis focused on specific facies that do not always correspond exactly with the facies tested in this study using the PDPK-400.

Comparing the permeability data from this study against that of Nexen Inc. for the same interval provides a means to test the consistency of permeability data gathered at similar scales but by slightly different processes.

X-Ray Micro-Computed Tomography

To characterize pore geometry and connectivity, and to visualize the complex three-dimensional heterogeneity within Medicine Hat reservoir facies, high-resolution X-ray computed tomography (CT) was performed on four of the five samples used in the spot-minipermeametry experiments. Samples ranged from moderately biouturbated silty sandstones to weakly burrowed silty

Sample Number (this study)	Nexen Inc. Sample Number	Approx. Sample Depth (m)	Air Permeability (mD)	Local Bioturbation Intensity (%)
	843		12.7	35
1	844	507.65	34.7	60
	845		18.6	80
	889		0.186	55
2	890	509.00	0.523	35
	891		108	65
3	898	509.20	81.2	15
	899		160	35
	946		23.9	40
4	947	510.60	4.59	20
	948		4.80	50
	949		1.01	30
	1031		0.0599	5
5	1032	513.80	0.448	10
	1033		0.0799	2.5

Table IV-2: The PDP — 200 data provided by Nexen Inc. used to plot on the graphs of burrowing intensity versus permeability. The data allowed for comparison between two different permeametry methods and assessment of the overall nature of fluid flow in bioturbated media.

claystones.

X-ray computed tomography is emerging as an important and valuable tool for geological investigation. CT scans generate cross-sectional images by rotating objects at angular increments, and measuring the attenuation of a focused X-ray beam. The interactions responsible for attenuation are primarily Compton scattering and photoelectric absorption (Mees et al., 2003). Based on the set of measurements, Fourier transform algorithms are applied to reconstruct a cross-sectional image (Akin and Kovscek, 2003). Thus, the cross-sectional images map the variation in X-ray attenuation within objects, a property that is closely related to density variation. As transitions in density often correspond to material or phase boundaries, the resulting images and volumes are intuitive and straightforward to interpret in a geological framework (Ketcham and Carlson, 2001). For a detailed description and discussion of the theory and methodology of X-ray CT and its geological applications refer to Ketcham and Carlson (2001), Akin and Kovscek (2003), and Mees et al. (2003).

The CT analysis in this study was undertaken on a SkyScan 1172 Desktop X-ray Microtomograph, whereas data processing used an array of four PCs (Figure IV-1B). The CT equipment comprises an X-ray microfocus tube with high-voltage power supply, a rotating specimen stage with a precision manipulator, and a two-dimensional X-ray CCD-camera feeding a frame-grabbing program. For more details on the system components and their specifications refer to the SkyScan 1172 user manual (SkyScan, 2005). During the analysis the X-ray microfocus tube was operated at 110 kV and 250 μA, resulting in a 5 μm focal spot. Copper and aluminium filters were applied to reduce noise and produce cleaner images. The camera was positioned in such a way as to attain 33 μm resolution.

A four-fold process was used to generate and visualize three-dimensional volumes of the attenuation (density) heterogeneity in this analysis. The first step comprised scanning each sample. This was done by placing the sample on the rotating specimen stage and using plastic putty to secure it, adjusting to the necessary parameters (as mentioned above), and waiting for the batch X-ray images to be generated. On average, for the size of samples used (~ 50 mm diameter and 40-60 mm height), the scanning process would take between four and six hours. Oversize scans were necessary to image the relatively large samples used, which were near the upper limit of the SkyScan 1172. A number of individual scans were taken as the stage rotated through 180º at 0.5º increments. The scan process was the single most time-intensive part of the entire analysis.

Once X-ray images were generated, the next step was reprocessing the data to remove errors and make the images suitable for building models. A number of errors and artifacts occur during X-ray CT scanning. It is necessary to remove as much of the error as possible in order to model true heterogeneity and not heterogeneity occurring because of the CT process. The most important and readily occurring errors, and the primary concern, were ring artefacts and so-called "beam hardening". Circular, or ring-shaped artefacts originate from the image reconstruction and back propagation process, as a result of the varying thickness of the material being scanned. Beam hardening is error produced because the X-ray source contains a spectrum of energy levels (polychromatic), and lower energy (soft) X-rays are preferentially attenuated at the air-object interface. The remaining X-rays shift the average energy of the beam towards the higher (hard) end of the spectrum (Akin and Kovscek, 2003). Often beam hardening is manifested as dark bands surrounding the object image. The errors can be minimized, or even eliminated, however, by applying the correction algorithms included in the program N-Recon (SkyScan, 2005). The algorithms use a technique called *linearization*, a calibration that depends on the material being scanned and the thickness (Van Geet et al., 2003).

To derive quantitative parameters and construct visual models from the scanned dataset (series of X-ray images), the application CT-Analyser (SkyScan,

2005) was used after ring artefacts and beam hardening were corrected for. CT-Analyser allowed the dataset to be opened, a region of interest within the object to be allocated, a histogram of the attenuation coefficients of the entire dataset to be generated, and finally a three-dimensional model of a particular attenuation range to be constructed. The region of interest chosen was cylindrical, approximately two centimeters in diameter, oriented with the long axis (z-axis) in the same direction as the core plug, and passing roughly through the center of the samples. The region of interest balanced processing time and resolution versus computer power necessary to generate the volumes. Histograms of the attenuation coefficients were generated for each dataset, and the range of values chosen for volume rendering were based upon what was interpreted to be the most illustrative low-density heterogeneity. The low end of the spectrum of density was chosen because in general, sand- and silt-filled burrows, as well as sand laminae, contain more pore space, and thus, are lower density relative to the surrounding matrix. Upon applying a region of interest and determining the range of attenuation to be modelled, a three-dimensional volume was rendered. On average, the processing in CT-Analyser took from three to five hours, depending on the sample.

Manipulation and viewing of the three-dimensional surface-rendered models was done using SkyScan's CT-Volume application (SkyScan, 2005). Figures IV-10 and IV-11 were captured using the CT-Volume application. Thus, the fourth and final step in identifying and displaying heterogeneity in X-ray attenuation/density in the Medicine Hat 6-31-14-1W4 core was done using CT-Volume.

RESULTS

The facies association chosen for analysis in this paper (FA2) is described and interpreted in Chapter II. Several sedimentological and ichnological characteristics of the association are important to note. Overall, FA2 is typified by a coarsening-upwards profile, in which sandstone facies increase in thickness and frequency with a concurrent decrease in siltstone and claystone. However, the facies association is ultimately composed of numerous stacked fining-upwards successions that become sandier upwards. These fining-upwards units are between 3 and 7 cm, but most commonly are between 4 and 5 cm thick. Planar laminated sandstone, comprising a portion of storm deposits, is absent at the base of the succession, but becomes common 2 to 3 m above the lower contact, and the dominant facies near the top of FA2. Siltstone and claystone facies are primarily found as top to the fining-upwards units that recur throughout the association, or more rarely, as isolated strata.

Bioturbation in FA2 is moderately common in the siltstone and claystone facies (up to BI 2; Taylor and Goldring, 1993), but is less common in the sandstones, with an overall sporadic appearance. Trace fossils are often indistinct forms, but when identifiable, correspond to a depauperate expression of the distal *Cruziana* ichnofacies. Biogenic structures indicate that the primary life strategy was horizontal deposit-feeding.

Spot-Minipermeametry Results

Core photos, with corresponding spot-permeability test locations and permeability measurements (in millidarcy) are presented in Figures IV-2 to IV-4. Next to each core photo is a contour map showing the distribution of permeability in each sample. These contoured permeability fields are used to exhibit, compare, and contrast the distribution of permeability in Facies Association 2 as discussed later.

The results of the spot-minipermeametry testing suggest that overall the permeability in burrowed intervals can be preserved in trace fossils, and is often greater than the permeability of the surrounding muddy matrix (by up to two orders of magnitude). Measured permeability values range between 1.0×10^{-2} and 10 mD for the most clay rich portions of FA2, corresponding to the stratigraphic bottom of the association (e.g., Figure IV-4). Permeability varies between 2.0×10^{-1} and 68 mD in the stratigraphic middle of FA2, where siltstone and sandstone facies are approximately equal in proportion (e.g., Figure IV-3). In the sandiest parts of FA2, occurring near the top of the succession, measured permeability ranges from 2.0×10^{-1} to 1.5×10^{2} mD (e.g., Figure IV-2). Overall, the permeability fields indicate that the flow occurs in a dual-porosity system (*sensu* Gingras et al., 2007).

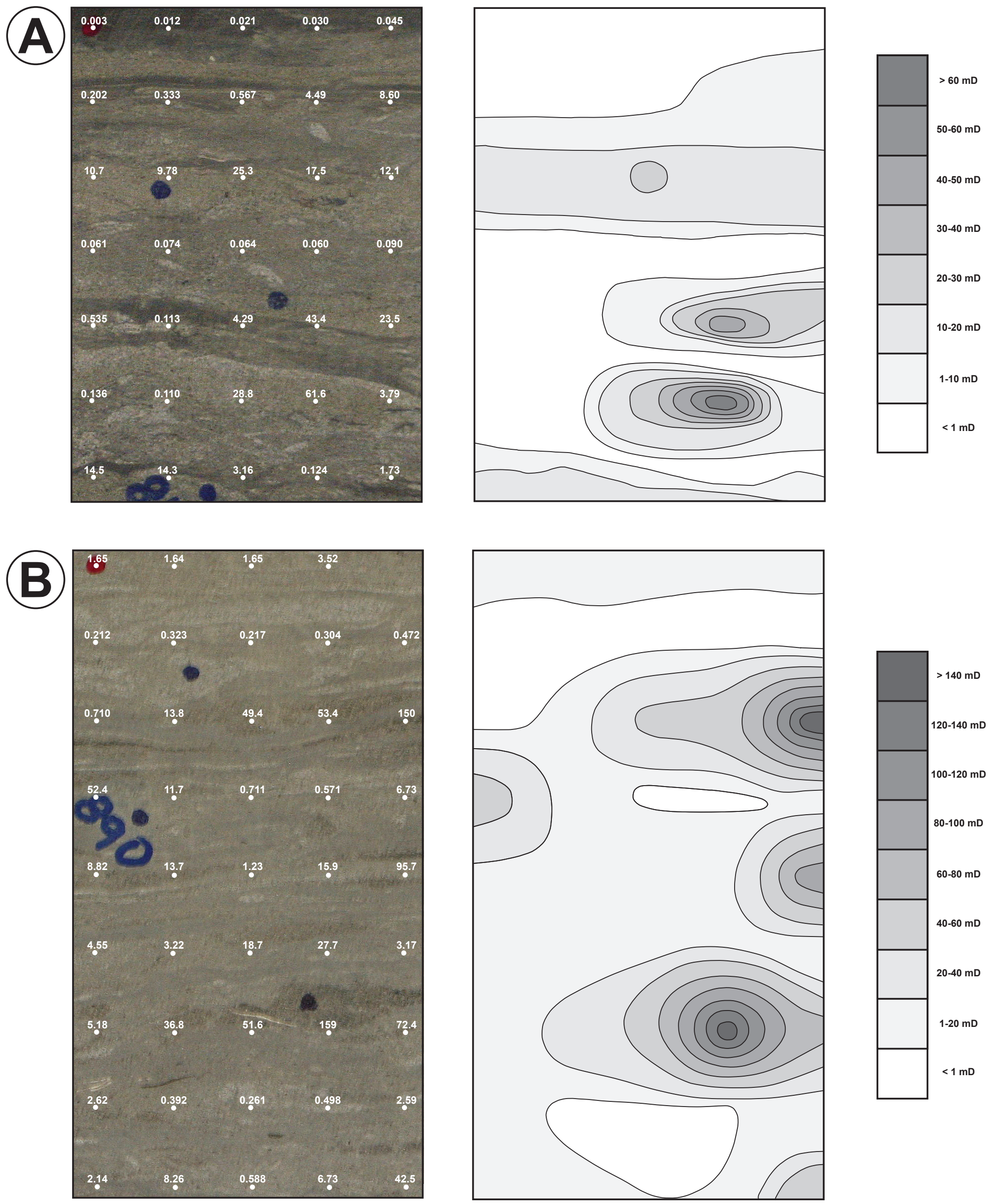

Figure IV-2: The results of spot-minipermeametry tests conducted on Medicine Hat Member facies. Shown on the left hand side are the core photos with annotated test locations and their corresponding permeability to air (K_a) measurements in millidarcy. On the right, contoured permeability fields highlight the most permeable streaks within the strata. Higher permeability values are illustrated by darker shades of grey, whereas, lower permeability values are ligher shades. All samples were tested using a one centimeter grid spacing. (A) Sample 1 (6-31-14-1W4, 507.65 m depth). Overall, burrow-associated permeability appears to be enhanced relative to the background muddy matrix with values ranging up to ~60 mD. (B) Sample 2 (6-31-14-1W4, 509.00 m depth). A slightly sandier part of the facies association (FA2), but again, overall, burrow-associated permeability is relatively higher than the surrounding muddy matrix permeability. Bioturbate textures show permeability values ranging up to ~140 mD. For all samples, any missing data points are discarded values occuring because of a poor probe tip seal.

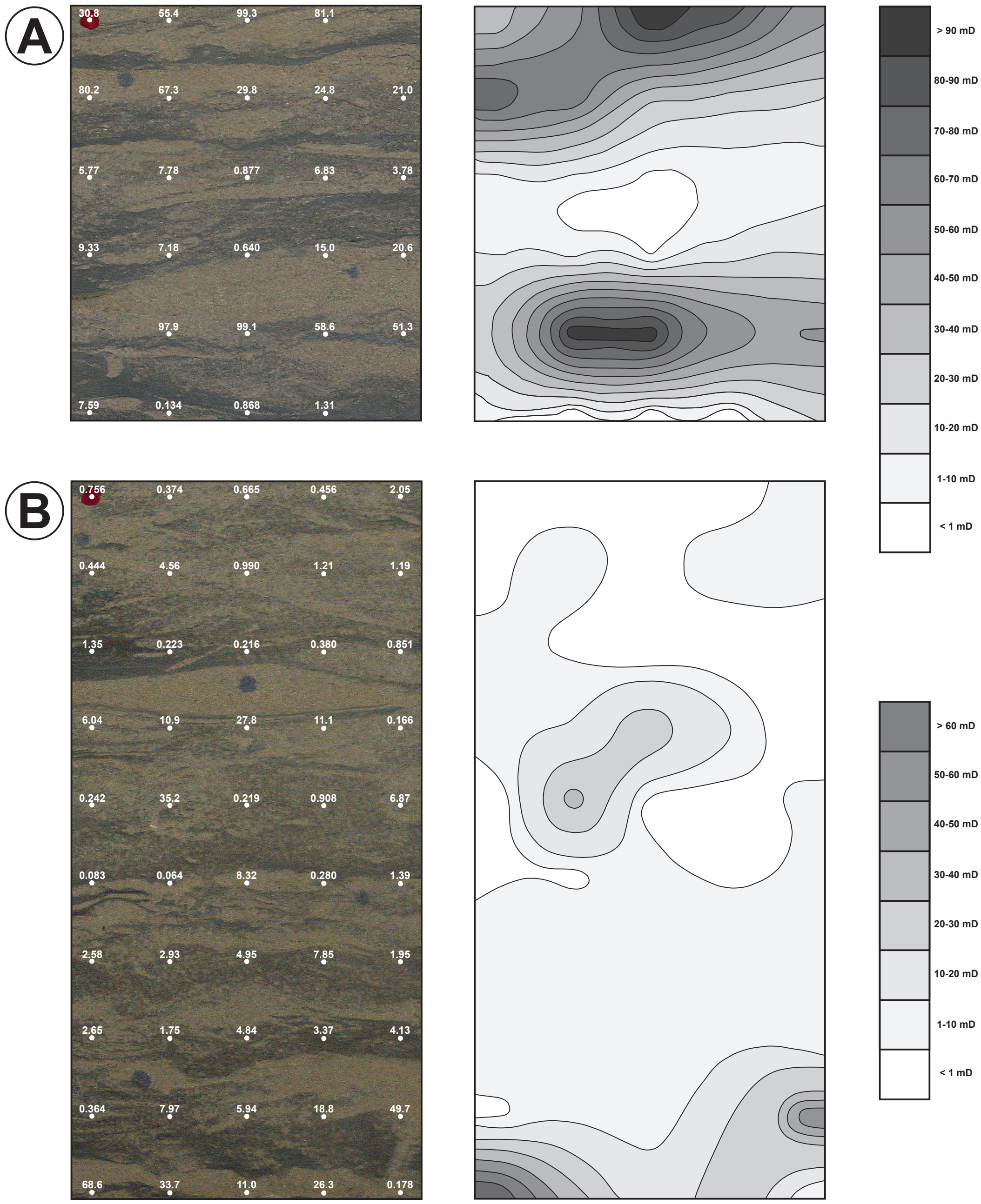

Figure IV-3: The results of spot-minipermeametry tests conducted on Medicine Hat Member facies. Shown on the left hand side are the core photos with annotated test locations and their corresponding permeability to air (K_a) measurements in millidarcy. On the right, contoured permeability fields highlight the most permeable streaks within the strata. Higher permeability values are illustrated by darker shades of grey, whereas, lower permeability values are ligher shades. All samples were tested using a one centimeter grid spacing. (A) Sample 3 (6-31-14-1W4, 509.20 m depth). Overall, burrow-associated permeability appears to be enhanced relative to the background muddy matrix with values ranging up to ~90 mD. (B) Sample 4 (6-31-14-1W4, 510.60 m depth). In general, burrow-associated permeability is relatively higher than the surrounding muddy matrix permeability. Bioturbate textures show permeability values ranging up to ~60 mD. Both samples are subtly less sandy than Samples 1 and 2 and occur stratigraphically lower in FA2. For all samples, any missing data points are discarded values occuring because of a poor probe tip seal.

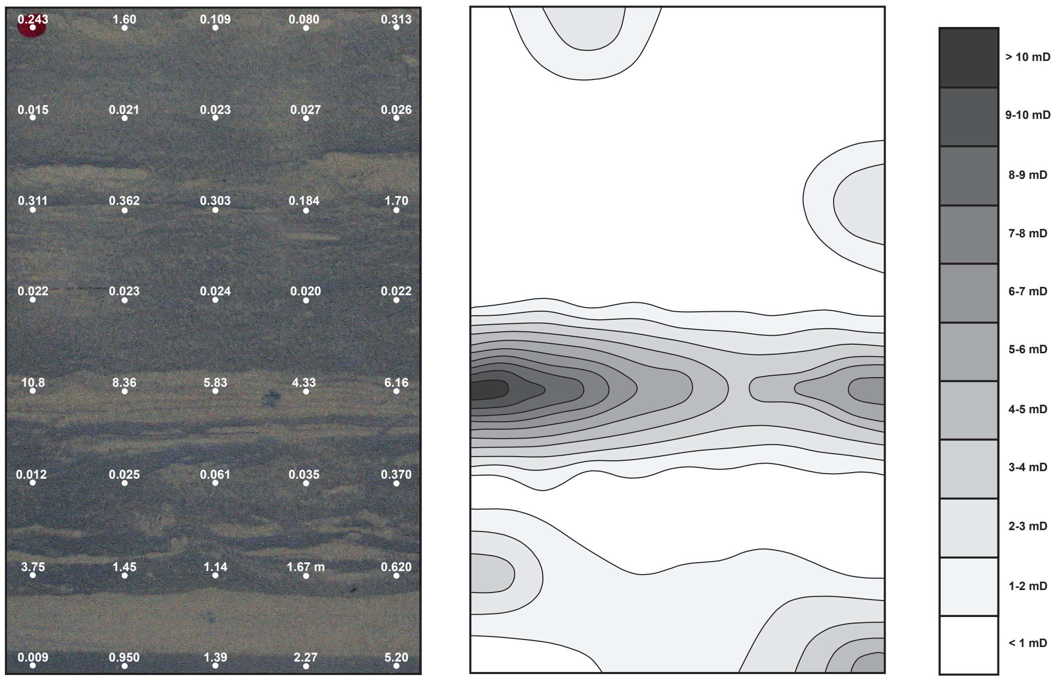

Figure IV-4: The results of spot-minipermeametry tests conducted on Medicine Hat Member facies. Shown on the left hand side are the core photos with annotated test locations and their corresponding permeability to air (K_a) measurements in millidarcy. On the right, contoured permeability fields highlight the most permeable streaks within the strata. Higher permeability values are illustrated by darker shades of grey, whereas, lower permeability values are ligher shades. All samples were tested using a one centimeter grid spacing. The sample shown is Sample 5 (6-31-14-1W4, 513.80 m depth). Overall, burrow-associated permeability appears to be enhanced relative to the background muddy matrix with values ranging up to ~10 mD. Sample 5 is the least sandy of all samples, occuring near the base of FA2. For all samples, any missing data points are discarded values occuring because of a poor probe tip seal.

The spot-minipermeability also suggests that permeability tends to be the highest, and least variable, where the thickest accumulation of sand occurs, regardless of the fabric (i.e., laminated or burrowed). That is, the permeability contrast in sandstone facies is generally high, but controlled by the overall degree of sorting/burrow homogenization (from visual examination). Therefore, burrow mottled sandstones, without well-sorted infills, have low permeability contrast with the surrounding matrix compared to discretely burrowed horizons.

Where siltstone and claystone facies are common (i.e., in the stratigraphic lower half of FA2; Figure IV-4), the range in permeability is significantly more variable than the sand-prone strata. In these intervals, permeability streaks comprise sand filled burrows and laminated sandstones in an otherwise silt and clay rich matrix.

The permeability contour maps highlight an interesting relationship between the intensity of bioturbation and the resulting permeability values. In locations where bioturbation is low to moderate (BI 1-3; Taylor and Goldring, 1993), permeability is localized to the burrowed zones compared to the matrix. In contrast, where bioturbation intensity is higher (BI 2-4; Taylor and Goldring, 1993), burrow mottling does not affect the measured permeability to the same degree.

Graphs of Burrowing Intensity Versus Permeability

The graphs comparing the intensity of bioturbation with measured permeability are shown in Figures IV-5 to IV-9. The three lines trace the harmonic, geometric, and arithmetic means in black, red, and blue, respectively. These represent the possible permeability behaviour of Medicine Hat strata resulting from burrow-associated heterogeneity. Superimposed upon the graphs are red stars marking data points from Nexen Inc.'s PDP-200 permeability analysis (Table IV-2).

Overall, the graphs illustrate that permeability in the facies tested behaves approximately arithmetically, indicating that fluid flow dominantly occurs in the high permeability portion of the strata (i.e., the burrows). Only a few data points occur on the lower end of the permeability spectrum, roughly approximated by the harmonic mean (Figures IV-6 and IV-9). However, these data points are the result of measurements taken solely in the matrix, without being in close proximity to burrows.

There is no obvious relationship between the proportionate volume of sediment that has been burrowed and the nature of burrow-associated fluid migration pathways. That is, in general, data points appear to approximate the arithmetic mean (or rarely the geometric mean), irrespective of the degree of burrowing. Moreover, as the relative proportion of burrows increase, so too does the average permeability.

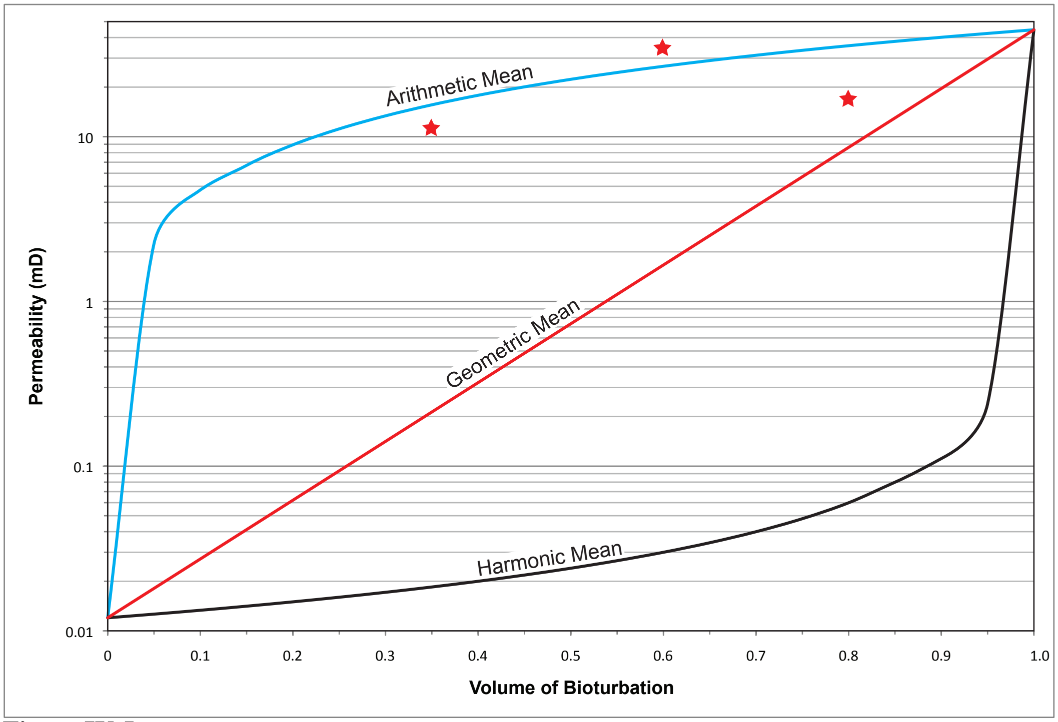

Figure IV-5

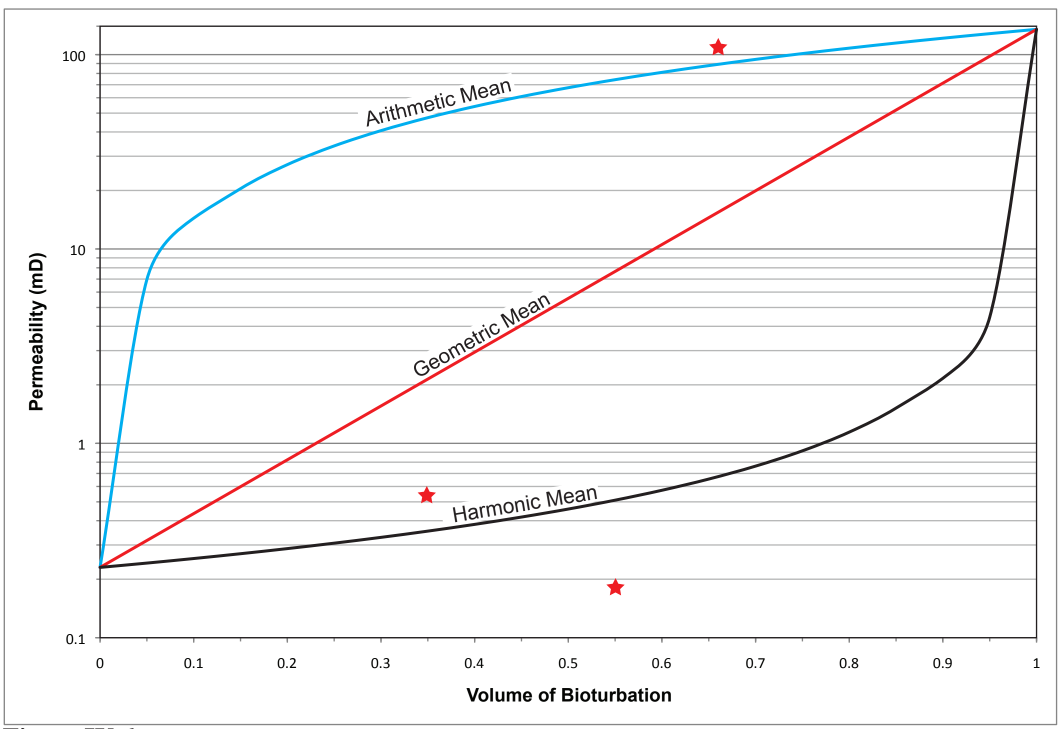

Figure IV-6

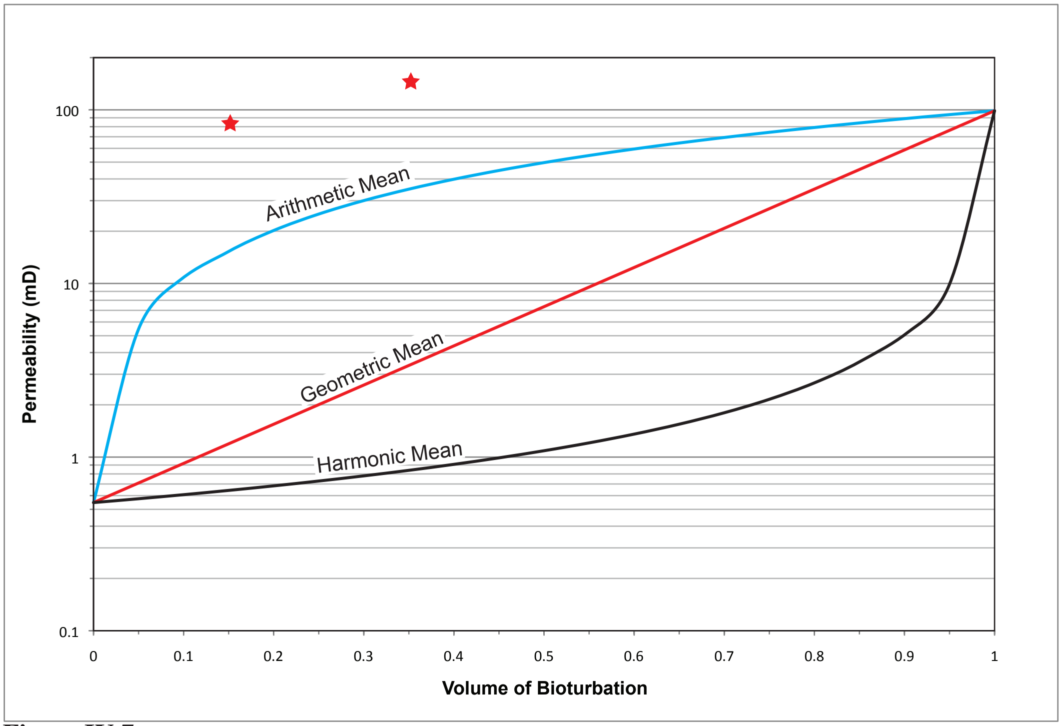

Figure IV-7

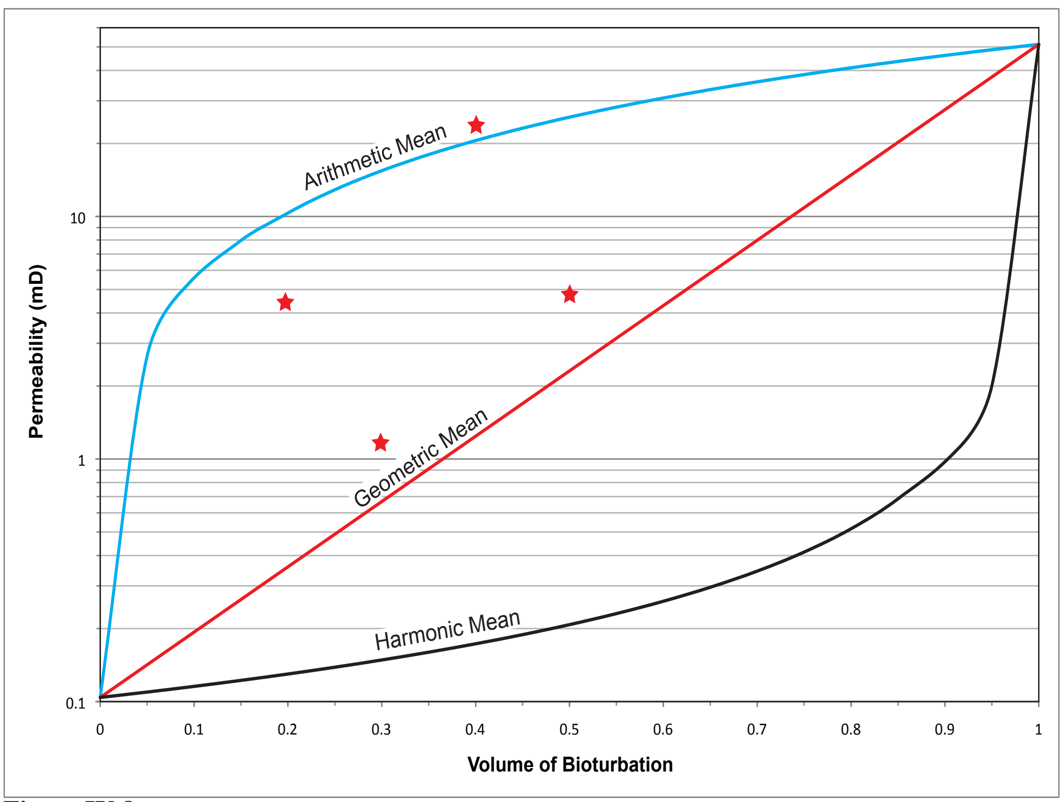

Figure IV-8

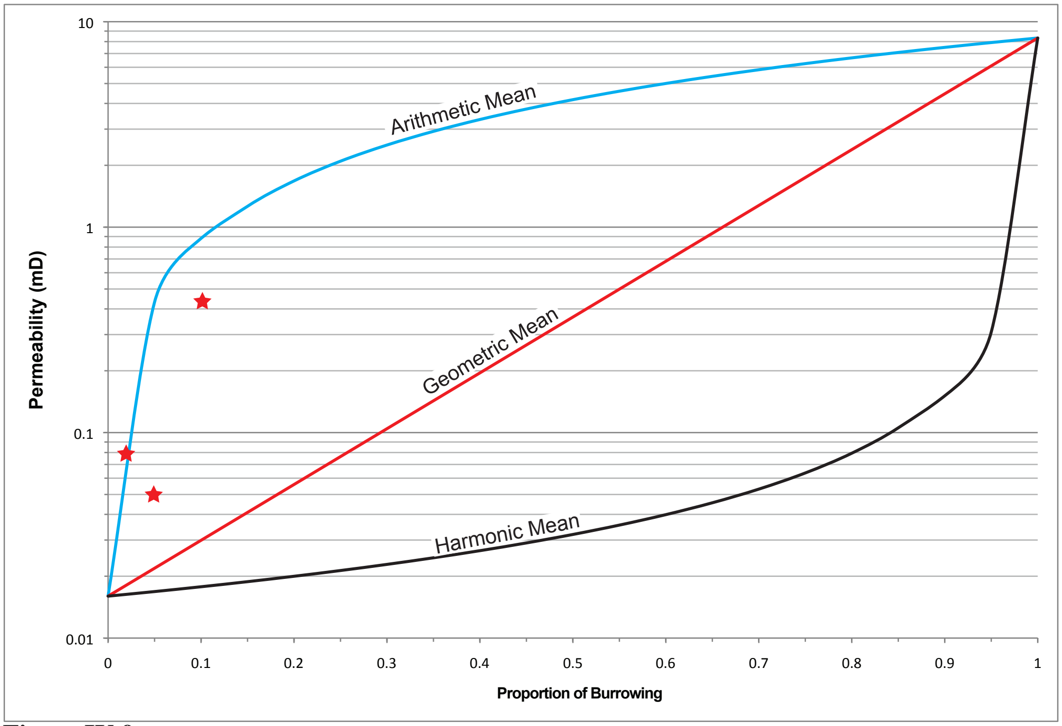

Figure IV-9

Figures IV-5 to IV-9 caption: Graphs of burrowing intensity versus permeability for Samples 1-5. The three lines represent the arithmetic mean (blue), geometric mean (red), and harmonic mean (black) of permeability calculated from the contribution of two end-member measurements (burrows and matrix, respectively), over the full range of bioturbation intensity. Data used to calculate the three mean relationships was derived from spot-minipermeametry and are summarized in Table IV-1. Data points shown as red stars are from permeability analysis undertaken by Nexen Inc., allowing for comparison between methods (Table IV-2). Overall, the results suggests that bulk permeability is characterized by the arithmetic mean of the volume-weighted burrow and matrix permeabilities. This arithmetic relationship supports the interpretation that the burrows form well-connected, planiform networks for the transmission and storage of natural gas.

X-Ray Micro-Computed Tomography Results

The rendered volumes of X-ray micro-computed tomography data are presented in Figures IV-10 and IV-11. Each figure shows the CT volume next to the corresponding core photograph, and an approximate outline of the region of interest visualized in the model. The volumes/models are used to illustrate, compare, and contrast X-ray attenuation (density) heterogeneity that is associated with burrowing and other porous features. These heterogeneity are discussed below in terms of their relationship to the permeability fields derived from spot-minipermeametry. Problems occurred when processing the data from stratigraphically highest sample, Sample 1, and therefore it was omitted from the

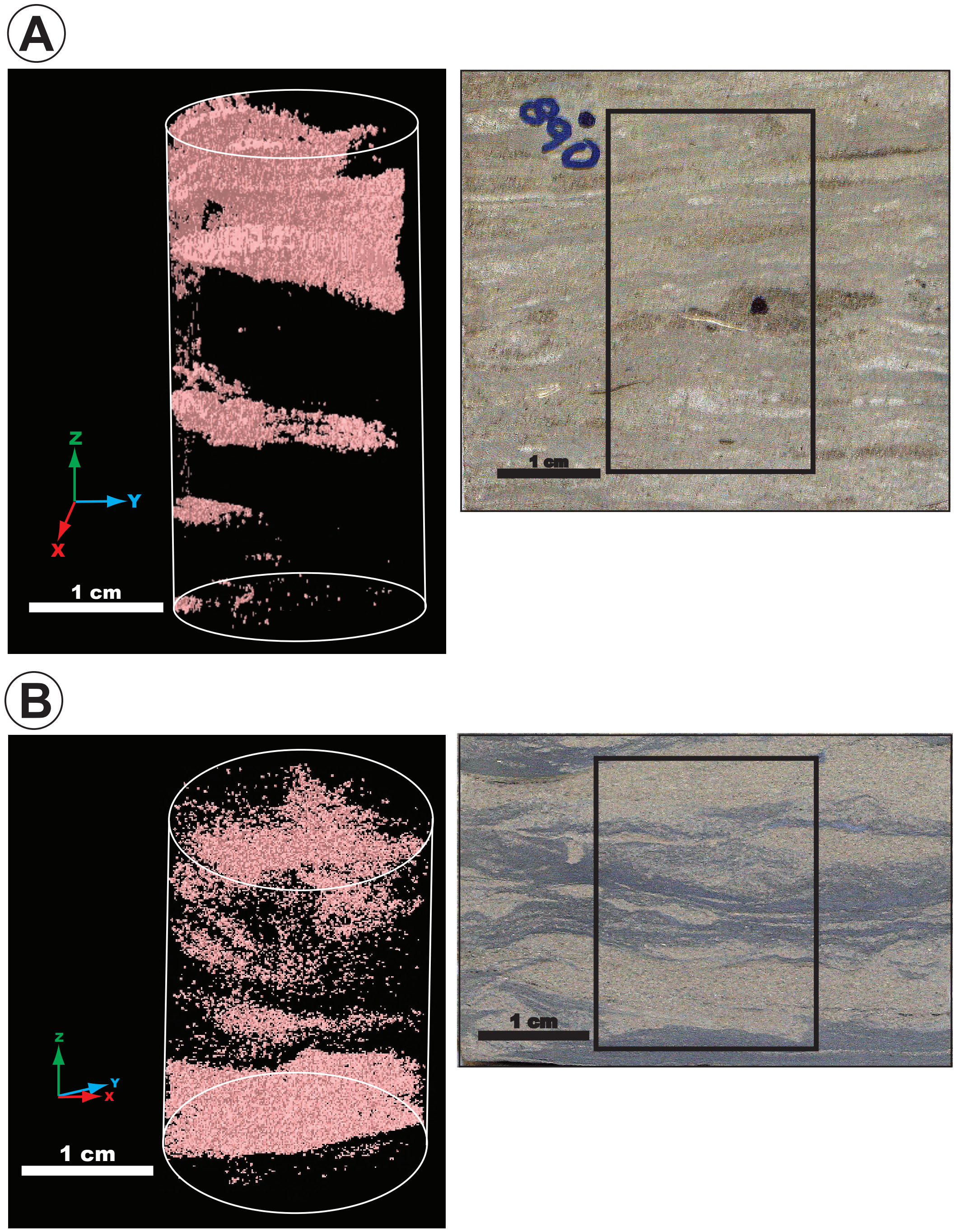

Figure IV-10: Micro-CT rendered volumes next to their corresponding core photos, with the approximate outline of the region of interest visualized in the 3-D model. (A) 3-D model of the low density heterogeneity in Sample 2. Overall, the heterogeneity is relatively planiform in geometry, however, the upper half of the model is homogeneous. The burrowed horizon occuring approximately in the middle of the model is clearly visualized. Traces form a burrow mottled texture, where specific ichnogenera cannot be readily identified. (B) 3-D model of the low density heterogeneity in Sample 3. Again, overall the heterogeneity forms planiform geometries where traces form burrow mottled textures, without easily identifiable ichnogenera. In both examples, the heterogeneity is interpreted as porosity, where porous horizons provide the preferential pathways for the transmission and storage of natrual gas.

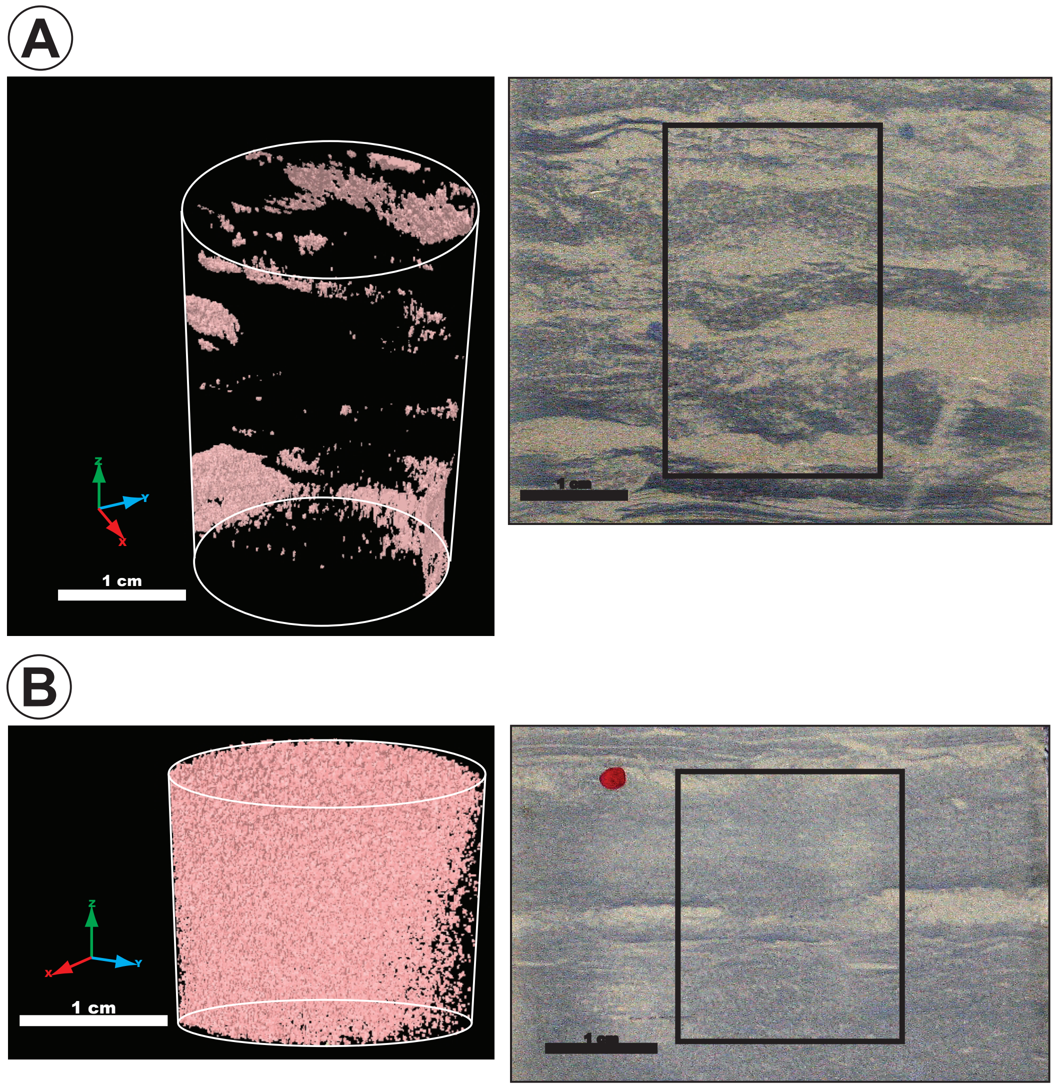

Figure IV-11: Micro-CT rendered volumes next to their corresponding core photos, with the approximate outline of the region of interest visualized in the 3-D model. (A) 3-D model of the low density heterogeneity in Sample 4. Overall, the heterogeneity is planiform with a patchy distribution. Burrow mottling does not allow for the identification of specific ichnogenera. (B) 3-D model of the low density heterogeneity in Sample 5. This sample has a highly burrow mottled texture, where very little of the original sedimentary fabric is preserved. In both examples, the heterogeneity is interpreted as porosity, where porous horizons provide the preferential pathways for the transmission and storage of natrual gas.

analysis.

In the micro-CT analysis low density was the proxy for higher porosity, which in turn was inferred to represent higher permeability. The results of the micro-CT analysis support the interpretation that burrowing, and thus permeability alteration by trace fossils, corresponds to the *nonconstrained textural heterogeneity* and *weakly defined textural heterogeneity* of Pemberton and Gingras

(2005). These classes were defined as discretely packaged trace fossils, not controlled by substrate consistency, with marked differences between the nature of burrow infills and surrounding matrix, and burrow infills which only show a subtle contrast in flow properties when compared to the surrounding matrix, respectively (Pemberton and Gingras, 2005).

In general, the CT volumes illustrate that the majority of density heterogeneity is planiform (roughly parallel to bedding). The ichnological assessment described and discussed in Chapter II observed that the trace fossil suite is dominated by horizontally oriented, shallow-tiered, deposit-feeding forms throughout the bulks of reservoir facies (i.e., archetypal to distal *Cruziana* Ichnofacies. Serial sections (Figures IV-12 to IV-15) and CT volumes through each of the samples supports these observations, showing that in three-dimensional space, most traces (or other density heterogeneity) occur as planar entities.

OVERVIEW AND DISCUSSION

Previously, the effects of bioturbation on permeability in the Medicine Hat Member were poorly understood. Spot-minipermeametry analysis was undertaken on five samples from 6-31-14-1W4, representing part of Facies Association 2 that was deposited on the distal foreset region of a subaqeous clinoform. Data from spot-minipermeametry illustrates that admixing of sand-sized particles into the silt and clay rich matrix is a favourable process through which permeability is locally increased. Discretely burrowed, and more commonly burrow-mottled fabrics are associated with higher permeability values, likely providing preferential fluid migration pathways. The dual-porosity nature of reservoir units, where burrow permeability is within two orders of magnitude of the surrounding matrix, suggests that bioturbated strata are locally as important as stratified sandstones with respect to reservoir quality.

X-ray micro-CT analysis was used to visualize the three-dimensional distribution of density heterogeneity, corresponding to porosity induced by biogenic processes. The CT volumes and serial sections through the samples provide evidence that density heterogeneity is planiform, oriented roughly parallel to bedding planes. The planiform nature of heterogeneity suggests that burrows

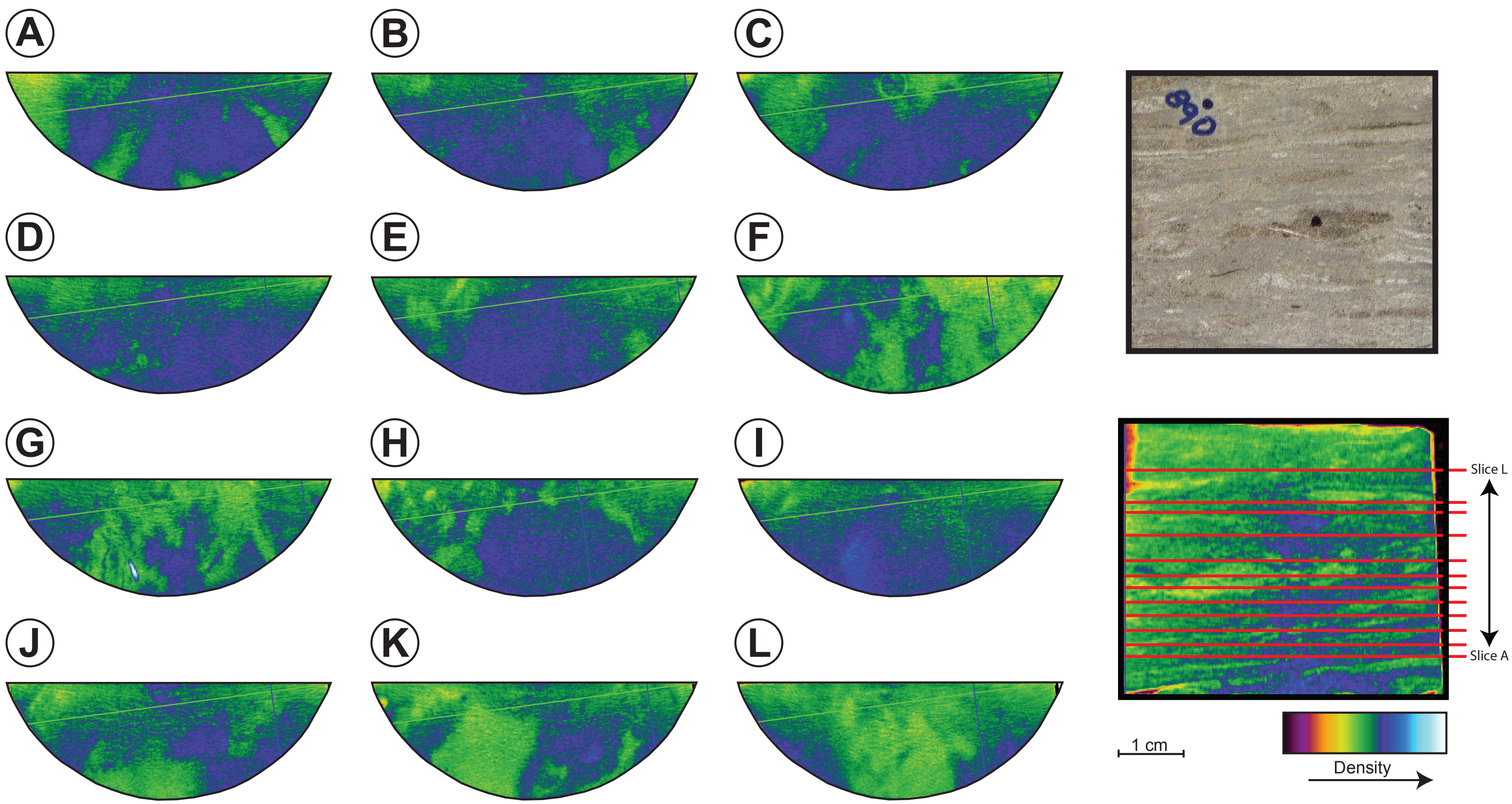

Figure IV-12: X-ray serial sections through Sample 2, with the corresponding core photo and vertical x-ray image for comparison. Slices A to L are arranged from the bottom to the top of the sample. Warm colours represent the lower densities, whereas cool colours are used to show the higher end of the density spectrum. Overall, the serial sections show the progressive changes in the nature of burrowing throughout the sample, where horizontally oriented traces can be observed in some of the slices (i.e., A and H).

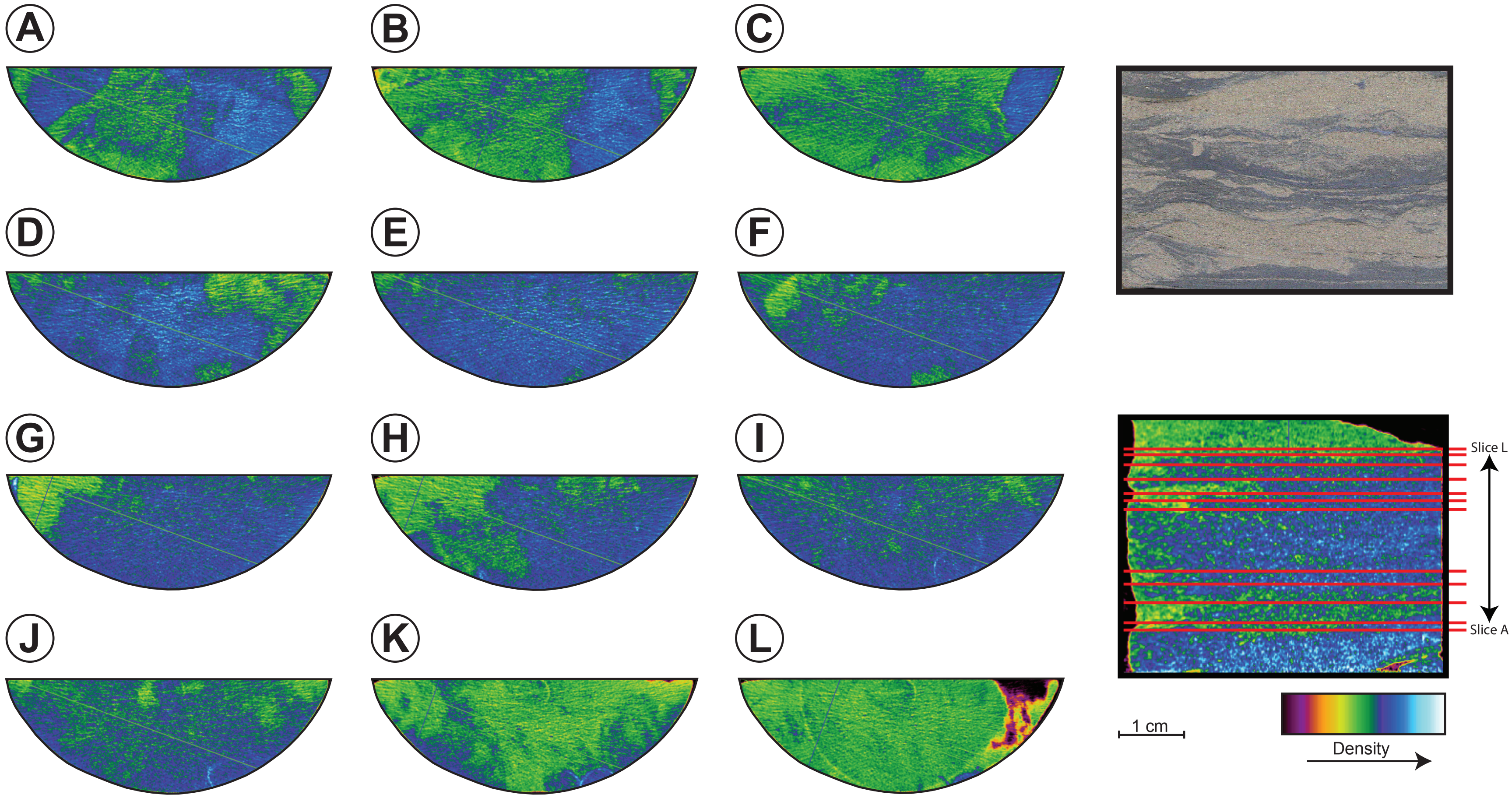

Figure IV-13: X-ray serial sections through Sample 3, with the corresponding core photo and vertical x-ray image for comparison. Slices A to L are arranged from the bottom to the top of the sample. Warm colours represent the lower densities, whereas cool colours are used to show the higher end of the density spectrum. Overall, the serial sections show the progressive changes in the nature of burrowing throughout the sample, where horizontally oriented traces can be observed in some of the slices (i.e., A).

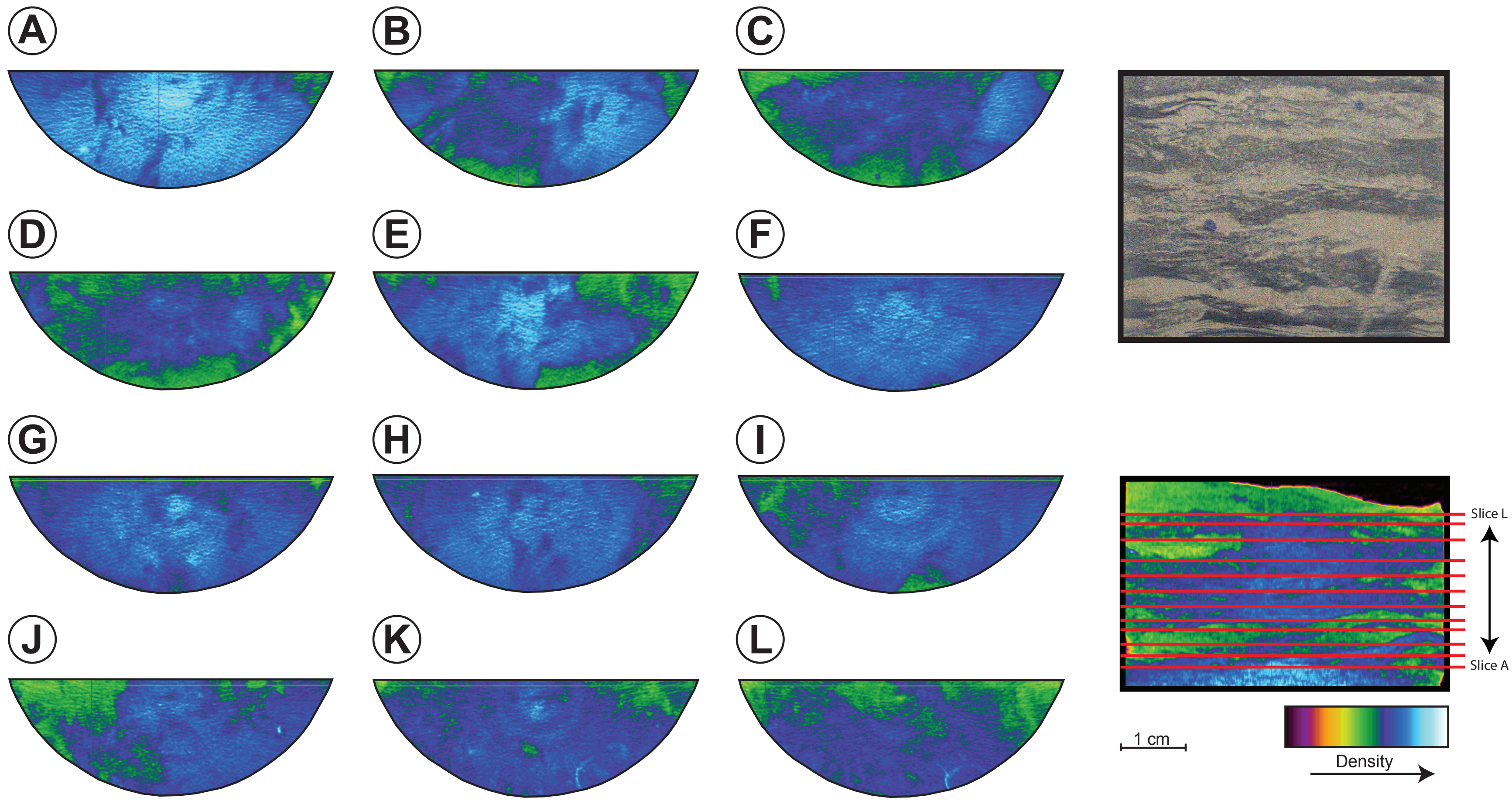

Figure IV-14: X-ray serial sections through Sample 4, with the corresponding core photo and vertical x-ray image for comparison. Slices A to L are arranged from the bottom to the top of the sample. Warm colours represent the lower densities, whereas cool colours are used to show the higher end of the density spectrum. Overall, the serial sections show the progressive changes in the nature of burrowing throughout the sample. Burrow mottling is the dominant texture, and no specific ichnogenera can be identified.

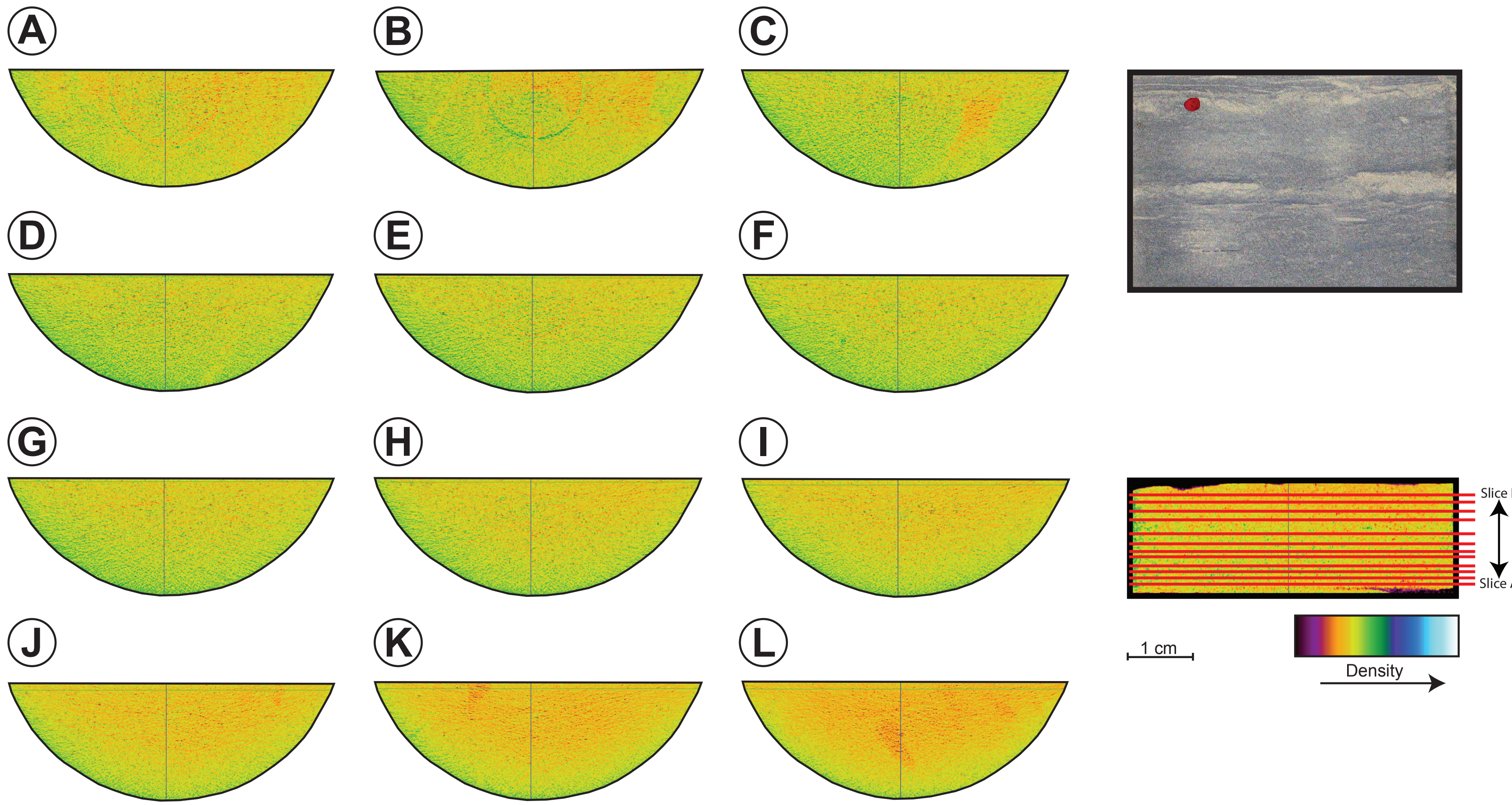

Figure IV-15: X-ray serial sections through Sample 5, with the corresponding core photo and vertical x-ray image for comparison. Slices A to L are arranged from the bottom to the top of the sample. Warm colours represent the lower densities, whereas cool colours are used to show the higher end of the density spectrum. Overall, the serial sections show that burrow mottling has obliterated all primary depositional fabric, and only a few subtle tubular biogenic structures are identifiable (i.e., K and L).

are significantly connected in the horizontal plane, forming a permeable network. However, the heterogeneity is not as important vertically, and thus communication between planiform burrowed horizons is probably minimal except in the most highly bioturbated horizons. On the whole, however, burrowing intensity is low to moderate (BI 1-3; Taylor and Goldring, 1993), except locally in FA2 or FA4. Vertical communication, when present, occurs through thin, often isolated *Skolithos*, *Cylindrichnus,* or *Thalassinoides* ichnogenera.

Permeability versus burrowing intensity graphs show that the permeability behaviour is best generalized by the arithmetic mean. The means were calculated from two volume-weighted permeability measurements, corresponding to the burrows and the matrix, respectively. The method stems from a model where burrows are interpreted to have the highest permeability, and the matrix represents the lowest measured permeability. The arithmetic mean is an estimation of the equivalent bulk permeability in a homogenous, anisotropic, layered unit. The statistical relationship emphasizes the high permeability values, indicating fluid preferentially flows through the most permeable horizons, without significant short-circuiting of the burrow networks. On the other hand, in the few instances where the permeability trend is more closely approximated by the geometric mean, the volume weighting emphasizes all values equally. The geometric mean is an estimation of the equivalent permeability in a homogeneous, isotropic porous medium.

Nexen Inc.'s permeability data allows for direct comparison with the spot-minipermeametry in this study. Their analysis used a PDP-200 permeameter, where data points were profiled roughly every 5 to 20 centimeters vertically, effectively providing a one-dimensional understanding of the effects of bioturbate textures on reservoir quality. In contrast, the PDPK-400 spot-minipermeameter used a closely spaced network of data points (in two-dimensions) to attain high-resolution permeability fields and understand both the vertical and lateral effects of traces on permeability. Since the spot-minipermeametry used a grid of data points, end member permeability was assessed (i.e., burrow permeability and matrix permeability) along with a volume-weighted range in mixtures between burrow and matrix permeability. In the permeability assessment undertaken by Nexen Inc., however, data points were not selected with specific reference to the bioturbation index and therefore, often measurements were taken at spots occurring only partially on burrows, and thus, partially on the matrix. Therefore, the PDP-200 method did not fully assess the influence of burrows on bulk permeability, and the bioturbation index was generalized by observing the nature of burrowing for the immediately surrounding rock package.

Using spot-permeability testing to understand the flow characteristics of intricate networks created by trace fossils is not without shortcomings. The methodology presented in this thesis was model driven, where permeable "streaks" were associated with the porous burrow infills, and the "tight", low permeability rock fabrics are inferred to comprise the silt and clay rich matrix. Understanding the three-dimensional distribution of permeability using measurements from flat core faces required supplemental information derived from x-ray micro-CT analysis to confirm that the distribution of burrows indeed formed an interconnected network.

Based upon data acquired from the permeametry and micro-CT analysis, I observed that above a critical burrowing intensity, approximately 30-40% burrowed (BI 2-3; Taylor and Goldring, 1993), trace fossils have little or no effect on permeability (in the horizontal plane). At this threshold, traces are interconnected and an increase in bioturbation only marginally increases the ease of fluid flow by providing alternate pathways and reducing the probability of dead ends. Once the network of burrows and their permeable fills is connected, increasing the relative abundance of traces only acts to churn sediment, decreasing its overall sorting and thereby reducing bulk permeability. Furthermore, increasing the abundance of burrows above the threshold increases the probability of cross-cutting and overlap, and therefore, decreases the probability of making new permeable fluid conduits in the otherwise silt and clay rich matrix. In light of this, ideal reservoir units comprise moderately burrowed (BI 2-3; Taylor and Goldring, 1993), sand-prone strata.

Intricate, highly tortuous fluid migration pathways characterize burrowed reservoirs. These tortuous flow networks are difficult to model and pose a serious obstacle for reservoir development. Gingras et al. (1999), and Gingras et al. (2004a), recognized that heterogeneous, dual-porosity flow systems potentially exhibit significant mobility of fluids; the tortuosity of fluid conduits generally slows but does not inhibit production (Gingras et al., 2004a). The fluid flow characteristics (porosity and permeability) and geometry of burrowing in the Medicine Hat Member suggests that the dual-porosity system likely contributes to the deliverability and storage capacity of gas. The reservoir properties of the burrowed intervals, in general, behave similarly to the laminated sandstone. But — owing to the extensive surface area shared between burrows and matrix — dual-porosity flow systems produce natural gas from both the bioturbated and matrix rock fabrics. This departs from dual-permeability flow networks (e.g. fracture production), where the lower permeability portion of the reservoir is nominally bypassed during production.

Although assessing the effects of bioturbation on bulk permeability is challenging, especially with respect to the scale of producing intervals, this study indicates that bioturbated media should not be overlooked when evaluating reservoir quality. As described in Chapter II, on the whole, bioturbation decreases up-section in each of the facies associations, so the relative influence of burrowed fabrics on the bulk reservoir quality concomitantly decrease. That being said, it is likely that upon perforating sand-starved intervals, where burrowing cannot be seen on wire-line logs, larger volumes of natural gas may be produced than previously realized. Considering the data and results from this study and understanding the flow dynamics of biogenic heterogeneity should allow geoscientists to improve production techniques in unconventional reservoirs. Applying the principles of ichnology to fluid flow dynamics provides a powerful reservoir development tool.

Three other facies associations recur throughout the study area, where burrowed fabrics comprise a portion of the strata. However, only in FA4 is bioturbation more common than in the succession that was tested herein, FA2 (see Chapter II). As FA4 is not particularly widespread, occurring in only a few isolated locals, it was not selected as a prime candidate for the analysis undertaken in this paper. Furthermore, bioturbation all but obliterates primary physical sedimentary structures in FA4, and thus comparison between laminated and burrowed strata would not have been possible. As such, FA2 was the obvious candidate for permeability and micro-CT analysis because bioturbation is relatively common, but occurs in close proximity to structured fabrics for direct comparison.

SUMMARY

Recognizing that bioturbated rock fabrics can enhance the storage capacity and transmission of subsurface fluids is a relatively recent advancement in our understanding of reservoir dynamics (e.g., Meadows and Tait, 1989; Bastardie et al., 2003; Pemberton and Gingras, 2005; Gingras et al., 2007; Cunningham et al., 2009; Lemiski, 2010). The results of this paper show that significant volumes of biogenic gas are potentially stored and produced from bioturbated claystones, siltstones, and fine-grained sandstones.

Though not examined herein, the relative contribution of trace fossils to permeability preservation in the sandier, but less bioturbated FA1, may be considerable. This stems from the observation that overall burrowing intensities in FA1 fall below a critical threshold. Above the threshold, somewhere between 30% and 40% burrowed, bioturbation does not always significantly enhance reservoir quality. Both reservoir intervals (FA1 and FA2) are volumetrically important rock packages for the production of hydrocarbons in the Medicine Hat field.

Burrowed rock fabrics have elaborate and tortuous fluid migration pathways that complicate the storage and transmission of gas. The trace fossil suites in the Medicine Hat Member dominantly comprise shallow-tiered, horizontally oriented ichnogenera, and thus, burrowing significantly affects the horizontal connectivity of permeable streaks as observed by integrating spot-minipermeametry and x-ray micro-CT analysis. Graphs comparing burrow intensity with permeability show that the permeability can be assessed using the arithmetic mean, and thereby burrowed horizons potentially form laterally extensive flow units. Since the zones are planiform flow units, they are analogous in some ways to structured sandstones (e.g., laminated, cross-laminated, etc), which comprise the most recognizable reservoir units.

Spot-minipermeametry data indicates that the Medicine Hat system represents a dual-permeability flow network, where matrix permeability is within two orders of magnitude relative to the burrowed fabrics. In dual-permeability systems, natural gas is produced from both the matrix and burrowed portions of strata, because flow conduits interact extensively with the surrounding porous matrix (Gingras et al., 2004a). It is essential to understand the interactions between burrow-associated heterogeneity and fluid flow to optimize production strategies in unconventional gas reservoirs.

REFERENCES

Akin, S., and Kovscek, A.R., 2003, Computed tomography in petroleum engineering research, *in* Mees, F., Swennen, R., Van Geet, M., and Jacobs, P., eds., Applications of X-ray Computed Tomography in the Geosciences, Geological Society of London, Special Publications, v. 215, p. 23-38.

Bastardie, F., Capowiez, Y., de Dreuzy, J.R., and Cluzeau, D., 2003, X-ray tomographic and hydraulic characterization of burrowing by three earthworm species in repacked soil cores, Applied Soil Ecology, v. 24, p. 3-16.

Bromley, R.G., 1996, Trace Fossils: Biology and Taphonomy, Unwin Hyman, London, p. 361.

Castle, J.W., Molz, F.J., Lu, S., and Dinwiddie, C.L., 2004, Sedimentology and fractal-based analysis of permeability data, John Henry Member, Straight Cliffs Formation (Upper Cretaceous), Utah, U.S.A., Journal of Sedimentary Research, v. 74, p. 270-284.

Core Laboratories Instruments, 1996, Profile Permeameter PDPK – 400 Operations Manual, 40p.

Cunningham, K.J., Sukop, M.C., Huang, H., Alvarez, P.F., Curran, H.A., Renken, R.A., and Dixon, J.F., 2009, Prominence of ichnologically influenced macroporosity in the karst Biscayne aquifer: stratiform “super-K” zones, Geological Society of America Bulletin, v. 121, p. 164-180.

Dawson, W.C., 1978, Improvement of sandstone porosity during bioturbation, American Association of Petroleum Geologists, Bulletin, v. 62, p. 508-509.

Freeze, R.A., and Cherry, J.A., 1979, Groundwater, eds., Prentice-Hall, New Jersey, USA, 604p.

Gingras, M.K., Pemberton, S.G., Henk, F., MacEachern, J.A., Mendoza, C., Rostron, B., O'Hare, R., Spila, M., and Konhauser, K, 2007, Applications of ichnology to fluid and gas production in hydrocarbon reservoirs, *in* MacEachern, J.A., Bann, K.L., Gingras, M.K., and Pemberton, S.G., eds., Applied Ichnology, SEPM Short Course Notes 52, p. 129-143.

Gingras, M.K., Mendoza, C., and Pemberton, S.G., 2004a, Fossilized worm-burrows influence the resource quality of porous media, AAPG Bulletin, v. 88, p. 875-883.

Gingras, M.K., Pemberton, S.G., Muehlenbachs, K., and Machel, H., 2004b, Conceptual models for burrow-related, selective dolomitization with textural and isotopic evidence from the Tyndall Limestone, Geobiology, v. 2, p. 21-30.

Gingras, M.K., MacMillan, B., Balcom, B.J., 2002a, Visualizing the internal physical characteristics of carbonate sediments with magnetic resonance imaging and petrography, Bulletin of Canadian Petroleum Geology, v. 50, p. 363-369.

Gingras, M.K., MacMillan, B., Balcom, B.J., Saunders, T., and Pemberton, S.G., 2002b, Using magnetic resonance imaging and petrographic techniques to understand the textural attributes and porosity distribution in *Macaronichnus*-burrowed sandstone, Journal of Sedimentary Research, v. 72, p. 552-558.

Gingras, M.K., Pemberton, S.G., Mendoza, C.A., Henk, F., 1999, Assessing the anisotropic permeability of *Glossifungites* surfaces, Petroleum Geoscience, v, 5, p. 349-357.

Gunatilaka, A., Al-Zamel, A., Sherman, A.J., and Reda, A., 1987, A spherulitic fabric in selectively dolomitized siliciclastic crustacean burrows, northern Kuwait, Journal of Sedimentary Petrology, v. 57, p. 927-992.

Hankel, R.C., Davies, G.R., and Krouse, H.R., 1989, Eastern Medicine Hat gas field: a shallow, Upper Cretaceous, bacteriogenic gas reservoir of southeast Alberta, Bulletin of Canadian Petroleum Geology, v. 37, p. 98-112.

Ketcham, R.A., and Carlson, W.D., 2001, Acquisition, optimization and interpretation of X-ray computed tomographic imagery: applications to the geosciences, Computers and Geosciences, v. 27, p. 381-400.

LEE, K.E., AND FOSTER, R.C., 1991, Soil fauna and soil structure, Australian Journal of Soil Research, v. 29, p. 745-775.

LEMISKI, R.T., 2010, Sedimentology, Ichnology, and Resource Characterization of the Low-Permeability Alderson Member, Hatton gas pool, southwest Saskatchewan, Canada, unpublished M.Sc. Thesis, University of Alberta, Canada.

LEMISKI, R.T., HOVIKOSKI, J., GINGRAS, M.K., AND PEMBERTON, S.G., in review, Sedimentological, ichnological, and resource characteristics of the low-permeability, gas-charged Alderson Member (Hatton Gas Pool, southwest Saskatchewan): Implications on resource development, Canadian Bulletin of Petroleum Geology.

MCKINLEY, J.M., LLOYD, C.D., AND RUFFELL, A.H., 2004, Use of variography in permeability characterization of visually homogeneous sandstone reservoirs with examples from outcrop studies, Mathematical Geology, v. 36, p. 761-779.

MEADOWS, P.S., AND TAIT, J., 1989, Modificatino of sediment permeability and shear strength by two burrowing invertebrates, Marine Biology, v. 101, p. 75-82.

MEES, F., SWENNEN, F., VAN GEET, M., JACOBS, P., 2003, Applications of X-ray computed tomography in the geosciences, *in* Mees, F., Swennen, R., Van Geet, M., and Jacobs, P., eds., Applications of X-ray Computed Tomography in the Geosciences, Geological Society of London, Special Publications, v. 215, p. 1-6.

PEMBERTON, S.G., AND GINGRAS, M.K., 2005, Classification and characterizations of biogenically enhanced permeability, AAPG Bulletin, v. 89, p.1493-1517.

PIERRET, A., CAPOWIEZ, Y., BELZUNCES, L., AND MORAN, C.J., 2002, 3D reconstruction and quantification of macropores using x-ray computed tomography and image analysis, Geoderma, v. 106, p. 247-271.

PIERRET, J., PRASHER, S.O., KANTZAS, A., AND LANGFORD, C., 1999, Three dimensional quantification of macropore networks in undisturbed soil cores, Journal of the Soil Science Society of America, v. 63, p. 1530-1543.

Rockware ®, Inc., 2009, Surfer 9.0 Gridding and Contouring Software.

SkyScan N.V., 2005, SkyScan 1172 Desktop X-ray Microtomograph Instruction Manual, 53p.

Sutton, S.J., Etheridge, F.G., Almon, W.R., Dawson, W.C., and Edwards, K.K., 2004, Textural and sequence-stratigraphic controls on sealing capacity of Lower and Upper Cretaceous shales, Denver Basin, Colorado, American Association of Petroleum Geologists, Bulletin, v. 88, p. 1185-1206.

Taylor, A.M., and Goldring, R., 1993, Description and analysis of bioturbation and ichnofabric, Journal of the Geological Society of London, v. 150, p. 141-148.

Van Geet, M., Lagrou, D., Swennen, R., 2003, Porosity measurements of sedimentary rocks by means of microfocus X-ray computed tomography (μCT), *in* Mees, F., Swennen, R., Van Geet, M., and Jacobs, P., eds., Applications of X-ray Computed Tomography in the Geosciences, Geological Society of London, Special Publications, v. 215, p. 51-60.

Weber, K.J., 1982, Influence of common sedimentary structures on fluid flow in reservoir models, Journal of Petroleum Technology, v. 34, p. 665-672.

Worden, R.H., and Morad, S., 2003, Clay minerals in sandstones: controls on formation, distribution and evolution, *in* Worden, R.H., and Morad, S. (eds.), Clay Mineral Cements in Sandstones, International Association of Sedimentologists, Special Publication #34, p. 3-41.

Zorn, M.E., Gingras, M.K., and Pemberton, S.G., 2010, Variation in burrow-wall micromorphologies of select intertidal invertebrates along the Pacific Northwest Coast, U.S.A.: behavioral and diagenetic implications, Palaios, v. 25, p. 59-72.

CHAPTER V — SUMMARY AND CONCLUSIONS

This thesis investigates the ichnological, sedimentological, and stratigraphic characteristics of the Medicine Hat Member (Niobrara Formation) in the Medicine Hat gas field of southeast Alberta. The study exhibits the wide-ranging and powerful applications of ichnology, when utilized in conjunction with sedimentology, stratigraphy, and hydrogeology. Overall, this research contributes to the geologic understanding of Santonian-aged strata in the Western Canada Sedimentary Basin in two regards. The first contribution is an alternative palaeoenvironmental and stratigraphic interpretation of the Medicine Hat Member than has previously been published. The second concerns the application of ichnology to reservoir characterization. The data and interpretations from both aspects of the study are valuable tools for the exploration and production of natural gas in this understudied interval.

PALAEOENVIRONMENTS AND STRATIGRAPHY

Chapter II develops a facies classification scheme based on ichnological and sedimentological criteria. From this, the identification of thirteen major facies was established, and organized into four recurring facies associations. These facies associations consist of silt- and clay-dominated, coarsening-upwards successions with persistent occurrences of sandy bedsets having subtly erosional bases and gradational tops. The trace fossil assemblages observed in the fair-weather siltstones and mudstones show indications of physico-chemical stresses present in the system during deposition. Such biogenic evidence is manifested as a depauperate suite of traces that is dominated by low diversity horizontal deposit-feeding ethologies. The trace fossils have a patchy distribution with an overall low bioturbation intensity. When taken in context, the ichnology points to periodic salinity reductions, heightened depositional rates, soft (thixotropic) substrates, highly turbid water, and common emplacement of high-energy storm beds. Together, these associations give rise to the interpretation that the strata represent various sub-environments present on a shallow marine subaqueous clinoform. Furthermore, the aforementioned data suggest that a significant portion of the Medicine Hat Member was deposited at relatively shallow depths, above storm wave-base.

Chapter III builds upon the palaeoenvironmental interpretations by using a network of seven stratigraphic cross-sections built from wire-line logs (gamma-gamma butterfly plots), and tied to measured core intervals. The facies associations are correlated across the sections, and five clinoform shaped geobodies that prograde northwards through the study area are established. Each clinoform is interpreted as a parasequence, and together these five clinoforms comprise one parasequence set.

Contour maps reveal that the facies associations are broadly lobate. Isolated bays occur between the thickest accumulations of the foreset region, and their distribution is herein proposed to relate to the protection of embayed regions from the dominant marine processes (e.g., waves and storms). Overall, the integration of ichnology and sedimentology, combined with the nature of stratigraphic stacking, suggest that the Medicine Hat system shares many similarities with river- and wave-influenced deltas.

The interpretation of a deltaic affinity for the Medicine Hat Member is a contentious issue. Authors such as Nielsen (2002), Nielsen et al. (2003), Nielsen et al. (2008), and Pedersen et al. (2010), albeit on larger scales, contend that the unit was deposited in a distal shelf setting. Their interpretations of "shelf sandstones", or "detached shelf edge wedges" are weighed against that proposed herein, and the merits of all models are assessed. Moreover, their sequence stratigraphic model differs locally. In this study, the Medicine Hat Member is the preserved part of a highstand systems tract (HST). The nature of bounding surfaces (co-planar sequence boundary/flooding surface below, and sequence boundary above) and the inferred progradation of strata demonstrate clearly that sedimentation outpaced the creation of accommodation space. Nielsen (2002), on the other hand, propose that the same units comprise two separate sequences.

ICHNOLOGY AND RESERVOIR GEOLOGY

Chapter IV explores the relationship between biogenic rock fabrics and porosity and permeability modification. Employing spot-minipermeametry and x-ray microtomography (Micro-CT) experiments, one of the main reservoir units (Facies Association 2) is analyzed to understand the relationship between bioturbate textures and heterogeneity. The spot-minipermeametry results indicate that the highly complex and tortuous biogenic-flow pathways in the Medicine Hat Member contribute significantly to the storage and transmission of natural gas. These bioturbated intervals have highly contrasting and well-defined permeability fields, where matrix- and burrow-associated permeability are within two orders of magnitude. Biogenic fluid conduits in the Medicine Hat Member therefore, construct a dual-porosity flow network system (*sensu* Gingras et al., 2007). In dual-porosity flow media, the majority of the rock volume conducts fluids, though flow is focused through the higher permeability zones. Furthermore, flow interaction between the burrowed and matrix horizons may be extensive (Gingras et al., 2007).

Volume-weighted averaging of the burrow- and matrix-associated permeability was employed on the data from spot-minipermeametry to approximate the bulk permeability of specific facies in FA2. The arithmetic mean of permeability is a good estimate of the bulk permeability occuring through well connected burrow networks; the harmonic mean is an estimator of the bulk permeability in less well-connected burrow networks where signifcant short circuiting of flow conduits occur; and the geometric mean provides an equivalent bulk permeability in homogeneous, isotropic flow media. Profile permeability data (provided by Nexen Inc.) is plotted on graphs of the three respective means for the full range of bioturbation intensity (i.e., 0-100%). The majority of data clustered near the arithmetic mean, indicating that trace fossils form well-connected planiform networks. The planiform burrow networks are in some ways analogous to the stratified sandstone facies because the spot-minipermeametry data were nominally similar. In some instances, rare traces with vertical components (e.g., *Skolithos, Teichichnus, Psilonichnus, Rhyzocorallium,* etc.) may provide hydraulic communication between discontinuous planiform burrow networks.

CONCLUSION

As the global demand for energy continues to rise, the unconventional natural gas occurring in the Medicine Hat Member will become increasingly important. These regionally extensive Upper Cretaceous strata have been problematic for understanding the depositional processes responsible for their accumulation, and for characterizing the flow dynamics of subsurface fluids. The reason for this lack of knowledge is the challenge of describing and interpreting the enigmatic sediments. Under careful and scrutinous observation, however, the important sedimentological and ichnological characteristics have been distilled and brought to the forefront to refine the palaeoenvironmental and stratigraphic models. Emerging technologies, such as micro-computed tomography, combined with spot-minipermeametry provides evidence supporting the hypothesis that biogenic rock fabrics appreciably enhance reservoir characteristics such as porosity and permeability. Together, the data presented in this thesis forge a framework upon which future scientists and industry can build to recognize similar deposits elsewhere, and maximize production potential from fine-grained, low-permeability gas reservoirs.

With meticulous and insightful consideration of cores and wire-line log signatures throughout the Medicine Hat gas field, geologists will be able to map the productive intervals with the knowledge that pervasively burrowed strata contribute significantly to the flow dynamics of these reservoirs. The anisotropic burrow-associated permeability will now be recognized as a significant contributor to overall natural gas production, and in light of this, bypassed pay may increase potential reserves and the resulting value of the field as a whole. Extrapolating these ideas to other stratigraphic levels with similar characteristics might further increase natural gas production from southeast Alberta and southwest Saskatchewan. Moreover, elevating the economic significance of the Upper Cretaceous unconventional reservoirs in the Western Canada Sedimentary Basin will spearhead further in-depth study to address other poorly understood aspects of the geology.

REFERENCES

Gingras, M.K., Pemberton, S.G., Henk, F., MacEachern, J.A., Mendoza, C., Rostron, B., O'Hare, R., Spila, M., and Konhauser, K, 2007, Applications of ichnology to fluid and gas production in hydrocarbon reservoirs, *in* MacEachern, J.A., Bann, K.L., Gingras, M.K., and Pemberton, S.G., eds., Applied Ichnology, SEPM Short Course Notes 52, p. 129-143.

Nielsen, K.S., 2002, Lithostratigraphy, sequence stratigrapy and palaeoenvironments of the Upper Colorado Group in southern Alberta and southwest Saskatchewan: definition of the Carlile and Niobrara formations (Upper Turonian to Upper Santonian), unpublished Ph.D. thesis, Carleton University, Ottawa, Canada.

Nielsen, K.S., Schröder-Adams, C.J., and Leckie, D.A., 2003, A new stratigraphic framework for the Upper Colorado Group (Cretaceous) in southern Alberta and southwest Saskatchewan, Canada, Bulletin of Canadian Petroleum Geology, v. 51, p. 304-346.

Nielsen, K.S., Schröder-Adams, C.J., Leckie, D.A., Haggart, J.W., and Elberdak, K., 2008, Turonian to Santonian paleoevironmental changes in the Cretaceous Western Interior Sea: The Carlile and Niobrara formations in southern Alberta and southwest Saskatchewan, Canada, Palaeogeography, Palaeoclimatology, Palaeogeography, v. 270, p. 64-91.

Pedersen, P.K., Macquaker, J.H., and Hart, B., 2010, Detached fine-grained shelf edge wedges within shale dominated successions, depositional model and reservoir significance, American Association of Petroleum Geologists, Conference Abstracts.

APPENDIX A

LEGEND

LITHOLOGY

- Silty Sand
- Siltstone
- Shale/Mudstone
- Sandy Silt
- Silty Shale
- Lost Core

CONTACTS

- Uncertain
- Sharp

PHYSICAL STRUCTURES

- Current Ripples
- Planar Tabular Bedding
- Hummocky Cross-Strat.
- Wavy Parallel Bedding
- Convolute Bedding
- Graded Bedding
- Oscillation Ripples
- Low Angle Tabular Bedding
- Scour
- Fault

LITHOLOGIC ACCESSORIES

- Silt Lamina
- Shale Lamina
- Sand Lamina
- Py Pyrite
- Bentonite
- Shell Fragments
- Calcareous

ICHNOFOSSILS

- Planolites
- Diplocraterion
- Rhyzocorallium
- Palaeophycus
- Phycosiphon
- Chondrites
- Schaubcylindrichnus freyi
- Zoophycos
- Teichichnus
- Thalassinoides
- Escape Draft

BIOTURBATION INDEX

- 0 Barren
- 3 Moderate
- 6 Complete
- 1 Sparse
- 4 Abundant
- 2 Low
- 5 Intense

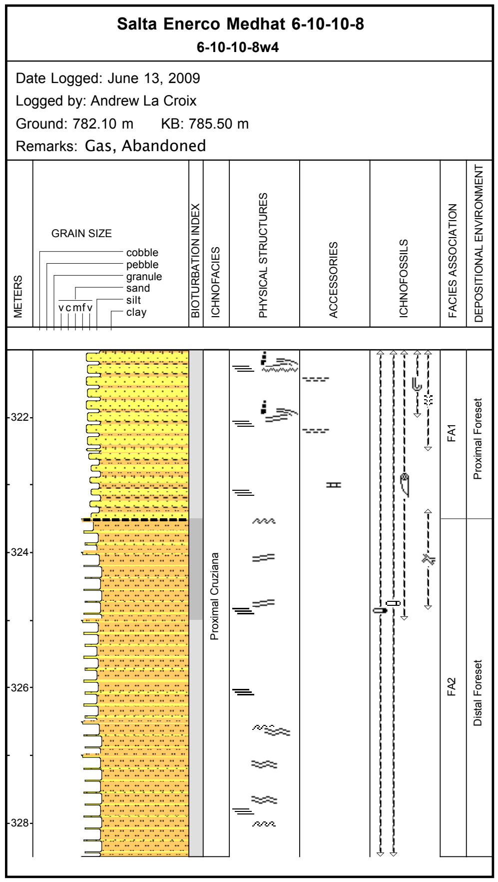
Salta Enerco Medhat 6-10-10-8
6-10-10-8w4
Date Logged: June 13, 2009
Logged by: Andrew La Croix
Ground: 782.10 m KB: 785.50 m
Remarks: Gas, Abandoned
METERS
GRAIN SIZE
cobble
pebble
granule
sand
silt
clay
v c m f v
BIOTURBATION INDEX
ICHNOFACIES
PHYSICAL STRUCTURES
ACCESSORIES
ICHNOFOSSILS
FACIES ASSOCIATION
DEPOSITIONAL ENVIRONMENT
322
324
326
328
Proximal Cruziana
FA1
Proximal Foreset
FA2
Distal Foreset

Salta Enerco Medhat 7-13MH-10-8

2/7-13-10-8w4

Date Logged: June 17, 2008
Logged by: Andrew La Croix
Ground: 768.40 m KB: 771.30 m
Remarks: Gas, Abandoned

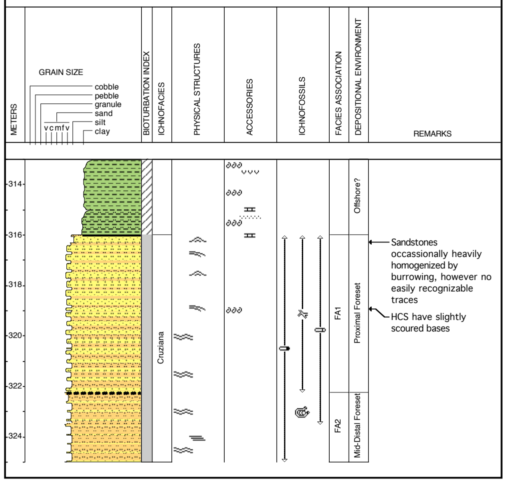

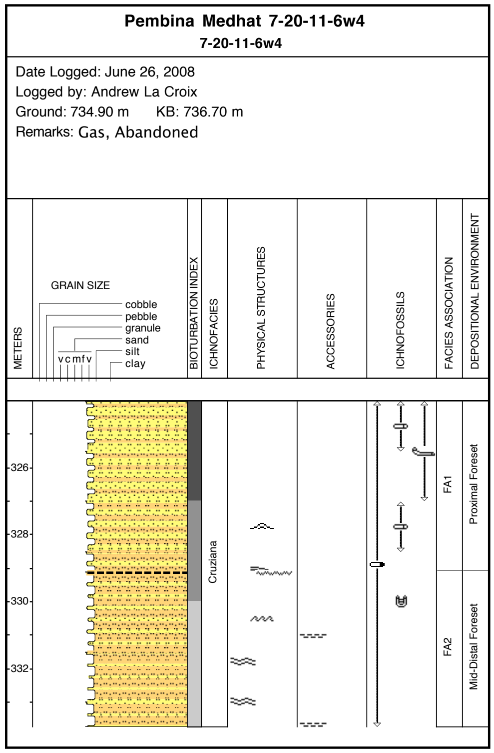
Pembina Medhat 7-20-11-6w4
7-20-11-6w4
Date Logged: June 26, 2008
Logged by: Andrew La Croix
Ground: 734.90 m KB: 736.70 m
Remarks: Gas, Abandoned
METERS
GRAIN SIZE
cobble
pebble
granule
sand
silt
clay
v c m f v
BIOTURBATION INDEX
ICHNOFACIES
PHYSICAL STRUCTURES
ACCESSORIES
ICHNOFOSSILS
FACIES ASSOCIATION
DEPOSITIONAL ENVIRONMENT
326
328
330
332
Cruziana
FA1
Proximal Foreset
FA2
Mid-Distal Foreset

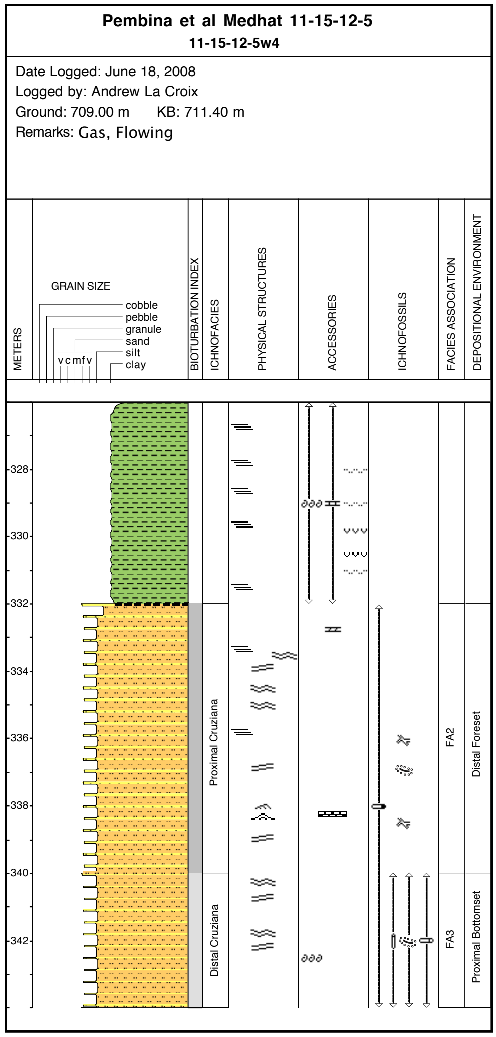
Pembina et al Medhat 11-15-12-5
11-15-12-5w4
Date Logged: June 18, 2008
Logged by: Andrew La Croix
Ground: 709.00 m KB: 711.40 m
Remarks: Gas, Flowing
METERS
GRAIN SIZE
cobble
pebble
granule
sand
silt
clay
v c m f v
BIOTURBATION INDEX
ICHNOFACIES
PHYSICAL STRUCTURES
ACCESSORIES
ICHNOFOSSILS
FACIES ASSOCIATION
DEPOSITIONAL ENVIRONMENT
-328
-330
-332
-334
-336
-338
-340
-342
Proximal Cruziana
Distal Cruziana
FA2
FA3
Distal Foreset
Proximal Bottomset

Ranchmen's et al Medhat 11-11-12-3

11-11-12-3w4

Date Logged: June 20, 2008
Logged by: Andrew La Croix
Ground: 783.30 m   KB: 786.40 m
Remarks: Gas, Abandoned

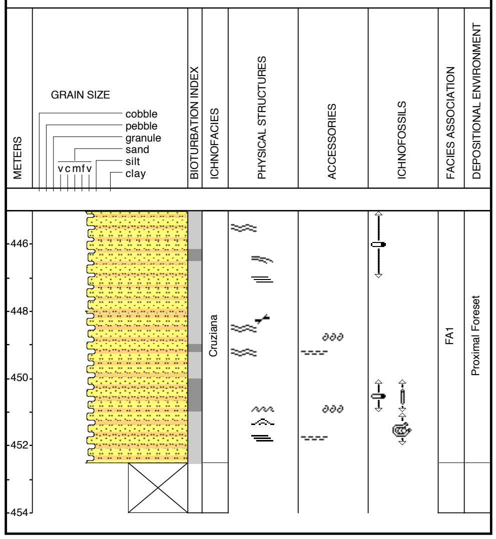

Esso Medhat 6-10-13-7

6-10-13-7w4

Date Logged: June 12, 2008

Logged by: Andrew La Croix

Ground: 752.60 m KB: 755.00 m

Remarks: Gas, Flowing

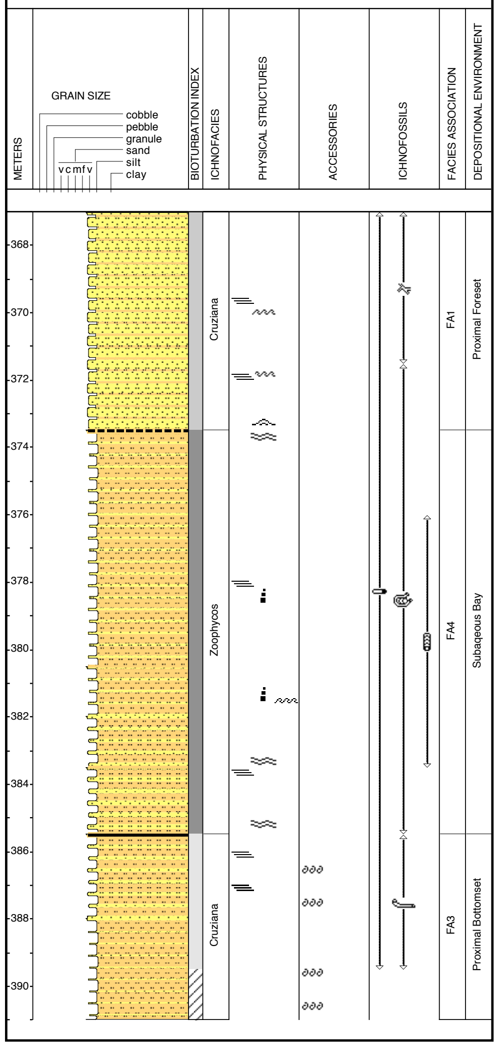

Nexen Medhat 14-36-13-4

14-36-13-4w4

Date Logged: June 9, 2008
Logged by: Andrew La Croix
Ground: 745.30 m KB: 750.10 m
Remarks: Gas, Flowing

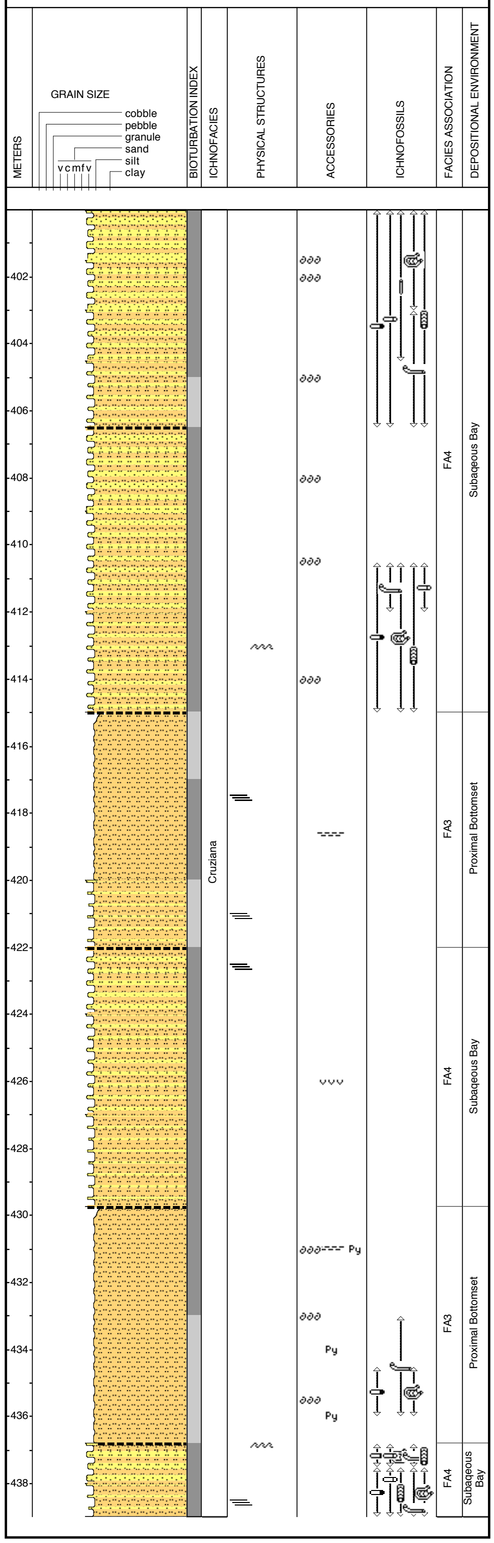

Saskoil Medhat 6-26-14-2

2/6-26-14-2w4

Date Logged: June 11, 2008
Logged by: Andrew La Croix
Ground: 809.20 m KB: 812.70 m
Remarks: Gas, Abandoned

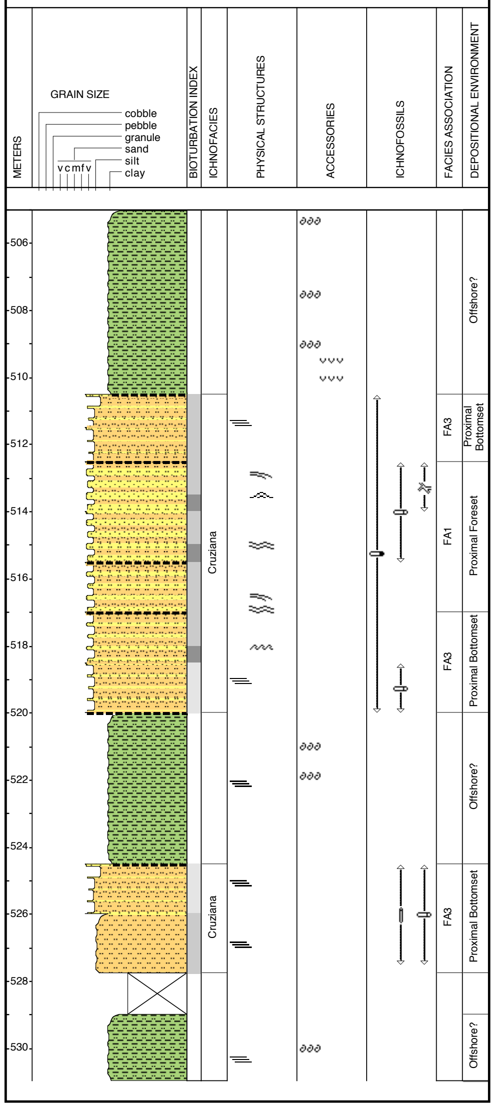

Nexen Medhat 6-31-14-1w4

6-31-14-1w4

Date Logged: July 13, 2009
Logged by: Andrew La Croix
Ground: 806.40 m KB: 810.20 m
Remarks: Gas, Flowing

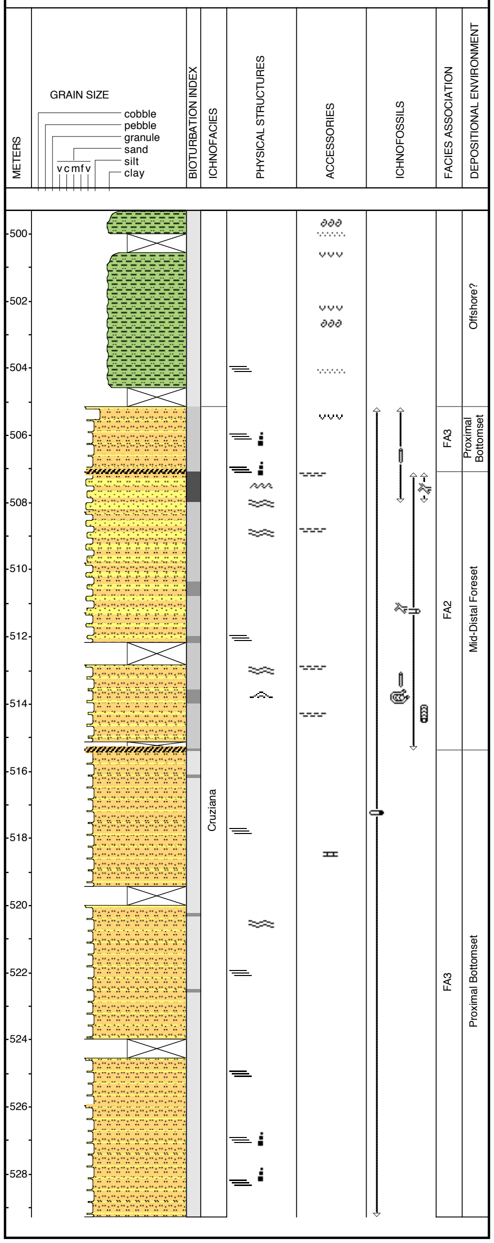

PC Medhat 7-17-15-4

7-17-15-4w4

Date Logged: June 24, 2008
Logged by: Andrew La Croix
Ground: 745.80 m KB: 748.30 m
Remarks: Gas, Flowing

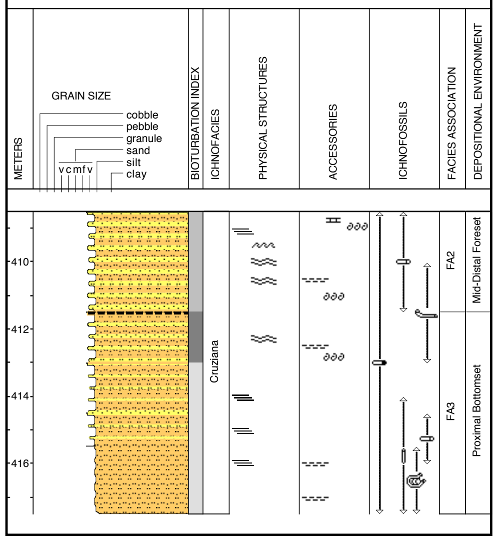

PC Medhat 7-35-15-4

7-35-15-4w4

Date Logged: June 25, 2008
Logged by: Andrew La Croix
Ground: 798.60 m KB: 801.30 m
Remarks: Gas, Flowing

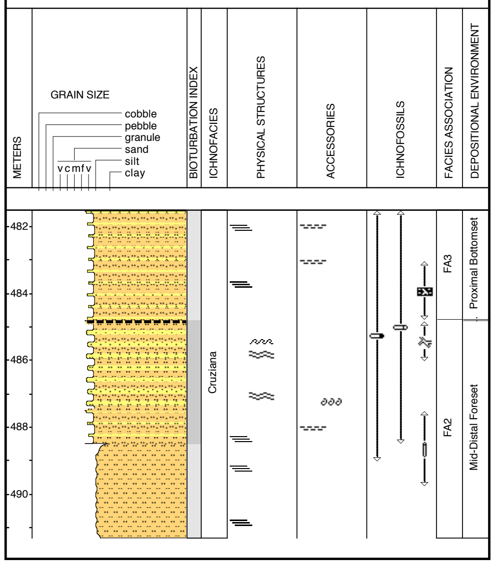

Esso Medhat 16-16-15-1
16-16-15-1w4

Date Logged: June 17, 2008
Logged by: Andrew La Croix
Ground: 796.10 m KB: 798.60 m
Remarks: Gas, Flowing

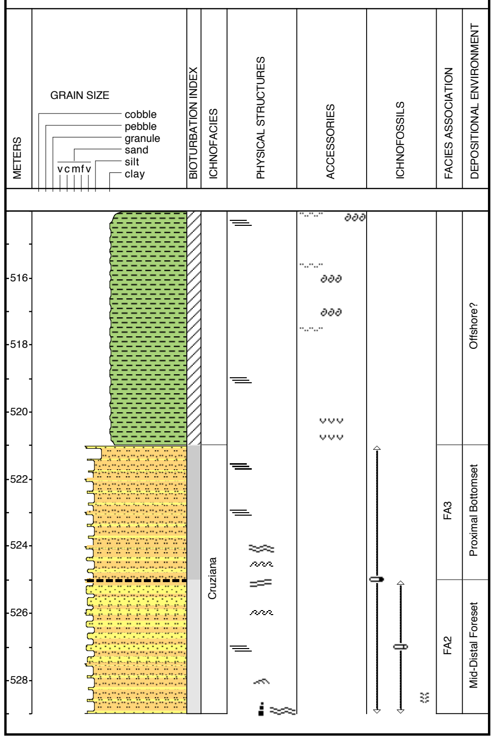

PC Medhat 10-5-16-4

10-5-16-4w4

Date Logged: June 24, 2008
Logged by: Andrew La Croix
Ground: 784.90 m KB: 787.00 m
Remarks: Gas, Flowing

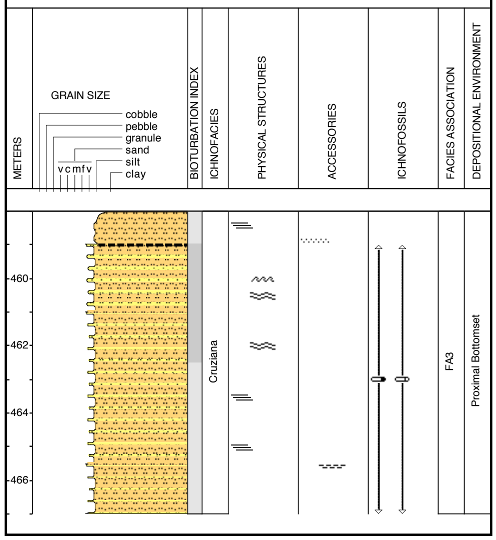

Esso Medhat 7-19-16-2
7-19-16-2w4

Date Logged: June 23, 2008
Logged by: Andrew La Croix
Ground: 827.80 m   KB: 830.30 m
Remarks: Gas, Flowing

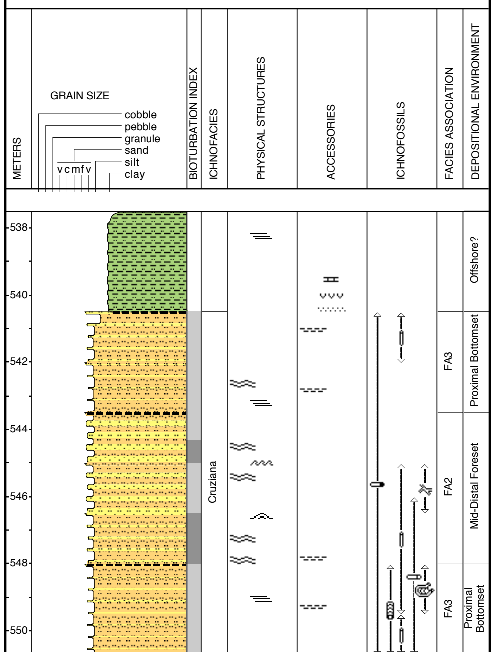

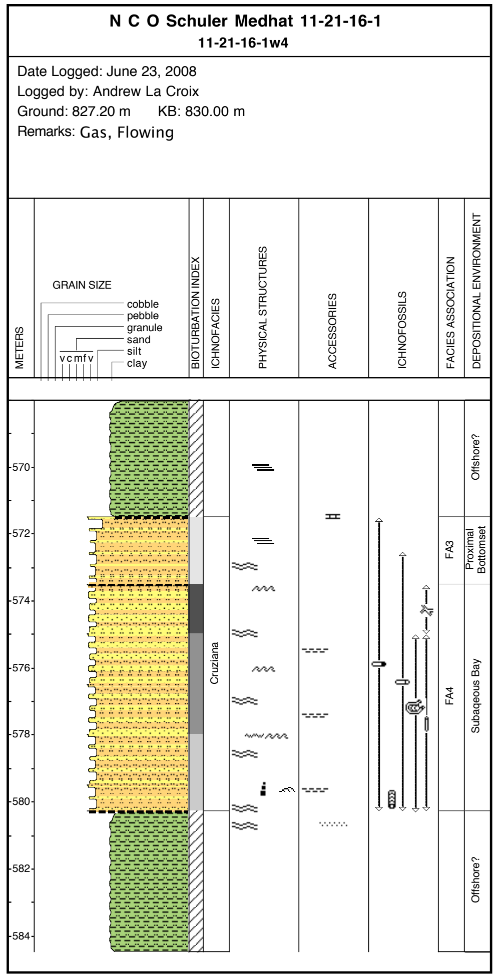
N C O Schuler Medhat 11-21-16-1
11-21-16-1w4
Date Logged: June 23, 2008
Logged by: Andrew La Croix
Ground: 827.20 m KB: 830.00 m
Remarks: Gas, Flowing
METERS
GRAIN SIZE
cobble
pebble
granule
sand
silt
clay
v c m f v
BIOTURBATION INDEX
ICHNOFACIES
PHYSICAL STRUCTURES
ACCESSORIES
ICHNOFOSSILS
FACIES ASSOCIATION
DEPOSITIONAL ENVIRONMENT
570
572
574
576
578
580
582
584
Cruziana
FA3
FA4
Offshore?
Proximal Bottomset
Subaqeous Bay
Offshore?

PC et al Hilda Medhat 16-15-17-2
16-15-17-2w4

Date Logged: June 16, 2008
Logged by: Andrew La Croix
Ground: 802.30 m KB: 805.30 m
Remarks: Gas, Flowing

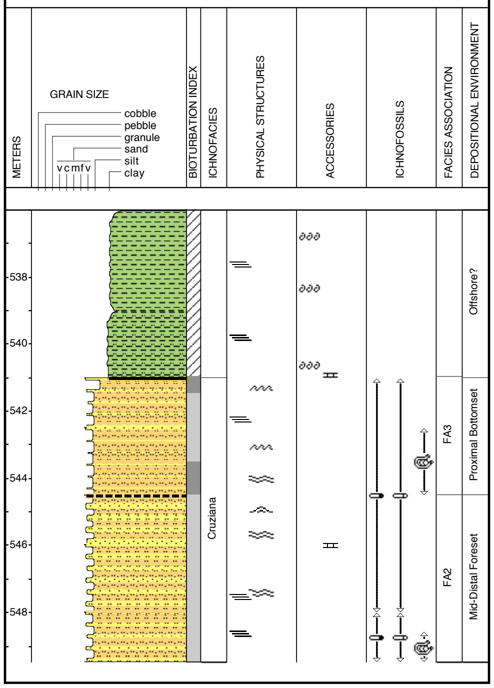

Pex Hilda Medhat 10-34-18-3

10-34-18-3w4

Date Logged: June 26, 2008
Logged by: Andrew La Croix
Ground: 740.10 m KB: 742.80 m
Remarks: Gas, Flowing

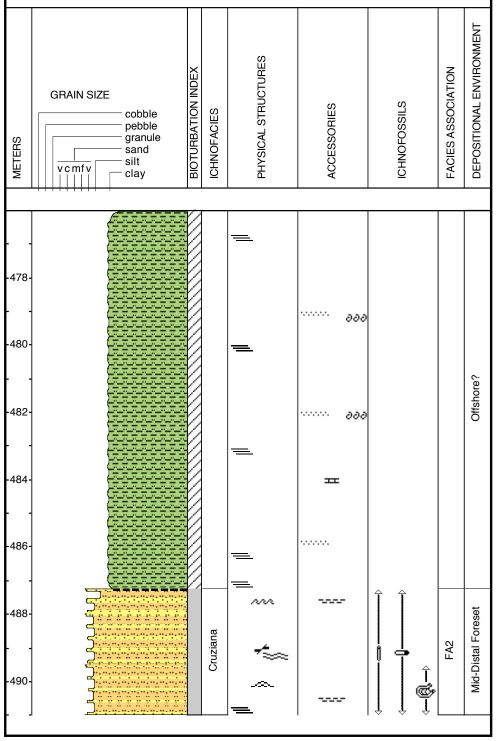

DEML Medhat 7-24-18-1

7-24-18-1w4

Date Logged: June 19, 2008
Logged by: Andrew La Croix
Ground: 740.70 m KB: 743.70 m
Remarks: Gas, Flowing

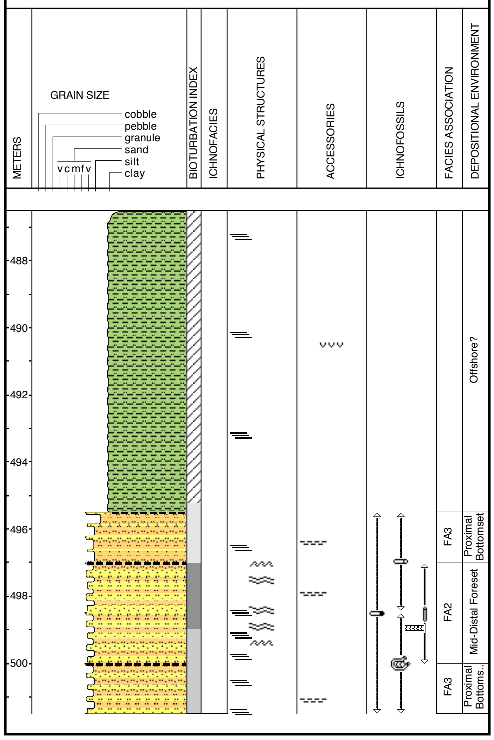

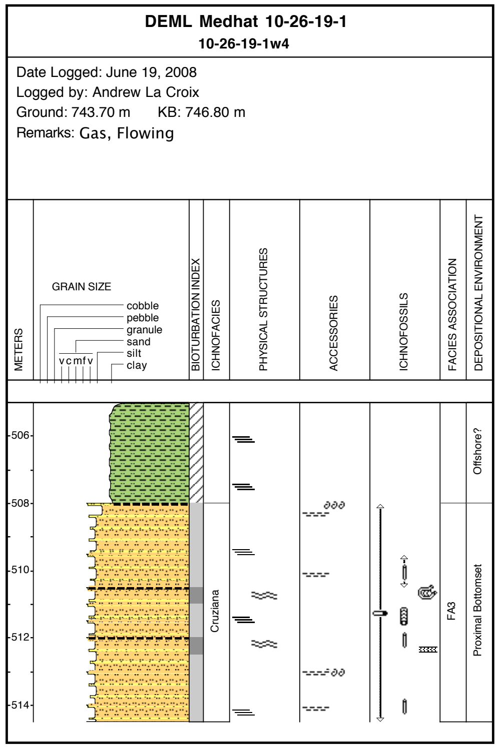
DEML Medhat 10-26-19-1
10-26-19-1w4
Date Logged: June 19, 2008
Logged by: Andrew La Croix
Ground: 743.70 m KB: 746.80 m
Remarks: Gas, Flowing
METERS
GRAIN SIZE
cobble
pebble
granule
sand
silt
clay
v c m f v
BIOTURBATION INDEX
ICHNOFACIES
PHYSICAL STRUCTURES
ACCESSORIES
ICHNOFOSSILS
FACIES ASSOCIATION
DEPOSITIONAL ENVIRONMENT
506
508
510
512
514
Cruziana
FA3
Offshore?
Proximal Bottomset

APPENDIX B

Isopach Map of Facies Association 1

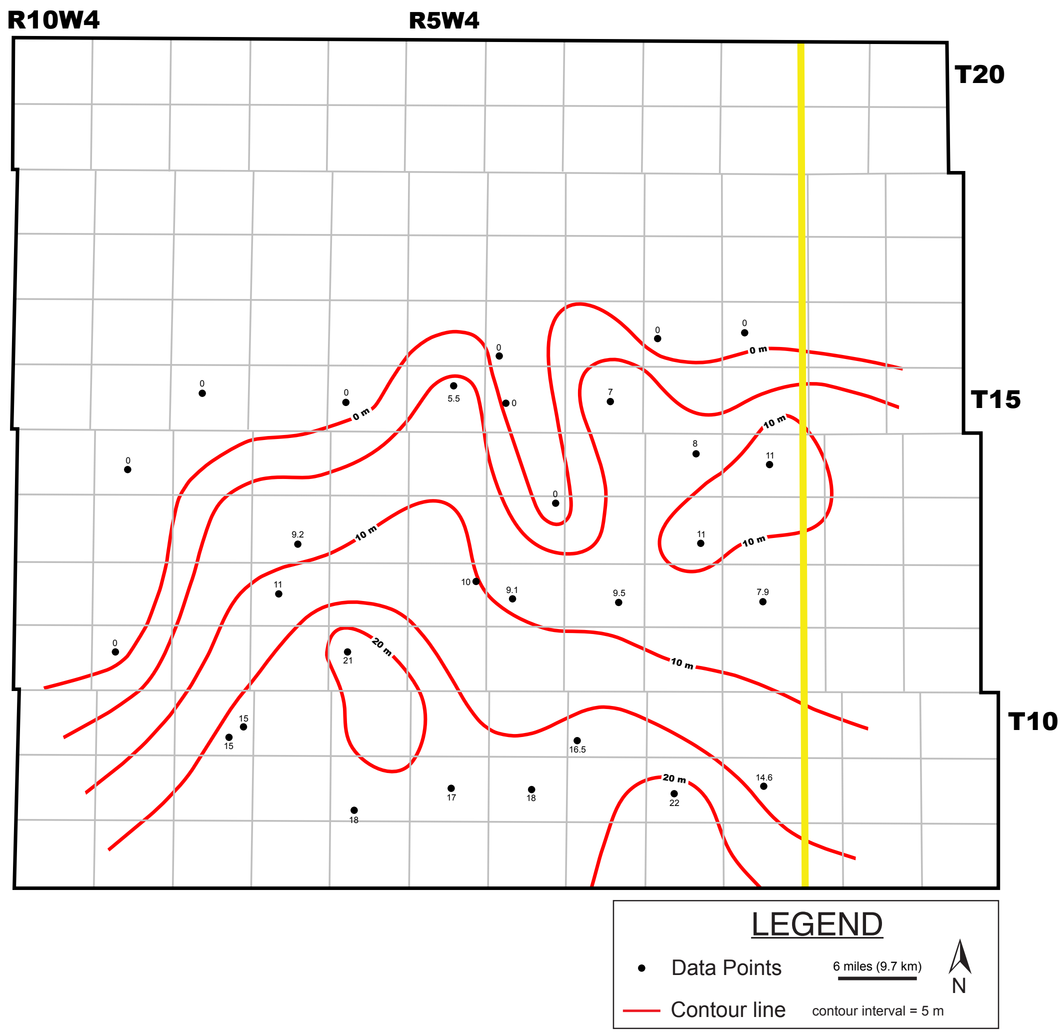

Isopach Map of Facies Association 2

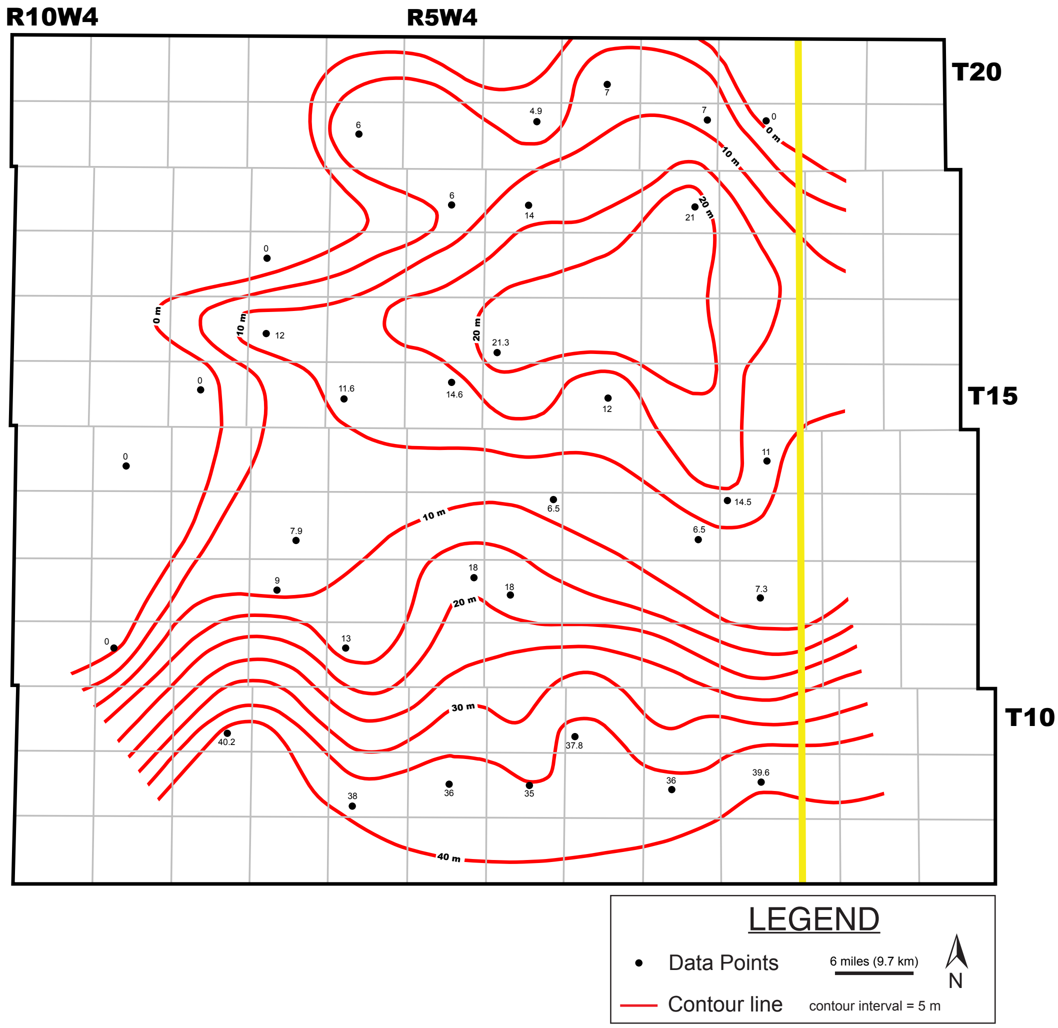

Isopach Map of Facies Association 3

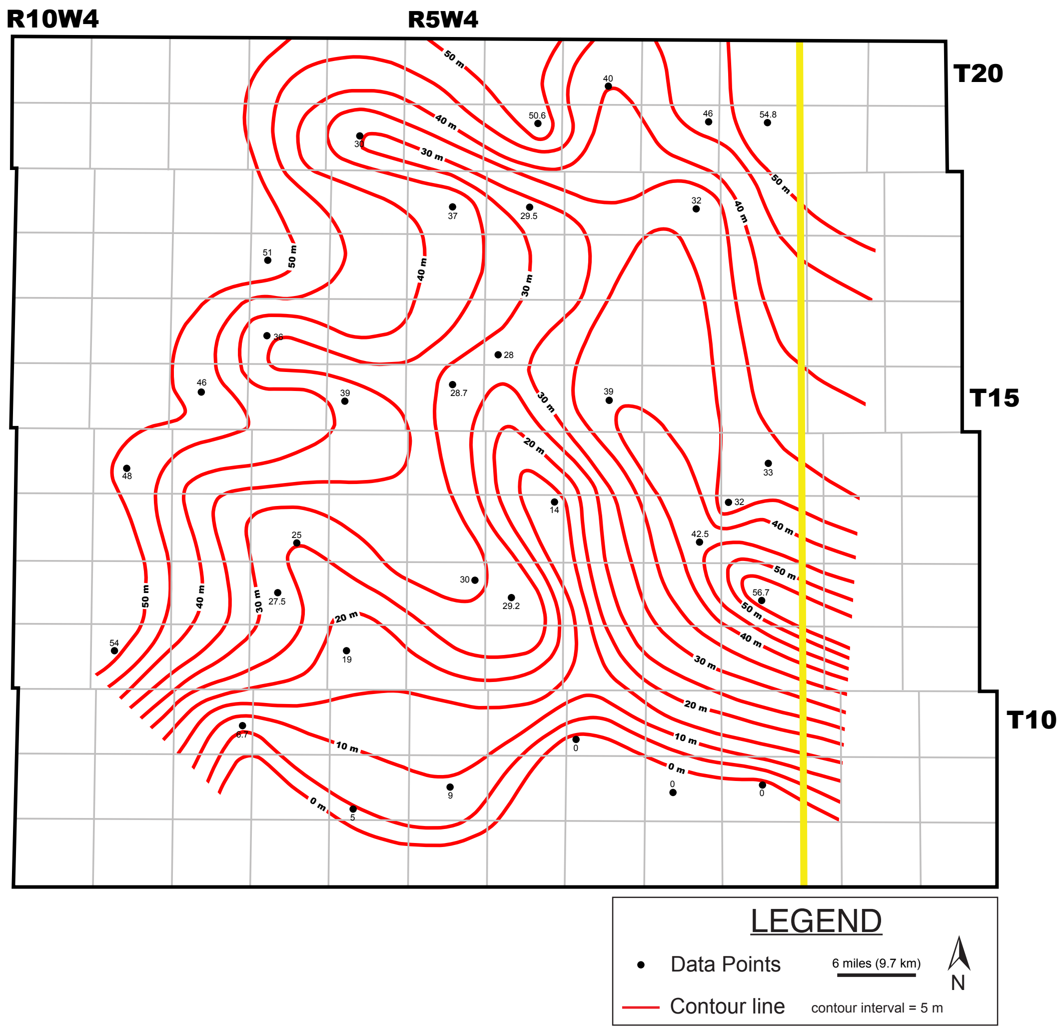

Isopach Map of the Medicine Hat Member